# Post-glacial coral reef growth on Kodakara Island in the Northwest Pacific: the relationship between high-latitude reef growth and millennial-scale global climate change

2013, 3

Nozomu HAMANAKA

A dissertation submitted to
Graduate School of
OKAYAMA UNIVERSITY

# Abstract

Recent studies have reported Holocene millennial-scale climate instability on a global scale. The distribution of modern coral reefs in the Northwest Pacific is restricted to approximately N30° latitude. Understanding the high-latitude reef growth process and its correlation to millennial-scale climate change may provide important insights into the expected reef growth in the future at even higher latitudes in response to global warming. It is still unclear whether or how such millennial-scale climate changes affect reef growth. To accurately evaluate this question, it is necessary to collect precise data on long-term natural changes in reef growth before the advent of human influence.

Kodakara Island (29°13'N, 129°19'E) is located in the pathway of the Kuroshio Current in the Northwest Pacific and has well-developed, raised coral reef terraces. The reef terraces display well-preserved coral reef features, such as spur and groove systems and reef mounds, and thus provide a rare opportunity to investigate Holocene-raised reef terraces in detail. In this thesis, I describe the details of high-latitude reef growth dynamics and their significant correlation to millennial-scale suborbital global climate variability during the Holocene, using field observations and high-precision geologic data obtained from three excavated trench walls and seven cores drilled from the raised reef on Kodakara Island, as well as absolute accelerator mass spectrometry (AMS) radiocarbon dating of 88 fossil coral samples.

The island is characterized by three Holocene raised reef terraces (Terraces I, II and III) approximately 9 m, 2 m, and 1 m above mean sea level, which uplifted approximately 2.4 ka, 1–0.4 ka, and during the modern era, respectively. I found three disconformities at excavated trench walls (E-1, E-2, and E-3 sites) on Terrace I, and the dating results indicated that disturbances with hiatuses in reef growth occurred at approximately 5.9 to 5.8, 4.4 to 4.0, and 3.3 to 3.2 cal yr BP. The timing of the disturbances corresponds well with the periods when the Kuroshio Current was relatively weak and was associated with a relatively cold sea surface temperature, which may have enhanced cold-winter Asian monsoons, and also with Holocene North Atlantic ice-rafting cold events. The coral composition clearly changed before and after the disturbances, with gradually reduced diversity resulting in a reef dominated by acroporid coral. These data led to the hypothesis that coral reef growth was interrupted by suborbital millennial-scale global climate change induced by persistent solar activity during the Holocene in high-latitude coral reefs, such as those in the Northwest Pacific, leading to low diversity in the reefs that experienced each disturbance.

The results also indicated that the second and third events were associated with sea-level oscillations. The late-Holocene sea-level oscillation (LHSO) observed at Kodakara Island was characterized by two oscillations; a 1.5 m fall and 0.7 m rise at 4.4–4.0 ka and a 0.8 m fall and 2.5 m rise at 3.3–3.2 ka, with relative low stand between 4–3.3 ka. The timing of these oscillations correspond well with events of weakening of the Kuroshio Current, that are linked to North Atlantic events 3 and 2 and may have led to a relative low sea-level. The timing of these events also corresponds to strong positive phases of Pacific Decadal Oscillation (PDO), which is related to El Niño Southern Oscillation (ENSO) activities. Similar oscillations have been reported in tectonically stable areas, such as eastern Australia, which implies that the changes extended to a global scale, although the magnitudes of the changes are inconsistent with our results. Thus, it is concluded that LHSO might have been induced by millennial-scale global climate change, which might have been able to invoke the extension or retreat of glaciers, and that changes in ENSO activity and

positive PDO positive phases that influenced the Kuroshio Current may have enhanced the magnitudes of the oscillations in the Northwest Pacific. The results indicate that the Holocene sea-level change may not have been as stable as previously estimated and may have had a significant regional impact on the pathways of major currents, such as the Kuroshio Current.

The reef began to grow at least 8 ka, and it experienced a relatively rapid vertical growth rate of 3.6-3.3 m $kyr^{-1}$ between 8 and 6 ka, despite terrigenous sedimentation on the reef slope. The reef started growing at landward sites and gradually extended seaward. Reef growth around the reef slope slowed after 6 ka, which most likely correlates with the first and second hiatus events detected landward. The timing of the second hiatus event corresponds to the onset of a period of weakening of the Kuroshio Current and a period of increased ENSO variability. In contrast to the reef flat, which resumed its growth after the third hiatus event, reef mound accretion on the reef slope ceased. Terrace I was uplifted approximately 2.4 ka. Reef growth was reactivated approximately 1.3 ka, and the reef grew at a pace of 9.1 m $kyr^{-1}$ between 1.3 and 1 ka, the fastest growth rate recorded in this study. This time interval corresponds to the Medieval Climatic Anomaly. The cause of the delayed reef growth between 2.4 and 1.4 ka remains unclear but may be attributable to a weaker Kuroshio Current approximately 1.7 ka and to the strong ENSO activity detected for the eastern Pacific between 2 and 1.5 ka.

The results indicate that post-glacial, high-latitude reef growth was apparently affected by millennial-scale climate change. In particular, the climate event approximately 4 ka caused the largest change in reef growth style and may have affected reefs throughout the Pacific region.

# Acknowledgements

The author would express to thank Prof. Hironobu Kan for his comprehensive supervise for this study. The author would also appreciate to follows. Prof. Shigeyuki Suzuki reviewed and gave important advises for this study. Prof. Tsugio Shibata was a supervisor when I was a student of doctoral course at the graduate school of Okayama University, and indicated a way of the study as a geologist. Dr. Yusuke Yokoyama of the University of Tokyo fully discussed on climate and sea-level changes in global scale for this study. Moreover, he kindly and readily accepted to carry out the radiocarbon dating using a tandem AMS at the Micro Analysis Laboratory Tandem Accelerator, University of Tokyo, with Dr. Hiroyuki Matsuzaki and Dr. Yosuke Miyairi of the University of Tokyo. Prof. Yosuke Nakashima of Ariake national college of technology assisted drilling operations at Kodakara Island and suggested helpful comments. Prof. Toshio Kawana of University of the Ryukyus, who was the supervisor when I was a student of the graduate school of University of the Ryukyus, and he first gave to me that the knowledge of physical geography, geomorphology and geology in the Ryukyu Islands and the Northwest Pacific. Prof. Nobuyuki Hori of Nara University suggested helpful comments. Mr. Hiroshi Adachi of Geo-act co. ltd. taught the techniques for drilling operations at Kitami city, Hokkaido by his kind invitation. Mr. Takehiro Okamoto fully supported of this study, in particular, assisted with all field works. Mr. Tomoya Ohashi also assisted with most field works.

Finally, the author would express to special thank Mr. Makoto Hamanaka and Mrs. Mieko Hamanaka of my parents, Mrs. Miho Hamanaka and Mr. Ray Hamanaka of my wife and a son, for their kind help throughout this study.

# Contents

# List of Tables

# List of Figures

# List of Appendix

# Chapter 1

# Introduction

The Holocene epoch corresponds to the marine isotope stage (MIS) 1. MIS 1 had a relatively warm and stable climate throughout the Quaternary, although there is evidence for unstable millennial-scale climate change characterized by North Atlantic ice-rafted cooling events (e.g., Bond et al., 1997; 2001; deMenocal et al., 2000). These changes occurred rapidly within decadal time-scales and with certain regularity such as 8200 yr BP cooling event (Alley et al., 1997; Rohling and Palike, 2005). Sea levels through some of these periods were recorded in sea level indicators such as coral reef sediments, marine notches, which obtained from worldwide (e.g. Fairbanks,1989; Bard et al., 1996; Pirazzoli, 1991; 1996). The recent realization that the rapid climate shifts of the Holocene were also associated with significant and abrupt changes in sea-level (e.g. Baker et al., 2001; Siddall et al., 2003; Martin et al., 2003; Lewis et al., 2008), may have implications on the evolutional patterns of coral reefs as during interglacial (Bruggemann et al., 2004; Blanchon et al., 2009; Thompson et al., 2011; Hamanaka et al., 2012) and glacial cycle (Yokoyama et al., 2001; Chappell, 2002; Esat and Yokoyama, 2006). The abrupt climate shifts has affected not only sea level, but oceanic and atmospheric conditions, such as variability, frequency, intensity and dynamics on sea surface temperature; SST (e.g. McCulloch et al., 1996 ; Gagan et al., 2000), Monsoon (e.g. Thompson et al., 2000 ;

Wang et al., 2005; Liew et al., 2006), El-Niño - Southern oscillation; ENSO (e.g. Haug et al., 2001; Moy et al., 2002; Gagan et al, 2004), major current such the Kuroshio (e.g. Jian et al., 2000; Ujiie et al., 2003; Xiang et al., 2007), which revealed on currently multi-proxies that deep sea sediments, corals, tropical ice, stalagmites, and their synchronous has assessed which generally based on Greenland ice cores (e.g., Dansgaad et al., 1993; Grootes et al., 1993) and North Atlantic sediments (Bond et al., 1997; 2001).

Therefore, the reef growth during the Holocene also may have effected by each or several and/or coupled climate variability, are sufficiently considered. Many studies have suggested that modern coral reef deterioration is related to increased anthropogenic activity (e.g., Pandolfi et al., 2003; 2011), including climate change such as global warming and ocean acidification (e.g., Kleypas et al., 1999; Hughes et al., 2003; Hoegh-Guldberg et al., 2007; 2011). It is still unclear whether or how such millennial-scale climate changes affect reef growth. To accurately evaluate this question, it is necessary to collect precise data on the long-term natural changes in reef growth before the advent of human influence.

The Ryukyu Islands in the Northwest Pacific are a high-latitude area where corals are already showing signs of poleward migration due to climate change (Yamano et al., 2011). Many post-glacial reef growth studies have been conducted in the Ryukyu Islands over the past three decades using drilling and by observing excavated trenches (e.g., Konishi et al., 1978; Takahashi et al., 1988; Kan and Hori, 1993; Kan et al., 1991; 1995; 1997; Webster et al., 1998; Ota et al., 2000; Yamano et al., 2001b; Kan and Kawana, 2006; Hongo and Kayanne, 2009; Hamanaka et al., 2012). However, there are few studies focused on how Holocene climate changes, such as millennial-scale climate change, have affected reef growth (Webster et al., 1998; Abram et al., 2001; Hamanaka et al., 2012).

High-latitude reefs in the Northwest Pacific typically have no lagoons and have relatively narrow reef flats with shallow reef slopes (Kan et al., 1995). These characteristics are common north of the Tokara strait (around N29°-N30°). Reef flats gradually narrow northward (Hori, 1977), and their lateral extent becomes restricted to small areas such as embayments. To understand the relationship

between the growth process and climate change during the Holocene, this area may provide new insights about the future poleward expansion of reef growth.

To date, a few studies have used geological and paleobiological data from uplifted fossil reefs, such as those near the Huon Peninsula, Papua New Guinea (Pandolfi et al., 2006), Kikai Island in the central Ryukyus (Webster et al., 1998; Abram et al., 2001), to examine how Holocene climate change influenced coral reef growth and whether coral reefs grew continuously before human impact. A well-developed Holocene fossil reef on the Huon Peninsula has provided data on reef growth that was interrupted by natural phenomena before the impact of humans; these particular data were obtained from high-resolution, quantitative geologic measurements of sea cliffs (Pandolfi et al., 2006). Kikai Island also provided a good location for studying the relationship between coral diversity and sea surface temperature (SST) through a detailed survey of paleodiversity in the reefs combined with paleo-SST data reconstructed from fossil corals (Webster et al., 1998; Abram et al., 2001). These studies provided important insights for predicting the impacts of climate changes on future coral reefs. I believe that the relationship between the Holocene millennial-scale climate variability and coral reef growth will also provide insights that are important for assessing future coral reef formation.

The uplifted Holocene reefs are developed in Kodakara Island as well as Huon Peninsula and Kikai Island, where paleo-reef morphology such as spur and groove system is well-preserved (Nakata et al., 1978; Koba et al., 1979). Therefore, Kodakara Island is a significantly valuable field in the world to study detailed geologic, geomorphologic and paleo-ecologic features of the Holocene coral reef on land. Moreover, around the Kodakara Island such as Tokara Islands, where is yet not study area for the anatomy and the growth process of the coral reefs in geographically, thus, the area is necessary to study for considering the Holocene coral reef formation variability in spatial and temporal. Hence, according to define the formation process of the raised reefs on Kodakara Island in detail, which not only contribute to advance for the reef formation process in the Ryukyu Islands, but also may be possible to demonstrate the relationship between the coral reef growth and the millennial-scale global climate change such as Kuroshio Current variability,

because the geographic, geomorphologic and geologic advantages of Kodakara Island.

Based on the above, it planned and carried out that the detailed geologic and geomorphologic research for defining the formation of the raised reefs and their correlation with millennial-scale global climate change. The three trenches resulting from road construction have cut into middle-to-late Holocene reef flats and spurs perpendicular to the coast, and both the lateral and vertical accretion sequences can be continuously identified. The trench walls provide a rare opportunity for studying continuous reef anatomy, which is difficult to detect in cores, and to confirm the existence of three sedimentological boundaries within the middle-to-late Holocene reef terrace rock. Moreover, drilling operations performed on Kodakara Island to understand the style of post-glacial reef growth at high latitudes. Herein, I present the detailed morphology and anatomy of the reef and its growth history based on accelerator mass spectrometry (AMS) radiocarbon dating, and I assess how these aspects correlate to millennial-scale climate change.

In this thesis show the first evidence for dynamic correlation between the climate, sea-level change and the reef growth during the Holocene revealed by such high-resolution geological evidences, and detailed growth history of the Holocene raised coral reef terraces of Kodakara Island, which are compiled from my published works (Hamanaka et al., 2008; 2009; 2012 and submitted) and unpublished data set.

# Chapter 2

# Setting

## 2.1 Geographical setting of Kodakara Island

Kodakara Island (29°13'N 129°19'E) is located near the Tokara Strait, an area greatly influenced by the Kuroshio Current (Fig. 2.1). Currently, coral reefs and communities grow in the pathway of the Kuroshio Current and its branches in the Northwest Pacific (Veron and Minchin, 1992). The Kuroshio Current originates in the North Equatorial Current and carries warm, salty water from the western tropical Pacific Ocean along the edge of the continental shelf above the Okinawa Trough northward through the Tokara Strait to the Northwest Pacific (Fig. 2.1). In the Northwest Pacific around Japan, the lower sea surface temperature (SST) limit for reef growth is typically 18°C (Veron and Minchin, 1992), except in cases of short-term or localized chilling. This low temperature is found near Tane Island (30°45'N) (Fig. 2.1). Coral reefs are replaced with non-reefal coral communities in locations where the SST regularly falls below 18°C (Veron and Minchin, 1992). The commonly accepted global geographic distribution of reefs is restricted to latitudes between approximately 31°40'S (Lord Howe Island) and 32°50'N (Bermuda), where the mean SST in winter is generally above 18°C (e.g., Wells, 1957). However, the faviid coral reef on Iki Island (33°48'N), Japan, is located at a higher latitude in which the lowest average winter SST is 13.3°C (Yamano et al., 2001a). Although there are no SST records for the waters around Kodakara Island, the SST here likely does not regularly fall below 18°C because the average SSTs for the coldest

month at nearby Amami and Tane Islands are 20.7°C and 19.3°C, respectively (Veron and Minchin, 1992) (Fig. 2.1).

## 2.2 Geology and Geomorphology

Kodakara Island, which has no rivers, is characterized by a central hilly part surrounded by uplifted Holocene coral reef terraces (Figs. 2.2 and 2.3). The highest point, at ~102 m above sea level (Figs. 2.2 and 2.3), is assumed to be a Pleistocene marine terrace because of its relatively flat top (Fig. 2.4). The hilly area consists of Tertiary tuff breccia topped by a Ryukyu group consist of Pleistocene reefal sediments (Fig. 2.5a, b and c). The Tertiary tuff is basement rock for Quaternary sediments (Figs. 2.5a and d). Three Holocene coral reef terraces (Terraces I, II, and III) are approximately 9 m, 2 m, and 1 m above mean sea level (AMSL), respectively (Fig. 2.3, 2.4, 2.5e and f) (Hamanaka et al., 2008; 2009).

The morphological features and $^{14}C$ dating of the surface corals indicate that the terraces developed as a result of a coseismic uplift at approximately 2.6 ka (I/II) and 1.5 ka (II/III) (Nakata et al., 1978; Koba et al., 1979); I calibrated these dates to calendar years using the CALIB 4.3 program with a 400-yr surface ocean reservoir correction (Stuiver and Reimer, 1993). The date for the latest event is unknown.

The Holocene reefs are divided by a low scarp, which is regarded as a normal fault or slumping morphology (Hamanaka et al., 2009). The low scarp crosses the southern part of the island in a WNW-ESE direction (Fig. 2.3). Terraces I and II were clearly displaced with the low scarp. However, the displacement is unclear on Terrace III because it is penetrated by numerous complicated grooves around the low scarp. The amount of vertical displacement observed for the well-flattened Terrace II on average is probably 0.7 m, although it reached up to 1.5 m at Terrace I (Hamanaka et al., 2009).

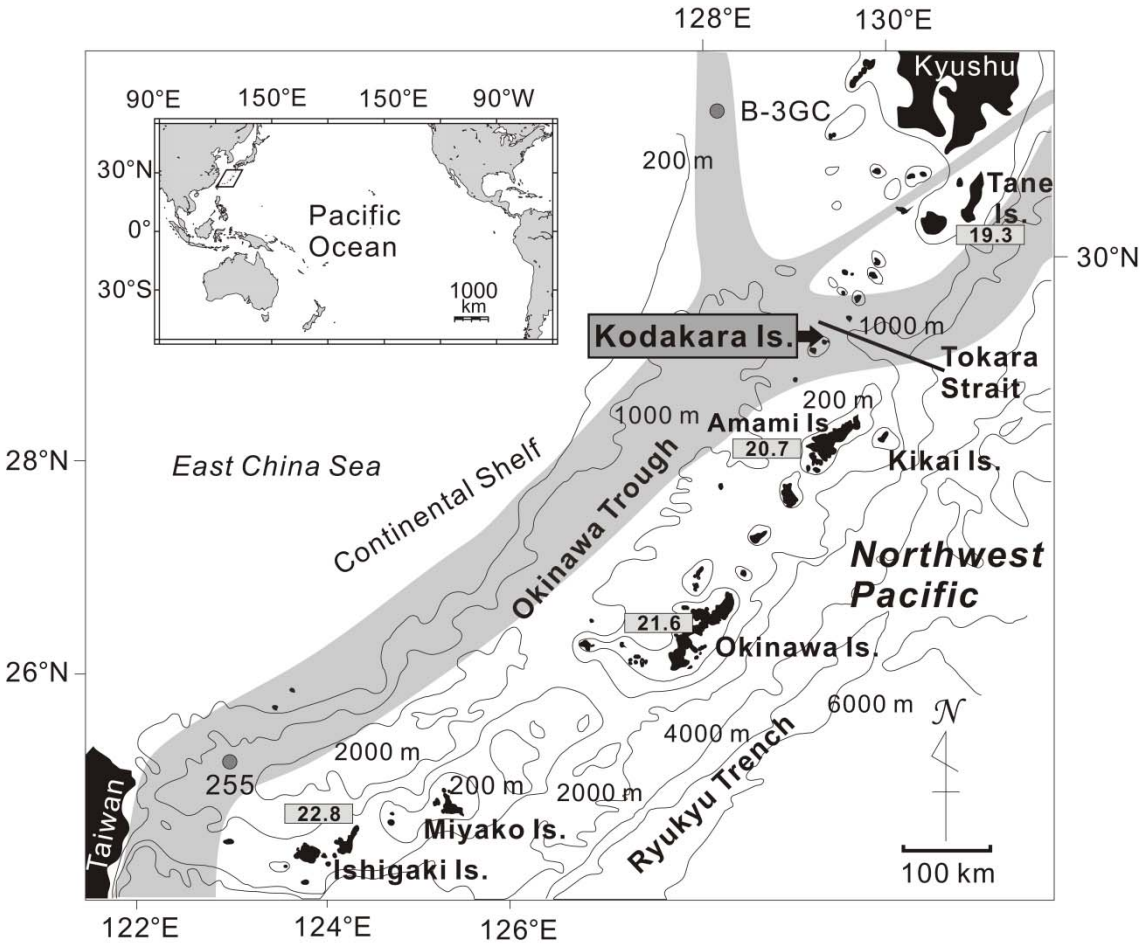


Fig. 2.1 A map of the study area. The Kuroshio Current is shaded. The averages of the coldest-month SSTs from some of the islands (Veron and Minchin, 1992) are shown in rectangles. The two circles with codes (255 and B-3GC) show the marine sediment core sites (left) (Jian et al., 2000).

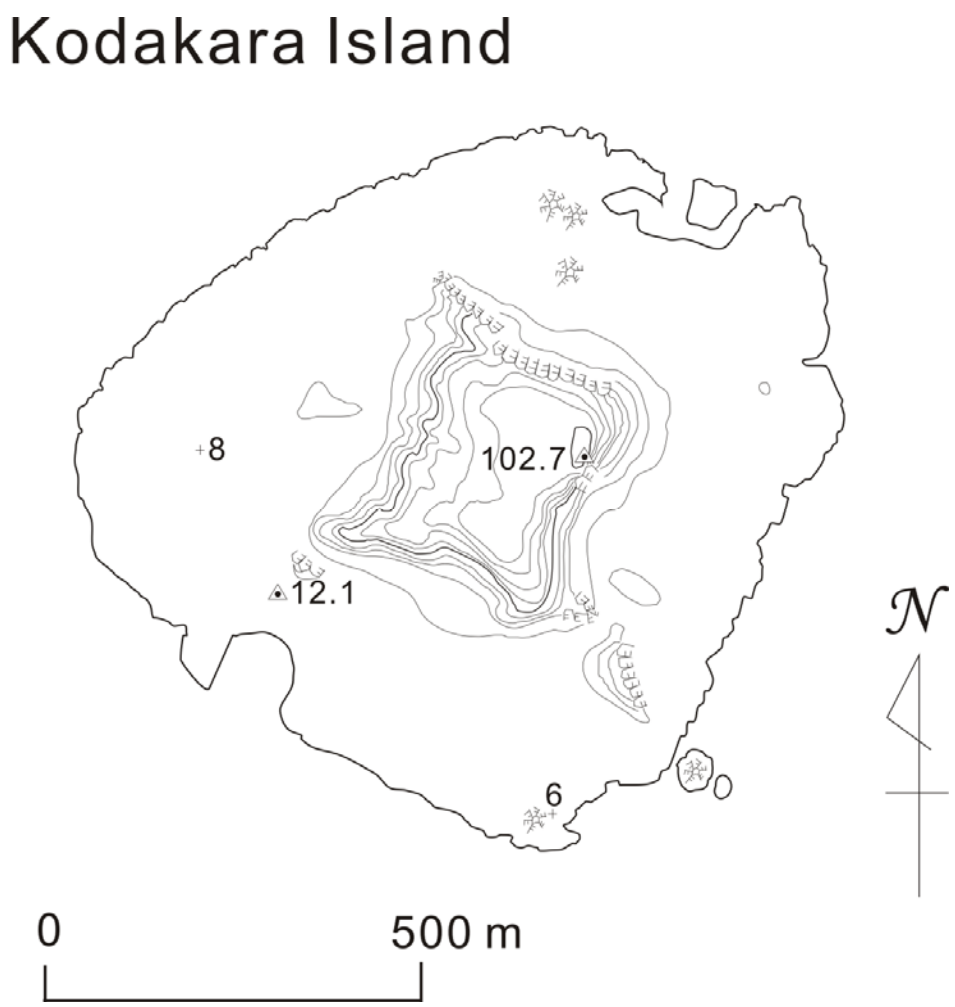


Fig. 2.2 A contour map of Kodakara Island based on 1:25000 map from the Geospatial Information Authority of Japan. The contour line interval is 10 m.

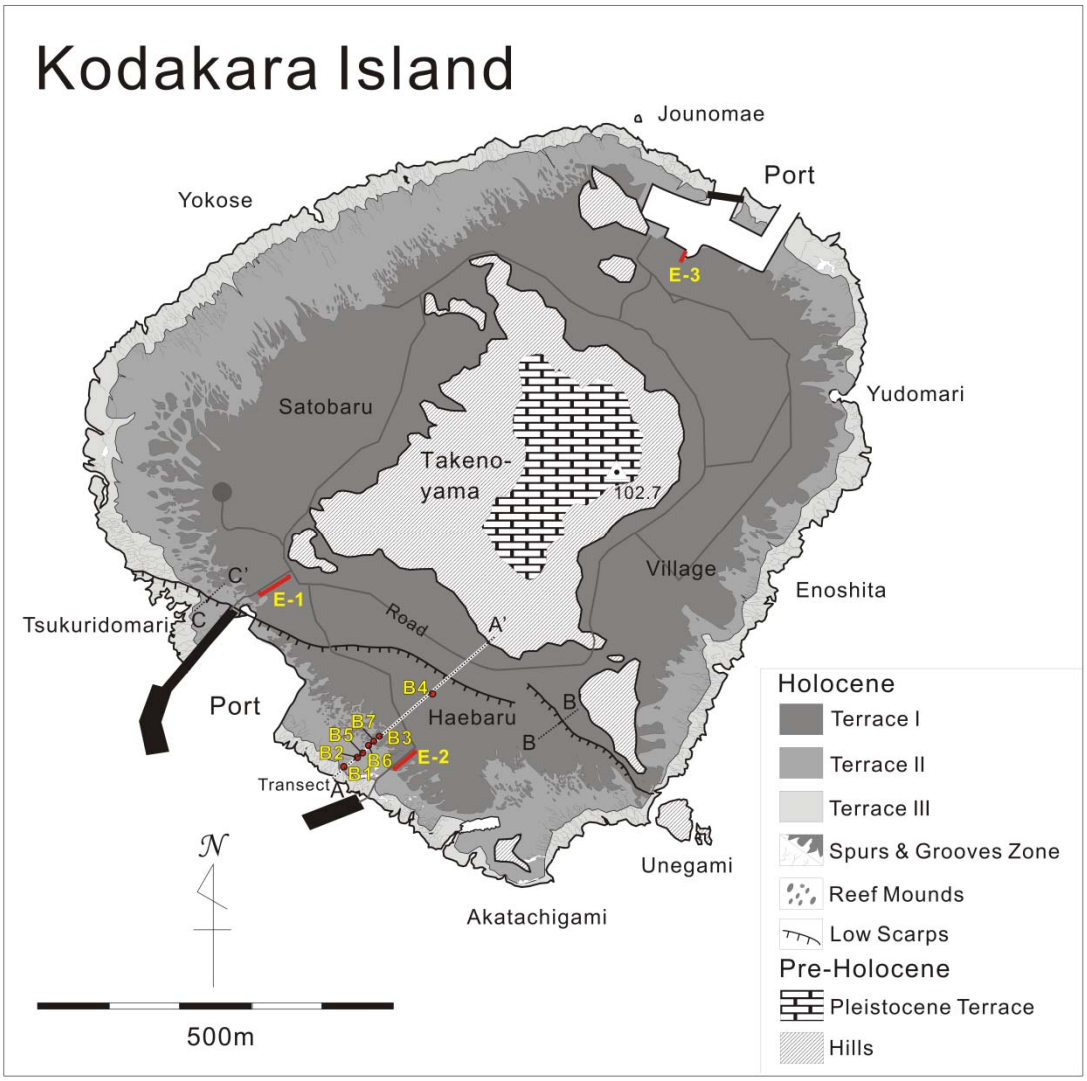


Fig. 2.3 A geomorphological map of Kodakara Island. The locations of the three excavated trench sites (E-1 to E-3, Hamanaka et al, 2012), the cores (B1 through B7) and the cross-sections around low-scarp (A-A', B-B' and C-C') are shown.

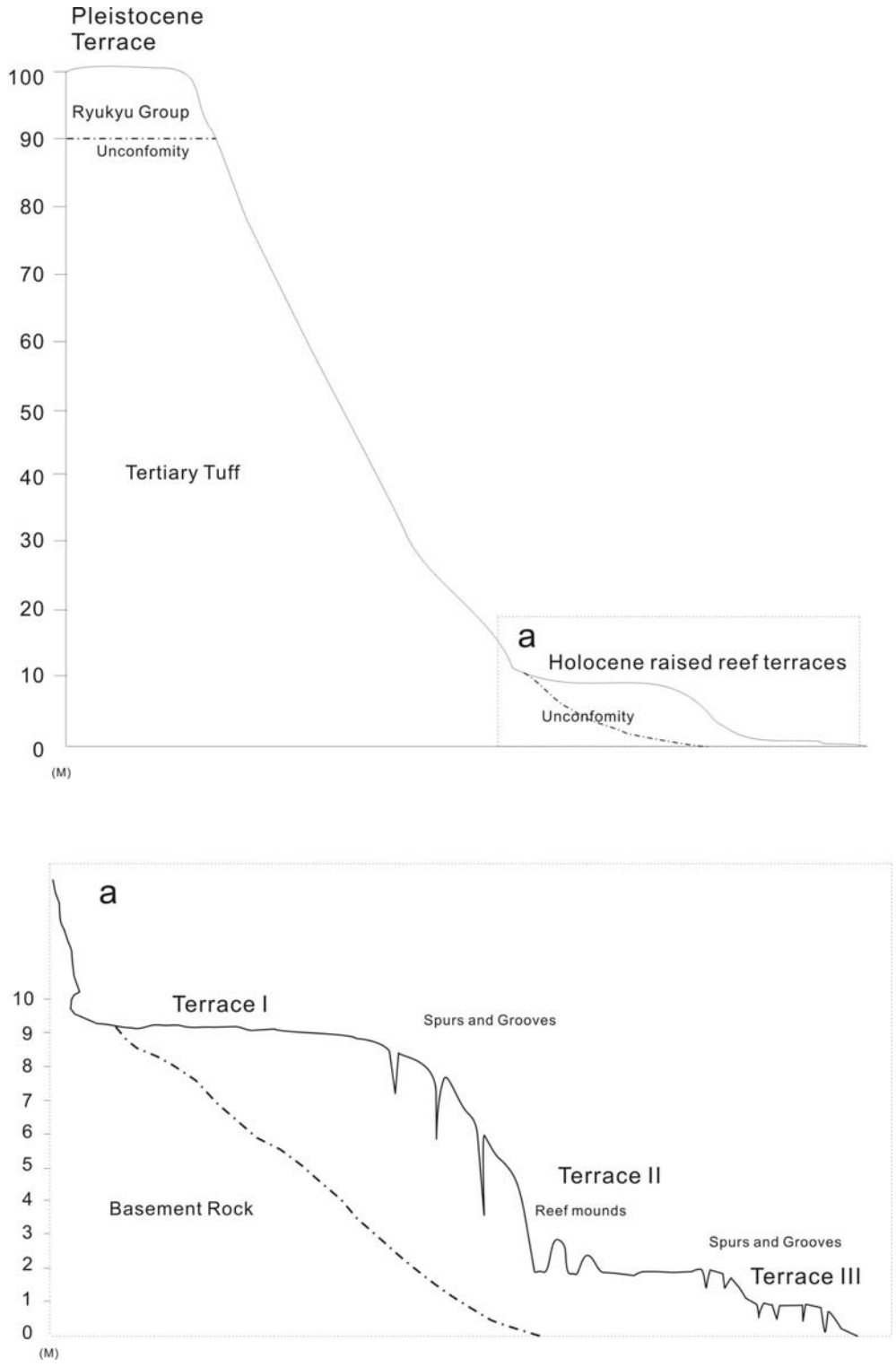


Fig. 2.4 Schematic diagram for general geology and geomorphology of Kodakara Island. The Holocene raised reef terraces are extended below (a).

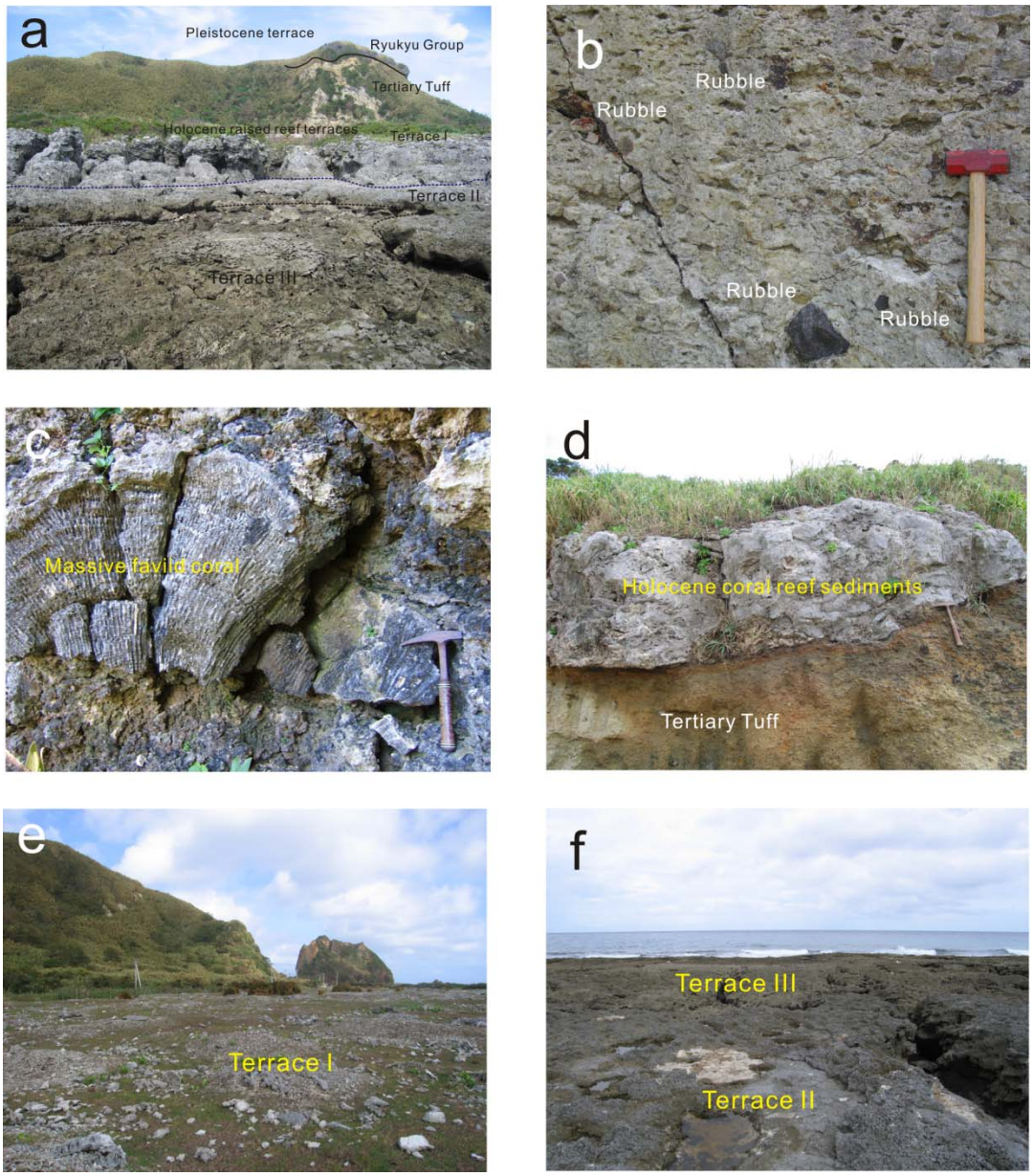


Fig. 2.5　Photos of characters of geology and geomorphology of Kodakara Island.

# Chapter 3

# Materials and Methods

## 3.1 Field survey

### 3.1.1 Classification of Holocene raised reef terraces

Firstly, the Holocene terraces were classified in three dimensional vision using a stereoscope and aerial photographs of Kodalara Island. Based on the above, the predicted geomorphological map on Kodakara Island was made. After them, it was carried out that the detailed field survey as observation and measurement, morphologic and geologic, on the Kodakara Island for mainly Holocene terraces in one month. Consequently, the terraces are divided into three, here named upper to lower, Terrace I (TI), Terrace II (TII), Terrace III (TIII), respectively (Fig. 2.3). TI~TIII are equivalent with Haebaru surface, Tsukuridomai surface, High-tide platform, respectively, labeled by Nakata et al. (1978) and Koba et al. (1979).

### 3.1.2 Excavated trench walls

I found excavated trench walls at sites E-1, E-2, and E-3 within TI (Fig. 2.1), which is composed of reef rock that formed before ~2.6 ka (see Setting). The trench

walls, which are up to ~8 m deep and 35 m long across the southern and northern parts of TI (see Fig. 2.3), show a continuous section of reef development that corresponds with the paleo upper reef zone (0-8 m). To delineate the excavation profiles accurately, I performed measurements using tape, a 5-m pole, and a level measure. Altitude data were obtained from the north and south ports and were revised by referencing tidal tables. To delineate the reef anatomy, measurements were performed from the terrace surface to the bottom of the excavations at 0.5-m intervals along the full sections. To define the centimeter-scale features, photographs were taken at 1-m intervals and were printed so that observations on the full sections could be sketched later. After delineating the trench walls, I investigated the coral characteristics in an effort to understand the vertical and lateral coral faunal variation. All the corals within the trench walls were completely documented by sketches on the printed photographs, and characteristics such as the genera were identified (Figs. 3.1, 3.2 and 3.3).

### 3.1.3 Drilling operations

I selected the coring points based on whether drilling was physically possible and whether the terraces were well developed. Consequently, I placed the drilling transects at Haeberu in the southern part of the island, where TI extends the furthest without artificial alterations, and seven drilling sites along the line transect were used (B1 to 7; Fig. 2.3). All drilling operations were permitted by the Toshima village office, Kagoshima Prefecture, Japan.

For drilling the B1-B4 sites (Fig. 2.3), my team used “Geoact Oil-fluid Drilling – KAN Type”, which was developed to perform underwater drilling operations (Kan et al., 1998). The present study represents the first attempt to use this device for drilling into raised reef terraces. The drilling operations consisted of the following steps (Fig. 3.4a, 3.5a and b): (1) construction of a stabilized turret for drilling on a horizontal square base composed of tube pipes with cramps; (2) secure placement of the drilling mast in the center of the turret; and (3) drilling using a double-core tube with sea water supplied by a circulating pump and water pipe. Whenever the

drilling site was far from the sea, the water pipe was either extended or a 500-liter poly tank filled with sea water was brought to the site. All drills were metal edged with buried tungsten tips.

For drilling the B5-B7 sites (Fig. 2.3), my team used a "Geo-act handy-boring machine" with a double-core tube, circulation pump, water tube, and sea water (Figs. 3.4b and 3.5c). A turret was not necessary for this machine. However, my team used concrete blocks as a vertical stabilizer.

## 3.2 Identification of corals

The coral genera identification is based on Veron and Pichon (1976; 1980; 1982), Veron et al. (1977), Veron and Wallace (1984) and Nishihira and Veron (1995). The morphology of the coral colonies also referenced Veron and Wallace (1984). In particular, the acroporiid corals at E-1 to E-3 are almost exclusively characterized by tabular or thick-plate/encrusting (see Fig. 4.13a), which is a typical characteristic of upper-reef zones in the Ryukyu Islands (e.g., Iryu et al., 1995; Sagawa et al., 2001). The tabular acroporiid corals are equivalent to those of the *Acropora hyacinthus* group (Veron and Wallace, 1984), which are presently distributed in the upper shallow reef slope of the Ryukyu Islands (e.g., Iryu et al., 1995; Humblet et al., 2009). The thick-plate/encrusting acroporiid corals are divided into two types: thick encrusting corymbose plate and thick encrusting plate. The former type is equivalent to the *Acropora humilis* group, and the latter is equivalent to the *A. (Isopora) palifera* group (see Fig. 4.13b and c) (Veron and Wallace, 1984). Both groups are also distributed in the shallow upper reef slope of the Ryukyu Islands (e.g., Iryu et al., 1995; Sagawa et al., 2001). In the trench walls, the corals that had developed in situ could be easily identified because their complete shapes, and growth forms were readily observable. I collected fossil corals that appeared to be autochthonous according to their growth forms, growth directions, and colony shapes for AMS radiocarbon dating. When characterizing the paleocoral diversity, I counted all the exposed in situ corals as genera and calculated the coral composition percentages, except for those in the lower seaward wall at E-3, which is always directly affected

by the wave energy.

## 3.3 AMS Radiocarbon Dating

I collected in situ fossil corals from terrace surfaces, excavations and cores for AMS radiocarbon dating. All the samples were cut into tips approximately 5 mm wide and 3 mm thick and were entirely cut down of their skeletal air space, such as coral calices. I observed the tips under a microscope to determine whether diagenesis had occurred and to carefully select the cleanest tips possible (there were at least five tips per sample). The tips were dipped into 4-N HCl for 60 seconds, rinsed in Milli-Q water in an ultrasonic bath, and dried in a 40 °C oven overnight. An X-ray diffraction (XRD) analysis before the dating confirmed that coral aragonite was well preserved in all the samples. The XRD was performed for total 125 samples at XRD laboratory, Department of Earth Sciences, Okayama University. The samples from excavated trench walls for the AMS dating was performed by the Beta Analytic Co., Miami, FL, USA. The samples from terraces surface are then converted into $CO_2$ by acidification with $H_3PO_4$ and finally into graphite by using $H_2$ as a reducing agent and Fe powder as a catalyst (Yokoyama et al., 2007). The $^{14}C/^{13}C$ and $^{14}C/^{12}C$ ratios of the graphite were measured using tandem AMS at the Micro Analysis Laboratory Tandem Accelerator, University of Tokyo (Matsuzaki et al., 2004). These samples were also dated in part at Beta analytic Co., FL, USA. All of the $^{14}C$ ages were calibrated to calendar years using the CALIB version 6.0 software (available online at http://calib.qub.ac.uKuroshio Currentalib) (Stuiver et al., 1998) based on a comparison to MARINE09 data (Hughen et al., 2004; Reimer et al., 2009). The ΔR value was assigned using the marine reservoir correction database, which gave a value of

$\Delta R = 29 \pm 18$ years.

This ΔR value was well suited for calibrating the $^{14}C$ age for Kodakara Islandbecause it was determined from five samples of pre-atomic molluscan shells from the Amami and Okinawa Islands (Yoneda et al., 2007), which are located in the Central Ryukyus near Kodakara Island (Hamanaka et al., 2012) (Fig. 2.1).


Fig. 3.1 A figure of sketched and counted corals at E-1 site. The outlines of corals are precisely sketched. All corals at trench sites were delineated by same method (see also Appendix A).


Fig. 3.2　A figure of sketched and counted corals at E-2 site.


Fig. 3.3　A figure of sketched and counted corals at E-3 site.


Fig. 3.4 Photos of drilling operations. (a) Drilling at B4 site (reef flat) using "Geoact Oil-fluid Drilling – KAN Type". (b) Drilling at B6 site (reef mound) using "Geo-act handy-boring machine".

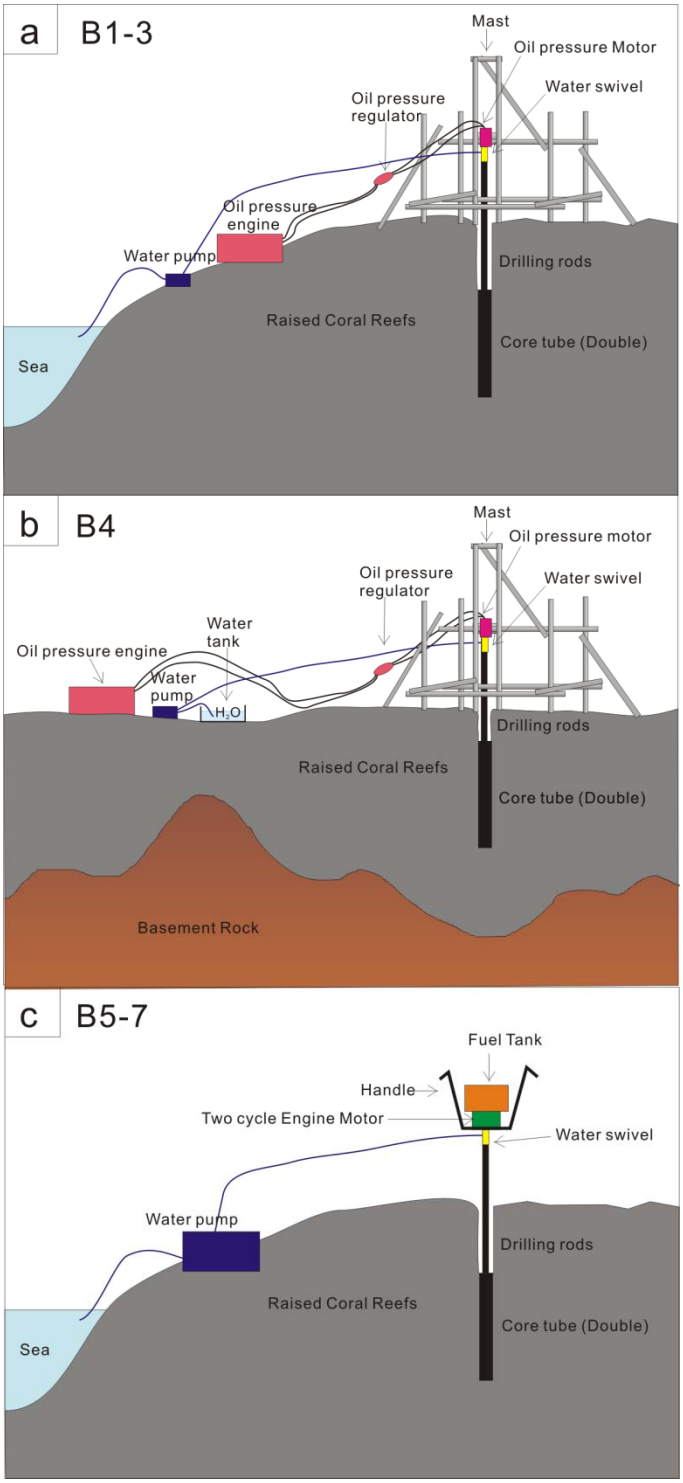


Fig. 3.5 Schematic diagrams show the drilling operations. (a) drilling at B1-3 sites. (b) Drilling at B4 site. (c) Drilling at B5-7 sites.

# Chapter 4

# Results

## 4.1 Characteristics of the Holocene raised reef terraces

### 4.1.1 Terrace I

Terrace I (TI), the uppermost Holocene terrace, is 9.7 m in altitude and up to 250 m in width (Figs. 2.3 and 4.1). TI corresponds to the "Haebaru Surface" of Nakata et al. (1978). The surface of TI represents a narrow reef flat without a lagoon or a reef crest (Fig. 4.1A), which is typical of high-latitude reefs in the Ryukyu Islands (Kan et al., 1995). The reef slope is characterized by a well-preserved spur and groove system and reef mounds (Figs. 4.1C and D). The landward margin of TI generally consists of basement rocks that were eroded or overlain by Holocene reef sediments (Hamanaka et al., 2008).

The surface of TI along the transect studied primarily consists of thick-plate/encrusting *Acropora* spp. (Fig. 4.2B), which belong to the *Acropora humilis* and *Acropora palifera* groups. Massive faviid corals and *Porites* spp. are

occasionally observed on the TI surface (Fig. 4.2A), whereas branching corals were not found. The groove walls offer the opportunity to examine in detail the nature of the reef slope. The upper portion of the slope primarily consists of thick-plate/encrusting *Acropora* spp. and is locally characterized by stacked tabular *Acropora* spp. (Fig. 4.2C), which probably belong to the *Acropora hyacinthus* group (Veron and Wallace, 1984). The lower part of the slope primarily consists of massive faviid corals and *Porites* spp. (Fig. 4.2D). A similar vertical faunal shift from massive corals to encrusting and tabular acroporiid corals was also reported from the Holocene raised reef terraces of Kikai Island (Webster et al., 1998).

The results of AMS radiocarbon dating of in situ corals indicate that TI was still forming ~2443 cal yr BP (Hamanaka et al., submitted)(see Table 4.2).

### 4.1.2 Terrace II

Terrace II (TII) is 2.4 m high and reaches 200 m in width on the northwest coast of the island (Figs. 2.3 and 4.1). TII corresponds to the "Tsukuridomari Surface" of Nakata et al. (1978). Like TI, the surface of TII is flat, and the seaward slope is characterized by a well-preserved spur and groove system (Figs. 4.1D and E). The contact between TII and the seaward slope of TI is erosive. In particular, reef mounds of Terrace I are eroded laterally and vertically. The area between the mounds is partly covered by in situ corals. The spur and groove system on the seaward side of TII is well developed, similar to TI, but the width of the grooves is narrower (Fig. 4.1E).

The landward part of TII primarily consists of eroded massive faviid corals and Porites spp. (Figs. 4.2D and E), which are equivalent to the TI reef slope sediment. The seaward part of the TII surface primarily consists of thick-plate/encrusting *Acropora* spp. (Fig. 4.2F). Encrusting faviid corals were observed across the entire surface of TII. Beach rocks are found in the southern part of Kodakara Island, from the port to Tsukuridomari, and they cover groove bottoms at the landward margin

of TII (Fig. 4.3).

The results of AMS radiocarbon dating of in situ corals indicate that TII was formed between 2316 and 967 cal yr BP (Hamanaka et al., submitted) (Table 4.2).

### 4.1.3 Terrace III

Terrace III (TIII) is the lowest Holocene terrace, with an altitude of 1.2 m and up to 50 m in width, and does not continuously enclose the Island (Figs. 2.3 and 4.1). TIII corresponds to the "Intertidal platform" and "High-tide platform" of Nakata et al. (1978) and Koba et al. (1979), respectively. TIII is separated from TII by a low scarp or slope corresponding to the spur and groove system of TII (Fig. 4.1E). TIII is generally submerged by large waves and during high tides or typhoons. The grooves penetrating the surface of TIII extend in TII, forming a grid-like pattern of flattened reef mounds (Fig. 4.1E). The width of these grooves is usually less than 2 m, and their depth gradually increases seaward. The spur and groove system, reef mounds, and the reef slope of TIII extend below sea level (Fig. 4.1F).

The surface of TIII primarily consists of in situ thick-plate/encrusting tabular *Acropora* spp., although branching *Pocillopora* spp. are also common. Therefore, TIII probably has a depositional origin but has been partly eroded.

The results of AMS radiocarbon dating of the in situ corals indicate that the surface of TIII formed between 440 cal yr BP and modern times (Hamanaka et al., submitted) (Table 4.2).

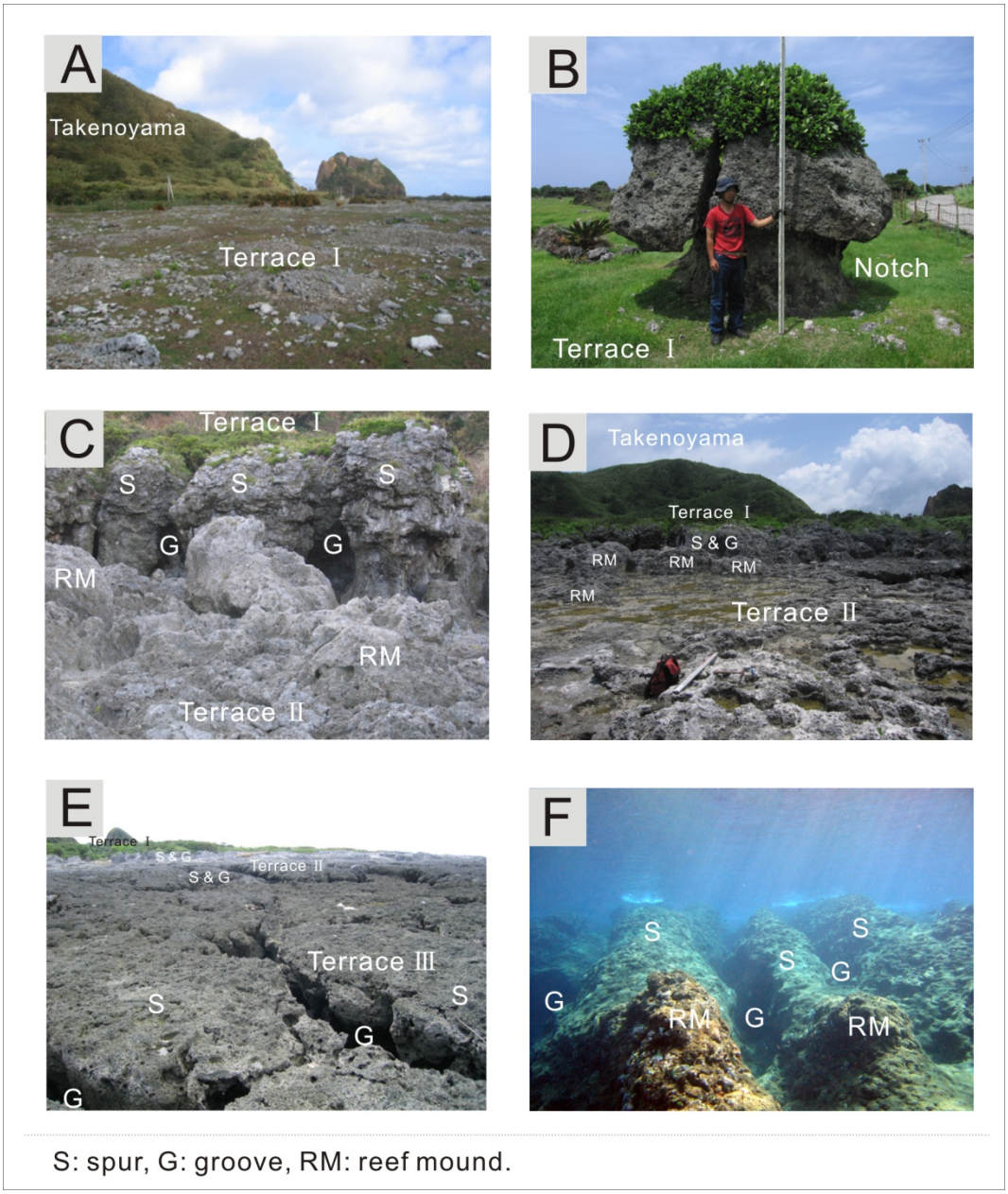


Fig. 4.1 Photos showing the detailed morphology on Holocene raised coral reef terraces (Terrace I~III). A: Reef flat of Terrace I at Haebaru ranch. B: Raised notch on Terrace I at Haebaru. C: Raised reef slope morphology consists of spur and grooves system and reef mounds between Terrace I and II at Enoshita. D: Reef flat of Terrace II at Yokose. Spurs and Grooves and reef mounds of Terrace I are shown. The reef mounds gradually lower toward outer TII (Seaward). E: Well-developed Terrace III at Yokose. There are narrow, complexity grooves which look like set of reef mounds. F: Modern reef slope morphology off drilling sites.

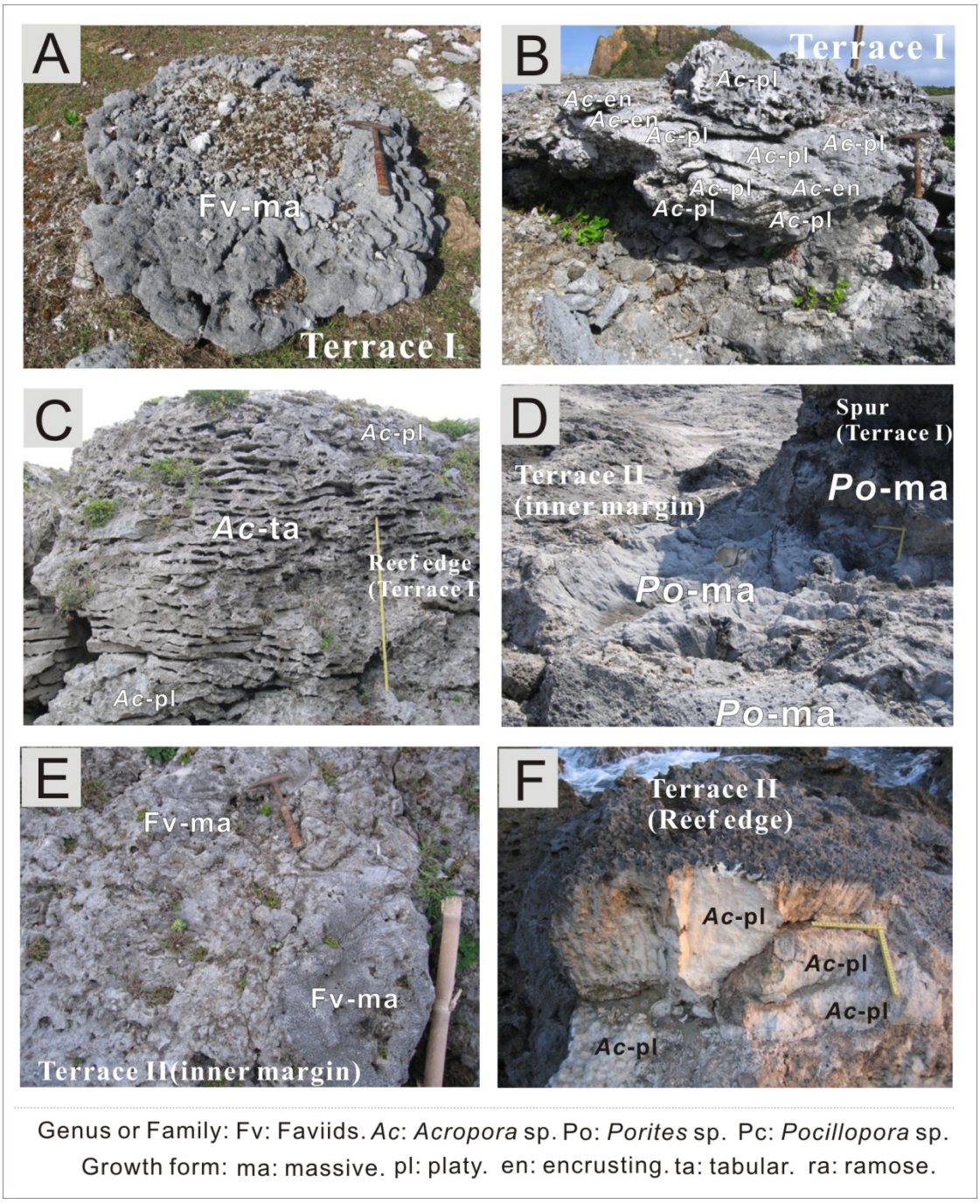


Fig. 4.2 Photos showing detailed lithology of the terrace surface. A: a massive Faviid coral formed like microatoll on reef flat of TI at Haebaru. B: accumulated platy and enclusting *Acropora*spp. on TI at Haebaru. It mainly consists of reef flat to spurs of the terraces. C: markedly accumulated tabular *Acropora* spp. on reef edge of TI at Enoshita. Scale bar is 1m. D: eroded huge massive Porites on inner margin of TII at near Akatachigami. Scale bar is 20×20cm E: massive or hemispherical Faviids on inner part of TII at Jounomae. F: accumulated thick-plate *Acropora* spp. on reef edge of TII at near Akatachigami. Scale bar is 20×20cm.

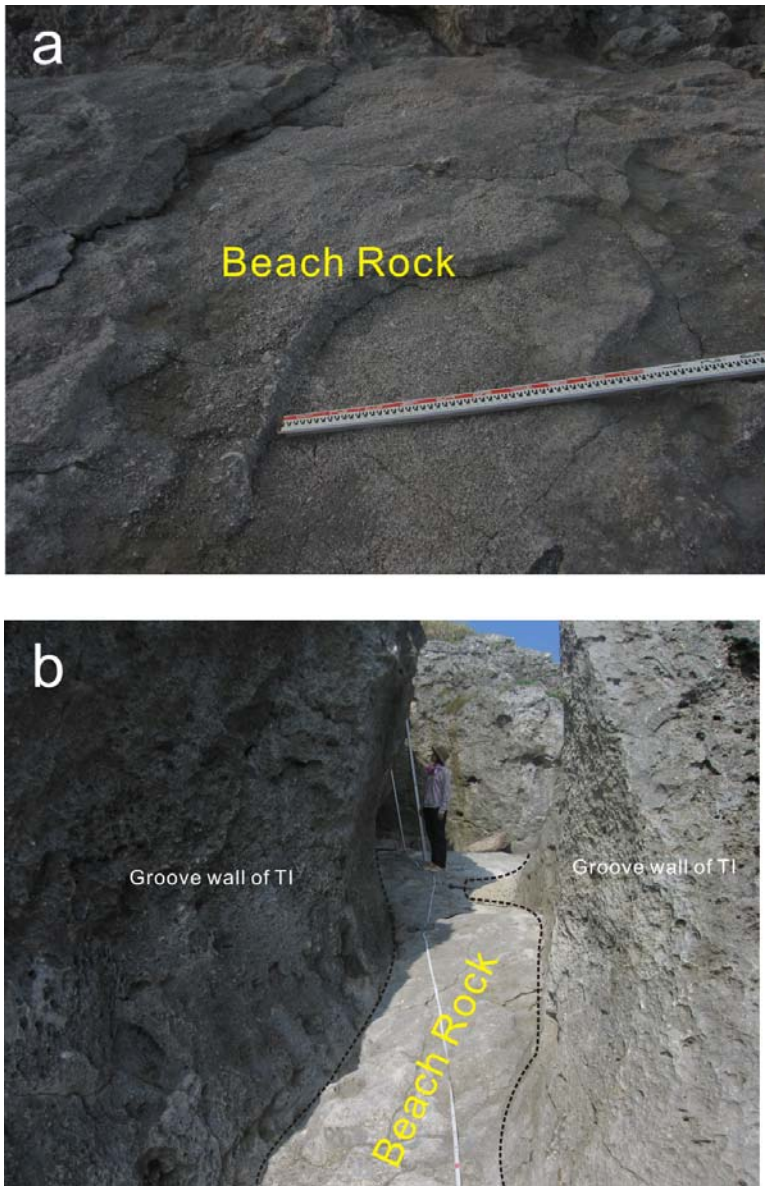


Fig. 4.3 Observed beach-rocks at near south port (a) and Tsukuridomari (b). The beach-rocks distribute intermittent on landward margin of TII at southern part of Kodakara Island, and has usually buried groove bottom.

## 4.2 Characteristics of the low-scarp morphology

### 4.2.1 Morphological characters

Koba et al. (1979) described that a fault exist at 100 m south from Okinose which extends N80W in direction and displaced of Tsukuridomari surface (TII in this study). In contrasting to Koba et al.(1979), Research group for active fault of Japan (1991) showed that a low-scarp exists at southern part of Kodakara Island which takes on curve to south and only displaced of Haebaru Surface (TI in this study). Thus, the both descriptions are different that the location of low-scarp and which terrace is displaced. Based on the above, I carried out to define that the locality with length and amount of displacement using 1:1000 map of Kodakara Island with GPS data and measurement.

The low-scarp extends 800 m in length at southern part of Kodakara Island which displaced TI, TII and TIII, respectively, and fallen southern part along the scarp (Hamanaka et al., 2009) (Fig. 2.3). The low-scarp is divided into two segments around Haebaru (Fig. 2.3). I set the three transects (A-A', B-B' and C-C') where displacement is clear, and measured the cross-section and amount of the displacements (Figs. 2.3 and 4.4) The amount of displacement is estimated to 1.5-0.7m which differs by the places (Fig. 4.4). The 1.5 m in maximum is observed at Haebaru on TI, whereas 0.7 m in minimum is observed at Tsukuridomari on TII (Fig. 4.4C). The low-scarp has usually associated with ground fissure (Figs. 4.4 and 4.5) which distributes intermittent. The width of the ground fissure is almost 0.5 m or below but reaches up to 1 m observed at Haebaru on TI (Fig. 4.5C). The ground fissure is almost buried by sands and gravels which is artificially on TI, although on TII is derived from waves (Fig. 4.5E). The surface of the low-scarp is partially smooth and it is observed that the surface was eroded like notch at Tsukuridomari on TII (Hamanaka et al., 2009) (Fig. 4.5E).

### 4.2.2 Altitude calibration based on vertical displacement along the low scarp

Hamanaka et al. (2009) suggested the amount of vertical displacement along the scarp is 0.7-1.5 m. I re-investigated this estimate and concluded that the displacement is probably 0.7 m. The 1.5 m value is a maximum and was only observed in TI, the surface of which is vertically irregular and partially collapsed. The displacement of the highest in situ corals at both the upper and lower sides observed at the transect location was 0.7 m (Fig. 4.4A). Moreover, the offset measured along the scarp on TII is also 0.7 m. Because all drilling and E-2 sites were located on the seaward side of the scarp, I calibrated the altitude of each core and terrace by adding 0.7 m (see Fig. 4.16 showing the calibrated topographic profile).

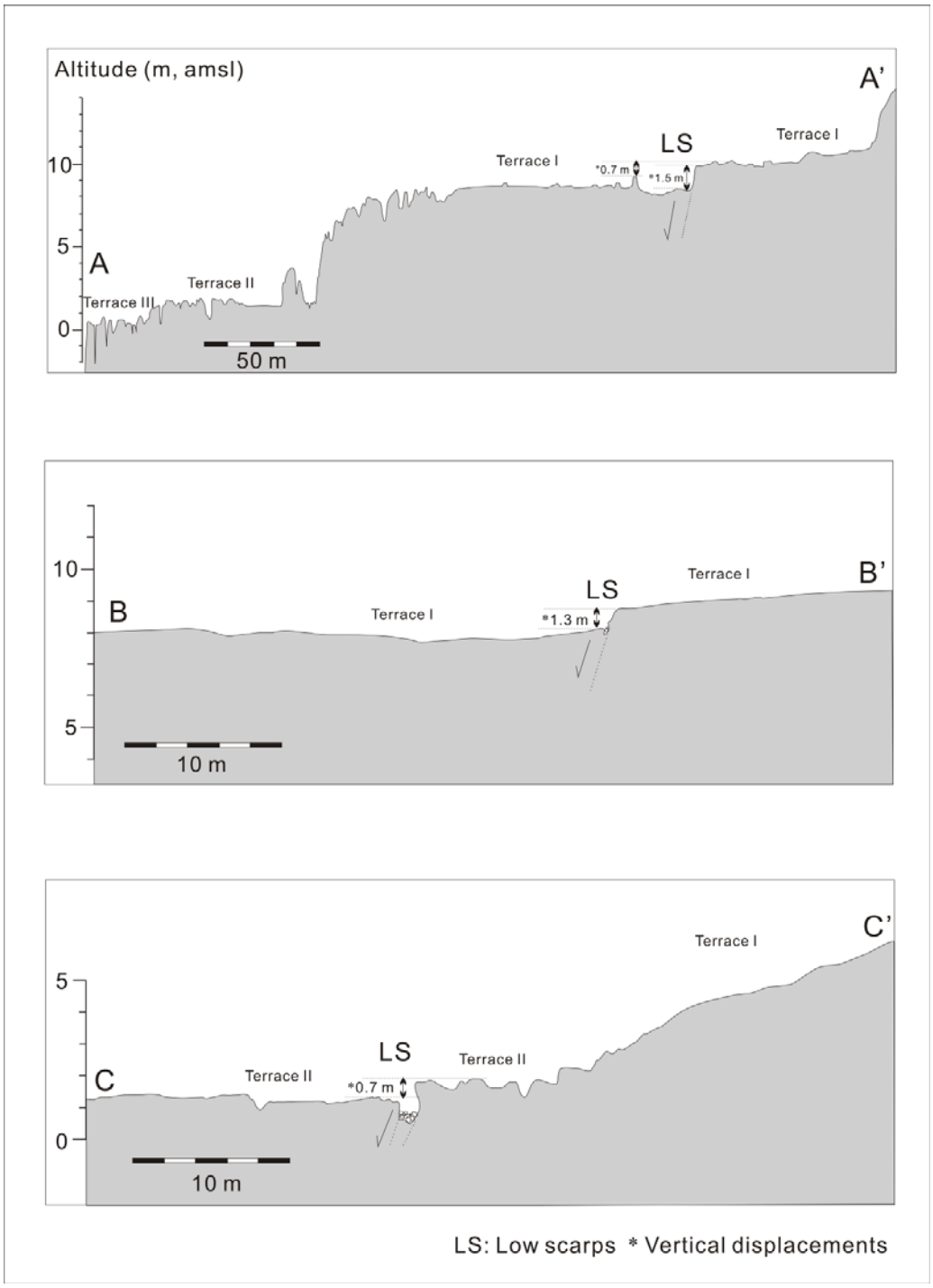


Fig. 4.4 Topographic profiles around the low scarps. Locations are shown in Fig. 2.3.

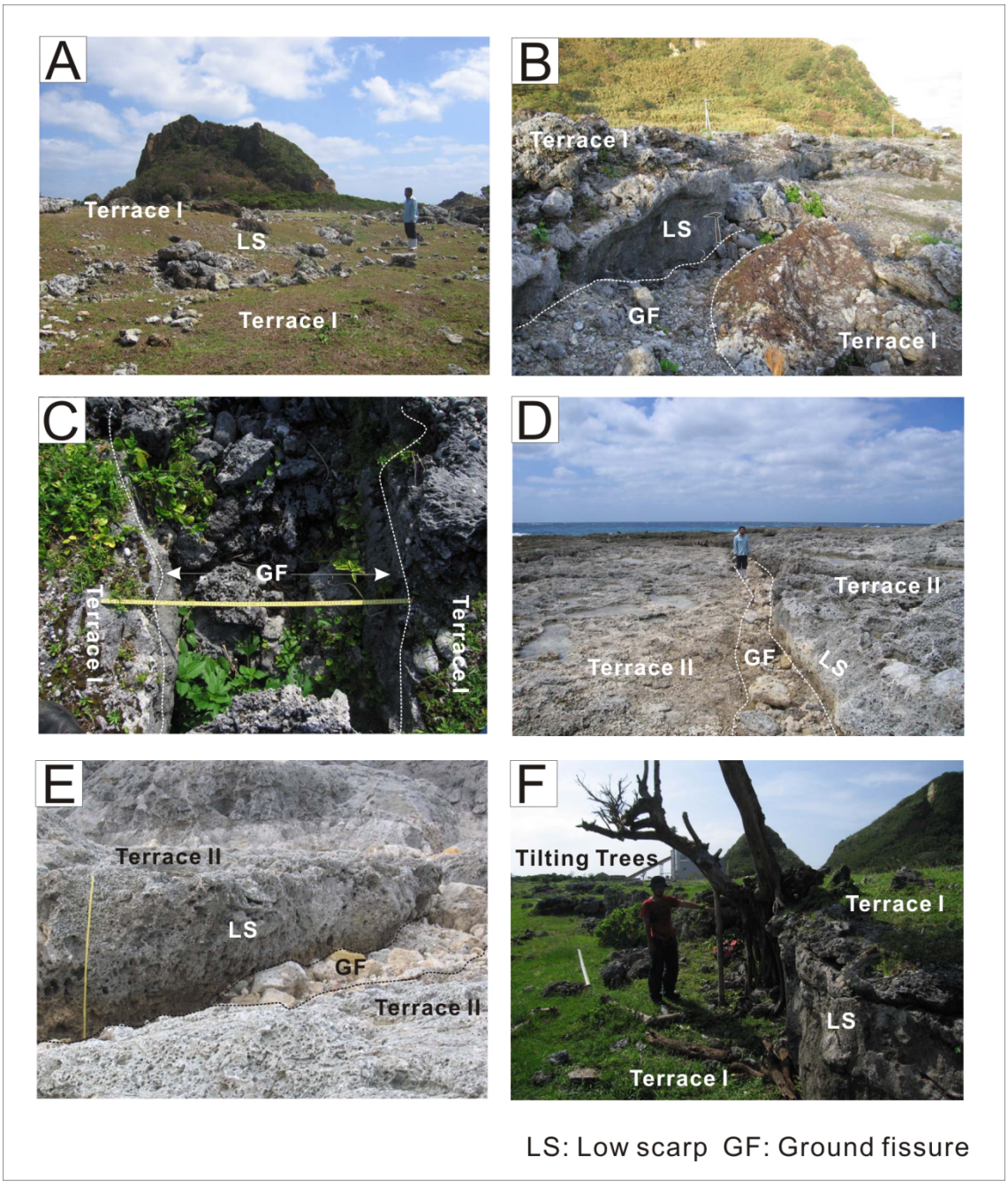


Fig. 4.5 Photos showing low scarps across raised coral reef terraces on Kodakara Island. A: Terrace I is clearly displaced in eastern Haebaru. B: Ground fissure (GF) is well developed along the scarp at Haebaru. Scale hammer is 30-cm long. C: Close-up of ground fissure at Haebaru. The width is around 90 cm, and has been filled in with gravel. Scale bar is 1-m long. D: Terrace II is displaced at Tsukuridomari. Ground fissure has been filled in with sand and gravel. Scale bar is 1-m long. E: Low scarp with leaning trees (*Ficus microcarpa*) in southwestern Haebaru, which imply recent scarp formation. The scarp surface is very smooth, which indicates it has been altered.

## 4.3 Characteristics of the Holocene raised reef from trenches

### 4.3.1 E-1 site

The trenches at E-1 are cut out of reef flats and a spur at the southwestern part of TI (Fig. 2.3). The trenches are up to 2-m deep and 35-m long (Fig. 4.6). The highest and lowest points are 8.5 m and 5.8 m AMSL, respectively. At E-1, the reef sediment is divided into four reef units by sharp boundaries (Figs. 4.6 and 4.7). I named these units (from lower to upper) Reef Unit 1 to Reef Unit 4 (RU1 to RU4), and they were confirmed to be of different in age by AMS dating results (Fig. 4.6 and Table 4.1).

RU1, the lowest unit, covers the basement rock, which is slightly exposed around the central part of E-1 (Fig. 4.6). RU1 is characterized by a brownish color because the matrix sediments and portions of the coral calices include brown mud that is derived from basement rock. RU1 has a mounded morphology similar to a reef crest, and it formed the basic morphology of the Holocene coral reef on Kodakara Island (Fig. 4.6). RU1 is mainly composed of tabular or thick-plate/encrusting *Acropora* spp. They constitute a framework with well-consolidated detrital reef materials that contains debris of marine organisms (Fig. 4.14), such as foraminifera, shells, mollusks, and that is associated with massive or encrusting faviid corals (*Goniastrea* spp., *Favites* spp., *Favia* spp., *Platygyra* spp.) and encrusting or columnar *Heliopora* spp. (Fig. 4.6 and 4.12A). Major changes are not observed in the vertical and lateral coral variation; however, dense accumulation of tabular *Acropora* spp. in the central part of E-1 is observed as minor changes (Fig. 4.12B).

RU2 covered RU1 with a sharp seaward boundary that consisted of a relatively white sediment composed of thick-plate and tabular *Acropora* spp. and massive or encrusting faviid corals in well-consolidated detrital reef materials; RU1 was similar, except for not containing brown mud from the basement rock. The boundary between RU1 and RU2 is recognized by a change in color, from brown to white, that formed an irregular line (Figs.4.6, 4.7a and 4.12A). Therefore, this boundary is

considered to result from sedimentary discontinuity rather than erosion, which indicates that the reef disturbance occurred between RU1 and RU2 formation. Landward, RU2 formed a reef mound morphology with thick-plate/encrusting and tabular *Acropora* spp. (Fig. 4.6). The seaward boundary is mainly occupied by thick-plate/encrusting acroporiid corals, with individual colony sizes over 1 m in diameter and 0.5 m thick and relative mere voids on the seaward side (Fig. 4.12A). The coral colonies tend to become gradually smaller toward the upper part (Fig. 4.12A), and detrital reef materials fill the spaces between the corals. Therefore, vertical colony size changes are observed at seaward side of the vertical and lateral coral variation within RU2, although characteristic lateral changes are not observed.

RU3 occurs above a sharp boundary with RU1 on the landward side. RU3 is composed of thick-plate/encrusting *Acropora* spp. and occasional massive *Favia* spp. (Fig. 4.6), with detrital reef materials as well as RU1 and RU2. The boundary is recognized as a nonlinear but smooth line compared with the boundary between RU1 and RU2. Therefore, this boundary may indicate that erosion occurred as a result of sea-level changes before RU3 formation. Major changes in the vertical and lateral coral variation are not observed.

RU4, the uppermost unit, fills morphological depressions between the reef mounds and lies on a significant linear salient of lower units that clearly indicates erosion (Figs.4.6, 4.7b~d and 4.12B). Therefore, this boundary indicates that the reef disturbance occurred from a sea-level change before RU4. RU4 is composed of a framework mainly consisting of tabular or thick-plate/encrusting *Acropora* spp. with detrital reef materials that is characterized by relatively high amounts of eroded branching coral debris (Fig. 4.6, 4.12B and 4.14c). The material was characterized by a relatively porous matrix. Massive or encrusting faviid corals (*Goniastrea* spp., *Favites* spp., *Favia* spp., *Platygyra* spp.) and encrusting or columnar *Heliopora* spp. (Fig. 4.6) are observed scattered through the acroporiid corals. Major changes in the vertical and lateral coral variation are not observed. RU4 created the flat reef morphology in Terrace I.

The coral content of RU1 is mainly *Acropora* spp. (70.3%), along with faviid corals (17.3%), *Pocillopora* spp. (2.6%), *Goniopora* spp. (2.6%), *Heliopora* spp. (6.7%), and unknown spp. (0.5%), see Fig. 4.15. The coral diversity is relatively high compared with the other reef units in E-1, although most units are occupied by both *Acropora* and faviid corals (87.6%). RU2, by contrast, is composed almost entirely of *Acropora* spp. (94.9%), and the fraction *of Acropora* spp. increases dramatically to 24.6%. However, the faviid coral fraction decreases to 12.2%, and no other corals are found, which is the main characteristic. The composition of RU3 changes to *Acropora* spp. (87.5%) and faviid corals (12.5%). Although *Acropora* decreases by 7.4% and faviid corals increase by 7.4%, there are no consistent changes in either the *Acropora* spp. or faviid corals. In RU4, the composition changes to *Acropora* spp. (95.8%), faviid corals (1.2%), *Pocillopora* spp. (1.8%), *Goniopora* spp. (0.6%), and *Heliopora* spp. (0.6%). In this change, the *Acropora* spp. content increases by 8.3%, that of faviid corals decreases by 11.3%, and the other corals recolonize slightly. Consequently, the composition of RU4 is more dominated by *Acropora* spp. than are other reef units at the E-1 site (Fig. 4.15).

### 4.3.2 E-2 site

E-2 is cut out of a reef-front spur at the southeast margin of TI (Fig. 2.3). The trenches are up to ~4.8 m deep and 35 m long (Fig. 4.8), and the highest and lowest points are 8.2 m and 3.4 m AMSL, respectively. At the E-2 site, the reef sediment is divided into four reef units by sharp boundaries, similar to the E-1 site (Figs 4.6 and 4.8). From their stratigraphical positions, sedimentary characteristics and AMS dating results, I concluded that these four units corresponded to RU1 to RU4 at the E-1 site (Figs. 4.6, 4.8 and Table 4.1).

RU1, the lowest unit, covers the basement rock, which is well exposed around the seaward side of E-2 (Fig. 4.8). RU1 is characterized by a brownish color (Fig. 4.14a), similar to RU1 at E-1, because the matrix sediments and portions of the coral cali-

ces include brown mud that is derived from basement rock. RU1 is mainly composed of a tabular or thick-plate/encrusting *Acropora* spp. framework with well-consolidated detrital reef materials and massive or encrusting faviid corals (*Favia* spp., *Favites* spp., *Goniastrea* spp., and *Platygyra* spp.) are occasionally observed (Figs. 4.8 and 4.13d). RU1 formed a rough morphology similar to the reef mounds developed according to the basement morphology, and the depressions are buried by whitish reef sediment that corresponds to RU2.

RU2 is mainly composed of an encrusting or thick-plate/encrusting *Acropora* spp. framework with well-consolidated detrital reef materials. The boundary is clearly defined by the color difference between RU1 and RU2. The boundary between RU1 and RU2 is recognized by a change in color, from brown to white, as the irregular line (Figs.4.8, 4.9b and c). Therefore, this boundary is considered to result from sedimentary discontinuity rather than erosion, which indicates that the reef disturbance occurred between RU1 and RU2 formation, similar to the E-1 site. Major changes in the vertical and lateral coral variation are not observed.

RU3 formed on a significantly sharp and linear boundary, which indicates that it clearly eroded before the formation of RU3 (see Figs. 4.8 and 4.9a). At the contact between RU1 and RU3, the former mounded morphology, which consists of RU1 and 2, is flattened out (Figs. 4.8 and 4.9a). Therefore, this boundary indicates that the reef disturbance occurred because of a sea-level change before RU3. RU3 is characterized by a thick-plate *Acropora* spp. framework, and each coral colony is approximately 1 m wide and 0.5 m thick (Fig. 4.12C). Massive or encrusting faviid corals (*Goniastrea* spp., *Favites* spp., *Favia* spp., *Platygyra* spp.) and encrusting or columnar *Heliopora* spp. (Fig. 4.8) scattered in the acroporiid corals are observed. Major changes in the vertical and lateral coral variation are not observed.

RU4, the uppermost unit, filled RU3 with a sharp boundary (Figs.4.8 and 4.9d), except for on the seaward side. The boundary between RU1 and RU2 is recognized by the irregular line (Fig.4.8) but partly linear (Fig. 4.9d). Therefore, this boundary is considered to result from sedimentary discontinuity with erosion, which indicates that the reef disturbance and sea-level change occurred between RU3 and RU4

formation. RU4 is composed of a framework consisting mainly of tabular or thick-plate/encrusting *Acropora* spp. with detrital reef materials that are characterized by a relatively high content of eroded branching coral debris, similar to the E-1 site (Fig. 4.8). The material was characterized by a relatively porous matrix. Massive or encrusting faviid corals (*Goniastrea* spp., *Favia* spp., *Platygyra* spp.) and encrusting or columnar *Heliopora* spp. (Figs. 4.8, 4.12C and 4.13d) scattered in the acroporiid corals are observed. Major changes in the vertical and lateral coral variation are not observed.

The coral composition of RU1 is *Acropora* spp. (41.8%), faviid corals (47.4%), *Pocillopora* spp. (1.5%), *Goniopora* spp. (2.6%), *Heliopora* spp. (6.7%), and unknown spp. (0.5%); see Fig. 4.15. The diversity is relatively high compared with the reef units at the E-2 and E-1 sites, although they are both mainly occupied by *Acropora* and faviid corals (89.2%). In RU2, the composition changes to *Acropora* spp. (78.7%), faviid corals (14.9%), *Pocillopora* spp. (4.3%), and *Heliopora* spp. (2.1%). In this change, *Acropora* spp. dramatically increased by 36.9%, and faviid corals decreased by 32.5%. The composition is dominated by *Acropora spp.* This composition trend is similar to the change from RU1 to RU2 at the E-1 site. In RU3, the composition changes to *Acropora* spp. (92.4%), faviid corals (3.5%), *Pocillopora* spp. (3.5%), and *Goniopora* spp. (0.6%). In this change, *Acropora* spp. further increases by 13.7%, faviid corals decrease by 11.4%, and the composition becomes *Acropora*-dominant. In RU4, the composition changes to *Acropora* spp. (92.2%), faviid corals (4.3%), *Pocillopora* spp. (1.7%), *Heliopora* spp. (0.9%), and unknown (0.9%). In this change, *Acropora* spp. decreased by 0.2%, and faviid corals increased by 0.8%. However, the composition remains dominated by *Acropora* corals (Fig. 4.15).

### 4.3.3 E-3 site

E-3 is cut out of a reef front spur at the northern part of TI (Fig. 2.3). The trenches are up to 7 m deep and 21 m long (Fig. 4.10). The highest and lowest points

are 7.5 m and -0.5 m AMSL, respectively. The basement rock is not exposed, and the trench wall consists entirely of Holocene reef sediment. The reef sediments at the E-3 site are divided into 3 units by two sharp boundaries (Figs. 4.10 and 4.11). From their stratigraphical positions, sedimentary characters and AMS dating results, I concluded that these three units correspond to RU2 to RU4 at the E-1 and E-2 sites (Figs. 4.10, 4.11 and Table 4.1).

RU2 is lowest unit at the E-3 site. RU2 is characterized by coral facies consisting of branching *Acropora* spp., *Montipora* spp., and *Caulastrea* spp. that are found in the lower seaward position (Fig. 4.10; note that coral numbers were not calculated in this area) and gradually change to tabular and thick-plate *Acropora* spp. and massive or encrusting faviids (*Favia* spp., *Favites* spp. *Goniastrea* spp., *Leptastrea* spp., *Cyphastrea* spp. and foliaceous *Echinopora* spp.) upward (Figs. 4.10, 4.12D and 4.13e). The individual coral colony sizes reach up to 30 cm, and the deposit is a complicated framework structure with detrital reef materials (Figs. 4.10, 4.12D and 4.13a). This change may reflect water depth associated with a wave energy gradient that corresponds to the middle to shallow upper reef environment (e.g., Sagawa et al., 2001).

RU3 occurs above a sharp boundary with RU1 at approximately 4–5 m AMSL, where an abrupt facies change is observed when the reef composition changes to accumulated thick-plate/encrusting *Acropora* spp. over 1 m in diameter (Fig. 4.13a). This change and differences in both sediments are clear, and the boundary is sharp (Figs.4.11b and 4.12D). The boundary gradually rises landward. The boundary between RU2 and RU3 is recognized by the irregular line (Figs. 4.10, 4.11a and 4.12D). Therefore, this boundary is recognized sedimentary discontinuity rather than erosion, which indicates that the reef disturbance occurred between RU3 and RU4 formation. RU3 consists of a framework of platy *Acropora* spp. and a scattering of other corals, such as faviids (*Goniastrea* spp. and *Favia* spp.) and *Heliopora* spp. The lower ~1 m of the unit is occupied by coral colonies that are over 1 m in diameter and 0.5 m thick, without voids. The coral colonies become gradually smaller toward the upper part (Fig. 12D), and the spaces between the corals are filled with

detrital reef materials. These observations are similar to RU2 at the E-1 site (Fig. 4.12A). Therefore, vertical colony size changes are observed at seaward side of the vertical and lateral coral variation within RU3, although characteristic lateral changes are not observed.

RU4 occurs above a sharp boundary with RU1 at approximately 6.5 m AMSL. The boundary between RU3 and RU4 is recognized by the linear line (Figs. 4.10, 4.11c and d). Therefore, this boundary is considered to result from erosion, which indicates that the reef disturbance with sea-level change occurred between RU3 and RU4 formation. RU4 is composed of a framework mainly consisting of tabular or thick-plate/encrusting *Acropora* spp. with detrital reef materials characterized by relative high contents of eroded branching coral debris, similar to the E-1 and E-2 sites (Figs. 4.10 and 4.14c). The material is characterized by a relatively porous matrix (Fig. 4. 14c). Major changes in the vertical and lateral coral variation are not observed. RU4 covers the surface of a spur (Fig. 4.10).

The coral composition of RU1 is *Acropora* spp. (48.5%), faviid corals (27.9%), *Pocillopora* spp. (11.8%), *Goniopora* spp. (4.4 %), *Heliopora* spp. (1.5%), and unknown spp. (5.9%), see Fig. 4.15. The diversity is relatively high compared with the other reef units in E-3 and to RU2 at the other sites. However, the RU1 composition is dominated by *Acropora* spp. and faviid corals (76.4%). A possible cause for the relatively high diversity is the position of RU2 on the reef slope (perhaps -5 m) and the relatively low wave energy conditions during reef growth. In support of this hypothesis, foliaceous corals, such as *Echinopora* spp., are commonly observed. In RU3, the composition changes to *Acropora* spp. (90.0%), faviid corals (6.2%), *Pocillopora* spp. (1.5%), *Heliopora* spp. (0.8%), and unknown spp. (1.5%). *Acropora* spp. increased by 41.5% while faviid and other corals inversely decreased. The change is also observed as a clear facies change between the boundary of RU2 and RU3 (Fig. 4.12). In RU4, the composition changes to *Acropora* spp. (87.2%), faviid corals (0%), *Pocillopora* spp. (6.4%), and *Goniopora* spp. (6.4%). *Acropora* spp. decrease by 2.8%, faviid corals disappear, and other corals increase. However, the fraction of other corals increases to 12%, and the reef sediment shows an *Acropora*

dominance as a result of a decrease in faviid corals (Fig. 4.15).

### 4.3.4 Ages of Reef Units and reef growth hiatuses

According to the stratigraphic and sedimentological characteristics of the reef sediments on Kodakara Island, I concluded that the boundaries indicate reef disturbances that may have extended throughout the island and that they are associated with reef-growth hiatuses. Thus, I selected nondiagenetic coral samples near the boundaries to identify the timings of the disturbances with hiatuses as accurately as possible. I obtained 50 AMS $^{14}C$ ages from the corals (Table 4.1). All the ages showed no discrepancy between their growth positions and the reef units. The following ages were calibrated: RU1, 7,102–5,894 (n=11) cal yr B.P.; RU2, 5,753–4,371 (n=11) cal yr B.P.; RU3, 3,970–3,343 (n=12) cal yr B.P.; and RU4, 3,177–2,614 (n=13) cal yr B.P. Therefore, the disturbances occurred at approximately 5,894–5,753 cal yr B.P., 4,371–3,970 cal yr B.P., and 3,343–3,177 cal yr B.P. (5.9–5.8, 4.4–4.0, and 3.3–3.2 cal yr BP) (Fig. 3 and Table 1). Hence, a sudden environmental change could have caused abrupt reef mortality without recovery on multi-decadal to centennial time scale (i.e., there were multi-decadal to centennial-scale hiatuses in reef growth following the disturbances).

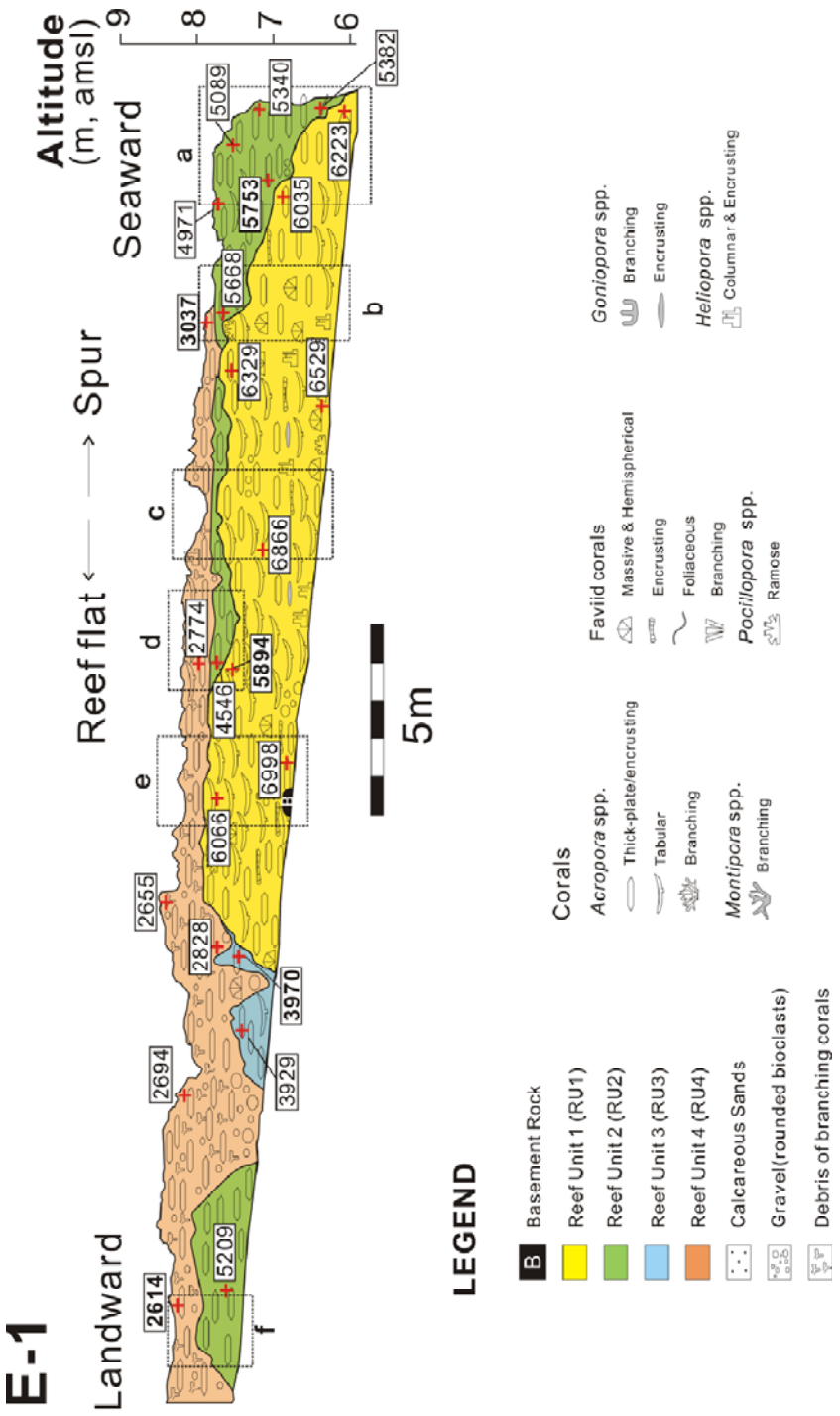


Fig. 4.6 The stratigraphic, sedimentological and paleoecological characteristics of the excavated trench site E-1. The AMS radiocarbon ages are also shown in rectangles. All the ages are in cal yr BP. The oldest and most recent ages in each reef unit appear in bold type. The dashed squares labeled a–f indicate the locations of the photos shown in Fig. 4.7.

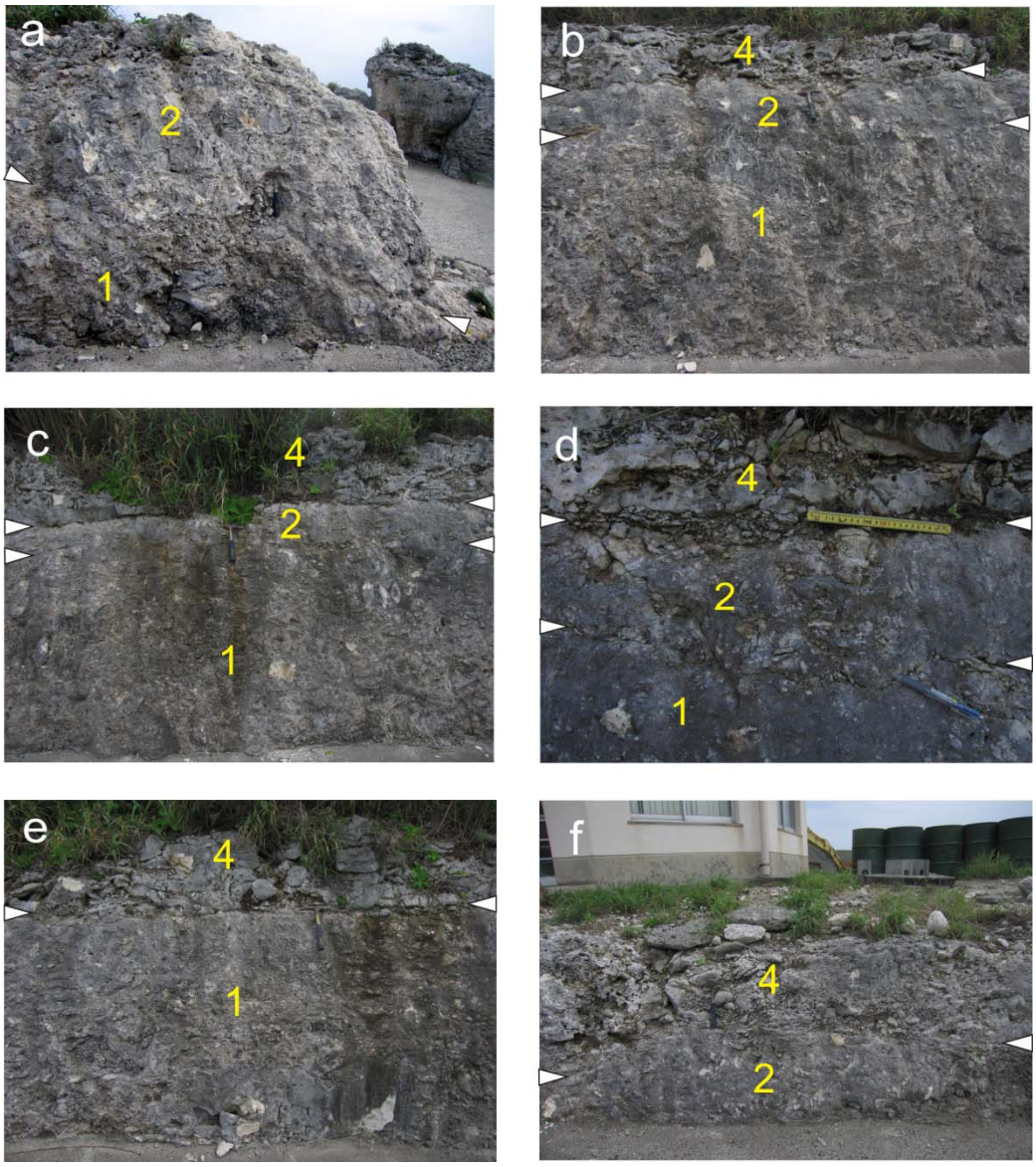


Fig. 4.7 Photos of the boundaries at E-1 site. The white triangles mark the boundaries. The locations of the photos are shown in Fig. 4.6. The numbers indicate the Reef Unit.

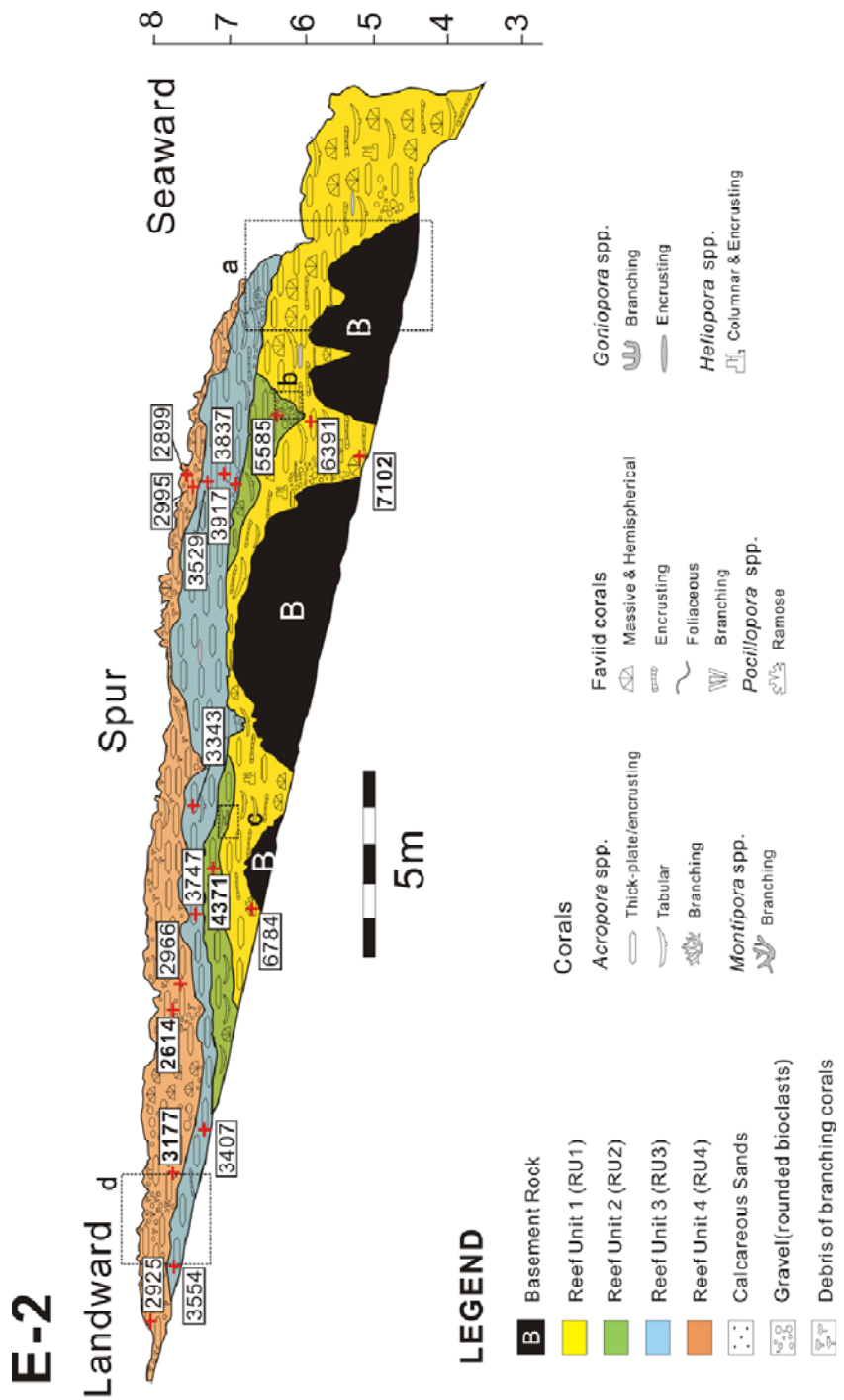


Fig. 4.8 The stratigraphic, sedimentological and paleoecological characteristics of the excavated trench site E-2. The AMS radiocarbon ages are also shown in rectangles. All the ages are in cal yr BP. The oldest and most recent ages in each reef unit appear in bold type. The dashed squares labeled a–d indicate the locations of the photos shown in Fig. 4.9.

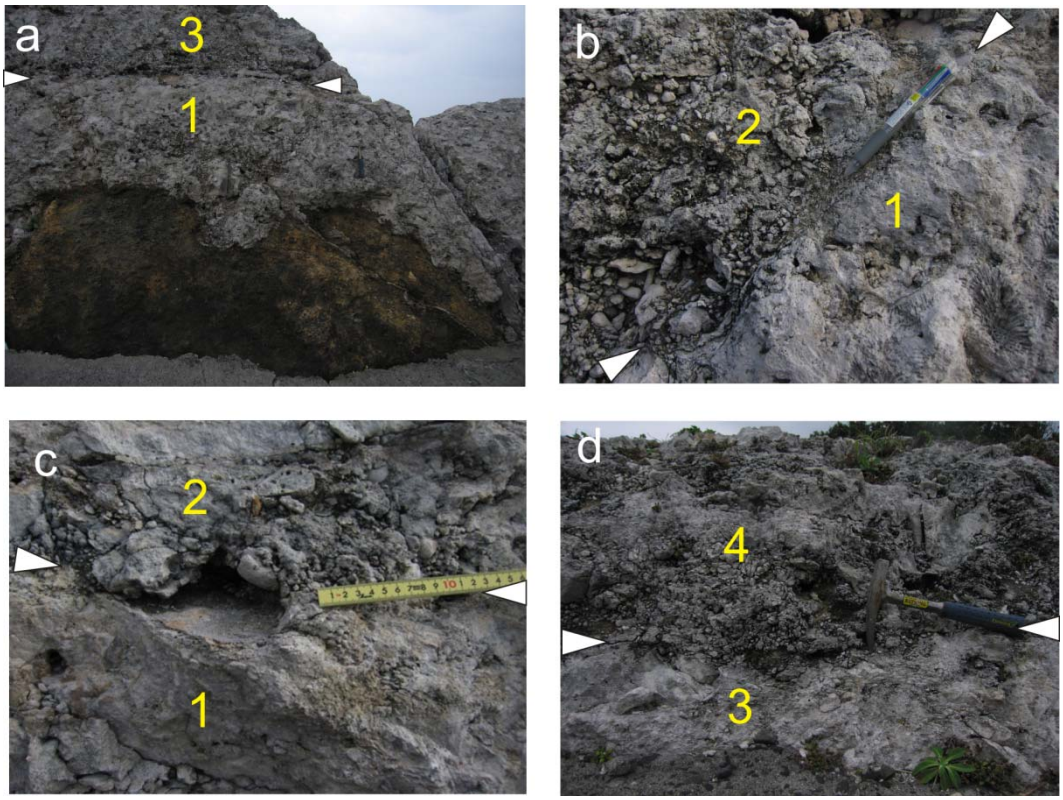


Fig. 4.9 Photos of the boundaries at E-2 site. The white triangles mark the boundaries. The locations of the photos are shown in Fig. 4.8. The numbers indicate the Reef Unit.

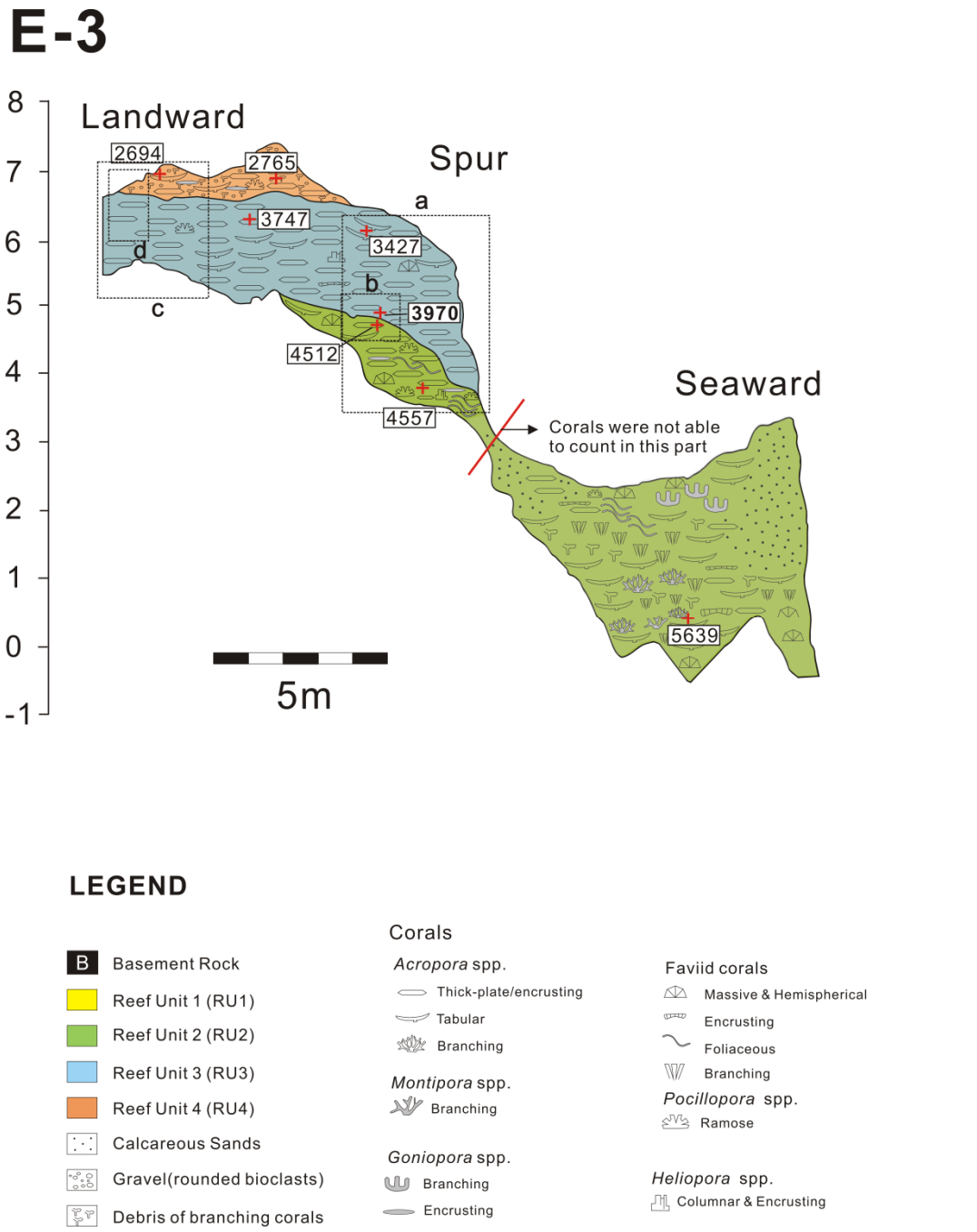


Fig. 4.10 The stratigraphic, sedimentological and paleoecological characteristics of the excavated trench sites E-3. The AMS radiocarbon ages are also shown in rectangles. All the ages are in cal yr B.P. The oldest and most recent ages in each reef unit appear in bold type. The coral composition at the seaward area at E-3 was not calculated (the red bar indicates its limit). The dashed squares labeled a–d indicate the locations of the photos shown in Fig. 4.11

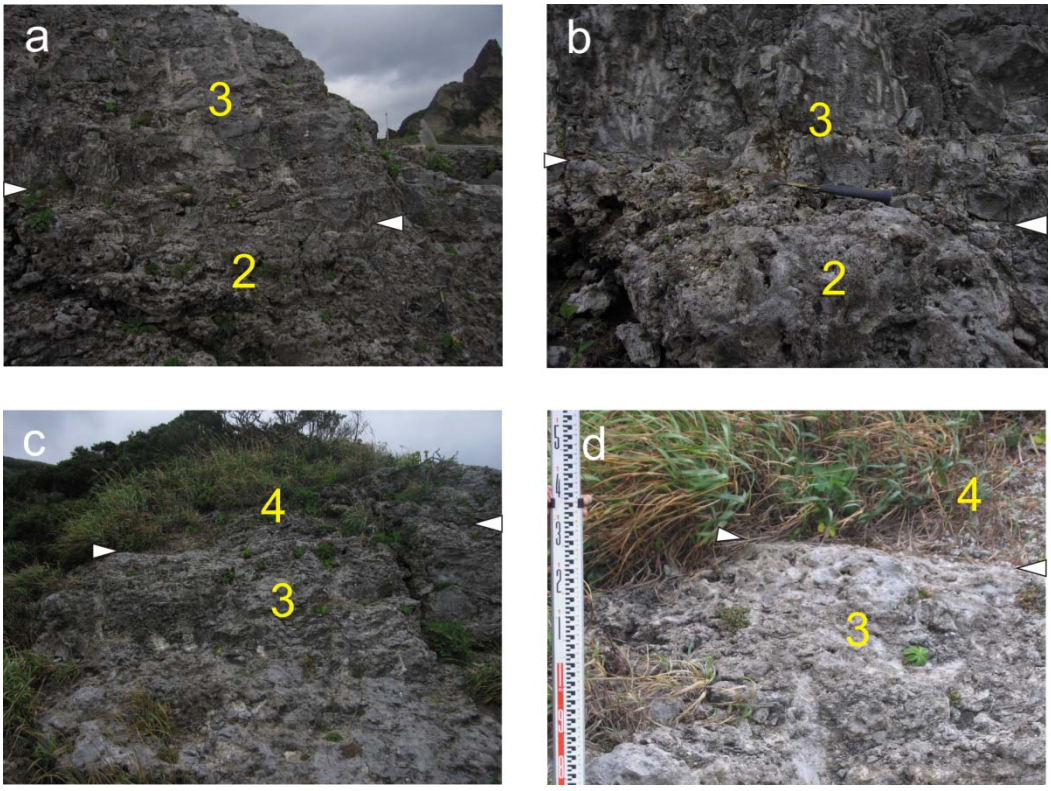


Fig. 4.11 Photos of the boundaries at E-2 site. The white triangles mark the boundaries. The locations of the photos are shown in Fig. 4.10. The numbers indicate the Reef Unit.

Table 4.1 AMS radiocarbon ages from excavations on Kodakara Island

| Lab. Code | Sample No. | Genus[1] | Coral morphology[2] | Conv.age (yr B.P.) | Calib. age (cal yr B.P.) | 1σ range (cal yr B.P.) | 2σ range (cal yr B.P.) | Locality | Reef Unit | Altitude (m, amsl) |
|---|---|---|---|---|---|---|---|---|---|---|
| Beta-233878 | KQ11-1 | *Pocillopora* sp. | Ramose | 5990±40 | 6784 | 6723-6846 | 6664-6902 | E-2 | 1 | 6.13 |
| Beta-233879 | NH-Pr-10 | *Favites* sp. | Massive | 6230±40 | 7102 | 7031-7160 | 6976-7219 | E-2 | 1 | 4.47 |
| Beta-233880 | NH-Pr-12 | *Acropora* sp. | Tabular | 5600±40 | 6391 | 6329-6441 | 6287-6496 | E-2 | 1 | 4.68 |
| Beta-233881 | NH-E-24 | *Acropora* sp. | T-P/E | 4840±40 | 5585 | 5544-5640 | 5473-5677 | E-2 | 2 | 5.71 |
| Beta-233882 | NH-E-39 | *Acropora* sp. | T-P/E | 3560±40 | 3917 | 3845-3974 | 3795-4066 | E-2 | 3 | 6.2 |
| Beta-233883 | NH-E-48 | *Acropora* sp. | T-P/E | 2750±40 | 2899 | 2832-2961 | 2773-3033 | E-2 | 4 | 6.8 |
| Beta-233884 | NH-KP-12 | *Acropora* sp. | T-P/E | 4920±40 | 5668 | 5609-5712 | 5574-5793 | E-1 | 2 | 7.53 |
| Beta-233885 | NH-KP-13 | *Acropora* sp. | T-P/E | 2850±40 | 3037 | 2957-3108 | 2894-3184 | E-1 | 4 | 7.9 |
| Beta-237235 | NH-KP-1 | *Platygyra* sp. | Massive | 5450±50 | 6223 | 6175-6276 | 6085-6340 | E-1 | 1 | 6.04 |
| Beta-237236 | NH-KP-4 | *Acropora* sp. | T-P/E | 5030±50 | 5753 | 5687-5838 | 5624-5881 | E-1 | 2 | 7.14 |
| Beta-237237 | NH-KP-9 | *Acropora* sp. | T-P/E | 4350±50 | 4971 | 4866-5034 | 4833-5180 | E-1 | 2 | 7.74 |
| Beta-237238 | NH-KP-10 | *Acropora* sp. | T-P/E | 5240±50 | 6035 | 5951-6103 | 5908-6170 | E-1 | 1 | 6.74 |
| Beta-237239 | NH-KP-14 | *Acropora* sp. | T-P/E | 5520±50 | 6329 | 6276-6381 | 6217-6443 | E-1 | 1 | 7.36 |
| Beta-237240 | NH-KP-16 | *Platygyra* sp. | Massive | 5730±50 | 6529 | 6462-6602 | 6397-6658 | E-1 | 1 | 6.34 |
| Beta-237241 | NH-KP-21 | *Goniastrea* sp. | Encrusting | 6020±50 | 6866 | 6789-6934 | 6717-7010 | E-1 | 1 | 7.12 |
| Beta-237242 | NH-KP-24 | *Acropora* sp. | T-P/E | 2620±40 | 2774 | 2727-2815 | 2695-2874 | E-1 | 4 | 7.93 |
| Beta-237243 | NH-KP-25 | *Acropora* sp. | T-P/E | 4040±50 | 4546 | 4441-4615 | 4399-4740 | E-1 | 2 | 7.72 |
| Beta-237244 | NH-KP-26 | *Acropora* sp. | T-P/E | 5130±50 | 5894 | 5839-5972 | 5733-6022 | E-1 | 1 | 7.51 |
| Beta-237245 | NH-KP-27 | *Acropora* sp. | T-P/E | 6120±50 | 6998 | 6919-7081 | 6855-7149 | E-1 | 1 | 6.77 |
| Beta-237246 | NH-KP-31 | *Acropora* sp. | Tabular | 5300±50 | 6066 | 5990-6138 | 5926-6194 | E-1 | 1 | 7.62 |
| Beta-237247 | NH-KP-37 | *Acropora* sp. | T-P/E | 3590±40 | 3970 | 3903-4045 | 3838-4101 | E-1 | 3 | 7.43 |
| Beta-237248 | NH-KP-40 | *Acropora* sp. | T-P/E | 2470±40 | 2614 | 2549-2698 | 2460-2726 | E-1 | 4 | 8.2 |
| Beta-237249 | NH-KP-41 | *Acropora* sp. | T-P/E | 4490±40 | 5209 | 5132-5289 | 5040-5312 | E-1 | 2 | 7.6 |
| Beta-237250 | NH-KP-44 | *Acropora* sp. | Tabular | 4650±40 | 5382 | 5319-5432 | 5279-5495 | E-1 | 2 | 6.39 |
| Beta-237251 | NH-KP-45 | *Acropora* sp. | T-P/E | 4570±40 | 5340 | 5281-5399 | 5236-5453 | E-1 | 2 | 7.2 |
| Beta-237252 | NH-KP-46 | *Acropora* sp. | T-P/E | 4390±40 | 5089 | 5011-5198 | 4932-5254 | E-1 | 2 | 7.49 |
| Beta-237253 | NH-KP-47 | *Acropora* sp. | Encrusting | 2480±40 | 2655 | 2601-2728 | 2493-2746 | E-1 | 4 | 8.38 |
| Beta-237254 | NH-KP-48 | *Acropora* sp. | T-P/E | 3550±40 | 3929 | 3852-3986 | 3809-4072 | E-1 | 3 | 7.41 |
| Beta-237255 | NH-KP-49 | *Acropora* sp. | T-P/E | 2540±40 | 2694 | 2652-2747 | 2526-2776 | E-1 | 4 | 8.1 |
| Beta-237256 | NH-KP-50 | *Acropora* sp. | T-P/E | 2670±40 | 2828 | 2763-2872 | 2734-2943 | E-1 | 4 | 7.67 |
| Beta-237257 | NH-J-1 | *Acropora* sp. | Tabular | 4930±40 | 5639 | 5586-5678 | 5557-5744 | E-3 | 2 | 0.42 |
| Beta-237258 | NH-J-2 | *Leptastrea* sp. | Encrusting | 3990±40 | 4557 | 4479-4635 | 4414-4720 | E-3 | 2 | 3.8 |
| Beta-237259 | NH-J-4 | *Acropora* sp. | T-P/E | 3590±40 | 3970 | 3903-4045 | 3838-4101 | E-3 | 3 | 4.9 |
| Beta-237260 | NH-J-7 | *Acropora* sp. | T-P/E | 3420±40 | 3747 | 3686-3814 | 3618-3870 | E-3 | 3 | 6.23 |
| Beta-237261 | NH-J-9 | *Acropora* sp. | T-P/E | 2600±40 | 2765 | 2719-2804 | 2688-2864 | E-3 | 4 | 7.05 |
| Beta-239676 | NH-E-41 | *Acropora* sp. | T-P/E | 3500±40 | 3837 | 3765-3905 | 3695-3963 | E-2 | 3 | 6.4 |
| Beta-239677 | NH-E-45 | *Acropora* sp. | T-P/E | 3250±40 | 3529 | 3462-3586 | 3411-3653 | E-2 | 3 | 6.55 |
| Beta-239678 | NH-J-3 | *Favia stelligera* | Columnar | 3990±40 | 4512 | 4432-4567 | 4392-4669 | E-3 | 2 | 4.75 |
| Beta-239679 | NH-J-6 | *Acropora* sp. | T-P/E | 3140±40 | 3427 | 3364-3473 | 3329-3549 | E-3 | 3 | 6.1 |
| Beta-239680 | NH-J-10 | *Acropora* sp. | T-P/E | 2530±40 | 2694 | 2652-2747 | 2526-2776 | E-3 | 4 | 6.95 |
| Beta-241426 | NH-E-47 | *Acropora* sp. | T-P/E | 2790±40 | 2995 | 2920-3065 | 2856-3141 | E-2 | 4 | 6.74 |
| Beta-241427 | NH-Pr-39 | *Acropora* sp. | T-P/E | 3260±40 | 3554 | 3485-3614 | 3433-3677 | E-2 | 3 | 7.03 |
| Beta-241428 | NH-Pr-40 | *Acropora* sp. | T-P/E | 2870±40 | 2925 | 2852-2987 | 2793-3064 | E-2 | 4 | 7.35 |
| Beta-253384 | NH-Pr-29 | *Acropora* sp. | T-P/E | 2790±40 | 2966 | 2890-3035 | 2833-3116 | E-2 | 4 | 7.08 |
| Beta-253385 | NH-Pr-30 | *Platygyra* sp. | Massive | 2500±40 | 2614 | 2549-2698 | 2460-2726 | E-2 | 4 | 7.13 |
| Beta-253386 | NH-Pr-32 | *Acropora* sp. | T-P/E | 3160±40 | 3407 | 3351-3453 | 3307-3532 | E-2 | 3 | 6.64 |
| Beta-253387 | NH-Pr-36 | *Acropora* sp. | T-P/E | 2930±40 | 3177 | 3106-3249 | 3036-3314 | E-2 | 4 | 7.06 |
| Beta-254560 | KQ-11-10 | *Acropora* sp. | T-P/E | 3430±40 | 3747 | 3686-3814 | 3620-3871 | E-2 | 3 | 6.75 |
| Beta-254561 | NH-Pr-24 | *Acropora* sp. | T-P/E | 3080±40 | 3343 | 3289-3399 | 3225-3446 | E-2 | 3 | 6.82 |
| Beta-254562 | NH-Pr-25 | *Favia stelligera* | Columnar | 3890±40 | 4371 | 4293-4428 | 4234-4501 | E-2 | 2 | 6.5 |

1. All Samples for AMS dating are in situ corals.
2. T-P/E means thick-plate/encrusting.

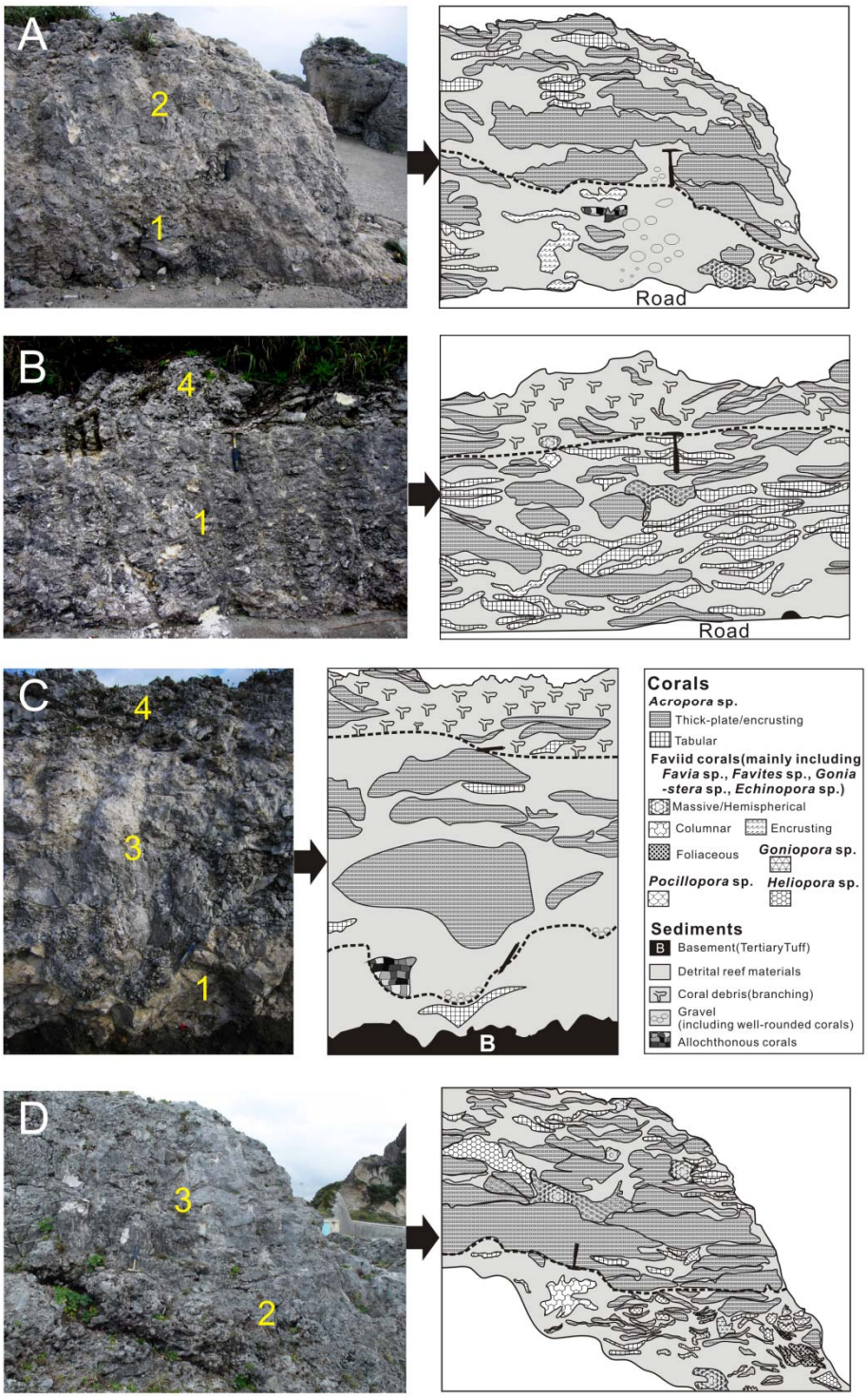


Fig. 4.12 Accurate coral compositions from the sketches and photos. The scale hammer is 30 cm and the pen is 10 cm. The dashed lines indicate the boundaries. (A) The seaward part of the E-1 site is identical to that in Fig. 4.6. (B) The central part of the E-1 site. (C) The central part of the E-2 site is identical to that in Fig. 4.8. (D) The seaward part of the E-3 site is identical to that in Fig. 4.10.

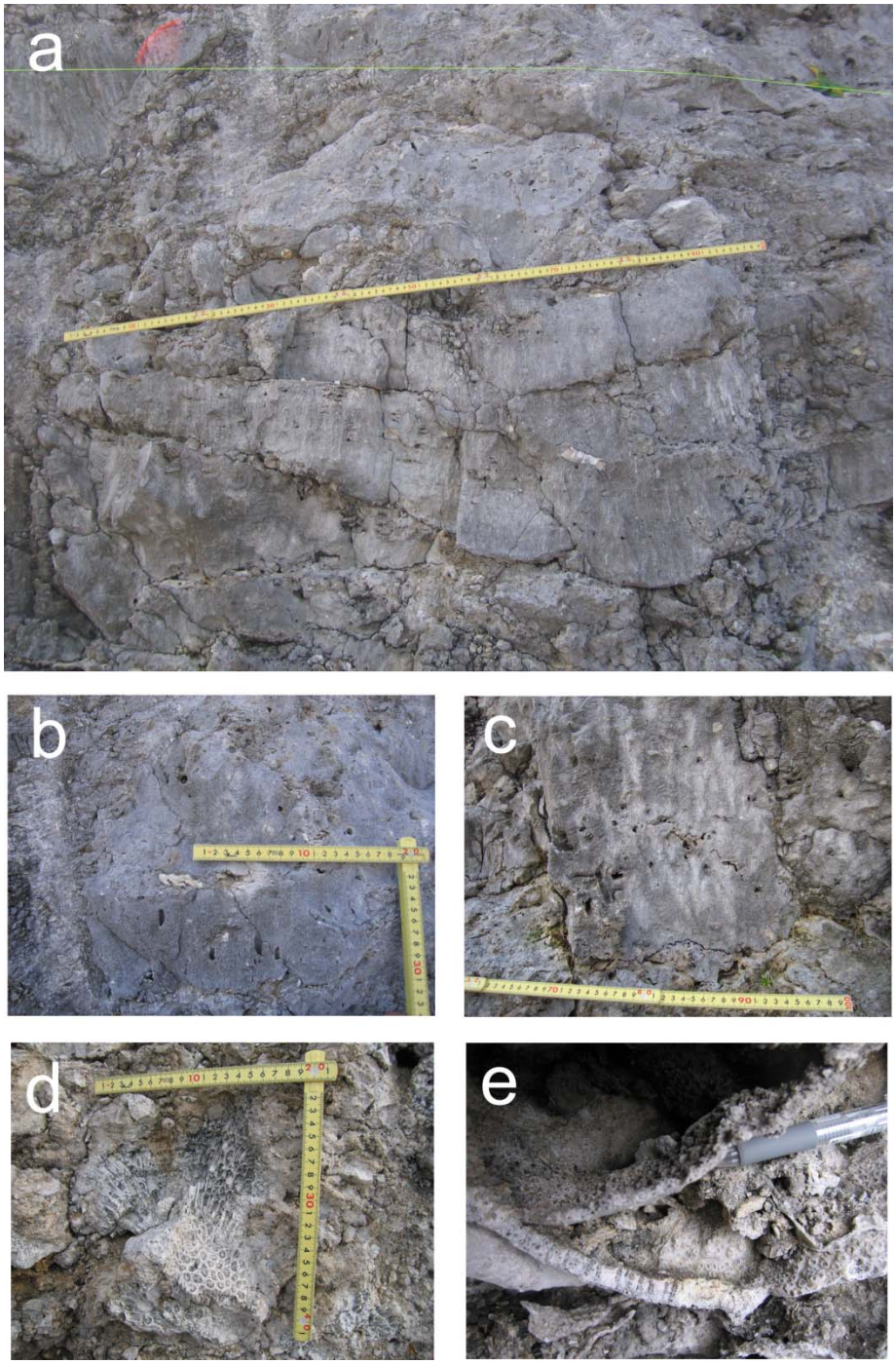


Fig. 4.13 Typical facies at trench sites. (a)Well-developed thick-plate/encrusting *Acropora* spp. in RU3 observed at E-3 site. (b) *A. (Isopora) palifera* group in thick-plate/encrusting *Acropora* spp. observed at E-3 site in RU3. (c) *Acropora humilis* group in thick-plate/encrusting *Acropora* spp. observed at E-3 site in RU3. (d) Massive faviid corals in RU1 observed at seaward of E-2 site. Foliaceous *Echinopora* spp. in RU2 observed at E-3 site.

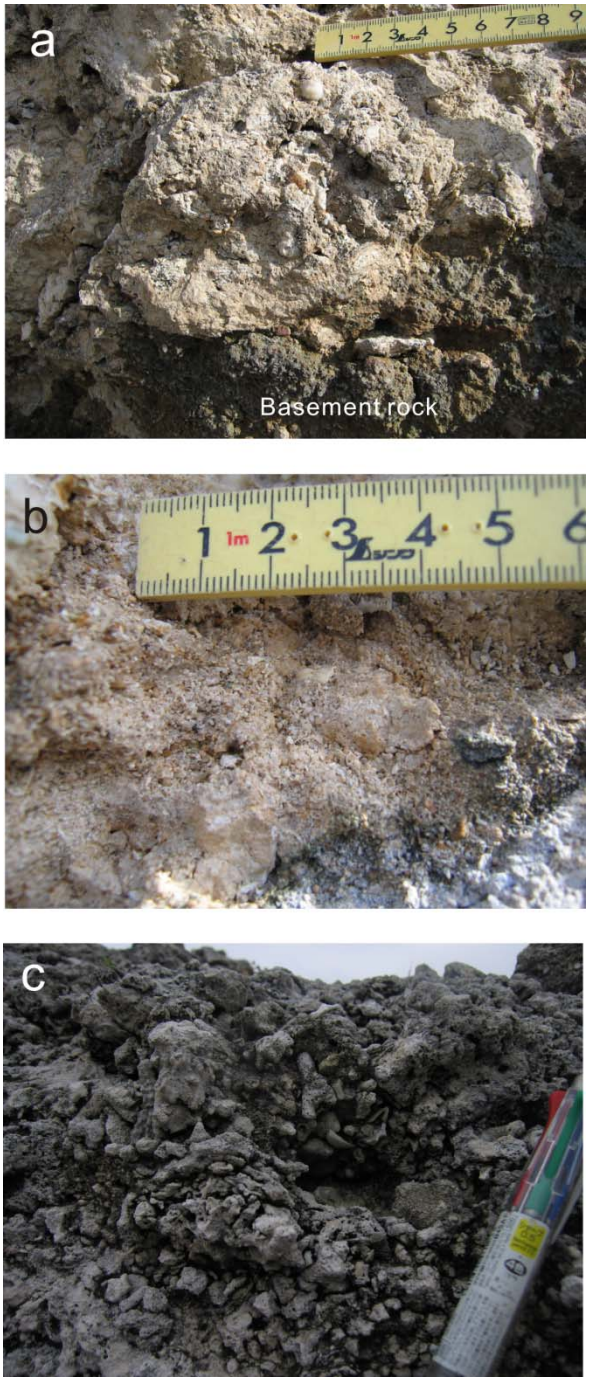


Fig. 4.14 Typical matrix of reef sediment at trench sites. (a) Consolidated detrital reef materials with terrigenous mud, sands and gravels above basement rock observed at E-2 site. (b) Consolidated detrital reef materials observed at E-2 site. Terrigenous sediments are rare. (c) Consolidated detrital reef materials consist of mostly debris of branching corals observed at E-2 site. This typically observed in RU4 at all trench sites.

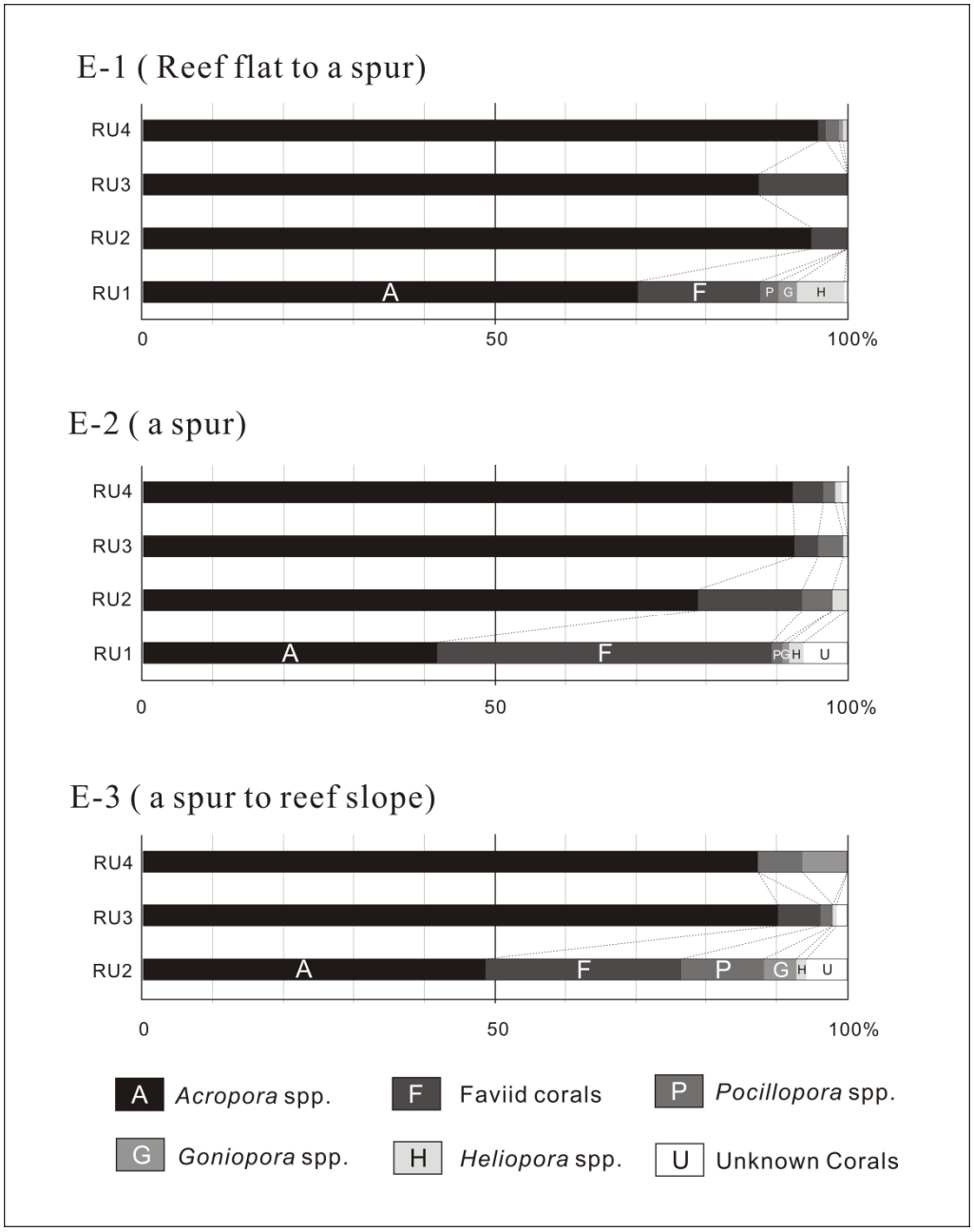


Fig. 4.15 The changes in coral compositions at E-1, E-2, and E-3.

### 4.3.5 Coral composition change with the hiatuses

Our results indicate that there were four stages of coral reef growth at Kodakara Island in the Northwest Pacific during the middle-to-late-Holocene; these stages were distinguished by three disturbances with hiatuses. The total coral compositions of sites E-1 to E-3 on Kodakara Island are compiled in Fig. 4.16.

Around 7.1 ka, reef growth on Kodakara Island was initiated in the RU1 formation. The coral composition of RU1 (ca. 7.1–5.9 ka) is *Acropora* spp. (59.4%), faviid corals (28.8%), *Pocillopora* spp. (2.2 %), *Goniopora* spp. (2.0%), *Heliopora* spp. (4.9 %), and unknown spp. (2.7%; see Fig. 8). These proportions indicate that diversity was relatively high compared with other reef units, although over half of the reef was occupied by *Acropora* spp. Moreover, the proportion of both *Acropora* and faviid corals was as high as 88.2%.

The disturbance in RU1 and the onset of the first hiatus occurred at 5.9 ka. Reef growth resumed after this hiatus, and RU2 formation was initiated at 5.8 ka. In RU2 (ca. 5,800–4,400 yr BP), the composition proportions changed to *Acropora* spp. (74.6 %), faviid corals (15.5%), *Pocillopora* spp. (5.2 %), *Goniopora* spp. (1.6 %), *Heliopora* spp. (1.0 %), and unknown spp. (2.1%). *Acropora* spp. increased dramatically (by 15.2%), and faviid corals decreased by 13.3%; the fractions of the other corals did not change significantly. The combined proportion of *Acropora* and faviid corals was 90.1%, which was relatively unchanged from that of RU1 (88.2%). The most significant change observed was that the percentage of *Acropora* spp. dramatically increased. The colony size increase observed at the E-1 site may suggest reef re-initiation or recovery.

The RU2 disturbance occurred and the onset of the second hiatus began at 4.4 ka. Reef growth resumed after this hiatus, and RU3 formation was initiated at 4.0 ka. In RU3 (ca. 4,000–3,300 yr BP), the composition changed to *Acropora* spp. (91.1%), faviid corals (5.1%), *Pocillopora* spp. (2.6%), *Goniopora* spp. (0.3%), *Heliopora* spp. (0.3%), and unknown spp. (0.6%). In this change, *Acropora* spp. dramatically increased by 16.5%, and faviid corals decreased by 10.4%. The trend in this change is

similar to that between RU1 and RU2. The composition of RU3 was dominated by *Acropora* corals (over 90%); thus, RU3 was an *Acropora* reef. The proportion of other corals decreased to below 5%, suggesting that the reef during the 4.0–3.3 ka period may have had a low diversity.

The disturbance in RU3 occurred at 3.3 ka, initiating the third hiatus. The reef growth resumed after this hiatus, and RU4 formation began at 3.2 ka. In RU4 (ca. 3,200–2,600 yr BP), the composition changed to *Acropora* spp. (93.3%), faviid corals (2.1%), *Pocillopora* spp. (2.5%), *Goniopora* spp. (1.2%), *Heliopora* spp. (0.6%), and unknown spp. (0.3%). In this change, *Acropora* spp. increased by 2.2%, faviid corals inversely decreased by 2.0%, and the other corals recovered. Therefore, *Acropora* became more dominant in the reef, although the other corals slightly increased.

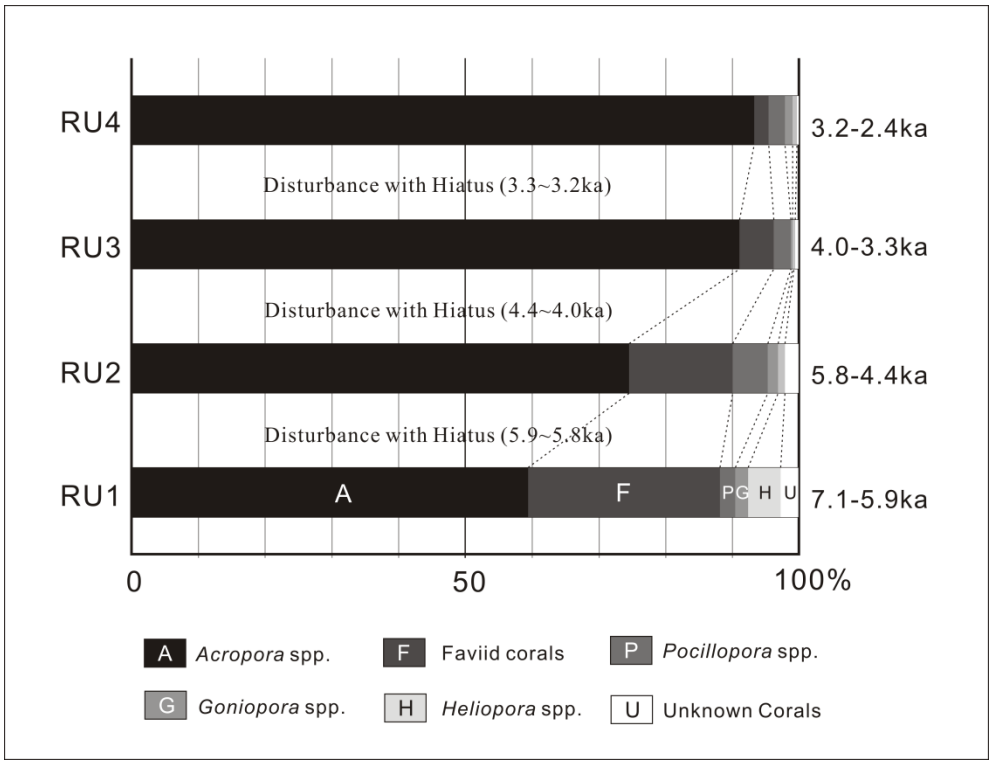


Fig. 4.16 The changes in total coral composition with disturbance hiatuses during the middle-to-late Holocene on Kodakara Island.

## 4.4 Characteristics of the Holocene raised reefs based on cores

In this section, I describe the sedimentary characteristics of cores along the transect, from seaward to landward sites (Figs. 2.3 and 4.17).

### 4.4.1 Core B1

Core B1 was located at the most seaward site and was situated at the edge of TII at an altitude of 2.3 m (Figs. 4.17 and 4.18). The total core length is 5.08 m, and the recovery ratio is approximately 75% (Fisg. 4.18, 4.19 and Table 4.3). The interval 5-3.5 meters below surface (mbs) consists of in situ massive *Porites* sp. and gravels derived from *Pocillopora* sp. They constitute a framework with poorly consolidated detrital reef materials that generally contain the debris of marine organisms, such as corals, foraminifera, shells, and mollusks. Major changes in the components of the reef materials were not observed in all cores despite the consolidation. The upper 3.5 m of the core consists of thick-plate/encrusting and tabular *Acropora* spp., which are equivalent to the *Acropora humilis* group, *Acropora(Isopora) palifera* group, and *Acropora hyacinthus* group (Veron and Wallace, 1984), as well as massive and encrusting faviid corals containing well-consolidated detrital reef materials. Encrusting calcareous algae up to 1 cm in thickness are commonly observed in this part. Ages measured in the B1 core range from 5027 cal yr BP to 967 cal yr BP (Figs. 4.17, 4.18, 4.19 and Table 4.2). Vertical growth rates were 0.2 m $kys^{-1}$ between 5 and 1.3 ka and 9.1 m $kyr^{-1}$ between 1.3 and 1 ka (Fig. 4.17).

Description

0.00 – 0.14 m Thick-plate/encrusting *Acropora* sp. (KD-B1-1; 967 cal yr BP) + well-consolidated detrital reef materials

0.14 – 0.36 m Thick-plate/encrusting *Acropora* sp. + well-consolidated detrital reef materials

0.36 – 0.52 m Thick-plate/encrusting *Acropora* sp. + encrusting calcareous algae and well-consolidated detrital reef materials

0.52 – 0.64 m Encrusting faviid coral + encrusting calcareous algae + well-consolidated detrital reef materials

0.64 – 0.72 m Thick-plate/encrusting *Acropora* sp. + encrusting calcareous algae + well-consolidated detrital reef materials

0.72 – 1.05 m Thick-plate/encrusting *Acropora* sp.

1.05 – 1.19 m Thick-plate/encrusting *Acropora* sp. + well-consolidated detrital reef materials

1.19 – 1.31 m An encrusting faviid coral + encrusting calcareous algae

1.31 – 1.40 m Thick-plate/encrusting *Acropora* sp. + encrusting calcareous algae

1.40 – 1.44 m Calcareous sands and gravels

1.44 – 1.73 m Thick-plate/encrusting *Acropora* sp. + an encrusting faviid coral + encrusting calcareous algae + well-consolidated detrital reef materials

1.73 – 1.77 m An encrusting faviid coral + encrusting calcareous algae + well-consolidated detrital reef materials

1.77 – 2.00 m Fragments of bioclastics + calcareous sands

2.00 – 2.05 m Consolidated detrital reef materials

2.05 – 2.30 m A massive faviid coral + encrusting calcareous algae + consolidated detrital reef materials

2.30 – 2.45 m Thick-plate/encrusting *Acropora* sp. (KD-B1-2; 1267 cal yr BP)

2.45 – 2.62 m Calcareous sands and gravels

2.62 – 2.72 m Consolidated detrital reef materials

2.72 – 3.00 m Not in situ coral (*Porites* sp.)＋fragments of consolidated detrital reef materials

3.00 – 3.09 m Consolidated detrital reef materials

3.09 – 3.14 m Thick-plate/encrusting *Acropora* sp. (KD-B1-5; 1288 cal yr BP)＋calcareous algae

3.14 – 3.42 m Consolidated detrital reef materials

3.42 – 3.45 m Encrusting faviid coral

3.45 – 3.48 m Consolidated detrital reef materials

3.48 – 3.64 m No recovery

3.64 – 3.97 m Massive *Porites* sp. (KD-B1-3; 5027 cal yr BP)

3.97 – 4.00 m Rounded gravel

4.00 – 4.07 m Ramose *Pocillopora* sp. + consolidated detrital reef materials

4.07 – 4.20 m Fragments of consolidated detrital reef materials

4.20 – 4.82 m No recovery

4.82 – 4.92 m Not in situ *Porites* sp. (KD-B1-4; 5027 cal yr BP)

4.92 – 5.08 m Fragments of consolidated detrital reef materials

### 4.4.2 Core B2

Core B2 was located at the center of TII (Figs. 4.17 and 4.18). The total core length is 10 m, and the recovery ratio is approximately 79% (Figs. 4.18, 4.20 and Table 4.3). The interval 10-9 mbs consists of encrusting faviid corals, such as *Montipora* spp. and *Porites* sp., with poorly consolidated reef materials. The interval 9-6.8 mbs consists of calcareous sands and gravels, which derive mostly from branching corals. The interval 6.8-3.5 mbs consists of massive *Porites* spp., encrusting and massive faviid corals, encrusting *Acropora* spp., and *Montipora* spp. with poorly consolidated reef materials. The interval 3.5-0 mbs consists of thick-plate/encrusting and tabular *Acropora* spp. as well as massive and encrusting faviid corals with well-consolidated reef materials. Encrusting calcareous algae up to 1 cm in thickness are commonly observed in this part. The ages measured in core B2 range from 7412 cal yr BP to 1262 cal yr BP (Figs. 4.17, 4.18, 4.20 and Table 4.2). Vertical growth rates were 3.6 m $kyr^{-1}$ between 7.4 and 5.9 ka, 1.5 m $kyr^{-1}$ between 5.9 and 4.2 ka, and 0.7 m $kyr^{-1}$ between 4.2 and 1.3 ka (Fig. 4.17).

Description

0.00 – 0.22 m Thick-plate/encrusting *Acropora* sp.(KD-B2-1; 1262 cal yr BP) +

encrusting calcareous algae and well-consolidated detrital reef materials

0.22 – 0.37 m Thick-plate/encrusting *Acropora* sp.

0.37 – 0.40 m Well-consolidated detrital reef materials

0.40 – 0.62 m Thick-plate/encrusting *Acropora* sp. + well-consolidated detrital reef materials

0.62 – 0.65 m No recovery

0.65 – 0.81 m Encrusting calcareous algae and well-consolidated detrital reef materials

0.81 – 1.03 m Thick-plate/encrusting *Acropora* sp. + consolidated detrital reef materials

1.03 – 1.29 m Massive *Goniastrea* sp. + consolidated detrital reef materials

1.29 – 1.41 m Thick-plate/encrusting *Acropora* sp. + consolidated detrital reef materials

1.41 – 1.51 m Thick-plate/encrusting *Acropora* sp. + well-consolidated detrital reef materials

1.51 – 1.60 m Thick-plate/encrusting *Acropora* sp.

1.60 – 1.80 m Massive *Favia* sp. + consolidated detrital reef materials.

1.80 – 1.85 m Coral fragments (faviids and *Pocillopora* sp.)

1.85 – 2.00 m Thick-plate/encrusting *Acropora* sp. (KD-B2-2; 4151 cal yr BP) + encrusting *Goniastrea* sp. + consolidated detrital reef materials with encrusting calcareous algae

2.00 – 2.07 m Encrusting *Montipora* sp. + consolidated detrital reef materials with encrusting calcareous algae

2.07 – 2.14 m Consolidated detrital reef materials + coral gravels

2.14 – 2.19 m Consolidated detrital reef materials

2.19 – 2.39 m Thick-plate/encrusting *Acropora* sp. + consolidated detrital reef materials with calcareous algae

2.39 – 2.57 m Columnar *Favia* sp. + consolidated detrital reef materials

2.57 – 2.62 m Gravels

2.62 – 2.69 m Consolidated detrital reef materials

2.69 – 2.80 m Encrusting *Goniastrea* sp. + consolidated detrital reef materials.

2.80 – 2.91 m Encrusting *Cyphastrea* sp. + consolidated detrital reef materials

2.91 – 3.09 m Encrusting *Favites* sp. + encrusting *Acropora* sp. + calcareous algae and consolidated detrital reef materials

3.09 – 3.19 m Encrusting *Goniastrea* sp. + consolidated detrital reef materials

3.19 – 3.26 m Encrusting *Montipora* sp. + consolidated detrital reef materials

3.26 – 3.31 m Fragments of consolidated detrital reef materials

3.31 – 3.40 m Encrusting *Acropora* sp. + consolidated detrital reef materials

3.40 – 3.47 m Encrusting *Acropora* sp. + consolidated detrital reef materials

3.47 – 3.52 m Encrusting *Platygyra* sp.

3.52 – 3.58 m Encrusting *Acropora* sp. + consolidated detrital reef materials

3.58 – 3.80 m Massive *Porites* sp.

3.80 – 3.94 m Rounded coral gravels

3.94 – 4.01 m Encrusting *Acropora* sp. + encrusting *Goniastrea* sp.

4.01 – 4.11 m Massive *Favia* sp.

4.11 – 4.40 m Massive *Favia* sp.

4.40 – 4.60 m No recovery

4.60 – 4.69 m Encrusting *Acropora* spp.

4.69 – 4.80 m Tabular *Acropora* sp. (KD-B2-3; 5939 cal yr BP) + calcareous algae + consolidated detrial reef materials

4.80 – 4.91 m Foliaceous *Montipora* sp.

4.91 – 5.29 m Encrusting *Cyphastrea* sp. + massive *Porites* sp.

5.29 – 5.34 m Fragments of consolidated detrital reef materials

5.34 – 5.44 m Encrusting *Echinopora* sp.

5.44 – 5.65 m Encrusting *Acropora* spp. + an encrusting faviid coral + consolidated detrital reef materials

5.65 – 5.80 m Massive *Favia* sp. + consolidated detrital reef materials

5.80 – 5.90 m Debris of branching corals

5.90 – 6.05 m Consolidated detrital reef materials

6.05 – 6.21 m Encrusting *Montipora* spp.

6.21 – 6.33 m No recovery

6.33 – 6.62 m Massive *Porites* sp. (KD-B2-4; 6691 cal yr BP)

6.62 – 6.68 m No recovery

6.68 – 6.80 m Massive *Goniopora* sp. + encrusting *Montipora* sp. + consolidated detrital reef materials

6.80 – 8.23 m Calcareous sands and gravels of branching corals and shells

8.23 – 8.31 m Not in situ *Favia* sp.

8.31 – 8.40 m Calcareous sands and gravels of branching corals

8.40 – 8.49 m Not in situ *Porites* sp.

8.49 – 8.60 m Calcareous sands and gravels

8.60 – 8.62 m Not in situ *Favites* sp.

8.62 – 8.97 m Calcareous sands and gravels

8.97 – 9.02 m Fragments of poorly-consolidated detrital reef materials

9.02 – 9.21 m Debris of branching corals

9.21 – 9.28 m Encrusting *Montipora* spp.

9.28 – 9.31 m Fragments of poorly-consolidated detrital reef materials

9.31 – 9.37 m Encrusting *Montipora* sp.

9.37 – 9.42 m No recovery

9.42 – 9.48 m Encrusting *Favites* sp.

9.48 – 9.53 m Poorly-consolidated detrial reef materials

9.53 – 9.60 m Encrusting *Porites* sp.

9.60 – 9.66 m Encrusting *Favia* sp. + poorly-consolidated detrial reef materials

9.66 – 9.82 m Massive *Favia* sp. + poorly-consolidated detrial reef materials

9.82 – 9.87 m Encrusting *Montipora* sp. + poorly-consolidated detrial reef materials

9.87 – 10.0 m Encrusting *Favites* sp. (KD-B2-5; 7412 cal yr BP) + poorly-consolidated detrial reef materials

### 4.4.3 Core B5

Core B5 was located nearer the landward margin of TII at an altitude of 2.1 m (Figs. 4.17 and 4.18). The total core length is 3 m, and the recovery ratio is approximately 79% (Fig. 4.18, 4.21 and Table 4.3). The interval 3-1.3 mbs consists of encrusting faviid corals, *Montipora* spp., *Acropora* spp. with well or moderately consolidated reef materials.The interval 1.3-0 mbs consists of thick-plate/encrusting and tabular *Acropora* spp., as well as massive and encrusting faviid corals with well-consolidated reef materials. Encrusting calcareous algae were not observed. The ages measured in core B5 range from 5385 cal yr BP to 2316 cal yr BP (Figs. 4.17a, 4.18, 4.21 and Table 1). Vertical growth rates were 1.3 m $kyr^{-1}$ between 5.4 and 4.5 ka, 1.1 m $kyr^{-1}$ between 4.5 and 3.3 ka, and 0.5 m $kyr^{-1}$ between 3.3 and 2.3 ka (Fig. 4.17a).

Description

0.00 – 0.09 m Encrusting *Goniastrea* sp. (KD-B5-1; 2316 cal yr BP).

0.09 – 0.14 m Well-consolidated detrital reef materials

0.14 – 0.15 m Encrusting *Acropora* sp.

0.15 – 0.17 m Well-consolidated detrital reef materials

0.17 – 0.18 m Encrusting *Acropora* sp.

0.18 – 0.29 m Well-consolidated detrital reef materials

0.29 – 0.66 m Thick-plate/encrusting *Acropora* sp. (KD-B5-2; 3274 cal yr BP)

0.66 – 0.84 m No recovery

0.84 – 0.87 m Tabular *Acropora* sp.

0.87 – 0.89 m Well-consolidated detrital reef materials

0.89 – 0.92 m Encrusting *Acropora* sp.

0.92 – 0.95 m Well-consolidated detrital reef materials.

0.95 – 0.98 m Encrusting *Acropora* sp.

0.98 – 1.00 m Rounded coral gravel

1.00 – 1.09 m Thick-plate/encrusting *Acropora* sp. (KD-B5-3; 3599 cal yr BP)

1.09 – 1.10 m Well-consolidated detrital reef materials

1.10 – 1.22 m Thick-plate/encrusting *Acropora* sp.

1.22 – 1.24 m Not in situ coral

1.24 – 1.27 m Not in situ coral + well-consolidated detrital reef materials

1.27 – 1.33 m Encrusting faviid coral + well-consolidated detrital reef materials

1.33 – 1.37 m Not in situ coral

1.37 – 1.39 m Well-consolidated detrital reef materials

1.39 – 1.46 m Tabular *Acropora* sp.

1.46 – 1.47 m Well-consolidated detrital reef materials

1.47 – 1.52 m Tabular *Acropora* sp.

1.52 – 1.61 m Unknown encrusting coral + well-consolidated detrital reef materials

1.61 – 1.62 m Well-consolidated detrital reef materials

1.62 – 1.66 m Encrusting *Acropora* sp.

1.66 – 1.73 m Encrusting *Montipora* sp. + consolidated detrital reef materials

1.73 – 1.78 m Encrusting *Montipora* sp.

1.78 – 1.84 m Thick-plate/encrusting *Acropora* sp. (KD-B5-4; 4459 cal yr BP)

1.84 – 1.88 m Fragments of consolidated detrital reef materials

1.88 – 1.90 m Not in situ coral

1.90 – 2.28 m No recovery

2.28 – 2.33 m Consolidated detrital reef materials + calcareous algae

2.33 – 2.36 m Unknown encrusting coral

2.36 – 2.40 m Encrusting *Montipora* sp.

2.40 – 2.54 m Encrusting *Montipora* sp.

2.54 – 2.60 m Encrusting *Acropora* sp.

2.60 – 2.66 m Encrusting *Acropora* sp.

2.66 – 2.71 m Encrusting *Platygyra* sp.

2.71 – 2.83 m No recovery

2.83 – 3.00 m Thick-plate/encrusting *Acropora* sp. (KD-B5-4; 5385 cal yr BP)

### 4.4.4 Core B6

Core B6 was located at the top of a reef mound with an elevation of 4.4 m, equivalent to that of the TI reef slope (Figs. 4.17 and 4.18). The total length is 3 m, and the recovery ratio is approximately 79% (Figs. 4.18, 4.22 and Table 4.3). The interval 3-2 mbs consists of encrusting faviid corals, such as *Montipora* spp., with consolidated reef materials and thinner encrusting calcareous algae. The interval 2-0 mbs consists of thick-plate/encrusting and tabular *Acropora* spp. as well as massive and encrusting faviid corals with well-consolidated reef materials. Encrusting calcareous algae were not observed in this part. The ages measured in core B6 range from 4820 cal yr BP to 3297 cal yr BP (Figs. 4, 17a, 4.18, 4.22 and Table 4.2). Vertical growth rates were 1.8 m $kyr^{-1}$ between 4.8 and 4.2 ka and 1.4 m $kyr^{-1}$ between 4.2 and 3.3 ka (Fig. 4.17a).

Description

0.00 – 0.15 m Encrusting *Goniastrea* sp. (KD-B6-1; 3297 cal yr BP) + well-consolidated detrital reef materials

0.15 – 0.17 m Well-consolidated detrital reef materials

0.17 – 0.27 m An massive faviid coral

0.27 – 0.29 m Well-consolidated detrital reef materials

0.29 – 0.42 m Fragments of well-consolidated detrital reef materials

0.42 – 0.63 m Well-consolidated detrital reef materials

0.63 – 0.70 m Tabular *Acropora* sp.

0.70 – 0.96 m Well-consolidated detrital reef materials

0.96 – 1.00 m Encrusting Acropora sp.

1.00 – 1.02 m Well-consolidated detrital reef materials

1.02 – 1.06 m Tabular *Acropora* sp.

1.06 – 1.09 m Not in situ corals

1.09 – 1.11 m Well-consolidated detrital reef materials

1.11 – 1.18 m Tabular *Acropora* sp.

1.18 – 1.42 m Massive *Favia* sp.

1.42 – 1.50 m No recovery

1.50 – 1.56 m Consolidated detrital reef materials

1.56 – 1.90 m Thick-plate/encrusting *Acropora* sp. (KD-B6-3; 4160 cal yr BP)

1.90 – 1.92 m Consolidated detrital reef materials

1.92 – 1.99 m Tabular *Acropora* sp.

1.99 – 2.00 m Consolidated detrital reef materials

2.00 – 2.05 m Encrusting *Echinopora* sp.

2.05 – 2.18 m No recovery

2.18 – 2.23 m Not in situ coral

2.23 – 2.26 m Consolidated detrital reef materials

2.26 – 2.27 m Not in situ coral

2.27 – 2.37 m Consolidated detrital reef material + encrusting calcareous algae

2.37 – 2.43 m Encrusting *Montastrea* sp. (KD-B6-4; 4820 cal yr BP)

2.43 – 2.54 m No recovery

2.54 – 2.62 m Not in situ coral

2.62 – 3.00 m No recovery

### 4.4.5 Core B7

Core B7 was located at the landward margin of TII at an elevation of 1.9 m, equivalent to that of a groove top (Figs. 4.17 and 4.18). The total core length is 3 m, and the recovery ratio is approximately 87% (Figs. 4.18, 4.23 and Table 4.3). The interval 3-2.1 mbs consists of massive faviid coral, encrusting *Montipora* spp., *Acropora* spp. and *Porites* sp., with consolidated reef materials and rounded coral gravels. The interval 2.1-0.1 mbs consists of not in situ corals, well-rounded coral gravels and consolidated reef materials with encrusting calcareous algae. The core is capped by a 10-cm thick in situ thick-plate/encrusting *Acropora* sp. The ages measured in core B7 range from 5479 cal yr BP to 2227 cal yr BP (Figs. 4.17a, 4.18, 4.22 and Table 4.2). Vertical growth rates were 0.3 m $kyr^{-1}$ between 5.5 and 2.5 ka

and 8.7 m $kyr^{-1}$ between 2.5 and 2.2 ka (Fig. 4.17a).

Description

0.00 – 0.09 m Thick-plate/encrusting *Acropora* sp.(KD-B7-1; 2227 cal yr BP)

0.09 – 0.13 m Consolidated detrital reef materials

0.13 – 0.30 m Well-rounded coral gravels

0.30 – 0.33 m Consolidated detrital reef materials

0.33 – 0.52 m Not in situ coral (*Acropora* sp.; KD-B7-2; 3037 cal yr BP)

0.52 – 0.55 m Consolidated detrital reef materials

0.55 – 0.60 m Encrusting *Acropora* sp. + encrusting calcareous algae

0.60 – 0.77 m No recovery

0.77 – 0.86 m Consolidated detrital reef materials

0.86 – 1.00 m Consolidated detrital reef materials + encrusting calcareous algae

1.00 – 1.24 m Well-rounded coral gravels

1.24 – 1.27 m Fragments of consolidated detrital reef materials

1.27 – 1.35 m Not in situ coral

1.35 – 1.51 m Not in situ coral (*Favites* sp.; KD-B7-3; 2266 cal yr BP)

1.51 – 1.52 m Consolidated detrital reef materials + encrusting calcareous algae

1.52 – 1.70 m No recovery

1.70 – 2.10 m Rounded coral gravels + consolidated detrital reef materials

2.10 – 2.15 m Encrusting *Montipora* sp. (KD-B7-4; 2468)

2.15 – 2.37 m Well-consolidated detrital reef materials

2.37 – 2.45 m Well-consolidated detrital reef materials + rounded coral gravels

2.45 – 2.49 m Rounded coral gravel

2.49 – 2.55 m Consolidated detrital reef materials

2.55 – 2.58 m Encrusting unknown coral

2.58 – 2.63 m No recovery

2.63 – 2.72 m Encrusting *Acropora* sp.

2.72 – 2.74 m Encrusting *Montipora* sp.

2.74 – 2.78 m Encrusting *Montipora* sp.

2.78 – 2.81 m Rounded coral gravels

2.81 – 2.89 m Encrusting *Porites* sp.

2.81 – 2.92 m Encrusting *Montipora* sp.

2.92 – 2.93 m An encrusting unknown coral

2.92 – 3.00 m Massive *Favia* sp. (KD-B7-5; 5479 cal yr BP)

### 4.4.6 Core B3

Core B3 was located at the edge of TI at an elevation of 7.2 m (Figs. 4.17 and 4.18). The total core length is 14 m, and the recovery ratio is approximately 79.5% (Figs. 4.18, 4.24 and Table 4.3). The interval 14-5.8 mbs consists of encrusting *Goniopora* spp., encrusting and tabular *Acropora* spp., encrusting and foliaceous faviid corals and *Montipora* spp. The corals are embedded in a poorly consolidated brownish reef material composed of debris of marine organisms, such as foraminifera, shells, and mollusks and basement rock. The proportion of mud, sand, and gravel derived from the basement rock increases gradually down the length of the core. The interval 5.8-2.3 mbs consists of massive *Porites* spp. and thick-plate/encrusting and tabular *Acropora* spp. with poorly consolidated reef materials and well-rounded branching coral debris. The interval 2.3-0 mbs consists of thick-plate/encrusting and tabular *Acropora* spp., encrusting faviid corals, and ramose *Pocillopora* spp. with well-consolidated reef materials. Encrusting calcareous algae up to 1 cm in thickness were commonly observed in this part. The ages measured in core B3 range from 7927 cal yr BP to 2858 cal yr BP (Figs. 4.17, 4.18, 4.24 and Table 4.2). Vertical growth rates were 3.3 m $kyr^{-1}$ between 7.9 and 5.9 ka, 1.9 m $kyr^{-1}$ between 5.9 and 4.3 ka, and 2.2 m $kyr^{-1}$ between 4.3 and 2.9 ka (Fig. 4.17).

Description

0.00 – 0.16 m Thick-plate/encrusting *Acropora* sp. (KD-B3-1; 2858 cal yr BP) + well-consolidated detrital reef materials with calcareous algae

0.16 – 0.71 m Ramose *Pocillopora* spp. + encrusting *Acropora* spp. + well-consolidated detrital reef materials + calcareous algae

0.71 – 0.85 m Thick-plate/encrusting *Acropora* sp. + well-consolidated detrital reef

materials

0.85 – 0.91 m Thick-plate/encrusting *Acropora* sp. + well-consolidated detrital reef materials with calcareous algae

0.91 – 0.96 m Thick-plate/encrusting *Acropora* sp. + well-consolidated detrital reef materials

0.96 – 1.01 m Well-consolidated detrital reef materials

1.01 – 1.05 m Massive *Favia* sp.

1.05 – 1.13 m Massive *Platygyra* sp. + well-consolidated detrital reef materials

1.13 – 1.31 m Thick-plate/encrusting *Acropora* sp. + well-consolidated detrital reef materials

1.31 – 1.45 m Well-consolidated detrital reef materials with calcareous algae

1.45 – 1.50 m Tabular *Acropora* sp.

1.50 – 1.59 m Massive Favia sp. + well-consolidated detrital reef materials with calcareous algae

1.59 – 1.64 m Fragments of corals and consolidated detrital reef materials

1.64 – 1.75 m Tabular and encrusting *Acropora* sp. + well-consolidated detrital reef materials with calcareous algae

1.75 – 1.94 m Thick-plate/encrusting *Acropora* sp.

1.94 – 1.96 m Calcareous sands

1.96 – 2.02 m Encrusting *Goniastrea* sp.

2.02 – 2.10 m Tabular *Acropora* sp. + well-consolidated detrital reef materials

2.10 – 2.17 m Encrusting *Goniastrea* sp.

2.17 – 2.20 m Well-consolidated detrital reef materials

2.20 – 2.24 m No recovery

2.24 – 2.31 m Encrusting *Favites* sp. + consolidated detrital reef materials with calcareous algae

2.31 – 2.42 m Encrusting *Montipora* sp. + consolidated detrital reef materials

2.42 – 2.46 m Consolidated detrital reef materials with calcareous algae

2.46 – 2.56 m Tabular *Acropora* sp. + consolidated detrital reef materials

2.56 – 2.65 m Fragments of corals and consolidated detrital reef materials

2.65 – 2.75 m Tabular *Acropora* sp. + consolidated detrital reef material

2.75 – 2.83 m Rounded coral gravels

2.83 – 3.02 m Thick-plate/encrusting *Acropora* sp.

3.02 – 3.21 m Not in situ thick-plate/encrusting *Acropora* sp.

3.21 – 3.34 m Not in situ *Favites* sp.

3.34 – 3.39 m Rounded coral gravels

3.39 – 3.65 m Massive *Porites* sp. (KD-B3-2; 4344 cal yr BP)

3.65 – 3.75 m No recovery

3.75 – 3.79 m Encrusting *Acropora* sp. + consolidated detrital reef materials with calcareous algae

3.79 – 3.85 m Encrusting *Montipora* sp.

3.85 – 4.34 m Fragments of corals and consolidated detrital reef materials

4.34 – 4.47 m Thick-plate/encrusting *Acropora* sp.

4.47 – 4.59 m Rounded coral gravels

4.59 – 4.67 m Encrusting *Goniopora* sp. + consolidated detrital reef materials with terrigenous sands and gravels

4.67 – 4.77 m Encrusting *Acropora* sp.

4.77 – 4.81 m Encrusting *Favites* sp.

4.81 – 4.90 m Fragments of branching corals and consolidated detrital reef materials with terrigenous sands and gravels

4.90 – 4.96 m Tabular *Acropora* sp. + consolidated detrital reef materials with terrigenous sands and gravels

4.96 – 5.05 m Fragments of consolidated detrital reef materials with terrigenous sands and gravels and shells

5.05 – 5.16 m Thick-plate/encrusting *Acropora* sp.

5.16 – 5.59 m Thick-plate/encrusting *Acropora* sp.

5.59 – 5.77 m Consolidated detrital reef materials with terrigenous mud, sands and gravels

5.77 – 5.90 m Massive *Favia* sp. + poorly-consolidated detrital reef materials with terrigenous mud, sands and gravels

5.90 – 6.04 m Fragments of poorly-consolidated detrital reef materials with terrigenous mud, sands and gravels

6.04 – 6.18 m Tabular *Acropora* sp. + poorly-consolidated detrital reef materials with terrigenous mud, sands and gravels

6.18 – 6.23 m Encrusting *Goniopora* sp. + poorly-consolidated detrital reef materials with terrigenous mud, sands and gravels

6.23 – 6.28 m Encrusting *Goniopora* sp

6.28 – 6.33 m Encrusting *Goniopora* sp. + poorly-consolidated detrital reef materials with terrigenous mud, sands and gravels

6.33 – 6.40 m Poorly-consolidated detrital reef materials with terrigenous mud, sands and gravels

6.40 – 6.47 m Encrusting *Montipora* sp. + poorly-consolidated detrital reef materials with terrigenous mud, sands and gravels

6.47 – 6.59 m Encrusting *Goniopora* sp. (KD-B3-3; 5945 cal yr BP)

6.59 – 6.79 m Encrusting *Montipora* sp. + poorly-consolidated detrital reef materials with terrigenous mud, sands and gravels

6.79 – 6.95 m Encrusting *Montipora* sp. + encrusting *Goniopora* spp. + poorly-consolidated detrital reef materials with terrigenous mud, sands and gravels

6.95 – 7.04 m Encrusting *Goniopora* sp. + poorly-consolidated detrital reef materials with terrigenous mud, sands and gravels

7.04 – 7.13 m Tabular *Acropora* sp. + poorly-consolidated detrital reef materials with terrigenous mud, sands and gravels

7.13 – 7.17 m Tabular *Acropora* sp.

7.17 – 7.23 m Poorly-consolidated detrital reef materials with terrigenous mud, sands and gravels

7.23 – 7.45 m Massive *Goniopora* sp. + massive *Favia* sp.

7.45 – 7.62 m Poorly-consolidated detrital reef materials with terrigenous mud, sands and gravels

7.62 – 7.66 m Encrusting *Goniopora* sp. + encrusting *Goniastrea* sp. + poor-

ly-consolidated detrital reef materials with terrigenous mud, sands and gravels

7.66 – 7.71 m Encrusting *Favites* sp.

7.71 – 7.76 m Poorly-consolidated detrital reef materials with terrigenous mud, sands and gravels

7.76 – 7.84 m Encrusting *Goniopora* sp.

7.84 – 7.87 m Fragments of poorly-consolidated detrital reef materials with terrigenous mud, sands and gravels

7.87 – 7.94 m Encrusting *Favites* sp.

7.94 – 7.96 m Fragments of poorly-consolidated detrital reef materials with terrigenous mud, sands and gravels

7.96 – 8.00 m Not in situ faviid coral

8.00 – 8.08 m Fragments of poorly-consolidated detrital reef materials with terrigenous mud, sands and gravels

8.08 – 8.12 m Branching *Acropora* sp. + poorly-consolidated detrital reef materials with terrigenous mud, sands and gravels

8.12 – 8.21 m Encrusting *Montipora* sp. + poorly-consolidated detrital reef materials with terrigenous mud, sands and gravels

8.21 – 8.25 m Fragments of branching corals

8.25 – 8.40 m Encrusting *Goniopora* spp. + poorly-consolidated detrital reef materials with terrigenous mud, sands and gravels

8.40 – 8.49 m Fragments of branching corals + poorly-consolidated detrital reef materials with terrigenous mud, sands and gravels

8.49 – 8.53 m Encrusting *Gonipora* sp. + branching *Caulastrea* sp. + poorly-consolidated detrital reef materials with terrigenous mud, sands and gravels

8.53 – 8.70 m Encrusting *Acropora* sp. + encrusting *Goniopora* sp. + poorly-consolidated detrital reef materials with terrigenous mud, sands and gravels

8.70 – 8.91 m Fragments of poorly-consolidated detrital reef materials with

terrigenous mud, sands and gravels

8.91 – 9.08 m Encrusting *Montipora* sp. + poorly-consolidated detrital reef materials with terrigenous mud, sands and gravels

9.08 – 9.17 m Encrusting *Montipora* sp. + poorly-consolidated detrital reef materials with terrigenous mud, sands and gravels

9.17 – 9.49 m Encrusting *Acropora* spp. + encrusting *Goniopora* sp. + poorly-consolidated detrital reef materials with terrigenous mud, sands and gravels

9.49 – 9.54 m Massive *Favia* sp. (KD-B3-4; 7048) + poorly-consolidated detrital reef materials with terrigenous mud, sands and gravels

9.54 – 9.58 m Tabular *Acropora* sp.

9.58 – 9.93 m Poorly-consolidated detrital reef materials with terrigenous mud, sands and gravels

9.93 – 9.96 m No recovery

9.96 – 10.37 m Encrusting *Acropora* spp. + poorly-consolidated detrital reef materials with terrigenous mud, sands and gravels

10.37 – 10.44 m No recovery

10.44 – 10.60 m Tabular *Acropora* spp. + poorly-consolidated detrital reef materials with terrigenous mud, sands and gravels

10.60 – 10.77 m No recovery

10.77 – 10.83 m Tabular *Acropora* sp. + Poorly-consolidated detrital reef materials with terrigenous mud, sands and gravels

10.83 – 10.92 m Fragments of poorly-consolidated detrital reef materials with terrigenous mud, sands and gravels

10.92 – 11.00 m Encrusting *Goniopora* sp. + poorly-consolidated detrital reef materials with terrigenous mud, sands and gravels

11.00 – 11.07 m Fragments of poorly-consolidated detrital reef materials with terrigenous mud, sands and gravels

11.07 – 11.35 m Foliaceous *Echinopora* spp. + poorly-consolidated detrital reef materials with terrigenous mud, sands and gravels

11.35 – 12.00 m No recovery

12.00 – 12.15 m Encrusting *Montipora* spp. + poorly-consolidated detrital reef materials with terrigenous mud, sands and gravels

12.15 – 12.20 m Poorly-consolidated detrital reef materials with terrigenous mud, sands and gravels

12.20 – 12.31 m Unknown encrusting corals + poorly-consolidated detrital reef materials with terrigenous mud, sands and gravels

12.31 – 12.34 m Fragments of poorly-consolidated detrital reef materials with terrigenous mud, sands and gravels

12.34 – 12.42 m Encrusting *Acropora* spp. + Poorly-consolidated detrital reef materials with terrigenous mud, sands and gravels

12.42 – 12.46 m Encrusting *Acropora* spp.

12.46 – 12.59 m Poorly-consolidated detrital reef materials with terrigenous mud, sands and gravels with shells

12.59 – 12.64 m Encrusting *Goniopora* sp.

12.64 – 12.95 m No recovery

12.95 – 13.03 m Encrusting *Goniopora* spp. + poorly-consolidated detrital reef materials with terrigenous mud, sands and gravels

13.03 – 13.07 m Fragments of poorly-consolidated detrital reef materials with terrigenous mud, sands and gravels

13.07 – 13.09 m Poorly-consolidated detrital reef materials with terrigenous mud, sands and gravels

13.09 – 13.13 m Encrusting *Goniopora* sp. (KD-B3-6; 7927 cal yr BP)

13.13 – 13.19 m Poorly-consolidated detrital reef materials with terrigenous mud, sands and gravels

13.19 – 13.33 m Fragments of poorly-consolidated detrital reef materials with terrigenous mud, sands and gravels

13.33 – 13.39 m Encrusting *Acropora* sp. + poorly-consolidated detrital reef materials with terrigenous mud, sands and gravels

13.39 – 14.00 m No recovery

### 4.4.7 Core B4

Core B4 was located at the center of the reef flat on TI (Figs. 4.17 and 4.18). The total core length is 9 m, and the recovery ratio is approximately 92% (Figs. 4.18, 4.25 and Table 4.3). The interval 9-8.1 mbs consists of basement rock. The depth interval 8.1-7.8 mbs consists of gravel derived from the basement rock. The interval 7.8-5.2 consists of massive and branching *Hydnophora* spp., branching *Caulastrea* spp., and unknown encrusting and foliaceous corals. Corals in this interval are almost completely recrystallized. The interval 5.1-3.5 mbs consists of encrusting *Goniopora* spp., encrusting and tabular *Acropora* spp., encrusting and foliaceous faviid corals, and *Montipora* spp. with poorly consolidated brownish reef materials. The proportion of mud, sand, and gravel derived from the basement rock increases gradually down the length of the core. The interval 3.5-0 mbs consists of thick-plate/encrusting and tabular *Acropora* spp. with well-consolidated reef materials with terrigenous mud and sands. The ages measured in core B3 range from 7604 cal yr BP to 2543 cal yr BP (Figs. 4.17, 4.18, 4.25 and Table 4.2). Vertical growth rates were 1.3 m $kyr^{-1}$ between 7.6 and 5.9 ka and 0.7 m $kyr^{-1}$ between 5.9 and 2.5 ka (Fig. 4.17).

Description

0.00 – 0.11 m Thick-plate/encrusting *Acropora* sp. (KD-B4-1; 2543 cal yr BP)

0.11 – 0.23 m Thick-plate/encrusting *Acropora* sp.

0.23 – 0.42 m Thick-plate/encrusting *Acropora* sp.

0.42 – 0.47 m Well-consolidated detrital reef materials

0.47 – 0.51 m Tabular *Acropora* sp.

0.51 – 0.53 m Debris of corals

0.53 – 0.54 m Well-consolidated detrital reef materials

0.54 – 0.66 m Thick-plate/encrusting *Acropora* sp.

0.66 – 0.74 m Tabular *Acropora* sp. + encrusting calcareous algae

0.74 – 0.82 m Ramose *Pocillopora* sp. + consolidated detrital reef materials with terrigenous mud, sands and gravels

0.82 – 0.90 m Tabular *Acropora* sp. + consolidated detrital reef materials with terrigenous mud and sands

0.90 – 0.93 m Consolidated detrital reef materials with terrigenous mud and sands

0.93 – 1.00 m Tabular *Acropora* sp. + well-consolidated detrital reef materials with terrigenous mud and sands

1.00 – 1.04 m Well-consolidated detrital reef materials with terrigenous mud and sands

1.04 – 1.16 m Thick-plate/encrusting *Acropora* sp.

1.16 – 1.20 m Well-consolidated detrital reef materials with terrigenous mud and sands

1.20 – 1.24 m Tabular *Acropora* sp.

1.24 – 1.30 m Well-consolidated detrital reef materials with terrigenous mud and sands

1.30 – 1.35 m Thick-plate/encrusting *Acropora* sp. (KD-B4-2; 5870 cal yr BP)

1.35 – 1.67 m Well-consolidated detrital reef materials with terrigenous mud and sands with rounded coral gravels

1.67 – 1.75 m Encrusting *Cyphastrea* spp. + encrusting calcareous algae

1.75 – 1.92 m Well-consolidated detrital reef materials with terrigenous mud and sands with rounded coral gravels

1.92 – 1.94 m Encrusting calcareous algae + well-consolidated detrital reef materials with terrigenous mud and sands

1.94 – 2.00 m Well-consolidated detrital reef materials with terrigenous mud and sands with encrusting unknown corals

2.00 – 2.04 m Encrusting *Acropora* sp. + encrusting calcareous algae

2.04 – 2.06 m Tabular *Acropora* sp.

2.06 – 2.11 m Well-consolidated detrital reef materials with terrigenous mud and sands with encrusting unknown corals

2.11 – 2.23 m Thick-plate/encrusting *Acropora* sp. (KD-B4-3; 5945 cal yr BP) + well-consolidated detrital reef materials with terrigenous mud and

sands

2.23 – 2.34 m Well-consolidated detrital reef materials with terrigenous mud and sands

2.34 – 2.37 m Tabular *Acropora* sp.

2.37 – 2.49 m Well-consolidated detrital reef materials with terrigenous mud and sands

2.49 – 2.52 m Tabular *Acropora* sp.

2.52 – 2.59 m Well-consolidated detrital reef materials with terrigenous mud and sands

2.59 – 2.63 m Tabular *Acropora* sp.

2.63 – 2.70 m Well-consolidated detrital reef materials with terrigenous mud and sands

2.70 – 2.77 m Not in situ coral + well-consolidated detrital reef materials with terrigenous mud and sand

2.77 – 2.80 m Well-consolidated detrital reef materials with terrigenous mud and sands

2.80 – 2.86 m Tabular *Acropora* sp. + well-consolidated detrital reef materials with terrigenous mud and sands

2.86 – 2.89 m Well-consolidated detrital reef materials with terrigenous mud and sands

2.89 – 2.94 m Encrusting unknown corals and encrusting calcareous algae

2.94 – 3.09 m Well-consolidated detrital reef materials with terrigenous mud and sands

3.09 – 3.11 m Tabular *Acropora* sp.

3.11 – 3.14 m Well-consolidated detrital reef materials with terrigenous mud and sands

3,14 – 3.15 m Tabular *Acropora* sp.

3.15 – 3.19 m Tabular *Acropora* sp. + encrusting calcareous algae

3.19 – 3.23 m Not in situ coral

3.23 – 3.33 m Consolidated detrital reef materials with terrigenous mud, sands

and gravels

3.33 – 3.37 m Tabular *Acropora* sp. (KD-B4-4; 7604 cal yr BP)

3.37 – 3.45 m Consolidated detrital reef materials with terrigenous mud and sands

3.45 – 3.49 m Tabular *Acropora* sp.

3.49 – 4.02 m Poorly-consolidated detrital reef materials with terrigenous mud, sands and gravels

4.02 – 4.08 m Encrusting *Goniopora* sp.

4.08 – 4.11 m Encrusting *Goniopora* sp.

4.11 – 4.13 m Poorly-consolidated detrital reef materials with terrigenous mud, sands and gravels

4.13 – 4.24 m Poorly-consolidated detrital reef materials with terrigenous mud, sands and gravels + encrusting calcareous algae

4.24 – 4.27 m Encrusting *Goniopora* sp. + encrusting calcareous algae

4.27 – 4.29 m Poorly-consolidated detrital reef materials with terrigenous mud, sands and gravels

4.29 – 4.31 m Unknown encrusting coral + encrusting calcareous algae

4.31 – 4.42 m Poorly-consolidated detrital reef materials with terrigenous mud, sands and gravels

4.79 – 4.80 m Encrusting *Goniopora* spp. + encrusting unknown corals + poorly-consolidated detrital reef materials with terrigenous mud, sands and gravels

4.80 – 4.82 m Blackish poorly-consolidated sediments

4.82 – 4.87 m Poorly-consolidated detrital reef materials with terrigenous mud, sands and gravels

4.87 – 4.91 m Unknown encrusting corals

4.91 – 4.94 m Fragments of Poorly-consolidated detrital reef materials with terrigenous mud, sands and gravels

4.94 – 5.06 m Poorly-consolidated detrital reef materials with terrigenous mud, sands and gravels

5.06 – 5.12 m Unknown encruating coral + encrusting calcareous algae + blackish poorly-consolidated sediments

5.12 – 5.18 m Blackish poorly-consolidated sediments

5.18 – 5.20 m Poorly-consolidated detrital reef materials with terrigenous mud, sands and gravels

5.20 – 5.22 m Unknown encrusting coral

5.22 – 5.43 m Massive *Hydonophora* sp.

5.43 – 5.47 m Poorly-consolidated detrital reef materials with terrigenous mud, sands and gravels

5.47 – 5.65 m Branching *Caulastrea* sp.

5.65 – 5.69 m Poorly-consolidated detrital reef materials with terrigenous mud, sands and gravels

5.69 – 5.71 m Unknown foliaceous coral + detrital reef materials with terrigenous mud, sands and gravels

5.86 – 5.91 m Branching *Caulastrea* sp.

5.91 – 5.97 m Poorly-consolidated detrital reef materials with terrigenous mud, sands and gravels

5.97 – 6.00 m Encrusting *Goniopora* sp.

6.00 – 6.08 m Unknown foliaceous coral + poorly-consolidated detrital reef materials with terrigenous mud, sands and gravels

6.08 – 6.10 m Poorly-consolidated detrital reef materials with terrigenous mud, sands and gravels

6.10 – 6.11 m Unknown encrusting coral

6.11 – 6.26 m Massive *Hydonophora* sp.

6.26 – 6.31 m Unknown foliaceous coral + poorly-consolidated detrital reef materials with terrigenous mud, sands and gravels

6.31 – 6.32 m Poorly-consolidated detrital reef materials with terrigenous mud, sands and gravels

6.32 – 6.38 m Fragments of corals and poorly-consolidated detrital reef materials with terrigenous mud, sands and gravels

6.38 – 6.54 m Unknown foliaceous coral + poorly-consolidated detrital reef materials with terrigenous mud, sands and gravels

6.54 – 6.57 m Unknown foliaceous coral

6.57 – 6.65 m Unknown foliaceous coral

6.65 – 6.82 m Unknown encrusting and foliaceous corals + poorly-consolidated detrital reef materials with terrigenous mud, sands and gravels

6.82 – 6.90 m No recovery

6.90 – 6.92 m Unknown foliaceous coral

6.92 – 6.97 m Massive *Hydonophora* sp.

6.97 – 7.04 m Unknown foliaceous corals + poorly-consolidated detrital reef materials with terrigenous mud, sands and gravels

7.04 – 7.12 m Unknown massive or encrusting coral

7.12 – 7.14 m Poorly-consolidated detrital reef materials with terrigenous mud, sands and gravels

7.14 – 7.76 m Fragments of poorly-consolidated detrital reef materials with terrigenous mud, sands and gravels (almost no recovery)

7.76 – 8.00 m Gravel derived from basement rock (Tertiary Tuff)

8.00 – 8.11 m Gravels from basement rock + poorly-consolidated sediments

8.11 – 9.00 m Tertiary Tuff (Basement rock)

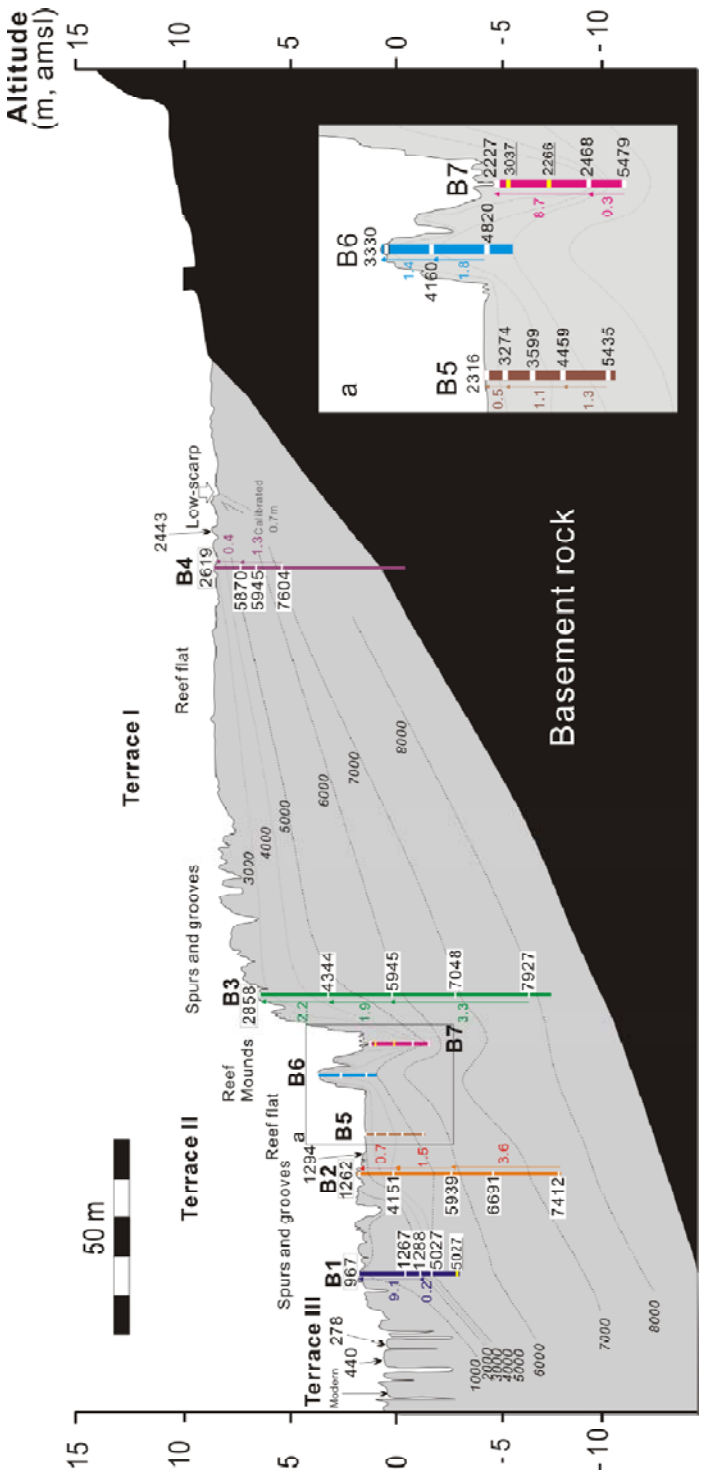


Fig. 4.17 Cross-section of the drilling transect. The colored bars show the cores. All of the AMS radiocarbon ages are shown for each core. The ages of the reworked corals are underlined. The numbers by the cores indicate the vertical growth rates (m kys$^{-1}$). The altitude of the seaward side from the low scarp is calibrated to +0.7 m (see text). (a) A detailed image of the inner part of Terrace II.

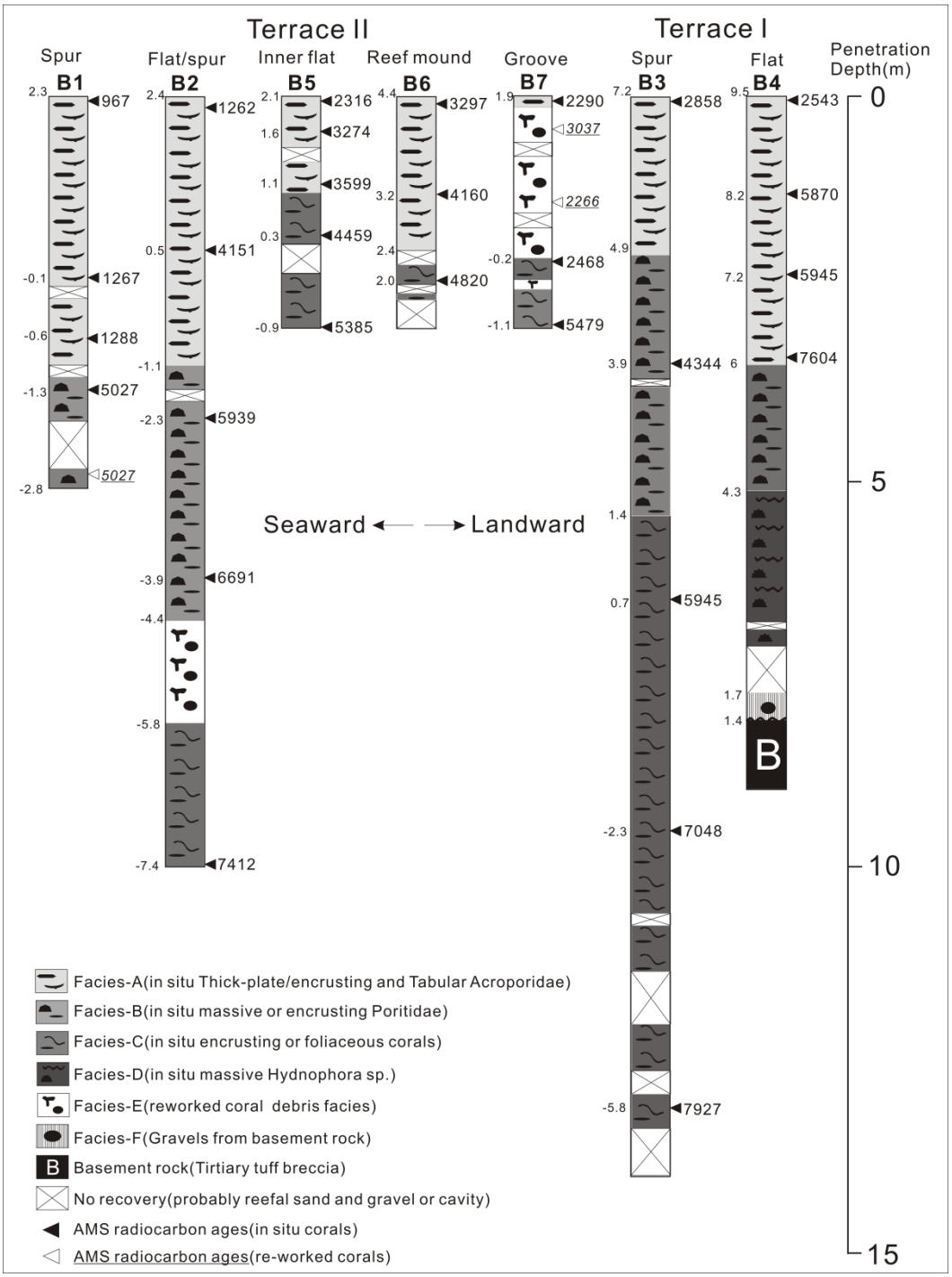


Fig. 4.18 Schematic showing the distribution of facies and AMS radiocarbon ages in the cores. The numbers to the left of the cores indicate their altitude (m, above or below msl).

Table 4.2 AMS radiocarbon ages from drilling cores and terraces surface on Kodakara Island

| Sample No. | Genus | Coral morphology | Conv.age (yr B.P.) | Calib. age (cal yr B.P.) | 1σ range (cal yr B.P.) | 2σ range (cal yr B.P.) | Locality | Altitude (m) |
|---|---|---|---|---|---|---|---|---|
| KD-B1-1 | *Acropora* sp. | T-P/E | 1450±30 | 967 | 920-1003 | 896-1054 | B1 core | 2.3 |
| KD-B1-2 | *Acropora* sp. | T-P/E | 1740±30 | 1267 | 1233-1299 | 1180-1334 | B1 core | -0.1 |
| KD-B1-3 | *Porites sp.* | Massive | 4800±30 | 5027 | 4948-5087 | 4887-5206 | B1 core | -1.3 |
| KD-B1-4 | *Porites sp.* | *(Gravel)* | 4800±30 | 5027 | 4948-5087 | 4887-5206 | B1 core | -2.4 |
| KD-B1-5 | *Acropora* sp. | T-P/E | 1765±50 | 1288 | 1240-1339 | 1173-1390 | B1 core | -0.6 |
| KD-B2-1 | *Acropora* sp. | T-P/E | 1740±85 | 1262 | 1171-1344 | 1060-1466 | B2 core | 2.4 |
| KD-B2-2 | *Acropora* sp. | T-P/E | 4130±30 | 4151 | 4090-4210 | 4016-4280 | B2 core | 0.5 |
| KD-B2-3 | *Acropora* sp. | Tabular | 5575±95 | 5939 | 5836-6088 | 5708-6176 | B2 core | -2.1 |
| KD-B2-4 | *Porites* sp. | Massive | 6270±40 | 6691 | 6633-6743 | 6564-6804 | B2 core | -3.9 |
| KD-B2-5 | *Favites sp.* | Encrusting | 6930±75 | 7412 | 7333-7481 | 7267-7551 | B2 core | -7.4 |
| KD-B3-1 | *Acropora* sp. | T-P/E | 3090±160 | 2858 | 2677-3078 | 2425-3265 | B3 core | 7.2 |
| KD-B3-2 | *Porites* sp. | Massive | 4270±40 | 4344 | 4280-4409 | 4211-4488 | B3 core | 3.9 |
| KD-B3-3 | *Goniopora* sp. | Encrusting | 5580±85 | 5945 | 5850-6065 | 5734-6166 | B3 core | 0.8 |
| KD-B3-4 | *Favia* sp. | Massive | 6560±40 | 7048 | 6989-7123 | 6920-7160 | B3 core | -2.3 |
| KD-B3-6 | *Goniopora* sp. | Encrusting | 7495±110 | 7927 | 7799-8037 | 7690-8158 | B3 core | -5.8 |
| KD-B4-1 | *Acropora* sp. | T-P/E | 2825±40 | 2543 | 2466-2616 | 2374-2686 | B4 core | 9.5 |
| KD-B4-2 | *Acropora* sp. | T-P/E | 5520±110 | 5870 | 5722-5988 | 5627-6151 | B4 core | 8.2 |
| KD-B4-3 | *Acropora* sp. | T-P/E | 5585±45 | 5945 | 5885-5992 | 5838-6108 | B4 core | 7.2 |
| KD-B4-4 | *Acropora* sp. | Tabular | 7160±40 | 7604 | 7564-7645 | 7510-7686 | B4 core | 6 |
| KD-B5-1 | *Goniastrea* sp. | Encrusting | 2660±45 | 2316 | 2252-2392 | 2157-2452 | B5 core | 2.1 |
| KD-B5-2 | *Acropora* sp. | T-P/E | 3400±50 | 3274 | 3178-3321 | 3077-3364 | B5 core | 1.6 |
| KD-B5-3 | *Acropora* sp. | T-P/E | 3715±50 | 3599 | 3528-3678 | 3446-3754 | B5 core | 1.1 |
| KD-B5-4 | *Acropora* sp. | T-P/E | 4355±145 | 4459 | 4252-4654 | 4065-4835 | B5 core | 0.3 |
| KD-B5-5 | *Acropora* sp. | T-P/E | 5060±55 | 5385 | 5309-5443 | 5271-5542 | B5 core | -0.9 |
| KD-B6-1 | *Goniastrea sp.* | Encrusting | 3450±45 | 3297 | 3239-3357 | 3163-3413 | B6 core | 4.4 |
| KD-B6-3 | *Acropora* sp. | T-P/E | 4135±60 | 4160 | 4064-4259 | 3969-4358 | B6 core | 3.2 |
| KD-B6-4 | *Montastrea* sp. | Encrusting | 4630±50 | 4820 | 4730-4747 | 4645-4961 | B6 core | 2 |
| KD-B7-1 | *Acropora* sp. | T-P/E | 2585±40 | 2227 | 2172-2295 | 2115-2328 | B7 core | 1.9 |
| KD-B7-2 | *Acropora* sp. | *(Gravel)* | 3250±45 | 3037 | 2954-3115 | 2884-3194 | B7 core | 1.6 |
| KD-B7-3 | Favites sp. | *(Gravel)* | 2625±60 | 2266 | 2178-2335 | 2105-2441 | B7 core | 0.7 |
| KD-B7-4 | *Montipora* sp. | Encrusting | 2770±50 | 2468 | 2345-2529 | 2327-2654 | B7 core | -0.2 |
| KD-B7-5 | *Favia sp.* | Massive | 5140±50 | 5479 | 5435-5558 | 5329-5573 | B7 core | -1.1 |
| KD-I-2 | *Acropora* sp. | T-P/E | 2745±120 | 2443 | 2303-2610 | 2137-2725 | Terrace I | 9.5 |
| KD-II-2 | *Acropora* sp. | T-P/E | 1770±80 | 1294 | 1215-1378 | 1125-1487 | Terrace II | 2.3 |
| KD-III-1 | *Acropora* sp. | T-P/E | 830±40 | 440 | 406-491 | 323-505 | Terrace III | 1 |
| KD-III-2 | *Acropora* sp. | T-P/E | 660±45 | 278 | 231-362 | 137-406 | Terrace III | 1.1 |
| KD-III-3 | *Acropora* sp. | T-P/E | 385±50 | Modern | Modern | Modern | Terrace III | 0.7 |

Table 4.3 Penetration depth and recovery ratio of cores

| Core No. | Penetration Depth(cm) | Recovery (cm) | Recovery Ratio(%) | Total Recovery Ratio(%) |
|---|---|---|---|---|
| B1 | 0-101 | 101 | 100 | |
| | 101-140 | 40 | 97.5 | |
| | 140-145 | 0 | 0 | |
| | 145-176 | 32 | 100+ | |
| | 176-194 | 13 | 72.2 | |
| | 194-245 | 51 | 100 | |
| | 245-262 | 0 | 0 | |
| | 262-271 | 9 | 100 | |
| | 271-300 | 14 | 48.2 | |
| | 300-345 | 44 | 97.8 | |
| | 345-364 | 8 | 42.1 | |
| | 364-395 | 31 | 100 | |
| | 395-400 | 5 | 100 | |
| | 400-420 | 15 | 75 | |
| | 420-428 | 0 | 0 | |
| | 428-493 | 10.5 | 16.2 | |
| | 493-508 | 10 | 66.7 | 75% |
| B2 | 0-62 | 62 | 100 | |
| | 62-65 | 0 | 0 | |
| | 65-81 | 16 | 100 | |
| | 81-180 | 99 | 100 | |
| | 180-257 | 76.5 | 99.4 | |
| | 257-262 | 4 | 80 | |
| | 262-280 | 15 | 83.3 | |
| | 280-380 | 98.5 | 98.5 | |
| | 380-440 | 58 | 96.7 | |
| | 440-460 | 0 | 0 | |
| | 460-469 | 7 | 77.8 | |
| | 469-480 | 10.5 | 95.5 | |
| | 480-580 | 94 | 94 | |
| | 580-662 | 75 | 91.5 | |
| | 662-668 | 0 | 0 | |
| | 668-680 | 10 | 83.3 | |
| | 680-800 | 17 | 14.2 | |
| | 800-823 | 19 | 82.6 | |
| | 823-840 | 10 | 58.8 | |
| | 840-860 | 14 | 70 | |
| | 860-897 | 8 | 21.6 | |
| | 897-900 | 3 | 100 | |
| | 900-902 | 2 | 100 | |
| | 902-1000 | 94 | 95.9 | 79% |

| Core No. | Penetration Depth(cm) | Recovery (cm) | Recovery Ratio(%) | Total Recovery Ratio(%) |
|---|---|---|---|---|
| B3 | 0-96 | 96 | 100 | |
| | 96-130 | 34 | 100 | |
| | 130-175 | 44 | 97.8 | |
| | 175-220 | 41 | 91.1 | |
| | 220-224 | 2 | 50 | |
| | 224-265 | 37 | 90.2 | |
| | 265-275 | 10.5(10) | 100+ | |
| | 275-283 | 6.5 | 81.3 | |
| | 283-365 | 84(82) | 100+ | |
| | 365-375 | 0 | 0 | |
| | 375-392 | 12 | 70.6 | |
| | 392-434 | 18 | 43.9 | |
| | 434-490 | 50 | 89.3 | |
| | 490-496 | 5 | 83.3 | |
| | 496-500 | 0 | 0 | |
| | 500-600 | 100 | 100 | |
| | 600-679 | 76 | 96.2 | |
| | 679-700 | 23(21) | 100+ | |
| | 700-800 | 100 | 100 | |
| | 800-840 | 38 | 95 | |
| | 840-870 | 25 | 83.3 | |
| | 870-891 | 8 | 38.1 | |
| | 891-900 | 9 | 100 | |
| | 900-993 | 92 | 98.9 | |
| | 993-996 | 0 | 0 | |
| | 996-1000 | 4 | 100 | |
| | 1000-1060 | 51.5 | 85.8 | |
| | 1060-1077 | 0 | 0 | |
| | 1077-1100 | 23 | 100 | |
| | 1100-1107 | 5 | 71.4 | |
| | 1107-1135 | 29(28) | 100+ | |
| | 1135-1200 | 0 | 0 | |
| | 1200-1264 | 58 | 90.6 | |
| | 1264-1300 | 4 | 11.1 | |
| | 1300-1339 | 28 | 71.8 | |
| | 1339-1400 | 0 | 0 | 79.50% |
| B4 | 0-100 | 100 | 100 | |
| | 100-200 | 100 | 100 | |
| | 200-300 | 100 | 100 | |
| | 300-400 | 96 | 96 | |
| | 400-500 | 97 | 97 | |
| | 500-600 | 100 | 100 | |
| | 600-682 | 82 | 100 | |
| | 682-690 | 0 | 0 | |
| | 690-700 | 9 | 90 | |
| | 700-776 | 20 | 26.3 | |
| | 776-800 | 22.5 | 93.8 | |
| | 800-811 | 9 | 81.8 | |
| | 811-900 | 88 | 98.9 | 92% |
| B5 | 0-100 | 82 | 82 | |
| | 100-200 | 90 | 90 | |
| | 200-300 | 66 | 66 | 79% |
| B6 | 0-100 | 100 | 100 | |
| | 100-200 | 100 | 100 | |
| | 200-300 | 38 | 38 | 79% |
| B7 | 0-100 | 83 | 83 | |
| | 100-200 | 82 | 82 | |
| | 200-300 | 95 | 95 | 87% |

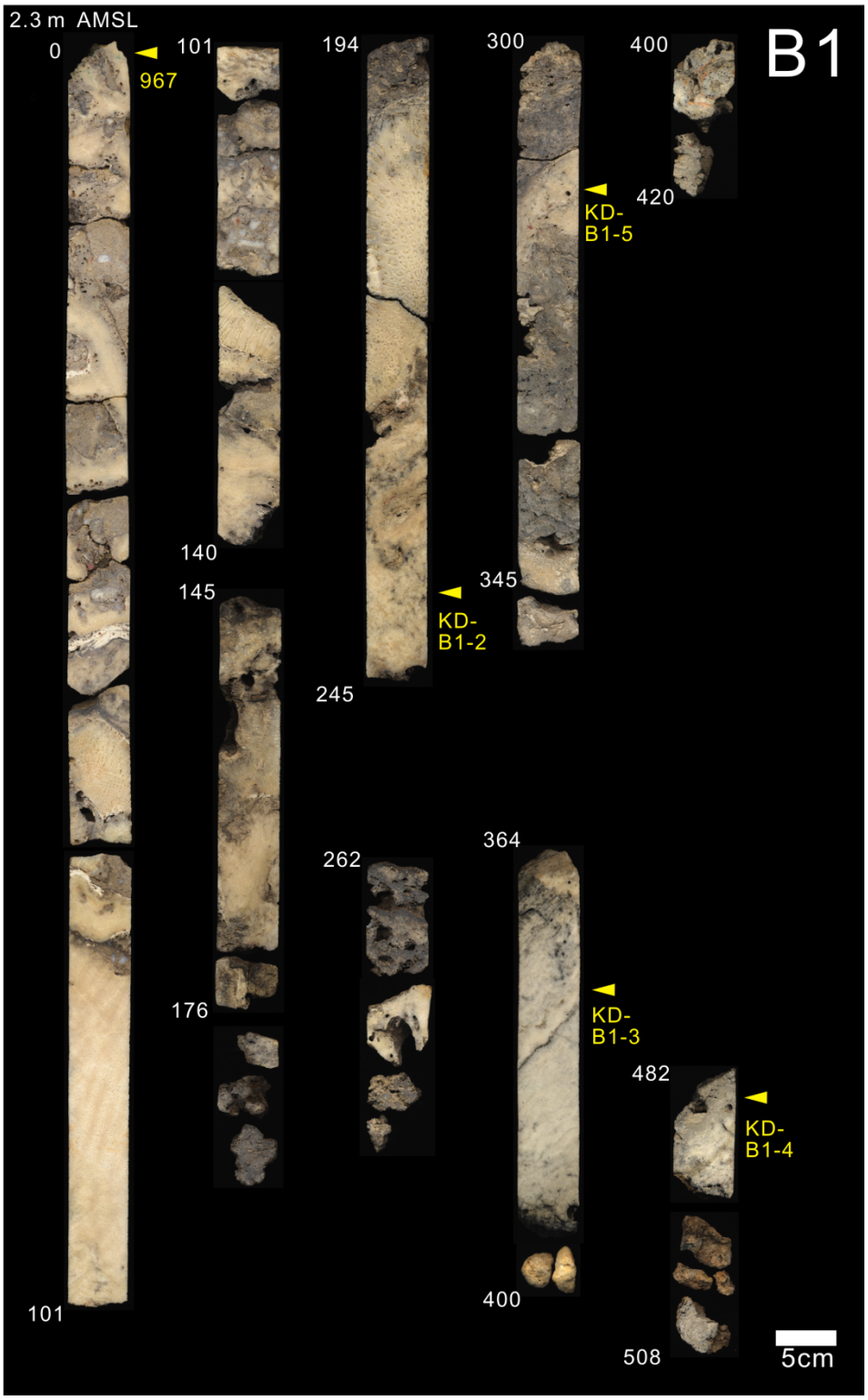


Fig. 4.19 Scanning image of cut out core B1. Triangles indicate position of coral samples for AMS radiocarbon dating. All ages are cal yr BP. The penetration depth is cm.

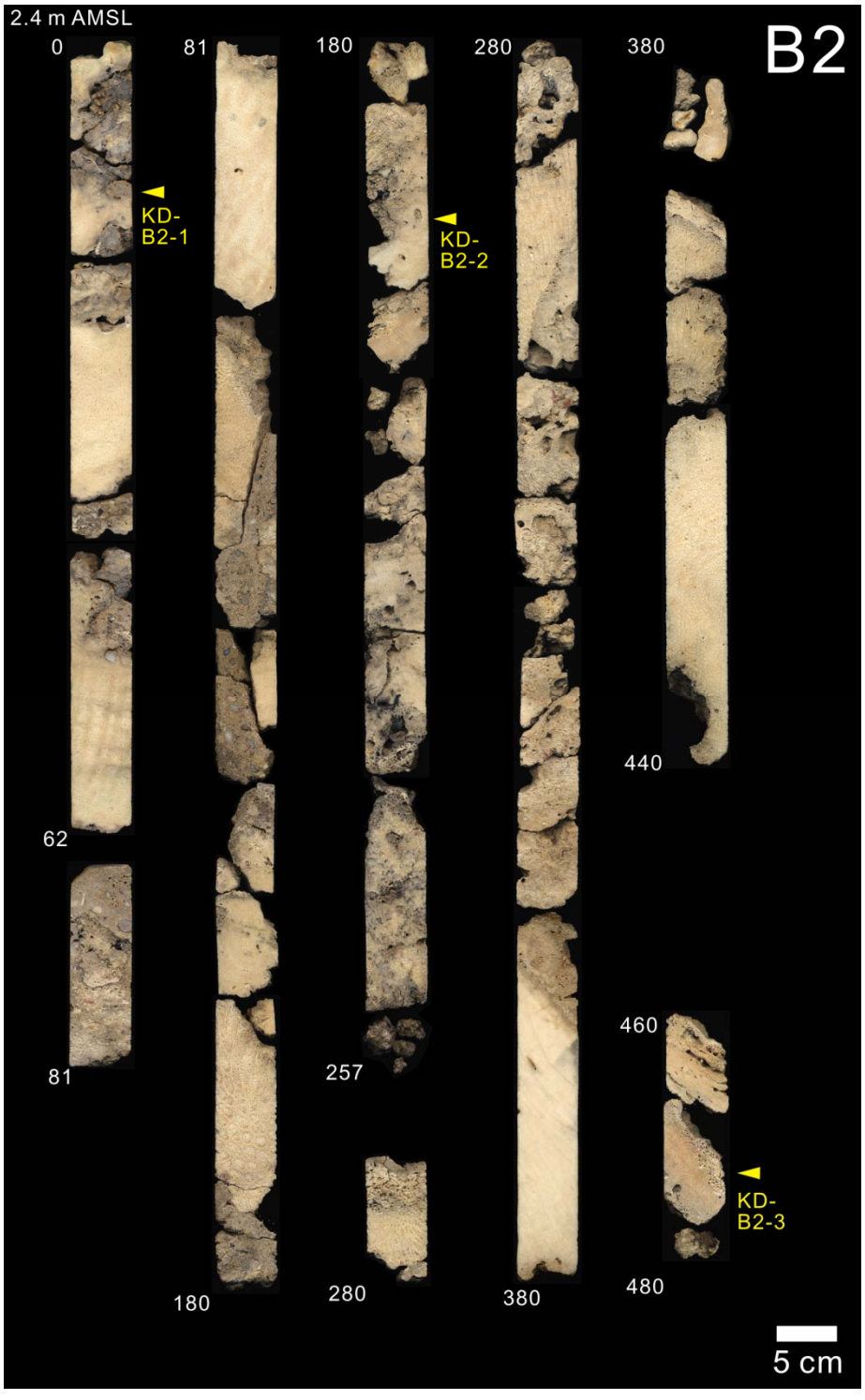


Fig. 4.20 Scanning image of cut out core B2. Triangles indicate position of coral samples for AMS radiocarbon dating. All ages are cal yr BP. The penetration depth is cm.

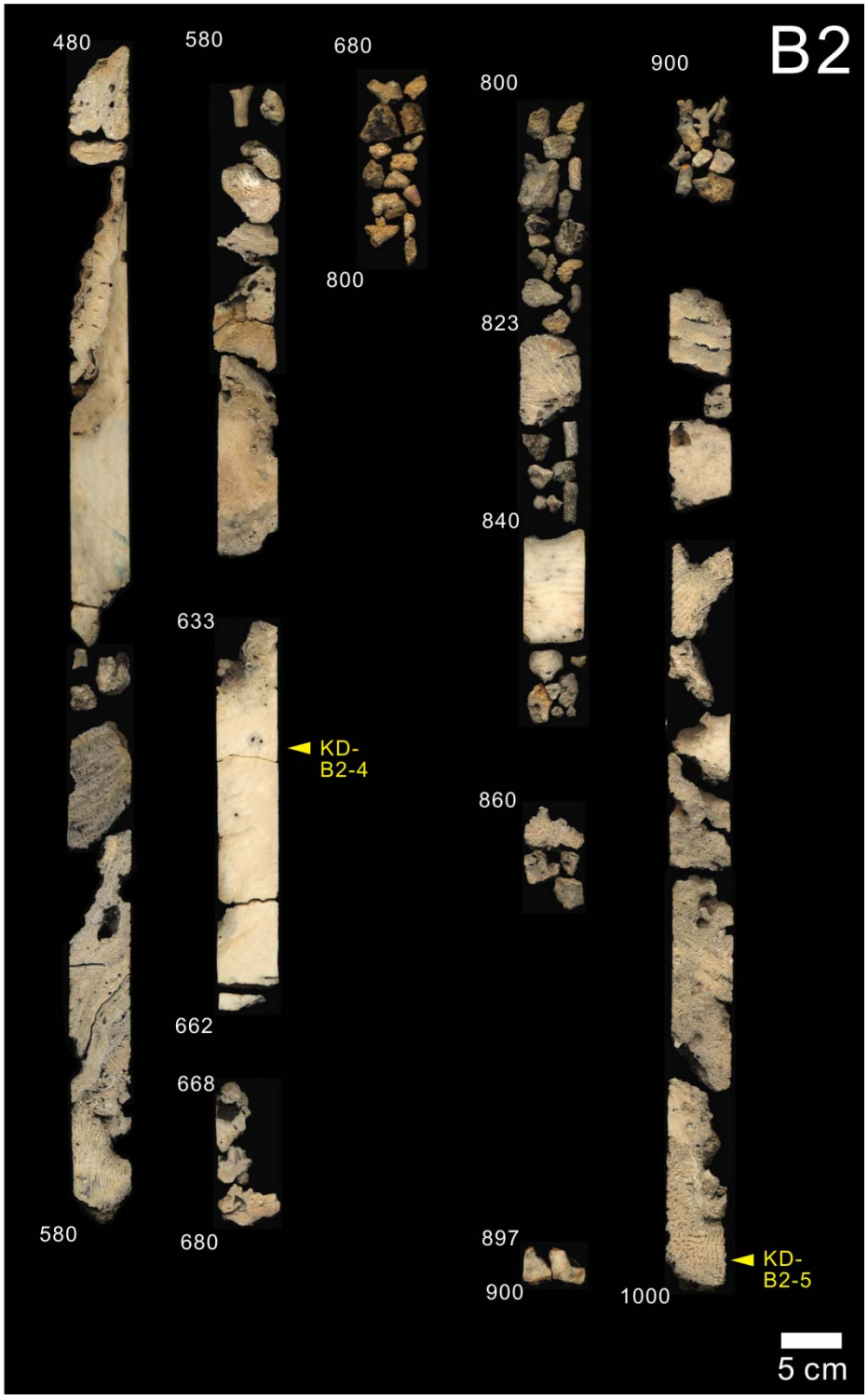


Fig. 4.20 *Continued.*

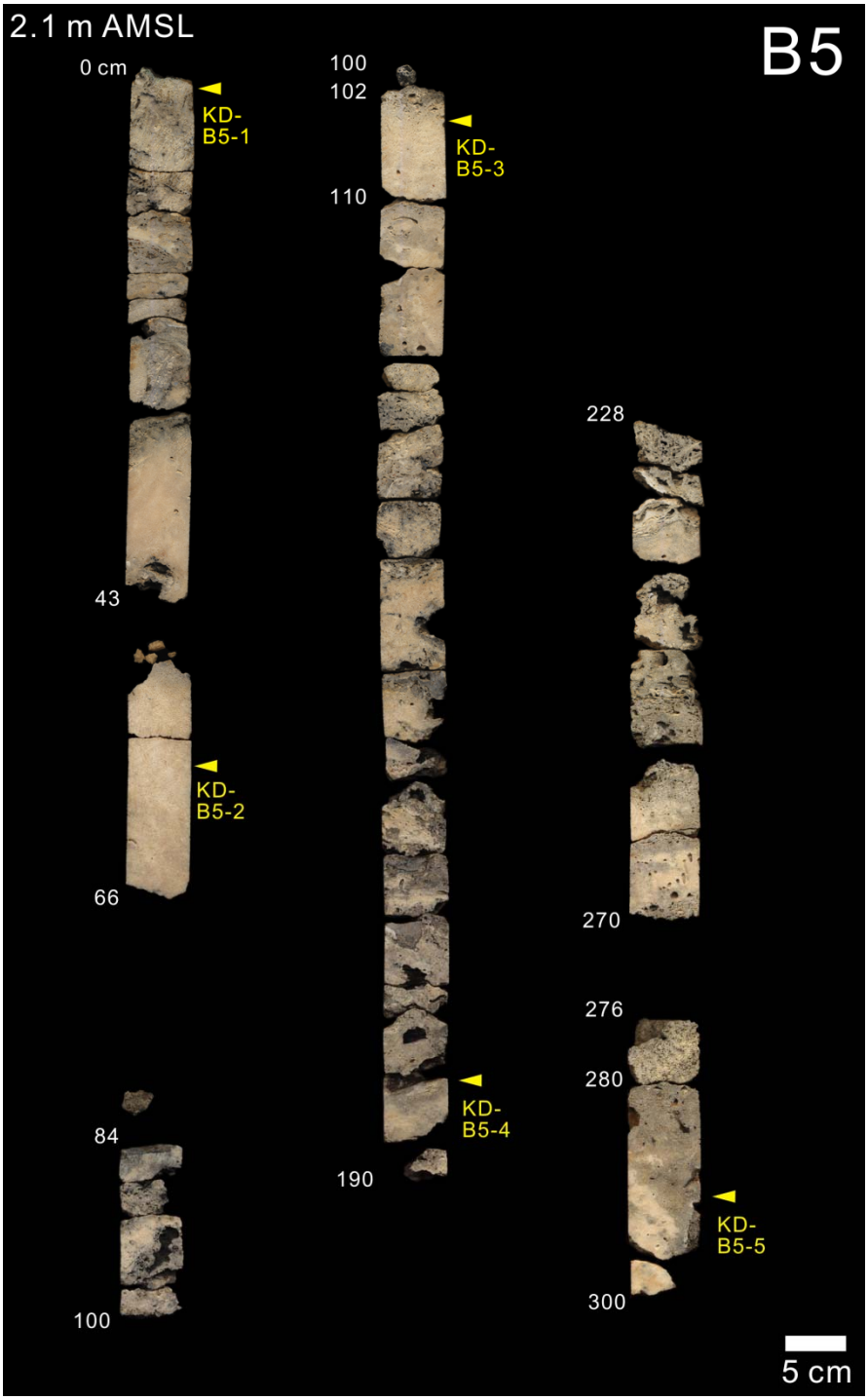


Fig. 4.21 Scanning image of cut out core B5. Triangles indicate position of coral samples for AMS radiocarbon dating. All ages are cal yr BP. The penetration depth is cm.

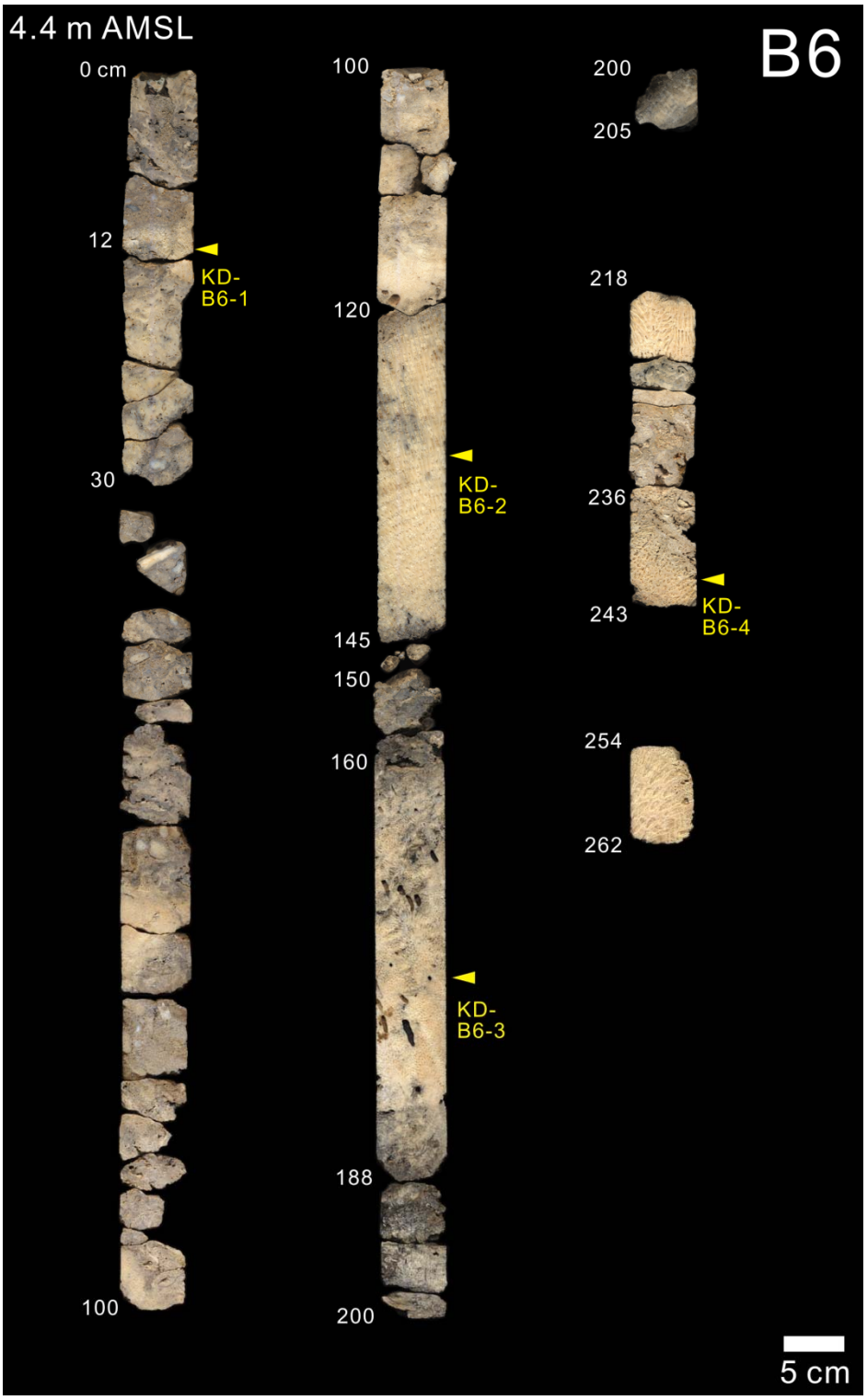


Fig. 4.22 Scanning image of cut out core B6. Triangles indicate position of coral samples for AMS radiocarbon dating. All ages are cal yr BP. The penetration depth is cm.

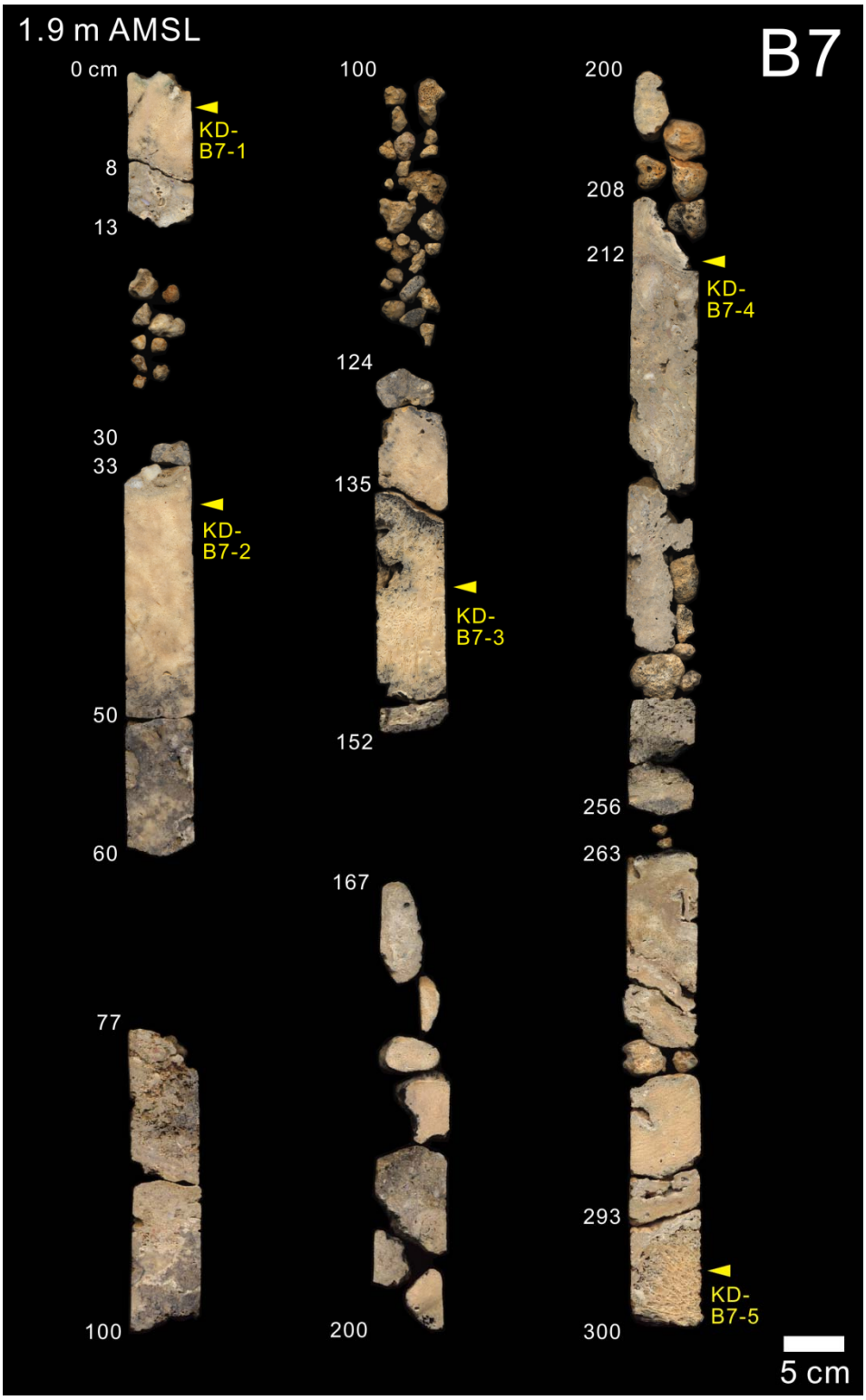


Fig. 4.23 Scanning image of cut out core B7. Triangles indicate position of coral samples for AMS radiocarbon dating. All ages are cal yr BP. The penetration depth is cm.

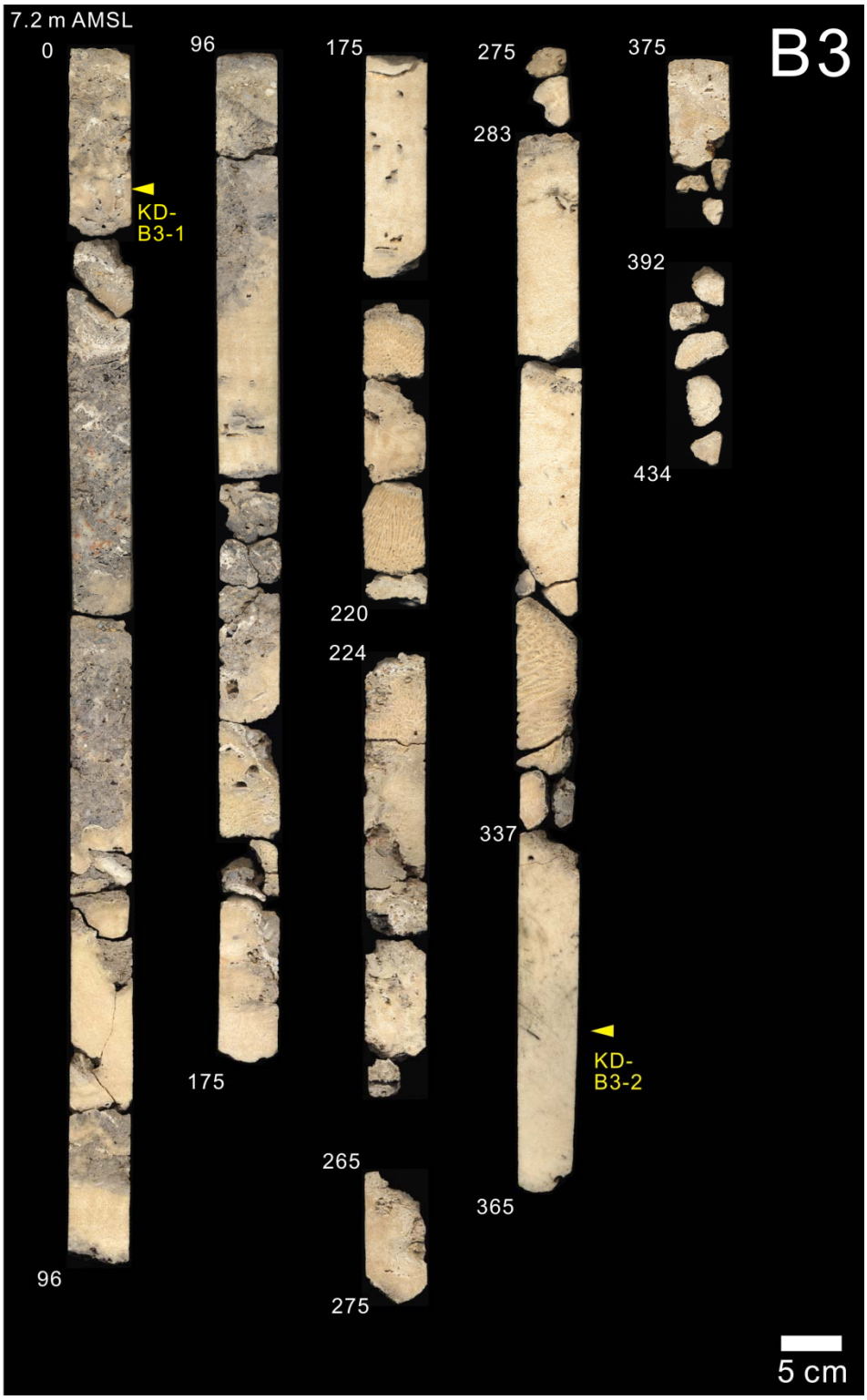


Fig. 4.24 Scanning image of cut out core B3. Triangles indicate position of coral samples for AMS radiocarbon dating. All ages are cal yr BP. The penetration depth is cm.

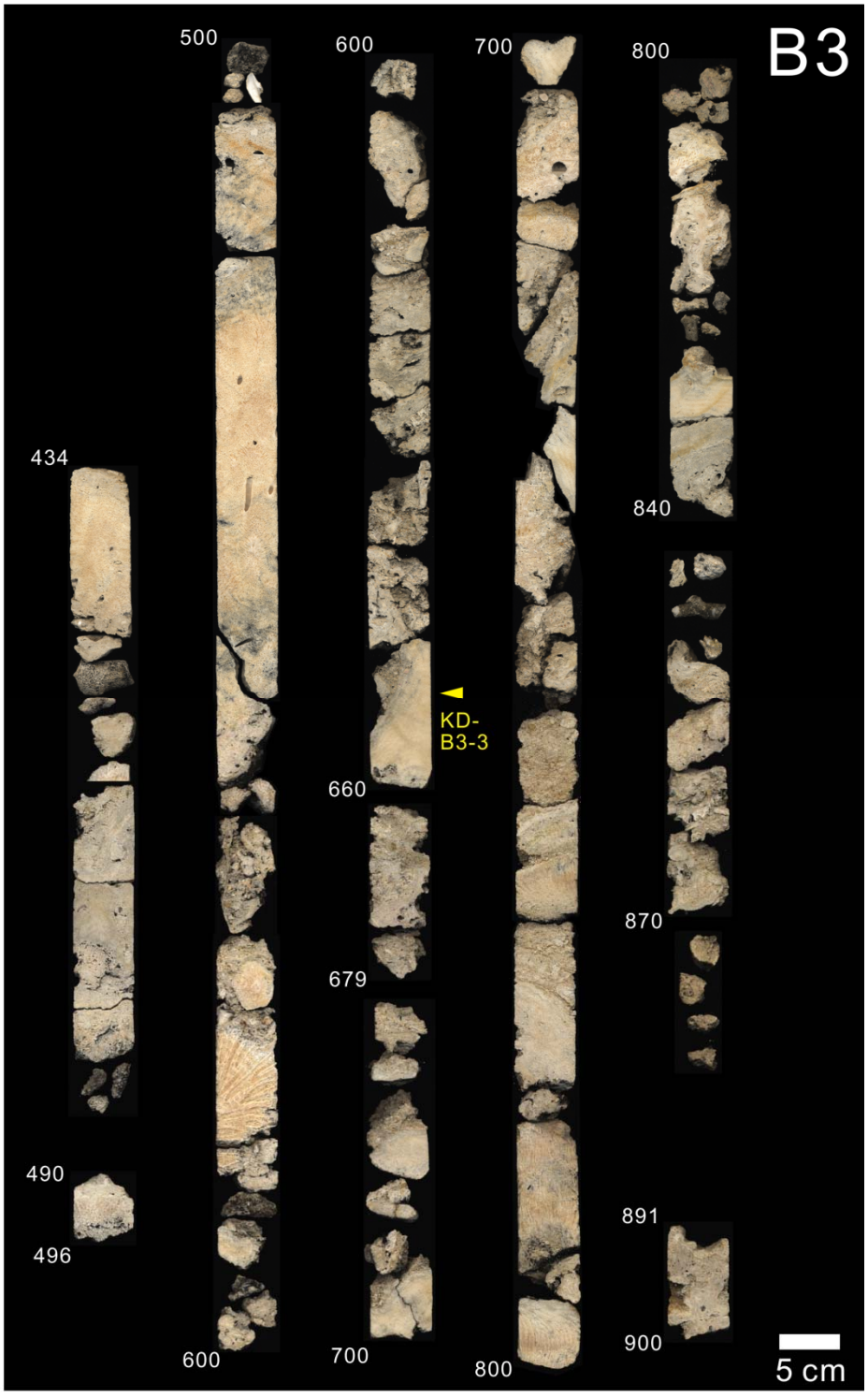


Fig. 4.24 *Continued.*

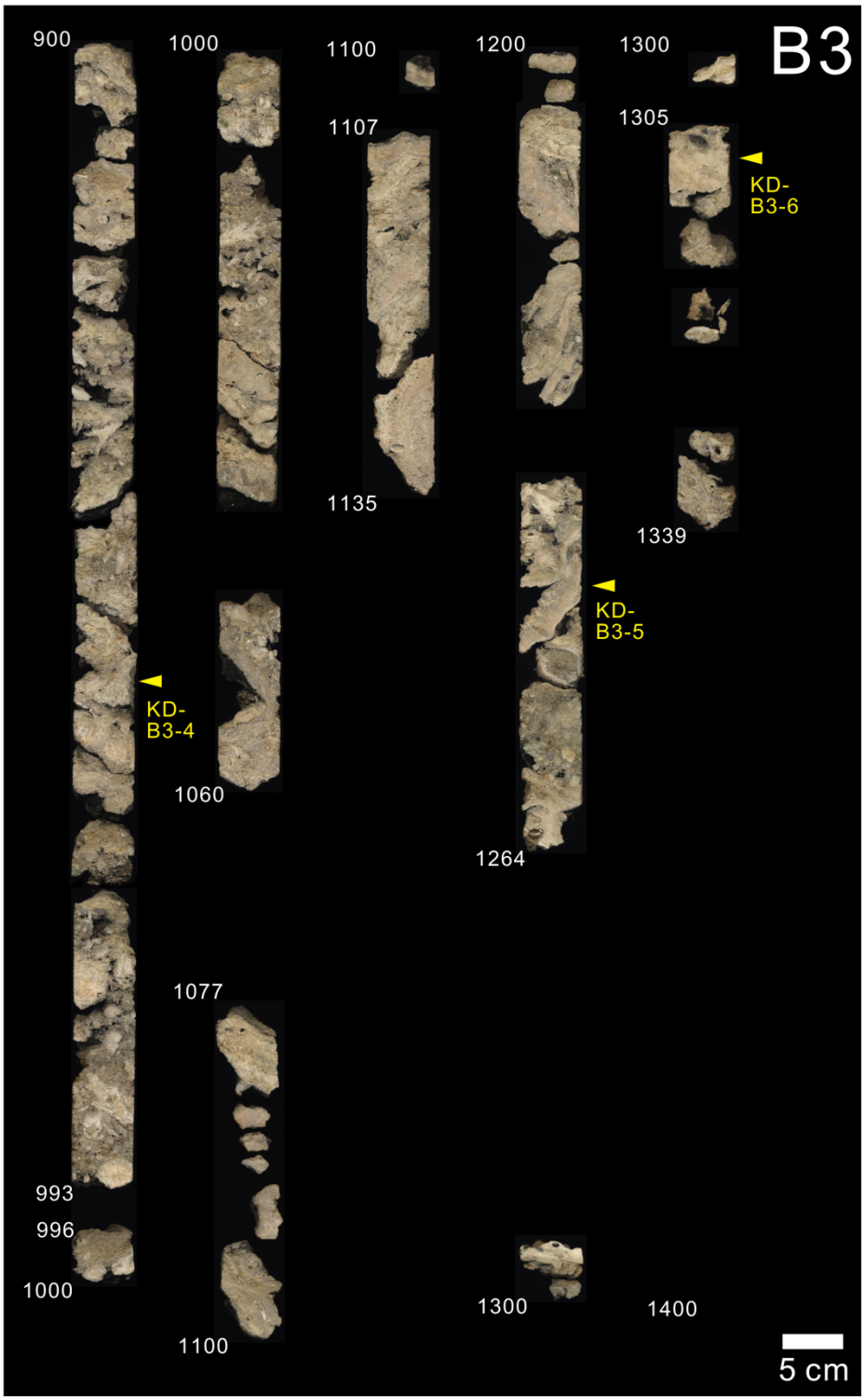


Fig. 4.24 *Continued.*

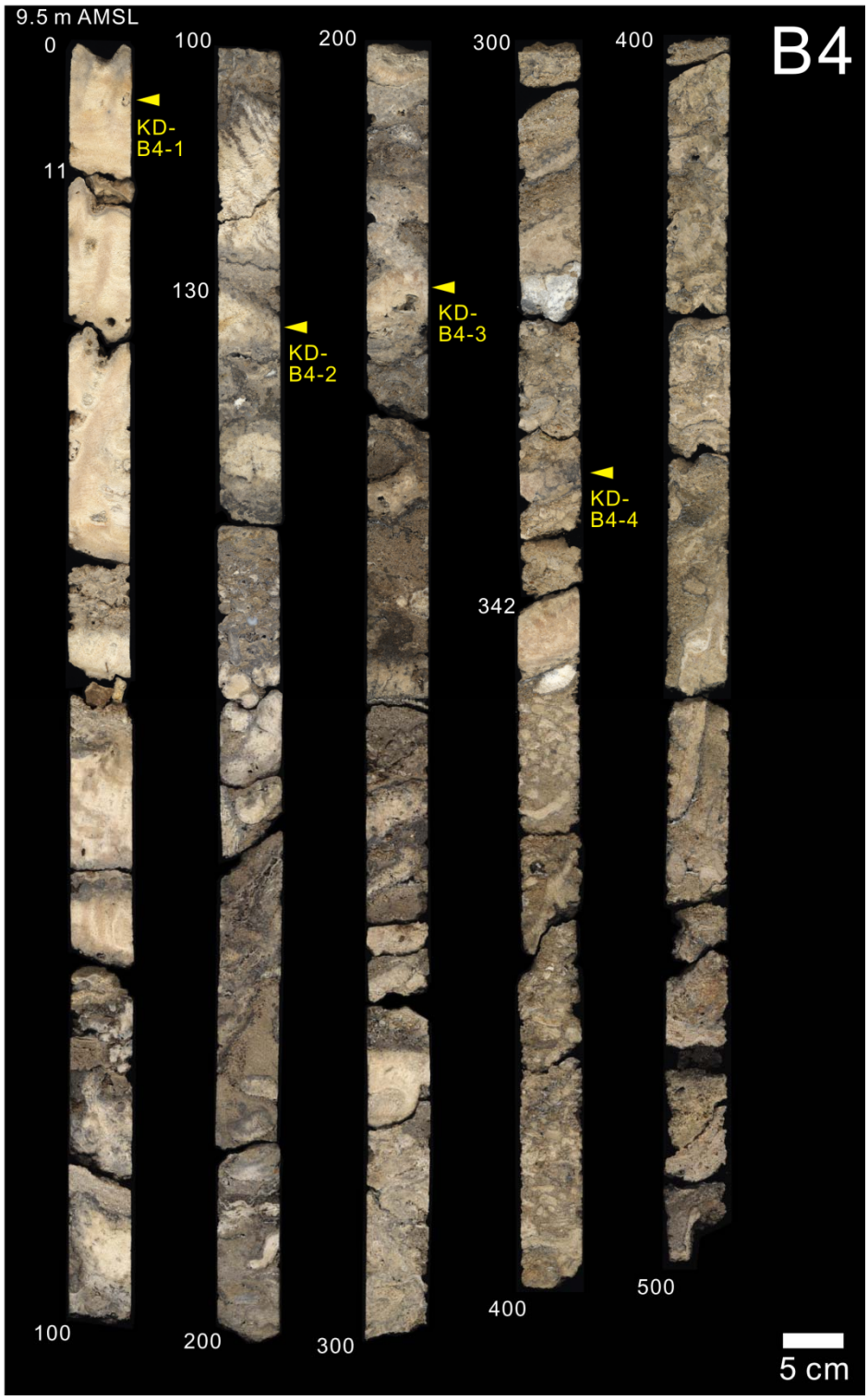


Fig. 4.25 Scanning image of cut out core B4. Triangles indicate position of coral samples for AMS radiocarbon dating. All ages are cal yr BP. The penetration depth is cm.

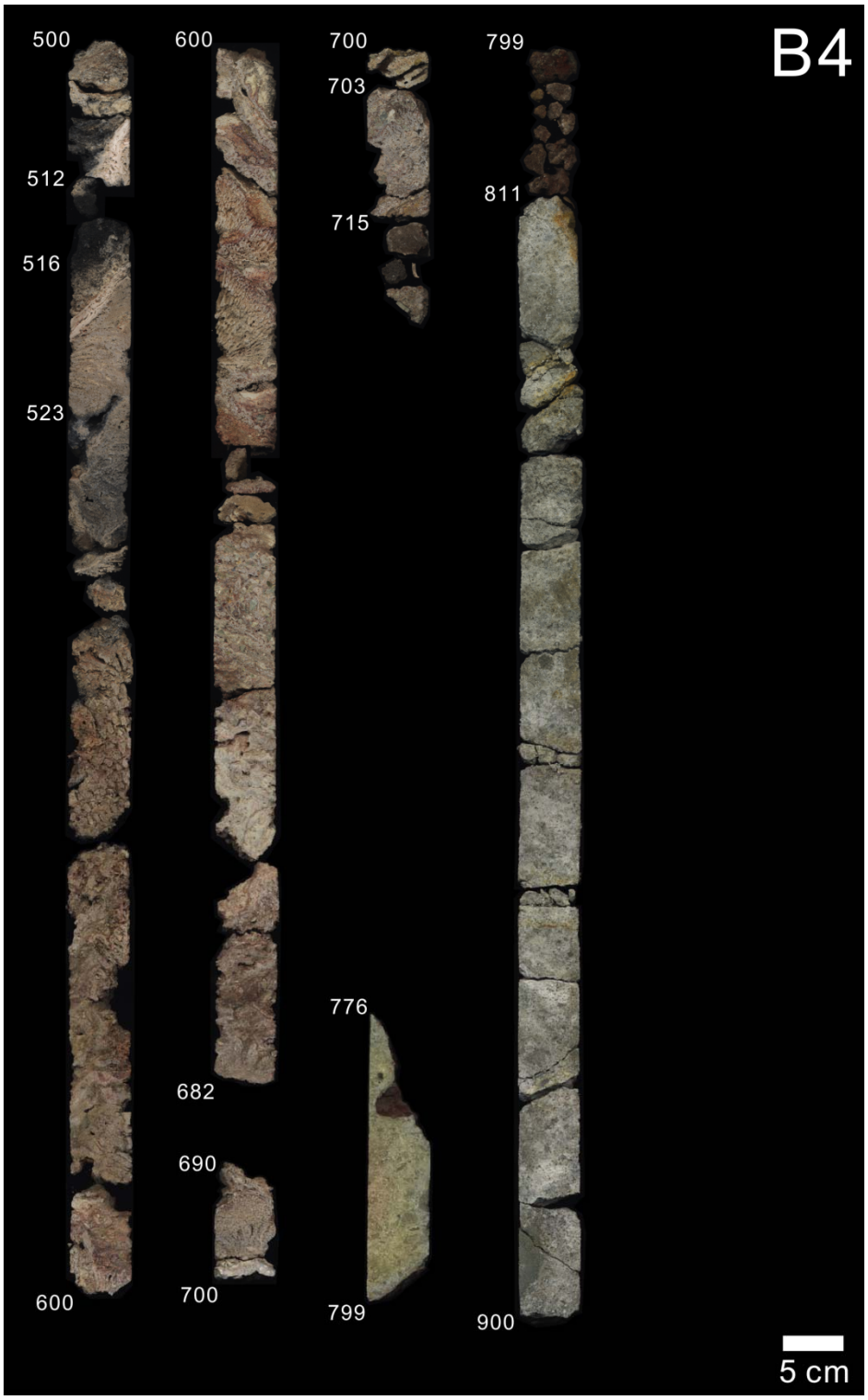


Fig. 4.25 *Continued.*

## 4.5 Facies

I identified seven sedimentary facies, Facies A through F, from the obtained cores and trenches (Figs. 4.18, 4.26, 4.27 and Table 4.4).

Facies A primarily consists of thick-plate/encrusting and tabular *Acropora* spp. with well-consolidated reefal detritus, which usually includes encrusting calcareous algae. Sediments derived from the basement rock are absent. *Acropora* spp. is associated with ramose *Pocillopora* spp., massive and encrusting faviid corals. Encrusting and columnar *Heliopora* spp. is only observed at E-1 and E-2 sites. This facies occurs in the upper part of the cores obtained from the reef flat to the reef edge in all but core B7, upper part of RU1 to 4 as well as TI surface. This facies forms the terrace surfaces at Kodakara Island and corresponds to high-wave energy, shallow upper-reef slope (0-5 m depth) in the Ryukyu Islands (Iryu et al., 1995; Sagawa et al., 2001) (Table 4.4).

Facies B primarily consists of massive and encrusting *Porites* spp., *Goniopora* spp., and faviid corals with consolidated reefal detritus. The other coral taxa present in this facies are tabular and encrusting *Acropora* spp. and encrusting *Montipora* spp. Sand from the basement rock are rare. Calcareous algae are also rare. This facies occurs below Facies A in cores B1, B2, and B3, lower part of RU1 at E-2, lower part of TI spurs and landward margin of TII. The coral assemblage of Facies B indicates an upper reef slope environment (5-20 m) (Sagawa et al., 2001) (Table 4.4).

Facies C primarily consists of encrusting *Goniopora* spp., encrusting *Montipora* spp., and encrusting and foliaceous faviid corals such as *Echinopora* spp. with poorly consolidated reefal detritus containing a large proportion of sediments derived from the basement rock. Calcareous algae are rare. This facies occurs below Facies B and A in all but core B1 and RU2 at E-3 site (Figs. 4.18 and 4.26). The coral assemblage of Facies C possibly indicates an upper to middle reef slope environment (about 5-30 m) according to the coral morphology such as the encrusting form (Sagawa et al., 2001) and their occurrence at specific altitudes in the cores (Figs.

4.18, 4.26 and Table 4.4)

Facies D primarily consists of massive *Hydnophora* spp. and branching *Caulastrea* spp. with poorly consolidated reefal detritus and abundant sand and gravel from the basement rock. Calcareous algae are rare. The facies only occurs in core B4, which is the most landward site. Most corals of this facies have been subject to diagenetic alteration and recrystallized into calcite. The coral assemblage of Facies D possibly indicates a reef slope environment near the basement rock (at least more than 5 m deep), inferred from their occurrence in core B4 (Fig. 4.18, 4.26 and Table 4.4)

Facies E consists of re-worked coral detritus. Fragments of branching *Acropora* spp. are the most common components of this detritus. This facies is mostly found in the grooves of site B7 and in the lower part of core B2. Facies E was likely deposited in topographic depressions, such as grooves (Fig. 4.18, 4.26 and Table 4.4).

Facies F is characterized by pebble to cobble sized debris derived from the basement rock. No calcareous material is observed. This facies is only found in core B4 above the basement rock. However, this facies was not found above the basement rock exposed in trenches near the top of TI (Hamanaka et al., 2012). Therefore, Facies F seems to occur only at lower elevations (Fig. 4.18, 4.26 and Table 4.4).

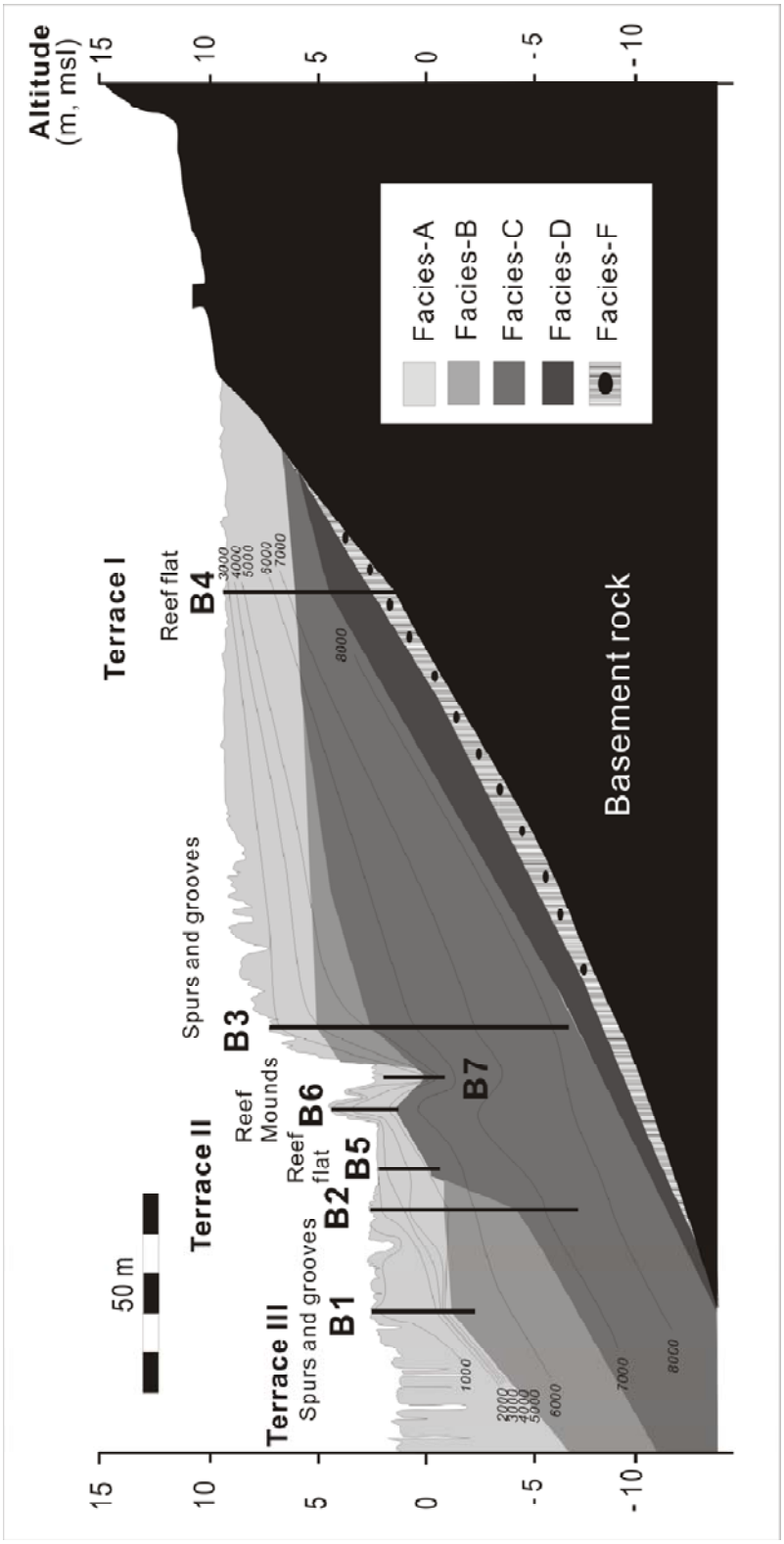


Fig. 4.26 Cross-section of the drilling transect showing changes in facies deduced from the core analysis. The interval between isochrones is 1000 yrs. Facies E (reefal sand and gravel) is not shown.

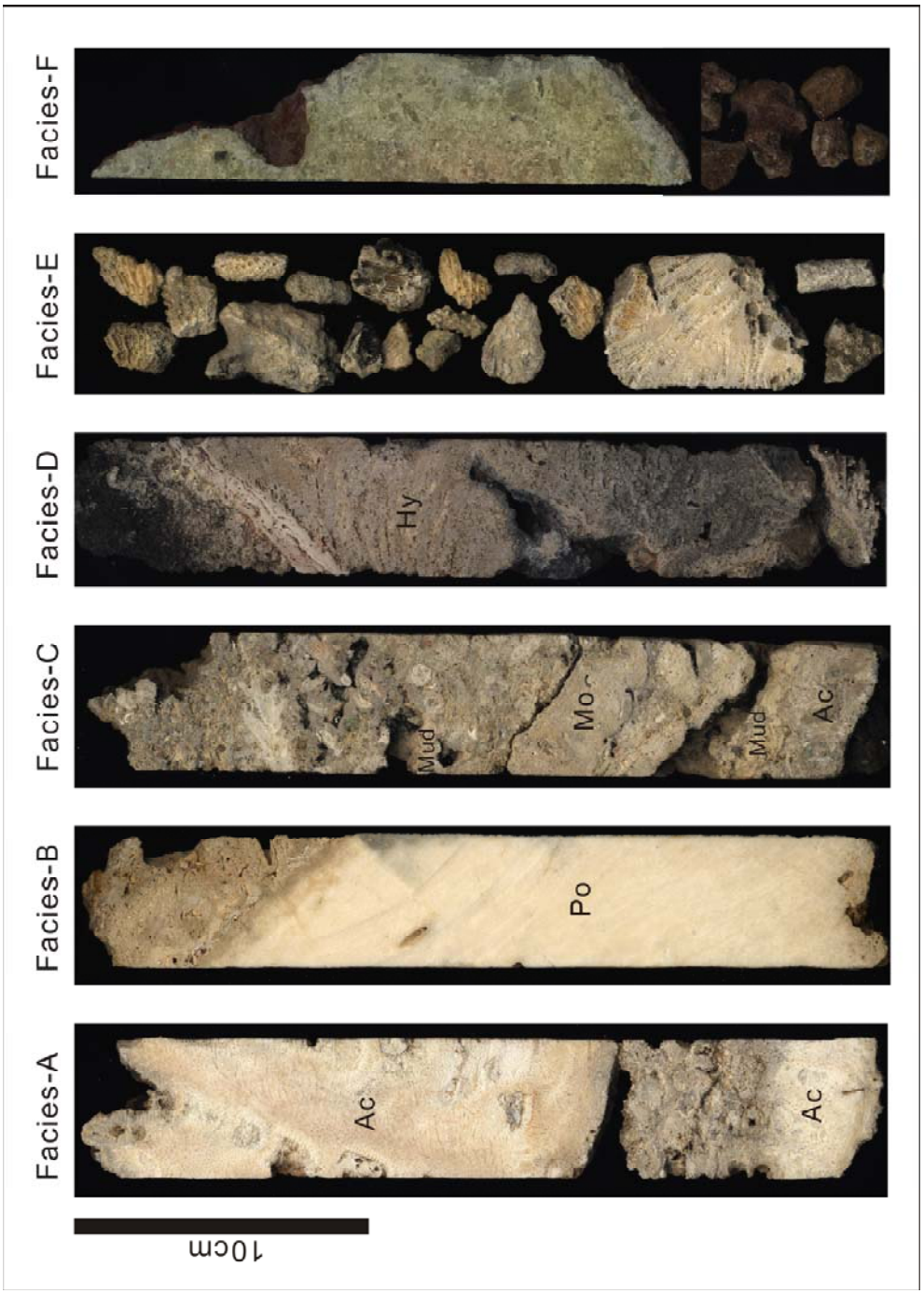


Fig. 4.27 Scanning image of cores showing facies A to F. Ac-*Acropora* sp., Po-*Porites* sp., Mo-*Montipora* sp., Hy-*Hydonophora* sp.

Table 4.4 Summary for the main characteristics of Facies in the Holocene raised reef sediments on Kodakara Island

| | Characteritic components | Dominant growth form of corals | Matrix | Paleoenvironment | Occurrence |
|---|---|---|---|---|---|
| Facies-A | *Acropora* spp.<br>Faviid corals<br>*Pocillopora* spp.<br>*Heliopora* spp. | Thick-plate/encrusting, tabular<br>Massive, encrusting<br>Ramose<br>Encrusting, columnar | Well-consolidated debris of corals, foraminifera, shells and mollusks associated with encrusting calcareous algae | Shallow upper reef slope(0-5m) with high-wave energy | Surface of TI, TII, TIII<br>E-1, E-2 and E-3 sites<br>Cores B1, B2, B3, B4, B5 and B6 |
| Facies-B | *Porites* spp.<br>Faviid corals<br>*Goniopora* spp.<br>*Acropora* spp.<br>*Montipora* spp. | Massive and encrusting<br><br>Encrusting<br>Encrusting, tabular<br>Encrusting | Consolidated debris of corals, foraminifera, shells and mollusks | Upper reef slope(5-20m) | Lower part of TI spurs, landward margin of TII<br>E-2 site<br>Cores B1, B2 and B3 |
| Facies-C | *Goniopora* spp.<br>*Montipora* spp.<br>Faviid corals | Encrusting<br>Encrusting<br>Encrusting, foliaceous, massive | Poorly consolidated debris of corals, foraminifera, shells and mollusks with sand and gravel from basement rock | Upper to middle reef slope (5-30m) | E-3 site<br>Cores B2, B3, B4, B5, B6 and B7 |
| Facies-D | *Hydonophora* spp.<br>*Caulastrea* spp. | Massive<br>Branching | Poorly consolidated debris of corals, foraminifera, shells and mollusks with sand and gravel from basement rock | | Core B4 |
| Facies-E | Not in situ *Acropora* spp. | Branching | - | Grooves and topographic depressions | Cores B2 and B7 |
| Facies-F | Pebble to cobble of Basement rock | - | - | Just above basement rock | Core B4 |

# Chapter 5

# Discussion

## 5.1 Tectonics

### 5.1.1 Uplifting

Kodakara Island experienced at least three periods of uplift during the Holocene. The timing of an uplift can be ascertained by comparing the youngest age of an uplifted terrace surface with the oldest age of the terrace surface that formed subsequently. Results of AMS dating indicate the following ages for the successive periods of uplift on Kodakara Island: 2443-2316 cal yr BP (TI), 967-440 cal yr BP (TII), and a modern age (TIII) (Fig. 4.17 and Table 4.2). These results indicate that the uplift events occurred abruptly on a centennial time scale. Specifically, the differentiation between TI and TII occurred during a time lapse of 130 years, suggesting that a 7-m vertical displacement was caused by one or a few large earthquakes approximately 2400 years ago. By contrast, the vertical displacement of Holocene terraces in islands located closer to the Ryukyu Trench, such as Kikai Island (28N 130E), is generally less than 5 m (Nakata et al., 1978; Ota et al., 1978).

The style of uplifts near Kodakara Island may have been different from that expe-

rienced by areas located near trench zones, such as Kikai in the Ryukyu Islands (Fig. 2.1) (Ota et al., 1978; 2000; Sugihara et al., 2003) and the Huon peninsula of Papua New Guinea (e.g., Ota and Chappell, 1996). Because Kodakara Island is located on an inner arc and near Tokara strait in the Northwest Pacific, the cause of the uplifts near Kodakara Island may have been related to not only subduction but also another activity.

The modern uplift event related to the formation of TIII is unrecorded in history. However, the inhabitants of Kodakara Island attest that they have experienced large earthquakes and have witnessed a decrease in the sea level during the past century, although the actual timing and frequency of these earthquakes remains unclear. The vertical displacement of Terrace III was estimated as at least 2 m because the altitude of TIII is 1.2 m amsl, whereas the modern living coral habitat is generally limited to ca. 1 m below the msl.

Therefore, I conclude that terrace differentiation on Kodakara Island was caused by coseismic uplift during large and non-periodic earthquakes, resulting in vertical displacements of ~7 m about 2,400 years ago, ~1 m between 1,000 and 400 years ago, and more than 2 m during the modern era.

### 5.1.2 Formation of low-scarp morphology

The timing of the low-scarp formation was after TII (Tsukuridomari surface) formed which estimated to at least 1.3 ka based on previous studies (Nakata et al., 1978; Koba et al., 1979). However, the inhabitants of Kodakara Island attest that they have experienced large earthquakes and have witnessed the low-scarp formation during the past century approximately 1970's and 1990's. This witness is supported by an evidence that two *Ficus microcarpa* along the upper part of the scarp inclined unnaturally to lower part of the one, and many aerial roots supported the trees at Haebaru (Fig. 4.5F). Hence, the low-scarp may have been made between 1970's and 90's with large earthquakes.

The earthquakes around Kodakara Island are recorded by Fukuoka district meteorological observatory (1975; 1998) and Japan meteorological agency (1976; 1995) which described that the earthquakes occurred at 1972, 1975 and 1995-6, respectively. The magnitudes (M) and the focal regions were M3.5 around N29°2′ E129°3′ at 1972, M5.1 around N29°05′ E129°19′ at 1976 and M5.4 around N29°19.8′ E129°3′ at 1995-1996, respectively.

There are no records and descriptions about the relationship between the earthquakes and low-scarp. However, Usami (2003) described that fissure was made with the earthquakes at 1972 and 1975 which may indicate formation of the low-scarp. The evidences and morphological characters of the low-scarp imply that the scarp means an active normal fault although the focal regions are not matched to Kodakara Island. According to above, I conclude that the low-scarp is normal fault but it difficult to deny at the present that the formation of the scarp may have caused slumping with the earthquakes.

## 5.2 Interpretation of the reef growth hiatuses

To assess the nature of the disturbance boundaries, I first considered whether they may have been caused by SST anomalies, relative sea-level changes, brief storm/cyclone horizons, "death" surfaces associated with previously unknown coseismic uplift events, or earthquake events without uplift but of sufficient size to impact the reefs. The boundaries of the Holocene reef sediments observed on the Huon Peninsula indicate that disturbances in reef growth occurred before the impact of humans (Pandolfi et al., 2006). These boundaries are similar to those that I discovered on Kodakara Island. However, the Huon boundaries are associated with disturbances, such as volcanic ash (Pandolfi et al., 2006), whereas the Kodakara boundaries are not associated with such characteristic sediments.

The timing of these hiatuses corresponds to the periods of weakened Kuroshio Current centered at 5.9 cal yr B.P., 4.6 cal yr B.P., and 3.3 cal yr B.P. recorded in

well-dated marine sediment cores (Jian et al., 2000) from the Okinawa Trough (Fig. 2.1). The disturbances also correspond to North Atlantic Holocene ice-rafted cold events 2–4 (Bond et al., 1997, 2001) (Fig. 5.1a). The production of $^{14}C$ and $^{10}Be$ indicates relatively low solar activity (Fig. 5.1b), leading to ice-rafting in the North Atlantic (Bond et al., 2001) and perhaps eventually to relatively low SSTs in the western tropical Pacific (Stott et al., 2004). Thus, the annual-to-centennial disturbances with hiatuses and their links with both cold events in the North Atlantic and low SSTs in the western tropical Pacific are partly attributable to isolation-forcing changes (Liu et al., 2003). The second and third disturbances (at 4.4–4.0 ka and 3.3–3.2 ka, respectively) are well correlated with the Middle/Late Jomon cold stage and the Latest Jomon cold stage, as recorded in Japan (Sakaguchi, 1983). The second disturbance (within 4.4–4.0 ka, Fig. 5.1) corresponds particularly well to the North Atlantic Holocene cooling event 3 (Bond et al., 1997, 2001), when abrupt climate shifts to cold and dry were reported at various places in East Asia (e.g., Wu and Liu, 2004; Wang et al., 2005; Xiang et al., 2007; Selvaraj et al., 2007). The Asian summer monsoon intensity abruptly decreased (Fig. 5.1c) at this time (Wang et al., 2005), in conjunction with a relatively strong cold Asian winter monsoon (Yancheva et al., 2007) that was induced by insolation forcing a southward migration of the Intertropical Convergence Zone (ITCZ) in the Northern Hemisphere (e.g., Haug et al., 2001). Hence, the second disturbance and hiatus are associated with both the Kuroshio Current weakening and the Asian winter monsoons strengthening (Fig. 5.1c). The strong Asian winter monsoon may have caused significantly cooler SST (Yu et al., 2004) in the Northwest Pacific. I believe that the correspondence between the disturbances with hiatuses and the global climate change events is not incidental because all of the disturbance events correspond closely with major climate-change events. Hence, our dating results revealed that these disturbance-with-hiatus events correspond to global-scale cooling conditions.

The global distribution of coral reefs is generally limited by the 18°C minimum isotherm because SST is directly related to coral growth through aragonite saturation states, physiology, and survival (e.g., Kleypas et al., 1999; Pandolfi et al., 2003).

Cold bleaching and mortality due to low winter SST may be a natural cause of reef mortality at high latitudes, where SSTs frequently fall below 18°C (Saxby et al., 2003). The Holocene SST around the Ryukyu Islands has been reconstructed from planktonic foraminifera and fossil corals. The estimated Holocene $\delta^{18}O$-derived SST from the foraminifera (*Pulleniatina obliquiloculata*) at the Core255 site in the southern Okinawa Trough (25°12′N, 123°07′E) was 21.5°C –26.6°C in winter and 28.2°C –29.1°C in summer. The SST for core B-3GC in the northern Okinawa Trough (31°29′N, 128°31′E) (Fig. 2.1) was 18.4°C –26.0°C in winter and 27.2°C –28.9°C in summer (Jian et al., 2000). The evidence shows larger SST variability in winter than in summer (Fig. 5.1d). During a disturbance event, the winter SST was clearly cooler than the present SST (Jian et al., 2000). However, the data show that the SST did not fall below 18°C during the disturbances with hiatuses (Fig. 5.1d). A possible explanation is that the coastal coral records are more variable than oceanic records because of stronger direct winter monsoon influences on the coastal sites (Yu et al., 2004).

Holocene coastal SST records have been reconstructed using fossil coral skeleton analysis. At Kikai Island (28°20'N) in the Northwest Pacific (Fig. 2.1), Abram et al. (2001) reconstructed the $\delta^{18}O$-based SST from *Porites* corals and discovered that the SST frequently fell below 18°C at approximately 3.7 ka. At the southernmost end of the Leizhou Peninsula (20°14'N 109°55'E), along the northern coast of the South China sea, the Holocene fossil coral (*Goniopora* spp.) records show that coral mortality and growth hiatuses frequently occurred at ~7.5–7.0 ka within the Holocene climatic optimum (Yu et al., 2004), when the average Sr/Ca-derived SST minima was estimated at 16.0–19.1°C. The calculated hiatus duration for the entire reef profile indicates that seriously stressed or deceased reef corals took between 20 and 25 years to recover (Yu et al., 2004). These data suggest that Holocene reefs have experienced severe winter SSTs that do not correspond to Holocene cooling events and that SSTs frequently fell below 18°C over multi-decadal scales. Thus, the Holocene cooling events may have created the conditions in which SST constantly fell below 18°C over multi-decadal to centennial scales, leading to disturbances with

hiatuses in the Northwest Pacific during the Holocene. The potential for low SSTs may have enhanced the Siberian High via atmospheric teleconnections, thus resulting in strengthened winter monsoons in East Asia (Yu et al., 2004).

Sea-level oscillations during the middle to late Holocene have also been reported in areas of the East Pacific region, such as the South China Sea (Zhao and Yu, 2002) and eastern Australia (e.g., Lewis et al., 2008), and in areas of the Atlantic region, such as eastern Brazil and South America (e.g., Martin et al., 2003). The timing of these oscillations is consistent with the Kodakara Island data from the Northwest Pacific. The observation that Holocene sea levels oscillated in other parts of the Pacific and the Atlantic indicates that eustatic changes may have influenced mid-late Holocene sea-level variations in the Northwest Pacific. Possible mechanisms for small-scale sea-level rises and falls invoke the repeated build up and break off of ice sheets (e.g., Gregory et al., 2004; Joughin et al., 2004; Alley et al., 2005), with warmer-to-cooler environmental changes during the Holocene that were induced by persistent solar activities (Bond et al., 2001). In any case, it is remarkable that the relative sea-level change associated with the second and third disturbances with hiatuses at Kodakara Island possibly coincided with the Holocene events in the North Atlantic (Bond et al., 1997; 2001). This coincidence argues for a link between the Holocene events and sea-level changes (Baker et al., 2003; 2005).

I thus interpret the main cause of reef growth disturbances as being low SSTs induced by sub-orbital millennial-scale global climate change induced by persistent solar activity and possibly enhanced by association with sea-level oscillations. The recovery of corals after disturbances with hiatuses seems to depend in large part on the type of disturbance causing the original decline (Cornell, 1997). More information and studies may therefore be required to assess reef growth in more detail.

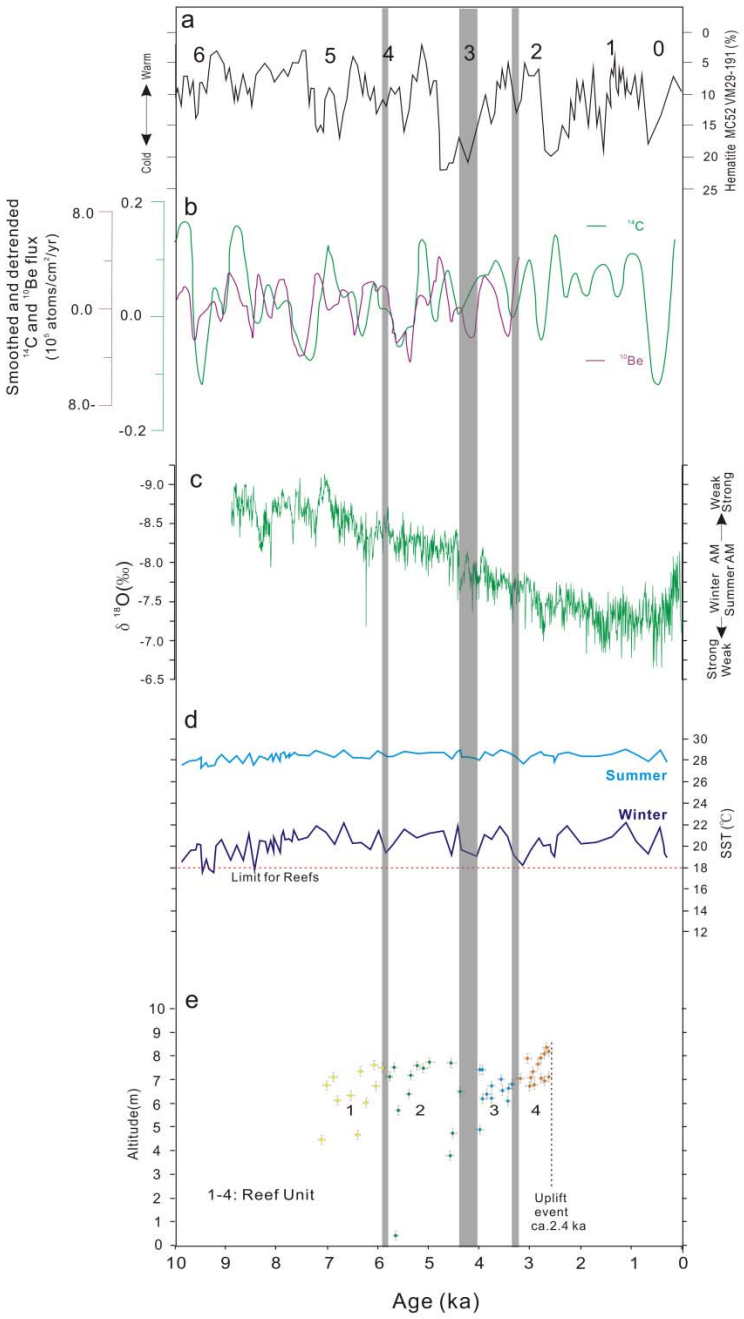


Fig. 5.1 Timing of the reef growth disturbances with hiatuses (vertical grey shading) relative to climate events. (a) Hematite (%) from North Atlantic sediment cores (MC52, VM29-191) and Holocene events 0–6 labeled by Bond et al., 2001. (b) $^{14}$C and $^{10}$B fluxes from the North Atlantic (Bond et al., 2001). (c) Green curve, the $\delta^{18}$O variability in a stalagmite from Dongge Cave, central China, indicating the summer Asian monsoon (AM) intensity (Wang et al., 2005). The winter AM trend is from a high-resolution lake sediment core from southern China (Yancheva et al., 2007). (d) The planktonic foraminifera-derived sea-surface temperature (SST) variability during the Holocene, from core B-3GC (Jian et al., 2000) (the locations are shown in Fig. 1). The dark and light blue curves indicate the winter and summer SSTs, respectively. (e) The age-height relationships of the collected corals and the relative sea-level curve from the excavated trench walls on Kodakara Island exhibit the timing of the disturbances with hiatuses and their linkage to climate change during the middle-to-late Holocene.

## 5.3 Interpretation of changes in coral composition during the middle-to-late Holocene

Our results suggest that coral compositions at Kodakara Island in the Northwest Pacific actually changed during the middle-to-late-Holocene; there were three disturbances with hiatuses, although they were limited to the upper reef zone. Moreover, coral diversity has gradually decreased from RU1 to RU4, which was particularly characterized by the dominance of *Acropora* spp. (Fig. 4.16).

The duration of RU1 formation corresponds to the Holocene climatic optimum, when SSTs of up to 1°C above the present were recorded in both the Pacific and Indian Oceans (e.g., Sonzogni et al., 1998; Gagan et al., 2000), and coincides with the main phase of sea-level stabilization. The reefs grew actively during this period in the Ryukyu Islands (e.g., Kan et al., 1995) and on Kodakara Island. During this period, corymbose, tabular, and arborescent *Acropora*, *I. palifera*, and *Porites* were the key species for reef growth in the Indo-Pacific (e.g., Cabioch et al., 1995; Kan et al., 1995; Kan and Kawana, 2006; Marshall and Davies, 1982; Montaggioni and Faure, 1997; Takahashi et al., 1988; Webster et al., 1998), and faviid corals were observed in the Indo-Pacific region during the reef-formation stage (e.g., Cabioch et al., 1995; Marshall and Davies, 1982; Montaggioni and Faure, 1997). Thus, the relatively high diversity of RU1 on Kodakara Island is interpreted as being due to the Holocene climatic optimum.

Between 4.6 ka and 2.7 ka, during the so-called *Pulleniatina obliquiloculata* minimum event (PME), the SSTs in the Northwest Pacific were relatively low (e.g., Li et al., 1997; Jian et al., 2000; Xiang et al., 2007). Moreover, the SSTs around Kikai Island were relatively low from 3.7 ka to 3.4 ka. The low SST correlates well with the reported increase in *Acropora* and the decrease in faviid corals (Abram et al., 2001). Therefore, the composition fluctuations in both the *Acropora* and faviid corals on Kodakara Island may be related to a cooling such as the PME that was

induced by a weakening of the Kuroshio Current.

It is natural that site-specific coral composition changes appear in each site because E-1, E-2, and E-3 are located on a reef flat to a spur, a spur, and a reef edge to a slope, respectively (Figs. 4.6, 4.8, 4.10 and 4.15). Throughout these sites, however, the dominant composition of *Acropora* spp. and faviid corals changed significantly with the disturbances with hiatuses; in these changes, the *Acropora* fraction increased and the faviid corals decreased (i.e., in every instance of a disturbance with hiatus, the coral reefs changed to *Acropora*-dominant reefs rather than becoming low coral-diversity reefs). The characteristic changes are interpreted to result from acroporiid coral's particular sensitivity to disturbances; however, their recolonization is rapid because of their relatively high growth rate and their mode of reproduction (Ninio and Meekan, 2002). In the Huon, the acroporiid corals were significantly affected by influences other than those that led to disturbances in the other coral genera in the Holocene reef (Pandolfi et al., 2006). According to them, acroporiid dominance may indicate that after the disturbances with hiatuses, *Acropora* spp. dominantly recolonized on bare substrates relatively faster than did other genera, even on Kodakara Island.

It is unknown whether similar disturbances with hiatuses occurred in other coral reefs in the area, although *Acropora* have gradually become the dominant genus and main reef builders in newer reefs in the Ryukyu Islands (e.g., Hongo and Kayanne, 2011), in agreement with our results. Hence, the area colonized by *Acropora* spp. may tends to increase when reefs experience disturbances with hiatuses that correlate with millennial-scale climate changes.

According to our results, the presence of *Acropora* spp., currently the most dominant genus on Ryukyu Island and in the Indo-Pacific region, increased for 4,500 yrs (from 7.1 ka to 2.6 ka) on high-latitude coral reefs, such as those on Kodakara Island. As the disturbances with hiatuses were repeated, *Acropora* spp. expanded to become the dominant genus, which may have been typical in high-latitude coral reefs.

## 5.4 Late Holocene sea-level oscillation

### 5.4.1 Interpretation of the sea-level indicators

I confirm the existence of three buried erosion surfaces (BES-1 to 3) equivalent with the horizontal sharp boundaries observed at E-1 to 3 sites, which clearly indicates remnant of sea-erosion at relative low stands, packed within the middle-to-late Holocene reef rock which formed ca.7-2.4 ka (Figs 5.2 and 5.3). The BES-1 to 3 are overlain by relative new reef sediments (Figs. 5.2 and 5.3). These characters clearly indicated relative sea-level low stands and following relative sea-level rise had occurred during mid-to-late Holocene during 7-2.4ka.

I also confirm the raised notches at south (SN) and north (NN) of the Island on TI (Fig. 5.4). The retreat point of marine notch is generally accepted to be excellent indicator for the mean sea-level (MSL) (Pirazzoli, 1991). The SN is characterized that have one retreat point at 9.9m (RP-1) and the morphology like mushroom which consists of Tertiary tuff. The NN is consists a Pleistocene limestone boulder which characterized two retreat points. The lower retreat point is at 10m which well correspond with RP-1 of SN, thus, I interpreted the altitude of retreat point is same as RP-1. The higher retreat point is at 10.9m which here named as RP-2. These characters are interpreted as relative sea-level high stands occurred at least two times ~2.4ka. Therefore, during 7-2.4ka, Kodakara reef had experienced three low-stands (from BES) and two relative high-stands (from RP-1 and 2).

The surface of TI is depositional origin which formed between 3037-2441 cal yr BP. (3-2.4ka; Figs.4.1 and 4.2) at below 9.7m. The inhabitant limit depth for corals has generally corresponded to mean low sea-level; thus, the paleo MSL at that time is regarded as ca. 1 m above the surface. Consequently, I interpreted that RP-2 at 10.9m indicate the MSL during 3.3-2.4ka. Alternatively, RP1 at 9.9m, the former

relative stabilized sea-level record during the mid Holocene, is corresponded with 6.3-4.4ka. Holocene high-stand (HHS) at 7-6ka~ in the far-field is not found at Kodakara Island. The relative high-stand at 3ka has been caused by hydro-isostatic effect in relation to the island shelf size, and the 3ka island group is distributed in the Ryukyu Islands (Koba et al., 1982).

The BES- 1 occurs at E-2 site, which erodes the RU1 (7.1-5.9ka) and RU2 (5.8-4.4ka), and is covered with RU3 (4.0-3.3ka). Therefore, the timing of formation of the BES was ca. 4.4-4.0ka (between RU2 and RU3). The altitude of BES-1 is centered at 7.0 m. The BES-2 occurs at E-1 site, which erodes the RU1 and RU2, and is covered RU4 (3.2-2.4ka). Therefore, the BES-2 formed between 4.4-3.2ka at least. However, the RU3 (4.0-3.3ka) is not eroded and is below ca. 0.3m of the BES-2 which indicates the age of BES-2 possibly correspond with RU3 formation and with limit (MLSL) of RU3 growth plus 0.3m above. These suggest that BES was approximately equivalent with 0.3m above paleo-MLSL. Thus, it is concluded that the BES-2 was formed at same time with RU3 growth. The BES-3 occurs at E-3 site, which erodes the RU3, and is covered RU4. Therefore, the BES-3 formed between 3.3-3.2ka. The altitude of BES-3 is 6.7m (Figs. 5.2 and 5.3).

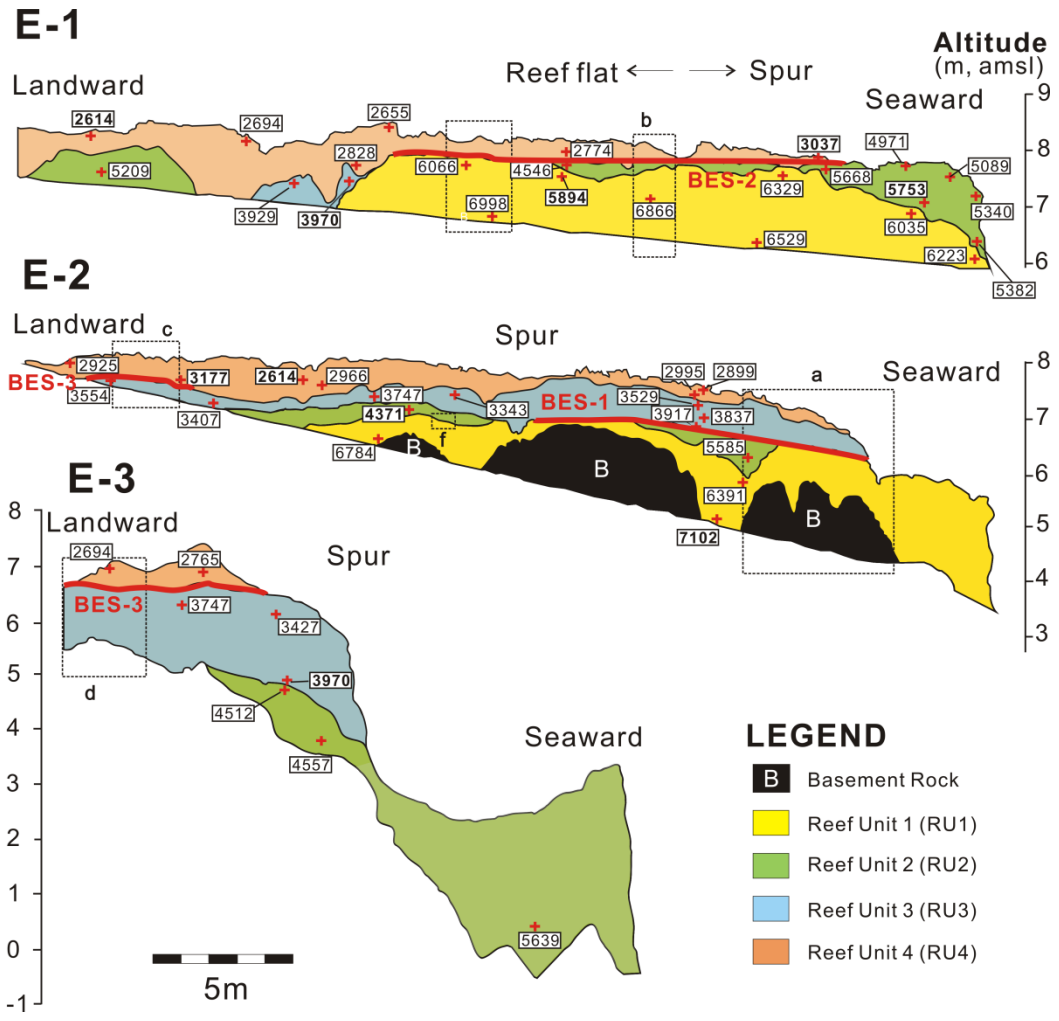


Fig. 5.2 The locality of Buried Erosion Surfaces (BES-1 to 3) at trench sites (E-1 to 3). The BES 1 to3 are shown by red line. The dashed squares labeled a–d indicate the locations of the photos shown in Fig. 5.3.

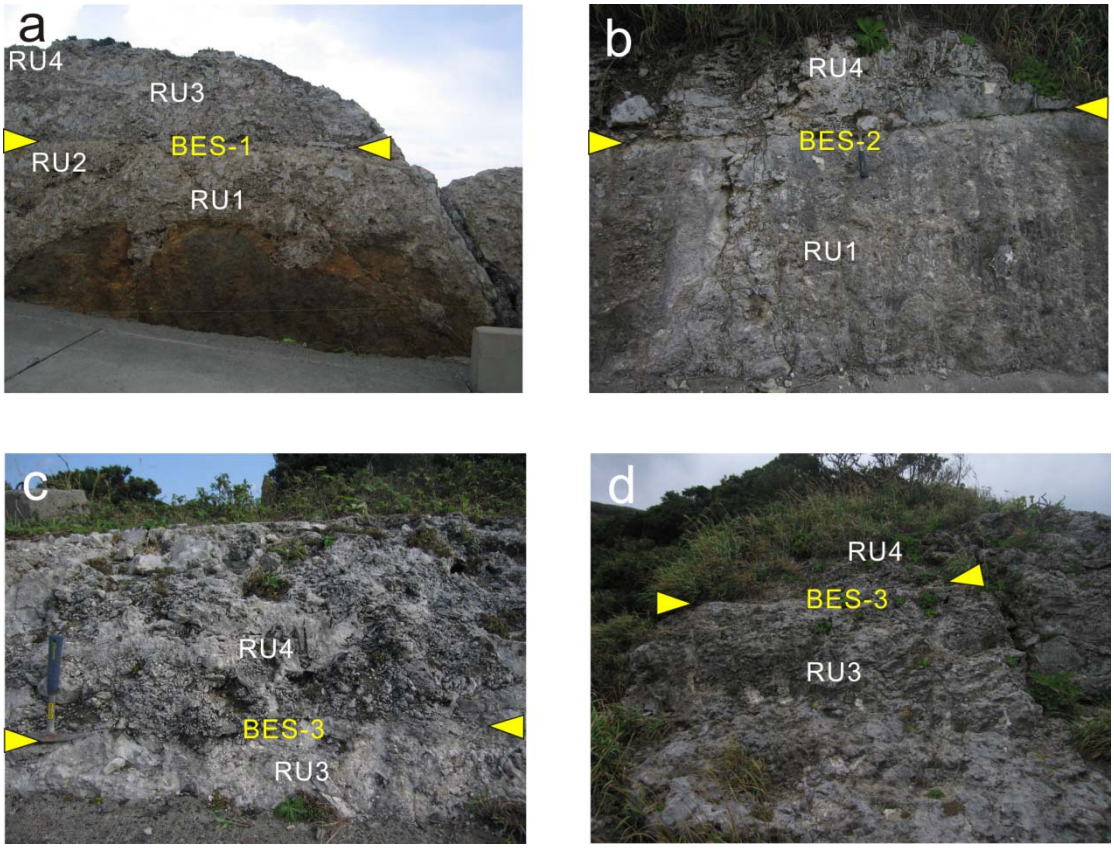


Fig. 5.3 The Buried Erosion Surfaces (BES-1 to 3) in TI sediments. The locations of the photos are shown in Fig. 5.3. The yellow triangles mark the BES. (a) BES-1 at E-2 site. (b) BES-2 at E-1 site. (c) BES-3 at E-2 site. (d) BES-3 at E-3 site.

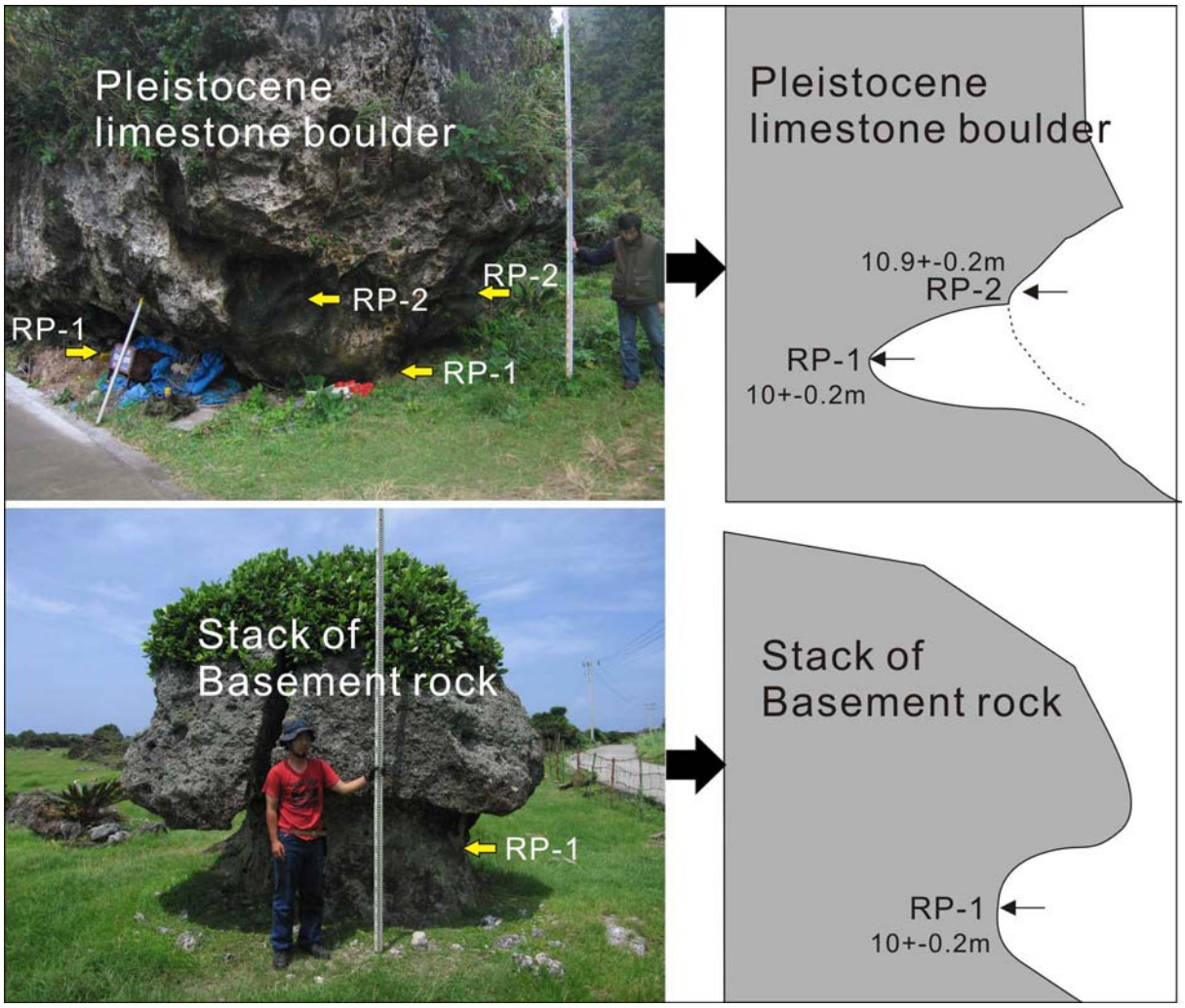


Fig. 5.4 The raised notches observed on TI at north (NN; upper part) and south (SN; lower part) of Kodakara Island. The RP indicates retreat points.

### 5.4.2 Sea-level change history

The hydro-isostatic adjustment after sea-level stabilized around the Kodakara is unknown. However, Kodakara is located in far-field from glacio-isostatic adjustment area. Moreover, island shelf around Kodakara is separated from continental shelf by Okinawa Trough, and is relatively small. Thus, I interpret that Kodakara reef provides an excellent place for measurements of recent sea-level changes due to the minimal hydro-isotatic contributions as well as Eastern Australia (<50 cm per 5000 yrs) (Lambeck, 2002).

Chronology and altitude data of the paleo sea-level indicators suggest that detailed sea-level change history at Kodakara Island, in the Northwest Pacific during the Holocene (Fig. 5.5a). At least, postglacial sea-level rise had ceased and the stabilization onset at least 6.3ka (Hamanaka et al., 2012) but possibly 7ka~ (Yokoyama et al., 1996). The sea-level had kept about 2000 yrs to ca. 4.4ka which had possibly recorded as RP1. At 4.4ka, the late Holocene sea-level oscillations (LHSO) had started. First, abrupt sea-level fall occurred with 1.5m. After sea-level fall, sea-level relative low stand had kept on within 400yrs. At ca.4ka, abrupt sea-level rise had occurred with 0.7m possibly within 100yrs (LHSO-1). The sea-level then had kept on lasting within 700yrs still 3.3ka. At 3.3ka, abrupt sea-level fall re-occurred with 0.9m within 100yrs. The sea-level then had kept on lasting within 100yrs still 3.2ka. At 3.2ka, abrupt sea-level rise had occurred with 2.5m possibly within 100yrs (LHSO-2). After 3.2ka, late-Holocene high-stand was onset and lasted to 2.4ka at least. Accordingly, LHSO occurred as two fluctuations in the relative long time sea-level fall during 4.4-3.2ka (Fig. 5.5a).

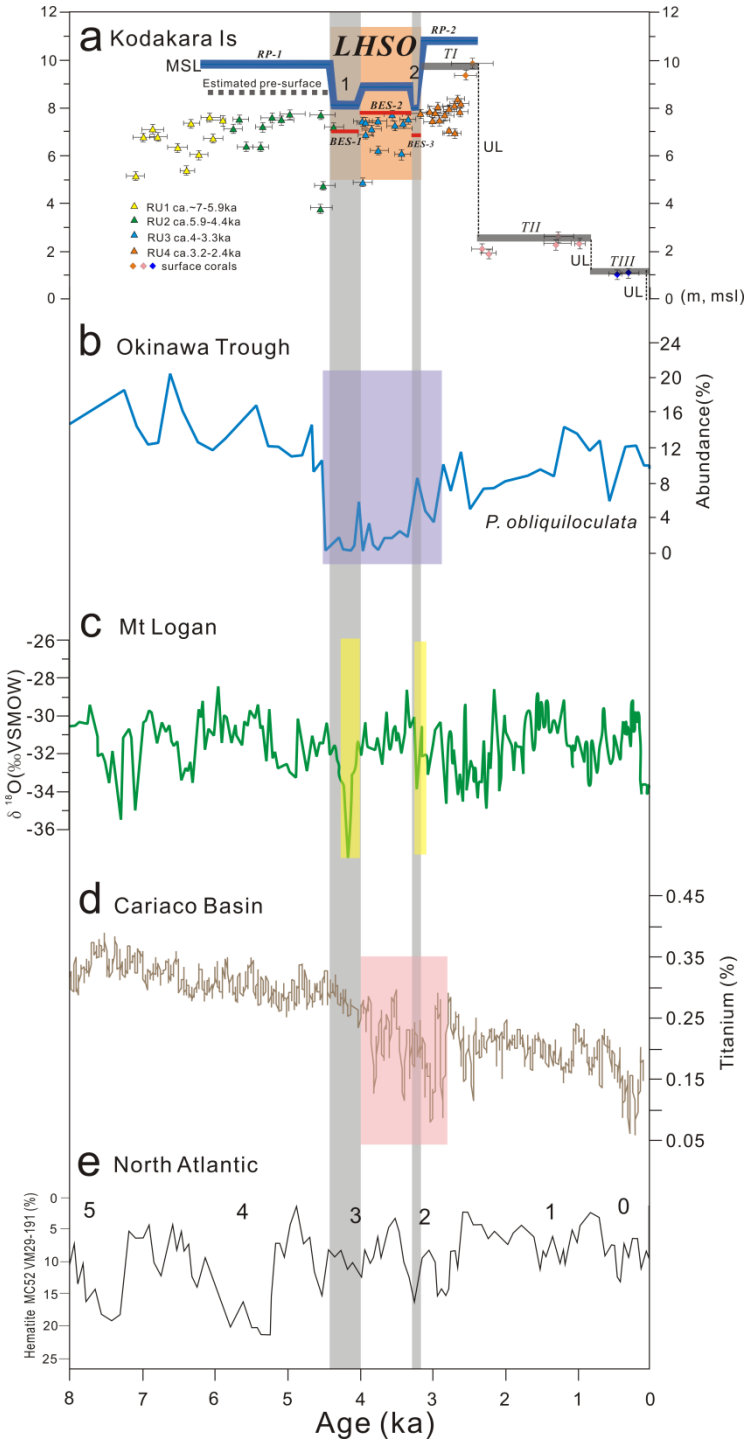


Fig. 5.5 The late Holocene sea-level oscillation (LHSO) with the millennial-scale climate change.(a) The age-height relationships of the collected corals and the relative sea-level changes from the excavated trench walls and terrace surfaces on Kodakara Island exhibit the timing of the disturbances with hiatuses and their linkage to climate change during the middle-to-late Holocene. (b) Percentage of *P. obliquiloculata* and the planktonic foraminifera-derived sea-surface temperature (SST) variability during the Holocene from core B-3GC (Jian et al., 2000). The PME is shaded. (c) $\delta^{18}O$ variability in a ice core form Mt. Logan, Yukon, Canada (Fisher et al., 2008). The strong PDO positive phase are shaded. (d) Percentage of titanium in a deep-sea core from the Cariaco Basin (Haug et al., 2001). The interval of strong El Nino is shaded. (e) Hematite (%) from North Atlantic sediment cores (MC52, VM29-191) (Bond et al., 1997) and Holocene events 0–6 labeled by Bond et al. (1997; 2001).

### 5.4.3 Interpretation for the cause of late Holocene sea-level oscillations

Sea-level and ice sheet

Although 70-75% of the projected sea-level rise is due to ocean temperature change ( IPCC, 2007), the influence of ice dynamical changes is identified as a major source of uncertainty (Milne et al., 2009). I believe the Holocene sea-level change have been effected by ice volume change at a global scale. However, it should be noted that it is difficult to detect which ices melted at that time.

The Antarctic deglaciation must have continued into the late Holocene (Nakada and Lambeck, 1989), in order to explain sea level changes on tectonically stable coasts far from the influence of glacio-isostatic rebound (Yokoyama et al., 2012). The recent sea-level model calls for meltwater addition equivalent 3-5m of sea-level from Antarctica and other sources, mostly in the period 7000 to 3000 years BP (Fleming et al., 1998; Ivins and James, 2005). The other sources, for example, the observed many glaciers in western Canada advanced between about 4.9 and 3.8 ka, about 4.2 ka, by a more extensive advance that may have lasted a few centuries (Menounos et al., 2008). These evidences suggest if the sea-level equivalent ice volume change is episodic, repeated extent and retreat, the observed LHSO at Kodakara may have been possible.

Similar to LHSO is recognized in the far-fields such as Eastern and Western Australia (Baker et al., 2005; Lewis et al., 2008), although the timings and magnitudes are inconsistent with our data. The reason is considered that difference of hydro-isostatic pattern which magnitudes and timings, however, even so, the difference of the magnitudes are significant.

The 4.4-3.2ka was corresponded with weakening duration of Kuroshio Current which characterized by abrupt decrease of *Pulleniatia obliculata*, so-called *Pelleniatia* minimum event (PME) between 4.6-2.7ka (Fig. 5.5b) (Jian et al., 2000; Xiang et al., 2007). The sea surface height (SSH) difference around Kuroshio Cur-

rent has reported around Japan within 1m scales (e.g., Kawabe, 1980; 1989). Moreover, Kuroshio Current volume transport anomaly in the Tokara Strait indicated by daily sea level difference (Ichikawa, 2001). Thus, I interpret the differences of SSH around the Northwest Pacific may have been affected by Kuroshio Current strength variability. During the PME, the relative weakening of Kuroshio Current may have enhanced the magnitudes of LHSO in the pathway.

ENSO and PDO

The Pacific Decadal Oscillation (PDO), a pattern of North Pacific SSH and SST variability that shifts phases every 20-30 years (Mantua et al., 1997). PDO spatial patterns broadly resemble El Niño (like positive phase) and La Niña (like negative phase) climate patterns (Mantua et al., 1997; Papineau, 2001). During a positive PDO phase is characterized by a cool wedge of lower than normal SSH /SST in the west Pacific Ocean becomes cool and the wedge in the east warms whereas they are inverse during a negative PDO phase. There were suppressed ENSO conditions during the middle Holocene between 8000 and 4000 cal BP with a North Pacific that generally resembled a La Niña-like or more negative PDO phase, and a climate transition between 4200 and 3000 cal BP (Fig. 5.5d) that appears to be the teleconnected expression to a more modern-like ENSO Pacific (Barron and Anderson, 2011). The climate transition well coincides to the duration of LHSO. Moreover, the two significant peaks of positive PDO phases are detected from $d^{18}O$ record of ice core which obtained at Mt. Logan, eastern Pacific (Fisher et al., 2008) (Fig. 5.5c). Therefore, the evidence indicates the positive phase of PDO may have been affected to the LHSO in the Northwest Pacific

Although the mechanism and magnitudes in detail is unclear at the present, I interpret that the LHSO was correlated with millennial-scale global climate change (Mayewski et al., 2004) induced by persistent solar activity (Bond et al., 2001) which may be able to invoke the extend or retreat of global ices, in particular, the Antarctic ice sheet (Ivins and James, 2005), the changes influenced Kuroshio Current (Jian et al. 2000), and the positive PDO phase (Fisher et al., 2008) with strong ENSO activity may have possibly enhanced the magnitude of the oscillations in the Northwest

Pacific. Thus, the results indicate that it is also important to assess the regional impact of future sea-level rise as well as the global impacts.

## 5.5 Interpretation of growth style of the raised reefs during the Holocene

The earliest post-glacial reef growth in the Ryukyu Islands began 9.9 to 8.5 ka ago on Kikai Island (Konishi et al., 1978; Webster et al., 1998; Ota et al., 2000). On Kodakara Island, reef growth initiated at least 8 ka ago, which is 2000 to 500 years earlier than at the nearby Kikai Island. However, I cannot determine precisely the date of reef initiation at Kodakara Island because corals near the bottom of core B4 are re-crystallized, and no other core penetrated the basement rock. The age of post-glacial reef initiation in the Ryukyu Islands ranges from 9 to 7 ka (Table 5.1; Kan and Kawana, 2006; Takahashi et al., 1988; Kan et al., 1995; Hongo and Kayanne, 2009). I can conclude that the timing of post-glacial reef growth initiation at Kodakara Island is similar to the rest of the Ryukyu Islands despite its high-latitude location.

It is possible that the sea environment supplied terrigenous sediments at the time of reef initiation on Kodakara Island because the coast was directly affected by wave attacks that eroded the basement rock surface. In fact, Facies D and C, which include relatively high quantities of terrigenous gravel, sand, and mud, are distributed near the basement rock (Figs. 4.26 and 4.27).

In the Ryukyu Islands, sea level stabilized between 7 and 5 ka (e.g., Kan et al., 1991). At Kodakara Island, the reef reached sea level at least approximately 6.3 ka, and subsequently the reef flat began prograding seaward (Hamanaka et al., 2012). When the sea level stabilized, the reef had not yet developed a reef edge, and the coastal area was exposed to high wave energy, like the “Holocene High-Energy Window” (HHEW; Hopley, 1984). It is possible that such condition resulted in the accretion of Facies A at landward sites (Figs. 4.26 and 4.27) and that the reef flat gradually extended seaward. The accretion of Facies A was also observed in exca-

vated trenches exposing vertical sections across the reef flat and reef edge (Hamanaka et al., 2012). By contrast, the seaward sites experienced relatively low wave energy conditions, and the reef slope morphology was constructed into Facies C (Figs. 4.26 and 4.27). After 6 ka, the reef-flat extended seaward, resulting in Facies A nearly covering the reef slope at the seaward sites. At that time, the facies of reef slope changed from Facies C to Facies B (Fig. 4.26). This transition corresponds to a relatively warm period, called the "Holocene climatic optimum" (e.g., Sonzogni et al., 1998; Gagan et al., 2000), during which reefs in the Ryukyu Islands grew more actively and reached sea level (e.g., Takahashi et al., 1988; Kan et al., 1991; Kan and Hori, 1993; Kan et al., 1995). Characteristic reef topographic features, such as reef flats, spur and groove systems, and reef mounds, formed at Kodakara Island at the same time as they did elsewhere in the Ryukyu Islands and match the timing of the Holocene climatic optimum.

Vertical growth on the lower reef slope decreased around 5 ka (core B1; Figs. 4.17 and 4.26), while the reef flat continued to grow seaward. In contrast with the lower reef slope, the upper reef slope, including the reef edge and mounds, continued its vertical growth after 4 ka (cores B2, B3, B5, B6; Figs. 4.17 and 4.26). At 3.3 ka, reef mound growth suddenly ceased, and reef slope accretion slowed (cores B6 and B5; Fig. 4). The upper reef growth continued after 3 ka. The 7-m uplift event occurred around 2.4 ka, which made the sea level fall relative to TI. The sea level restabilized at the level of TII. Both the reef flat and upper reef slope were exposed, while reef mounds protruded from the sea surface. Reef mounds with their tops near sea level were eroded. The depressions between mounds and the grooves were rapidly buried by detritus, including reworked corals, which correspond to Facies E, at a rate of 8.7 m $kys^{-1}$ as indicated by core B7 from a groove (core B7; Fig. 4.17a). Such conditions formed the relatively flat morphology on the landward side of TII (cores B1 and B2; Figs. 4.17 and 4.26). Reef growth was reactivated around 1.4 ka on the seaward side of TII (cores B1 and B2; Figs. 4.17 and 4.26). This new phase of reef accretion started on the reef slope of TII and constructed the spur and groove system that rapidly extended to the seaward sites (cores B2 and B1; Figs. 4.17 and 4.26). The

site of reef growth was under HHEW-like conditions, producing the flat morphology of the landward portion of TII through erosion processes, whereas Facies A dominantly accreted around the seaward sites in a zone of high wave energy (Fig. 4.26). At 1-0.4 ka, a coseismic uplift event caused a ~ 1.2 m vertical displacement of TII. Reef growth resumed before 0.4 ka and continued into the modern era. The third uplift event occurred during the past century and raised TIII approximately 2 m above its previous position.

In conclusion, the post-glacial reef anatomy of Kodakara Island, a high-latitude reef, appears to be controlled by a wave-energy gradient supplying terrigenous sediments. Apart from the effect of tectonic events, the reef initially reached sea level on the landward side and gradually extended seaward based on the spatial and temporal distribution of the cores (Fig. 5.6e), which is similar to the reef growth in Okierabu Island (27°20'N, 128°34'E) in the Northwest Pacific (Kan et al., 1995).

Table 5.1 Timings of post-glacial reef growth initiation in the Ryukyu Islands, Northwest Pacific

| Locality[1] | Timing of initial reef growth[2] | Reference |
|---|---|---|
| Kodakara Island (29°13′ N) | >7927 cal yr BP | Hamanaka et al. submitted |
| Kikai Island (28°21′ N) | 9900 years BP[3] | Ota et al. (2000) |
| Okinoerabu Island (27°20′ N) | 7380 years BP | Kan et al. (1995) |
| Minna Island (26°39′ N) | >5160 years BP | Kan and Hori (1993) |
| Kume Island (26°21′ N) | 7650 years BP | Takahashi et al. (1988); Kan et al. (1991) |
| Tonaki Island (26°22′ N) | >4960 years BP | Kan et al. (1997) |
| Okinawa Island (26°07′ N) | 7820 cal yr BP | Kawana and Kan (1996; 2002) |
| Ishigaki Island (24°30′ N) | >6040 cal yr BP | Hongo and Kayanne (2009) |
| Sekisei barrier reef (24°15′ N) | 8520 cal yr BP | Kan and Kawana (2006) |

1. Described from north to south
2. Oldest ages obtained from each Island and reef
3. $^{230}Th/^{234}U$ age

## 5.6 Correlation between the reef growth dynamics and millennial-scale climate change

Holocene reef growth on Kodakara Island has been interrupted at least three times, about 5.9-5.8 ka, 4.4-4.0 ka, and 3.3-3.2 ka, in response to millennial-scale climate changes (Hamanaka et al., 2012); however, it may be difficult to detect in the cores.

Reef growth during 8-6 ka corresponds to the interim between reef growth initiation and the first hiatus on Kodakara Island. The vertical growth rate of the seaward reef slope was estimated as 3.6-3.3 m $kys^{-1}$ (cores B2 and B3; Figs. 4.17 and 5.6e), and the growth rate of the landward sites was estimated as 1.3 m $kys^{-1}$ (core B4; Fig. 4.17), which occurred after the seaward site. The reason for the relatively low pace of growth at the landward site may have been due to the limitation of accommodation space for the vertical growth and the supply of relatively large portions of terrigenous sediments, which may have possibly disturbed the reef growth. The reef growth at the time window is equivalent to RU1 formation.

During the 6-4 ka which corresponds to the time between the first and second hiatus, the vertical reef growth rate of the seaward reef slope decreased to 1.9-1.3 m $kyr^{-1}$ (cores B2, B3, B5 and B6; Figs. 4.17 and 5.6), and the rates of growth of most landward and seaward sites abruptly decreased to 0.4-0.2 m $kyr^{-1}$, rates which continued into the late Holocene (cores B1 and B4; Figs. 4.17 and 5.6e). These altered growth rates may have been related to the first hiatus, which was caused by weakening of the Kuroshio Current. The reef growth at the time window is equivalent to RU2 formation.

In the 4-3 ka time period between the second and third hiatus which was associated with the LHSO (approximately 4.4-3.2 ka; Fig. 5.5). At ca. 4.4 ka, sea-level fall 1.7 m and seaward of TI was eroded which was lasting 400yrs until 4ka and is recorded as BES-1 at E-2 site. At ca. 4 ka, sea-level rose 0.7 m. At landward of TI was eroded, whereas the new reef (RU3) formed above BES-1 and more seaward reef

slope. The condition was lasting 700 yrs until ca. 3.3 ka which recorded as BES-2 at E-1 site (landward) and as RU3 on BES-2 at E-2 site (seaward). At ca. 3.3 ka, sea-level fall 0.9m and seaward of TI (RU3) was eroded which recorded as BES-3 at E-3 site. At ca. 3.2 ka, sea-level rose 2.5 m and new reef (RU4) formed above BES-2 (landward) and BES--3 (seaward). The condition was lasting 800 yrs until 2.4 ka uplifting event which recorded as RU4 on BES-2 at E-1 site (landward) and BES-3 at E-1 and E-2 sites (seaward). The vertical growth rates of the reef slope slowed to 1.4-0.5 m $kyr^{-1}$ (cores B5 and B6; Figs. 4.17 and 5.6e). This time interval corresponds to PME (Figs. 5.5b and 5.6d; Li et al., 1997; Jian et al., 2000; Xiang et al., 2007), and a period of increased ENSO variability (Figs 5.5d, 5.6b and c; Haug et al., 2001; Rein, 2007). The increase in ENSO variability significantly affected reef growth on the Panama coast in the tropical east Pacific and caused a hiatus in reef growth between 4 and 1.5 ka (Toth et al., 2012). The response of coral reef ecosystems to increased ENSO variability was probably different in the western and eastern Pacific. However, the timings of these events correspond with one another, indicating that changes in atmospheric and oceanic conditions may have affected reefs across the Pacific.

The third hiatus in reef growth is recorded at 3.3 ka (Hamanaka et al., 2012). At the same time, reef mound growth at site B6 ceased, and reef slope accretion slowed (cores B5 and B6; Figs 4.17 and 5.6e). The termination of reef growth reflects "give-up" conditions that occur when a reef cannot keep up with the rise in sea level (Neumann and Macintyre, 1985). This correlation implies that the hiatus may have changed, as the reef growth never restarted or slowed, and similar phenomenon may have existed at other reefs at high latitudes, such as those in the Northwest Pacific.

The rate of reef growth during the interval 1.3-1 ka was 9.1 m $kyr^{-1}$, the highest growth rate recorded in this study (Figs 4.17 and 5.6e). This time window corresponds to the Medieval Climate Anomaly (MCA), which is a period marked by a tendency for La Niña–like conditions in the tropical Pacific (Mann et al., 2009). The relative warmth in the central North Pacific MCA is consistent with the expected

extra-tropical signature for strong La Niña-like patterns in the tropical Pacific (strong cooling in the east and warming in the west) (Mann et al., 2009). Therefore, this condition may have accelerated the reef growth around Kodakara Island, which is situated in the Northwest Pacific. In contrast to that rapid growth, the TII reef barely grew between 2.4 (uplift event) and 1.4 ka. The Kuroshio Current weakened at 1.7 ka, which may correlate to the Holocene event at ca. 1.4 ka in the North Atlantic (Jian et al., 2000; Hamanaka et al., 2012), causing the less well understood growth hiatus in the reef at that time (Fig. 5.6). Moreover, a high El-Niño frequency about 2-1.5 ka can be detected from evidence at El Junco Lake, San Cristobal, Galápagos, in the Eastern Pacific (Conroy et al., 2008; Fig. 5.6c). Similarly, off the coast of Panama in the tropical east Pacific, a reef growth hiatus linked to increased ENSO variability occurred between 4 and 1.5 ka (Toth et al., 2012). Such a reef growth hiatus also occurred at Dunk Island in the southwest Pacific between 4.5 and 1.6 ka (Perry and Smithers, 2010). These findings suggest that hiatuses in reef growth between 4.4 and 1.4 ka on Kodakara Island could also be related to ENSO variability. The increased ENSO variability probably influenced reefs throughout the Pacific, although the patterns and causes of these disturbances varied from one region to another (Perry and Smithers, 2010; Hamanaka et al., 2012; Toth et al., 2012).

This study shows that millennial-scale climate change significantly affected reef growth at Kodakara Island in the Northwest Pacific. It will be necessary to collect precise data on the reef growth hiatuses from a wider area to better understand the processes controlling reef growth in the world. I hope that this study will contribute to the understanding of coral reef responses to climate change and aid in future studies on reef growth under conditions of global warming.

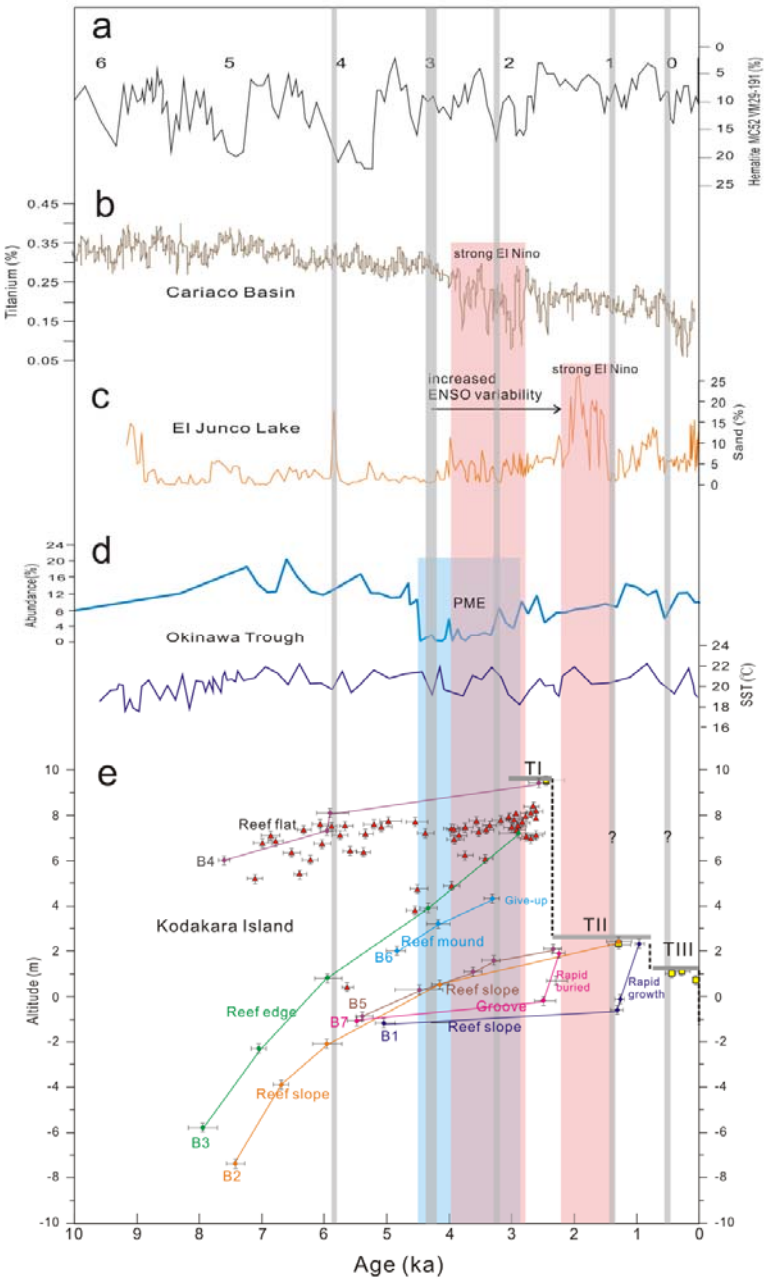


Fig. 5.6 The post-glacial reef growth on Kodakara Island with the millennial-scale climate change. (a) Hematite (%) from North Atlantic sediment cores (MC52, VM29-191) and Holocene events 0–6 labeled by Bond et al., 2001. (b) Percentage of titanium in a deep-sea core from the Cariaco Basin (Haug et al., 2001). The strong ENSO mode around 4ka is shown by pink shaded bar. (c) Percentage of sand in a core from El Junco Lake, San Cristobal, Galápagos (Conroy et al., 2008). The strong ENSO mode around 2ka is shown by pink shaded bar. (d) Percentage of *Pulleniatina obliquiloculata* and the planktonic foraminifera-derived sea-surface temperature (SST) variability during the Holocene from core B-3GC (Jian et al., 2000). The PME is shown by blue shaded bar. (e) The age-height relationships of the collected coral cores and excavated trenches on Kodakara Island. The diamonds indicate the age-height based on the cores. The triangles indicate the age-height from the excavated trench walls, E-1 to 3, from the upper reef flat to the edges (Hamanaka et al., 2012). The reef growth hiatus events are shown by grey shaded bars.

# Chapter 6

# Conclusions and Perspectives

Many factors, possibly varying across locations, influence coral reef formation (e.g., Kennedy and Woodroffe, 2002; Montaggioni, 2005). The results of this study suggest that the timing of the disturbances with hiatuses in high-latitude coral reef growth, i.e., the timing of the reef growth (Buddemeier and Hopley, 1988), was well-correlated with the millennial-scale global climate changes induced by persistent solar activity and that the paleodiversity changes were well-correlated with the variability in the major ocean currents, such as the Kuroshio Current. The Holocene reef growth trend in Kodakara Island may have occurred throughout the Holocene cooling events, such as the 8.2 ka event and the Little Ice Age, and may have been global in nature. Middle-to-late Holocene reef formation in Kodakara Island strongly suggests millennial-scale cycles in reef growth, thus reflecting global climate change. In particular, the reef growth has been possibly affected by ENSO and PDO activities after 4 ka. The results of thesis suggest that the timing of the rapid reef growth on Kodakara Island coincided to La-Niña tendency, whereas the hiatus coincided to strong El-Niño mode in the Pacific. Thus, it should be more needed to observation for long-term ENSO activity with PDO and how they affect

the future reef growth in the Pacific under global warming. New approaches are also needed to confirm disturbance with hiatus and growth phase timing in reef cores, because most ideas about current coral reef formation are based on evidence from cores. Moreover, more absolute SST and SSH data during disturbances with hiatuses elsewhere are needed to detect thresholds for continuous reef growth on a global scale. I can expect to understand the spatial and temporal variation of disturbances with hiatuses geographically using these additional data. I hope this study will contribute to the understanding of coral reef response to climate change and help to confirm theories of past and future reef formation.

# References


Abram N., Webster J., Davies P., and Dullo W., 2001. Biological response of coral reefs to sea surface temperature variation: evidence from the raised Holocene reefs of Kikai-jima (Ryukyu Islands, Japan). *Coral Reefs* 20, 221–234.

Alley, R.B., Mayewski, P. A., Sowers, T., Stuiver, M., Taylor, K. C. and Clark, P.U., 1997. Holocene climatic instability: Aprominent, widespread event 8200 yr ago. *Geology* 25, 483-486.

Alley, R.B., Clark, P.U., Huybrechts, P. and Joughin, I., 2005. Ice-sheet and sealevel changes. *Science* 310, 456–460.

Baker R.G.V., Haworth, R. J. and Flood, P. G. 2001. Warmer or Cooler Marine Late Holocene Palaeoenvironments?: Interpreting Southeast Australian and Brazilian Sea Level Curves Using Changes in Fixed Biological Indicators and their d $^{18}O$ Content." *Palaeogeography, Palaeoclimatology, Palaeoecology* 168, 249-272.

Baker, R.G.V., Davis, A.M., Aitchison, J.C., Flood, P.G., Morton, B.S. and Haworth, R.J., 2003. Comment on"Mid-Holocene higher sea level indicators from the south China coast" by W.W.-S. Yim and G. Huang: a regional perspective. *Marine Geology* 196, 91–98.

Baker, R.G.V., Haworth, R.J. and Flood, P.G., 2005. An oscillating Holocene sea-level? Revisiting Rottnest Island, Western Australia, and the Fairbridge eustatic hypothesis. *J. Coastal Res. Spec. Iss.*, 42, 3–14.

Bard, E., Hamelin, B., Arnold, M., Montaggioni, L. F., Cabioch, G., Faure, G and

Rougerie, F., 1996. Deglacial sea-level record from Tahiti corals and the timing of global meltwater discharge. *Nature* 382, 241-244.

Barron, J. A. and Anderson, L., 2011. Enhanced Late Holocene ENSO/PDO expression along the margins of the eastern North Pacific. *Quaternary International* 235, 3-12.

Blanchon, P., Eisenhauer, A., Fietzke, J. and Liebetrau, V., 2009. Rapid sea-level rise and reef back-stepping at the close of the last interglacial highstand. *Nature* 458, 881-884.

Bond G., Showers W., Cheseby M., Lotti R., Almasi P., deMenocal P., Priore P., Cullen H., Hajdas I., and Bonani G., 1997. A pervasive millennial-scale cycle in North Atlantic Holocene and glacial climates. *Science* 278, 1257–1266.

Bond G., Kromer B., Beer J., Muscheler R., Evans M.N., Showers W., Hoffmann S., Lotti-Bond R., Hajdas I., and Bonani G., 2001. Persistent solar influence on North Atlantic climate during the Holocene. *Science* 294, 2130–2136.

Bruggemann, J.H., Buffler, R.T., Guillaume, M.M.M., Walter, R.C., von Cosel, R., Ghebretensae, B.N., Berhe, S.M., 2004. Stratigraphy, palaeoenvironments and model for the deposition of the Abdur Reef Limestone: context for an important archaeological site from the last interglacial on the Red Sea coast of Eritrea. *Palaeogeography, Palaeoclimatology, Palaeoecology* 203, 179–206.

Buddemeier, R.W., and Hopley, D., 1988. Turn-ons and turn offs: causes and mechanisms of the initiation and termination of coral reef growth. *Proc. 6th Int. Coral Reef Symp.* 1, 253-261.

Cabioch, G., Montaggioni, L.F., Faure, G., 1995. Holocene initiation and development of New Caledonian fringing reefs, SW Pacific. *Coral Reefs* 14, 131–140.

Chappell, J., 2002. Sea level changes forced ice breakouts in the Last Glacial Cycle: New results from coral terraces. *Quaternary Science Reviews* 21, 1229–1240.

Conroy, J. L., Overpeck, J. T., Cole, J. E., Shanahan, T. M. and Steinitz-Kannan, M. 2008. Holocene changes in eastern tropical Pacific climate inferred from a Gala´pagos lake sediment record. *Quaternary Science Reviews* 27, 1166-1180.

Cornell, J. H., 1997. Disturbance and recovery of coral assemblages. *Coral Reefs* 16,

101-113.

Dansgaard, W., Johnsen, S. J., Clausen, H. B., Dahl-Jensen, D., Gundestrup, N. S., Hammer, C. U., Hviderberg, C. S., Steffensen, J. P., Sveinbjornsdottir, A. E., Jouzel, J. and Bond G., 1993. Evidence for general instability of past climate from a 250-kyr ice-core record. *Nature* 364, 218-220.

deMenocal P., Ortiz J., Guilderson T., and Sarnthein M., 2000. Coherent high and low-latitude climate variability during the Holocene warm period. *Science* 288, 2198–2202.

Esat, T. M., and Yokoyama. Y., 2006. Growth patterns of the last ice age coral terraces at Huon Peninsula. *Global and Planetary Change* 54, 216–224.

Fairbanks, R. G., 1989. A 17, 000-year glacio-eustatic sea level record: influence of glacial melting rates on the Younger Dryas event and deep-ocean circulation. *Nature* 342, 637-642.

Fisher, D., Dyke, A., Dahl-Jensen, D., Demuth, M., Zdanowicz, C., Bourgeois, J., Koerner, R.M.,Mayewski, P.,Wake, C., Kreutz, K., Steig, E., Zheng, J., Yalcin, K., Goto-Azuma,K., Luckman, B.,Rupper, S., 2008. The Mt. Logan Holocenedlate Wisconsin isotope record: tropical Pacific-Yukon connections. *The Holocene* 19, 667-677.

Fleming, K., Johnston, P., Zwartz, D., Yokoyama, Y., Lambeck, K. and Chappell, J., 1998. Refining the eustatic sea-level curve since the Last Glacial Maximum using far- and intermediate-field sites. *Earth Planet.Sci. Lett.* 163, 327-342.

Fukuoka district meteorological observatory, 1975. *Extraordinary weather report of Fukuoka district.* 52, 1-62.

Fukuoka district meteorological observatory, 1998. *Bulletin of the Fukuoka district meteorological observatory* 53, 435pp.

Gagan M.K., Ayliffe L.K., Beck J.W., Cole J.E., Druffel E.R.M., Dunbar R.B., Schrag D.P., 2000. New views of tropical paleoclimates from corals. *Quaternary Science Rev*iews 19, 45-64.

Gagan, M. K., Hendy, E. J., Haberle, S. G. and Hantoro, W. S., 2004. Postglacial evolution of the Indo-Pacific Warm Pool and El Niño-Southern Oscillation, *Qua-*

*ternary International* 118-119, 127-143.

Gregory, J.M., Huybrechts, P. and Raper, S.C.B., 2004. Threatened loss of the Greenland ice-sheet. *Nature* 428, 616.

Grootes, P.M., Stuiver, M., White, J.W.C., Johnsen, S., Jouzel, J., 1993. Comparison of oxygen isotope records from the GISP2 and GRIP Greenland ice cores. *Nature* 366, 552-554.

Hamanaka, N., Kan, H., Nakashima, Y., Hori, N., Okamoto, T., Ohashi, T., Adachi, H., 2008. Morphology and Anatomy of Holocene Raised Coral Reef Terraces in Kodakara Island, Tokara Islands, Northwestern Pacific, Japan. *Okayama Univ. Earth. Sci. Rep.*, 15, 33–65.

Hamanaka, N., Kan, H., Nakahima, Y., Yokoyama, Y., Okamoto, T., Ohashi, T., Adachi, H., Matsuzaki, H. and Hori, N. Response of high-latitude reef growth to Holocene millennial-scale climate change at Kodakara Island, Northwest Pacific. *Palaeogeography, Palaeoclimatology, Palaeoecology*, submitted.

Hamanaka, N., Kan, H., Yokoyama, Y., Okamoto, T., Nakashima, Y. and Kawana, T. 2012. Disturbances with hiatuses in high-latitude coral reef growth during the Holocene: Correlation with millennial-scale global climate change. *Global and Planetary Change* 80-81, 21-35.

Hamanaka, N., Okamoto, T., Ohashi, T., Kan, H., 2009. Low-scarp morphology on Holocene-raised coral reef terraces in Kodakara Island, the central Ryukyus, Japan. *Transac. Japanese Geomorphol. Union* 30, 125-135.

Haug, G., Hughen, K. A., Sigman, D. M., Peterson, L. C., Röhl, U., 2001. Southward Migration of the Intertropical Convergence Zone Through the Holocene. *Science* 293, 1304-1308.

Hoegh-Guldberg, O., Mumby, P.J., Hooten, A.J., 2007. Coral reefs under rapid climate change and ocean acidification. *Science* 318, 1737–1742.

Hoegh-Guldberg, O., Ortiz, J.C. and Dove, S. 2011. The future of coral reefs. *Science* 334**,** 1494-1495.

Hongo, C., Kayanne, H., 2009. Holocene coral reef development under windward and leeward locations at Ishigaki Island, Ryukyu Islands, Japan. *Sedimentary*

*Geology* 214, 62–73.

Hongo, C and Kayanne, H., 2011. Key species of hermatypic coral for reef formation in the northwest Pacific during Holocene sea-level change. *Marine Geology* 279, 162-177.

Hopley, D. 1984. The Holocene 'high-energy window' on the Central Great Barrier Reef. *In Thom, B. G. (ed.) Coastal geomorphology in Australia. Academic press,* 135-150.

Hori, N. 1977. A morphological study on the geographical distribution of coral reefs. *Geogr. Rep. Tokyo Metropol. Univ.* 12, 1-75.

Hughen K.A., Baillie M.G.L., Bard, E., Beck J.W., Bertrand C.J.H., Blackwell P.G., Buck C.E., Burr G.S., Cutler K.B., Damon P.E., Edwards R.L., Fairbanks R.G., Friedrich M., Guilderson T.P., Kromer B., McCormac G., Manning S., Ramsey C.B., Reimer P.J., Reimer R.W., Remmele S., Southon J.R., Stuiver M., Talamo S., Taylor F.W., van der Plicht J., and Weyhenmeyer C.E., 2004. MARINE04 marine radiocarbon age calibration, 0-26 cal kyr BP. *Radiocarbon* 46, 1059–1086.

Hughes, T.P., Baird, A.H., Bellwood, D.R., Card, M., Connolly, S.R., Folke, C., Grosberg, R., Hoegh- Guldberg, O., Jackson, J.B.C., Kleypas, J., Lough, J.M., Marshall, P., Nystro¨m, M., Palumbi, S.R., Pandolfi, J.M., Rosen, B., and Roughgarden, J., 2003. Climate change, human impacts, and the resilience of coral reefs. *Science* 301, 929–933.

Humblet ,M., Iryu, Y. and Nakamori T., 2009. Variations in Pleistocene coral assemblages in space and time in southern and northern Central Ryukyu Islands, Japan. *Marine Geol*ogy 259, 1–20.

Ichikawa, K., 2001. Variation of the Kuroshio in the Tokara Strait Induced by Meso-Scale Eddies. *J. Oceanography* 57, 55-68.

IPCC, 2007. Climate Change 2007: The Physical Science Basis. Contribution of Working Group I to the Fourth Assessment Report of the Intergovernmental Panel on Climate Change *[Solomon, S., D. Qin, M. Manning, Z. Chen, M. Marquis, K.B. Averyt, M. Tignor and H.L. Miller (eds.)]. Cambridge University Press, Cambridge, United Kingdom and New York, NY, USA*, 996 p.

*REFERENCES*


Iryu, Y., Nakamori, T., Matsuda, S., Abe, O., 1995. Distribution of marine organisms and its geological significance in the modern reef complex of the Ryukyu Islands. *Sedimentary Geology* 99, 243–258.

Ivins, E. R. and James, T. S., 2005. Antarctic glacial isostatic adjustment: a new assessment. *Ant. Sci*. 17, 541-553.

Japan meteorological agency, 1976. *Geophysical review* 913, 59pp.

Japan meteorological agency, 1995. *Geophysical review* 1156, 76pp.

Jian Z., Wang P., Saito Y., Wang J., Pflaumann U., Oba T., and Cheng X., 2000. Holocene variability of Kuroshio Current in the Okinawa Trough, northwestern Pacific Ocean. *Earth and Planetary Science Lett*ers 184, 305–319.

Joughin, I., Abdalati, W. and Fahnestock, M., 2004. Large fluctuations in speed on Greenland_s Jakobshavn glacier. *Nature* 432, 608–610.

Kan, H., Adachi, H., Nakashima, Y. and Naito, G. 1998. Development of a submersible, diver-operated coring device: a tool for reef science. *Chishitsu News* 527, 43-47.

Kan, H., Hori, N., 1993. Formation of topographic zonation on the well-developed fringing reef-flat, Minna Island, the Central Ryukyus. *Trans. Japan Geomorphol. Union* 14, 1–16.

Kan H., Hori N., Nakashima Y., and Ichikawa K., 1995. Narrow reef flat formation in a high-latitude fringing reef. *Coral Reefs* 14, 123–130.

Kan, H., Hori, N., Kawana, T., Kaigara, T. and Ichikawa, K., 1997. The evolution of a Holocene fringing reef and island: reefal environmental sequence and sea level change in Tonaki Island, the Central Ryukyus. *Atoll Research Bulletin* 443, 1-20.

Kan H., Kawana, T., 2006. 'Catch-up' of a high-latitude barrier reef by back-reef growth during post-glacial sea-level rise, Southern Ryukyus, Japan. *Proc. 10th Int. Coral Reef Symp*. 494-503.

Kan, H., Takahashi, T., Koba, M., 1991. Morpho-dynamics on Holocene reef accretion: drilling results from Nishimezaki Reef, Kume Island, the Central Ryukyus. *Geographical Review of Japan* 64B, 114–131.

Kawabe, M., 1980. Sea level variations along the south coast of Japan and the large

meander in the Kuroshio. *J. Oceanogr. Soc. Japan*, 36, 97-104.

Kawabe, M., 1989. Sea level changes south of Japan associated with the non large-meander path of the Kuroshio. *J. Oceanogr. Soc. Japan*, 45, 181-189.

Kennedy D.M., and Woodroffe C.D., 2002. Fringing reef growth and morphology: a review. *Earth-Science Reviews* 57, 255–277.

Kleypas, J. A., R. W. Buddemeier, D. Archer, J.-P. Gattuso, C. Langdon, and B. N. Opdyke, 1999. Geochemical consequences of increased atmospheric carbon dioxide on coral reefs. *Science* 284, 118– 120.

Koba, M., Nakata, T., and Watabe, S., 1979. Late Quaternary reef caps of Takara and Kodakara islands, Ryukyu archipelago, and sea-level changes of late Holocene. *Chikyu-Kagaku* 33, 173-191.

Koba M., Nakata T, and Takahashi T., 1982. Late Holocene eustatic sea-level changes deduced from geomorphological features and their $^{14}C$ dates in the Ryukyu Islands, Japan. *Palaeogeography, Palaeoclimatology, Palaeoecology* 39, 231–260.

Konishi, K., Tsuji, Y., Goto, T., Tanaka, T., 1978. Holocene raised reef drilling at Kikai-jima, central Ryukyus. *Science Report of Kanazawa University* 23, 129–153.

Lambeck, K., 2002. 'Sea Level Change From Mid Holocene to Recent Time: An Australian Example with Global Implications', *in Jerry X. Mitrovica, Bert L.A. Vermeersen (ed.), Ice sheets, sea level, and the dynamic earth*, *American Geophysical Union, Washington, DC, USA*, 33-50.

Lewis, S.E., Wüst, R.A.J., Webster J.M. and Shields, G.A., 2008. Mid-late Holocene sea-level variability in eastern Australia. *Terra Nova* 20, 74–81.

Li, B., Jian, Z. and Wang P., 1997. Pulleniatina obliquiloculata as a paleoceanographic indicator in the southern Okinawa Trough during the last 20,000 years, *Marine Micropaleontol*ogy 32, 59– 69.

Liew, P. M., Lee, C. Y. and Kuo, C. M., 2006. Holocene thermal optimal and climate variability of East Asian monsoon inferred from forest reconstruction of a subalpine pollen sequence, Taiwan. *Earth and Planetary Science Letters* 250,

596–605.

Liu, Z., Brady, E., Lynch-Stieglitz, J., 2003. Global ocean response to orbital forcing in the Holocene. *Paleoceanography* 18, 1041.

Mantua, N.J., Hare, S.R., Zhang, Y., Wallace, M., Francis, R.C., 1997. A Pacific decadal climate oscillation with impacts on salmon. *Bulletin of the American Meteorological Society* 78, 1069-1079.

Marshall, J.F., Davies, P.J., 1982. Internal structure and Holocene evolution of One Tree Reef, southern Great Barrier Reef. *Coral Reefs* 1, 21–28.

McCulloch, M., Mortimer, G., Esat, T., Xianghua, L., Pillans, B. and Chappell, J., 1996. High resolution windows into early Holocene climate: Sr/Ca coral records from the Huon Peninsula. *Earth and Planetary Science Letters* 138, 169-78.

Mann, M. E., Zhang, Z., Rutherford, S., Bradley, R. S., Hughes, M. K., Shindell, D., Caspar Ammann, C., Faluvegi, G. and Ni, F. 2009. Global Signatures and Dynamical Origins of the Little Ice Age and Medieval Climate Anomaly. *Science* 326, 1256-1260.

Martin, L., Dominguez, J. M. L. and Bittencourt, A. C. S. P., 2003. Fluctuating Holocene sea levels in eastern and southeastern Brazil: evidence from multiple fossil and geometric indicators. *Journal of Coastal Research* 19, 101–124.

Matsuzaki, H., Nakano, C., Yamashita, H., Maejima, Y., Miyairi, Y., Wakasa, S., Horiuchi, K., 2004. Current status and future direction of MALT, The University of Tokyo. *Nuclear Instruments and Methods B* 223–224, 92–99.

Mayewski, P.A., Rohling, E.E., Stager, J.C., Karlen, W., Maasch, K.A., Meeker, L.D., Meyerson, E.A., Gasse, F., van Kreveld, S., Holmgren, K., Lee-Thorp, J., Rosqvist, G. Rack, F., Staubwasser, M., Schneider, R.R. and Steig, E.J. 2004. Holocene climate variability. *Quaternary Research* 62, 243-255.

Menounos, B., Clague J. J., Osborn, G., Luckman, B. H., Lakeman, T. R. and Minkus, R., 2008. Western Canadian glaciers advance in concert with climate change circa 4.2 ka. *Geophysical Research Letters* 35, L07501.

Milne, G. A., Gehrels, W. R., Hughes, C. W. and Tamisiea, M. E., 2009. Identifying the causes of sea-level change. *Nature Geoscience* 2, 471 – 478.

Montaggioni L.F., 2005. History of Indo-Pacific coral reef systems since the last glaciation: Development patterns and controlling factors. *Earth-Science Rev*iews 71, 1–75.

Montaggioni, L.F., Faure, G., 1997. Response of reef coral communities to sea-level rise: a Holocene model from Mauritius (Western Indian Ocean). *Sedimentology* 44, 1053–1070.

Moy, C. M., Seltzer, G.O., Rodbell, D. T. and Anderson D. M. 2002. Variability of El Niño/Southern Oscillation activity at millennial timescales during the Holocene epoch. *Nature* 420, 162-165.

Nakada, M. & Lambeck, K., 1988. The melting history of the late Pleistocene Antarctic ice sheet. *Nature* 33, 36-40.

Nakata, T., Takahashi, T., and Koba, M., 1978. Holocene-emerged coral reefs and sea-level changes in the Ryukyu Islands. *Geographical Review of Japan* 51, 87-108.

Neumann, A.C. and Macintyre, I. G., 1985. Reef response to sea level rise: keep-up, catch-up, give-up. *Proc. Fifth. Int. Coral Reef Symp*. 3, 105–110.

Ninio, R. Meekan, M. G., 2002. Spatial patterns in benthic communities and the dynamics of a mosaic ecosystem on the Great Barrier Reef, Australia. *Coral Reefs* 21, 95–103.

Nishihira, M., Veron, J.E.N., 1995. Hermatypic Corals of Japan. *Kaiyusha, Tokyo.* 439 pp.

Ota, Y. and Chappell, J. 1996. Late Quaternary coseismic uplift events on the Huon Peninsula, Papua New Guinea, deduced from coral terrace data. *Journal of Geophysical Research* 101, 6071-6082

Ota, Y., Machida, H., Hori, N., Konishi, K., Omura, A., 1978. Holocene raised coral reefs of Kikai-jima (Ryukyu Islands) -an approach to Holocene sea level study. *Geographical Review of Japan*. 51A, 109– 130.

Ota, Y., Sasaki, K., Omura, A., Nozawa, K., 2000. Holocene sea level and tectonic history related to the formation of coral terraces at Kikai Island. *Quaternary Research (Daiyonki-Kenkyu)* 29, 81–95.

Pandolfi, J.M., Bradbury, R. H., Sala, E., Hughes,T. P., Bjorndal, K. A, Cooke, R.G, McArdle, D., McClenachan, L., Newman, M.J., Paredes, G., Warner, R.R. and Jackson, J.B., 2003. Global trajectories of the long-term decline of coral reef ecosystems. *Science* 301, 955-958.

Pandolfi, J.M., Connolly, S.R., Marshall, D.J. and Cohen, A.L. 2011. Projecting coral reef futures under global warming and ocean acidification. *Science* 333, 418-422.

Pandolfi, J.M., Tudhope, A.W., Burr, G., Chappell, J., Edinger, E., Frey, M., Steneck, R., Sharma, C., Yeates, A., Jennions, M., Lescinsky, H. and Newton, A. 2006. Mass mortality following disturbance in Holocene coral reefs from Papua New Guinea. *Geology* 34, 949-952.

Papineau, J.M., 2001. Wintertime temperature anomalies in Alaska correlated with ENSO and PDO. *International Journal of Climatology* 21, 1577-1592.

Perry, C. T. and Smithers, S. G. 2010. Evidence for the episodic "turn on" and "turn off" of turbid-zone coral reefs during the late Holocene sea-level highstand. *Geology* 38, 119-122.

Pirazzoli, P. A., 1991. World atlas of Holocene sea-level changes. *Elsevier Oceanography series* 58, 1-280.

Pirazzoli, P. A., 1996. Sea-level changes: the last 20,000 years. *Ed. John Wiley & Sons, Chichester*, 211 pp.

Reimer, P. J., Baillie, M.G.L., Bard, E., Bayliss, A., Beck, J. W., Blackwell, P.G., Bronk Ramsey, C., Buck, C. E., Burr, G.S., Edwards, R.L., Friedrich, M., Grootes, P.M., Guilderson, T.P., Hajdas, I., Heaton, T. J., Hogg, A. G., Hughen, K.A., Kaiser, K.F., Kromer ,B., McCormac, F.G., Manning, S.W., Reimer, R.W., Richards, D.A., Southon, J.R., Talamo, S., Turney, C.S.M., van der Plicht, J., and Weyhenmeyer, C.E., 2009. INTCAL09 and MARINE09 radiocarbon age calibration curves, 0–50,000 years cal BP. *Radiocarbon* 51, 1111–1150.

Rein, B. 2007. How do the 1982/83 and 1997/98 El Niño's rank in a geological record from Peru? *Quaternary International* 161, 56-66.

Research Group for Active Faults of Japan, 1991. Active Faults in Japan: sheet maps and inventories (revised edition). *University of Tokyo Press*, 437pp.

Rohling, E. J. and Palike, H., 2005. Centennial-scale climate cooling with a sudden cold event around 8,200 years ago. *Nature* 434, 975-979.

Sagawa, N., Nakamori, T., Iryu, Y., 2001. Pleistocene reef development in the southwest Ryukyu Islands, Japan. *Palaeogeography, Palaeoclimatology, Palaeoecology* 175, 303–323.

Sakaguchi, Y., 1983. Warm and cold stages in the past 7600 years in Japan and their global correlation. *Bull. Dep. Geogr. Univ. Tokyo* 15, 1-31.

Saxby T., Dennison W.C., and Hoegh-Guldberg O., 2003. Photosynthetic responses of the coral *Montipora digitata* to cold temperature stress. *Mar. Ecol. Prog. Ser.* 248, 85–97.

Selvaraj, K., Chen C.T.A. and J.Y. Lou, 2007. Holocene East Asian monsoon variability: links to solar and tropical Pacific forcing. *Geoph. Res. Lett.* 34, L01703.

Siddall, M., Rohling, E. J., Almogi-Labin, A., Hemleben, C., Meischner, D., Schmelzer, I. and Smeed, D. A. 2003. Sea-level fluctuations during the last glacial cycle. *Nature* 423, 853-858.

Sugihara, K., Nakamori, T., Iryu, Y., Sasaki, K., Blanchon, P., 2003. Holocene sea-level change and tectonic uplift deduced from raised reef terraces, Kikai-jima, Ryukyu Islands, Japan. *Sedimentary Geology* 159, 5–25.

Sonzogni, C., Bard, E., and Rostek, F., 1998. Tropical sea-surface temperatures during the last glacial period: A view based on alkenones in Indian Ocean sediments. *Quaternary Science Rev*iews 17, 1185– 1201.

Stott L., Cannariato K., Thunell R., Haug G.H., Koutavas A., and Lund S., 2004. Decline of surface temperature and salinity in the western tropical Pacific Ocean in the Holocene epoch. *Nature* 431, 56–59.

Stuiver, M., and Reimer, P. J., 1993. Extended 14C database and revised CALIB radiocarbon calibration program. *Radiocarbon* 35, 215-230.

Stuiver M., Reimer P.J., Bard E., Beck J.W., Burr G.S., Hughen K.A., Kromer B., Mccormac G., van Der Plicht J., and Spurk M., 1998. INTCAL98 radiocarbon age calibration 24,000-0 cal BP. *Radiocarbon* 40, 1041–1083.

Takahashi, T., Koba, M., Kan, H., 1988. Relationship between reef growth and sea

level on the northwest coast of Kume Island, the Ryukyus: Data from drill holes on the Holocene coral reef. *Proc. 6th Int. Coral Reef Symp.* 3, 491–496.

Thompson LG, Yao T, Mosley-Thompson E, Davis ME, Henderson KA, Lin P., 2000. A high-resolution millennial record of the South Asian monsoon from Himalayan ice cores. *Science* 289, 1916-1919.

Thompson, W. G., Curran, H. A., Wilson, M. A. and White, B., 2011. Sea-level oscillations during the last interglacial highstand recorded by Bahamas corals. *Nature Geoscience* 4, 684–687

Toth, L. T., Aronson, R. B., Vollmer, S. V., Hobbs, J. W., Urrego, D. H., Cheng, H., Enochs, I. C., Combosch, D. J., van Woesik, R. and Macintyre, I. G., 2012. ENSO Drove 2500-Year Collapse of Eastern Pacific Coral Reefs. *Science* 337, 81-84.

Ujiie, Y., Ujiie, H., Taira, A., Nakamura, T. and Oguri, K., 2003. Spatial and temporal variability of surface water in the Kuroshio source region, Pacific Ocean, over the past 21,000 years: evidence from planktonic foraminifera. *Marine Micropaleontology* 49, 335-364.

Usami, T., 2003. Materials for comprehensive list of destructive earthquakes in Japan, [416]-2001. *University of Tokyo Press*, 605pp.

Veron J.E.N., and Minchin P.R., 1992. Correlations between sea surface temperature, circulation patterns and the distribution of hermatypic corals of Japan. *Continental Shelf Research* 12, 835–857.

Veron, J.E.N. and Pichon, M., 1976. Scleractinia of eastern Australia. Part I. Families Thamnasteriidae, Astrocoeniidae, Pocilloporidae. *Australian Inst. Mar. Sci. Monogr. Ser.* 1, 86pp.

Veron, J.E.N. and Pichon, M., 1980. Scleractinia of eastern Australia. Part III. Families Agariciidae, Siderastreidae, Fungiidae, Oculinidae, Merulinidae, Mussidae, Pectiniidae, Caryophylliidae, Dendrophylliidae. *Australian Inst. Mar. Sci. Monogr. Ser.* 4, 443pp.

Veron, J.E.N. and Pichon, M., 1982. Scleractinia of eastern Australia. Part IV. Family Poritidae. *Australian Inst. Mar. Sci. Monogr. Ser.* 5, 159pp.

Veron, J.E.N., Pichon, M. and Wijsman-Best, M. 1977. Scleractinia of eastern Aus-

tralia. Part II. Families Faviidae, Trachyphylliidae. *Australian Inst. Mar. Sci. Monogr. Ser*. 3, 233pp.

Veron, J.E.N. and Wallace, C.C., 1984. Scleractinia of eastern Australia. Part V. Family Acroporidae. *Australian Inst. Mar. Sci. Monogr.Ser.6*, 485pp.

Wang Y., Cheng H., Edwards R.L., He Y., Kong X., An Z., Wu J., Kelly M.J., Dykoski C.A., and Li X., 2005. The Holocene Asian monsoon: links to solar changes and North Atlantic climate. *Science* 308, 854–857.

Webster, J.M., Davies, P.J., Konishi, K., 1998. Model of fringing reef development in response to progressive sea level fall over the last 7000 years—(Kikai-jima, Ryukyu Islands, Japan). *Coral Reefs* 17, 289–308.

Wells J.N., 1957. Coral Reefs: Treatise on Marine Ecology and Paleoecology 1. Ecology. *Geological Society of America Memoir* 67, 609–631.

Wu, W., and Liu,T., 2004. Possible role of the "Holocene Event 3" on the collapse of Neolithic Cultures around the Central Plain of China. *Quat. Int.*117, 153-166.

Xiang, R., Sun, Y., Li, T., Oppo, D.W., Chen, M., Zheng, F., 2007. Paleoenvironmental change in the middle Okinawa Trough since the last deglaciation: evidence from the sedimentation rate and planktonic foraminiferal record. *Palaeogeography, Palaeoclimatology, Palaeoecology* 243, 378–393.

Yamano H., Hori K., Yamauchi M., Yamagawa O., and Ohmura A., 2001a. Highest-latitude coral reef at Iki Island, Japan. *Coral reefs* 20, 9–12.

Yamano, H., Kayanne, H., Yonekura, N., 2001b. Anatomy of a modern coral reef flat: a recorder of storms and uplift in the late Holocene. *J. Sediment. Res*. 71, 295–304.

Yamano, H., Sugihara, K. and Nomura K. 2011. Rapid poleward range expansion of tropical reef corals in esponse to rising sea surface temperatures. *Geophysical Reserach Letters* 38, L04601

Yancheva G., Nowaczyk N.R., Mingram J., Dulski P., Schettler G., Negendank J.F.W., Liu J., Sigman D.M., Peterson L.C., and Haug G.H., 2007. Influence of the intertropical convergence zone on the East Asian monsoon. *Nature* 445, 74–77.

Yokoyama, Y., Esat, T. M. and Lambeck. K., 2001. Last Glacial sea-level change

deduced from uplifted coral terraces of Huon Peninsula, Papua New Guinea. *Quaternary International* 83–85,275–283.

Yokoyama, Y., Miyairi, Y., Matsuzaki H. and Tsunomori F. 2007. Relation between acid dissolution time in the vacuum test tube and time required for graphitization for AMS target preparation, *Nuclear Instruments and Methods in Physics Research Section B*, 259, 1, 330-334

Yokoyama, Y., Nakada, M., Maeda, Y., Nagaoka, S., Okuno, J., Matsumoto, E., Sato, H., Matsushima, Y., 1996. Holocene sea-level change and hydro-isostasy along the west coast of Kyusyu, Japan. *Palaeogeography, Palaeoclimatology, Palaeoecology* 123, 29–47.

Yoneda, M., Uno, H., Shibata, Y., Suzuki, R., Kumamoto, Y., Yoshida, K., Sasaki, T., Suzuki, A., Kawahata, H., 2007. Radiocarbon marine reservoir ages in the western Pacific estimated by pre-bomb molluscan shells. *Nucl. Instr. Meth.* B 259, 432–437.

Yu K., Zhao J., Liu T., Wei G., Wang P., and Collerson K.D., 2004. High-frequency winter cooling and reef coral mortality during the Holocene climatic optimum. *Earth and Planetary Science Letters* 224, 143–155.

Zhao, J. and Yu, K., 2002. Timing of Holocene sea-level highstands by mass spectrometric U-series ages of a coral reef from Leizhou Peninsula, South China Sea. *Chinese Pollut. Bull.* 47, 348–352.

# Appendix A

## Photos of excavated trenches with sketched corals

### A.1 E-1 site


1


2

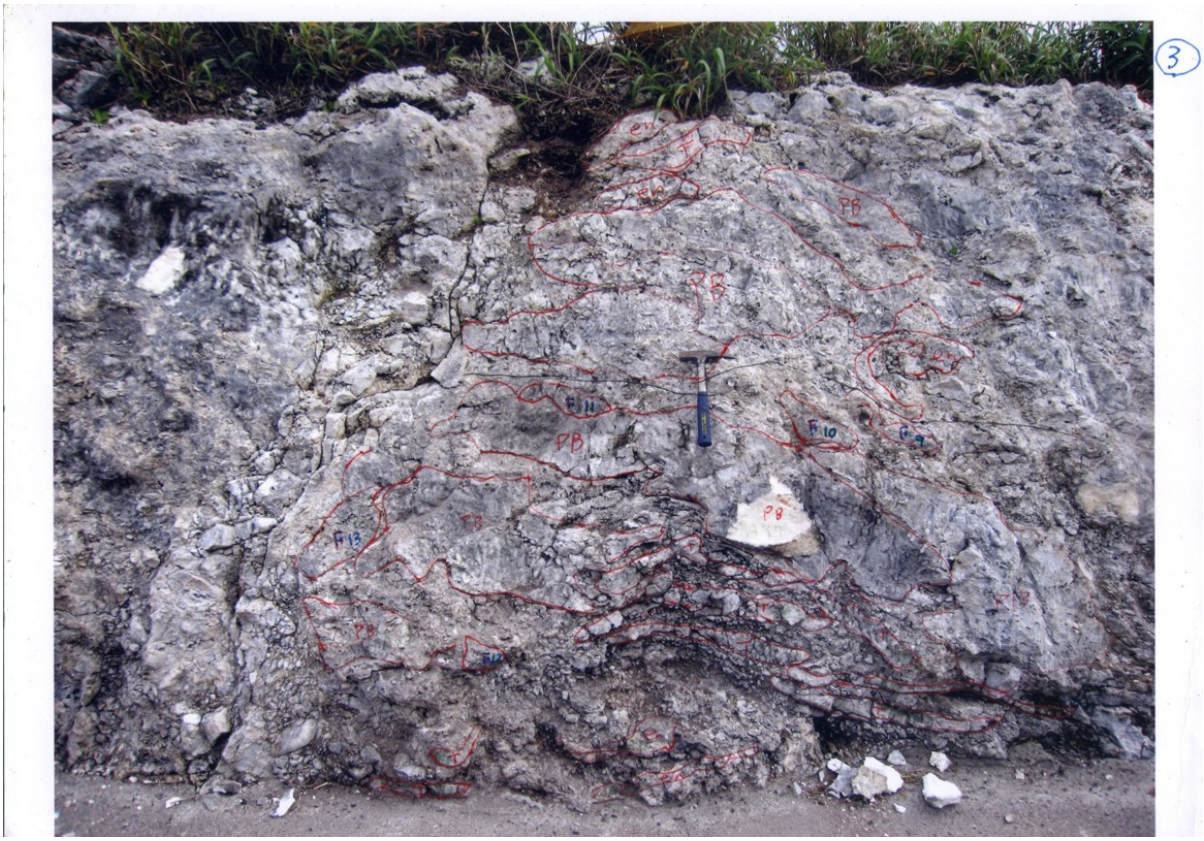
3
PB
PB
PB
PB
PB
PB
PB


4
PB
PB
PB


5

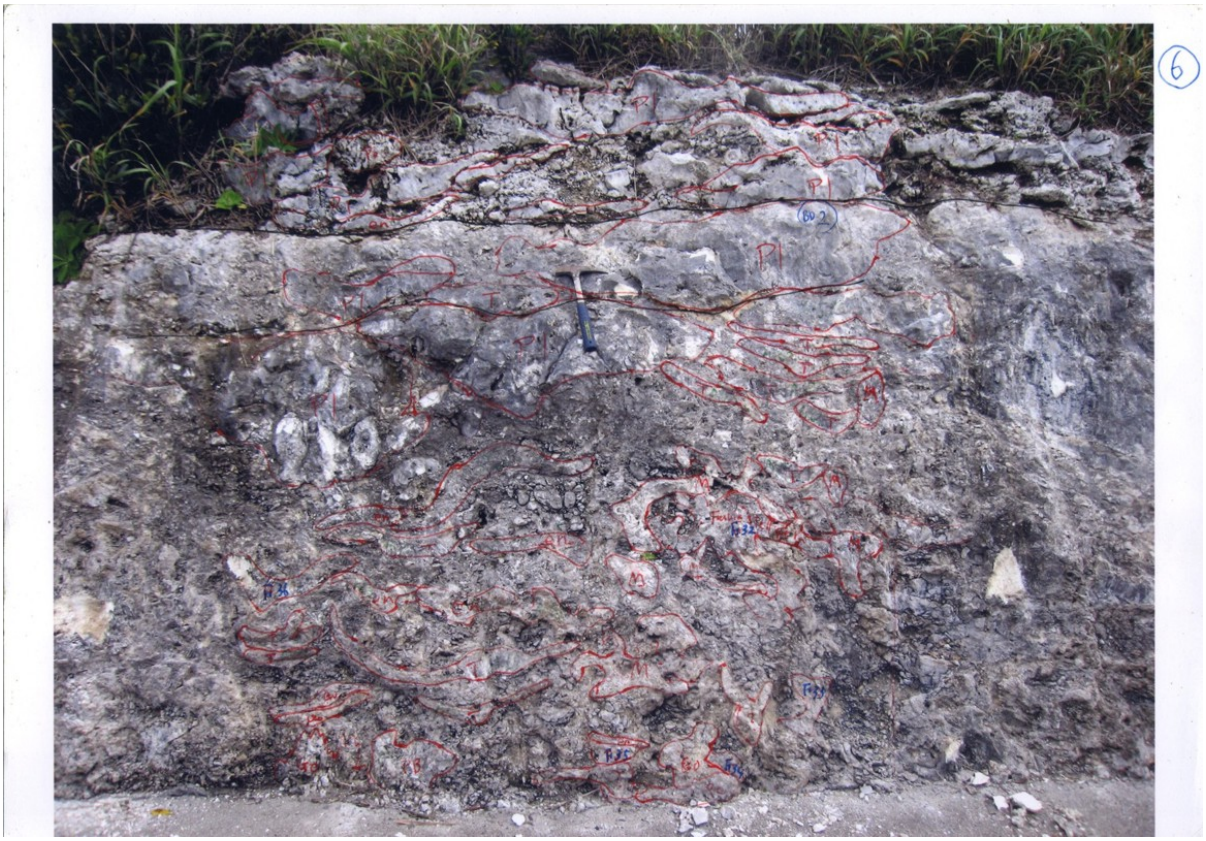
6


7
P1
P13
P1
P1
P38


8
P1
P1
P1
P1


9


10

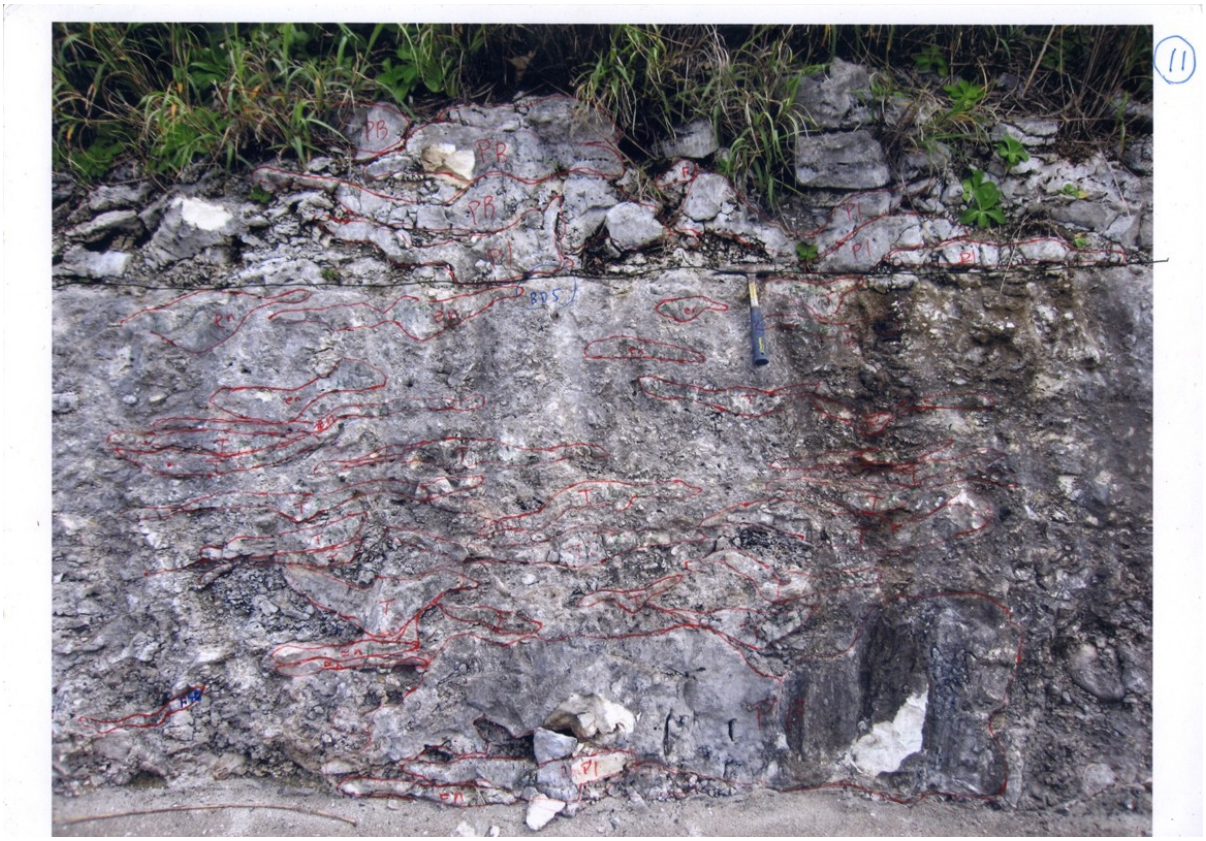
11


12
U4
U1
U4
U1


13

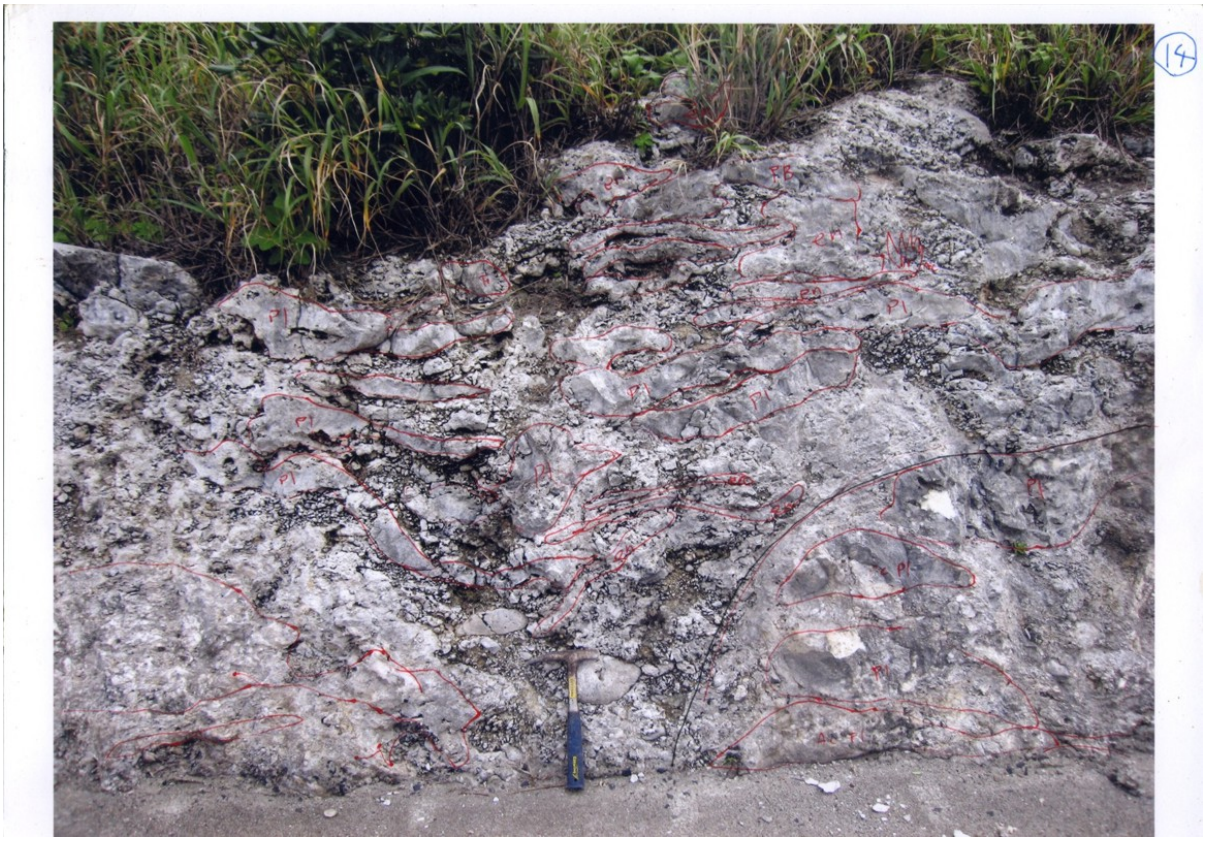
14


15
P1
P1
P8
P8

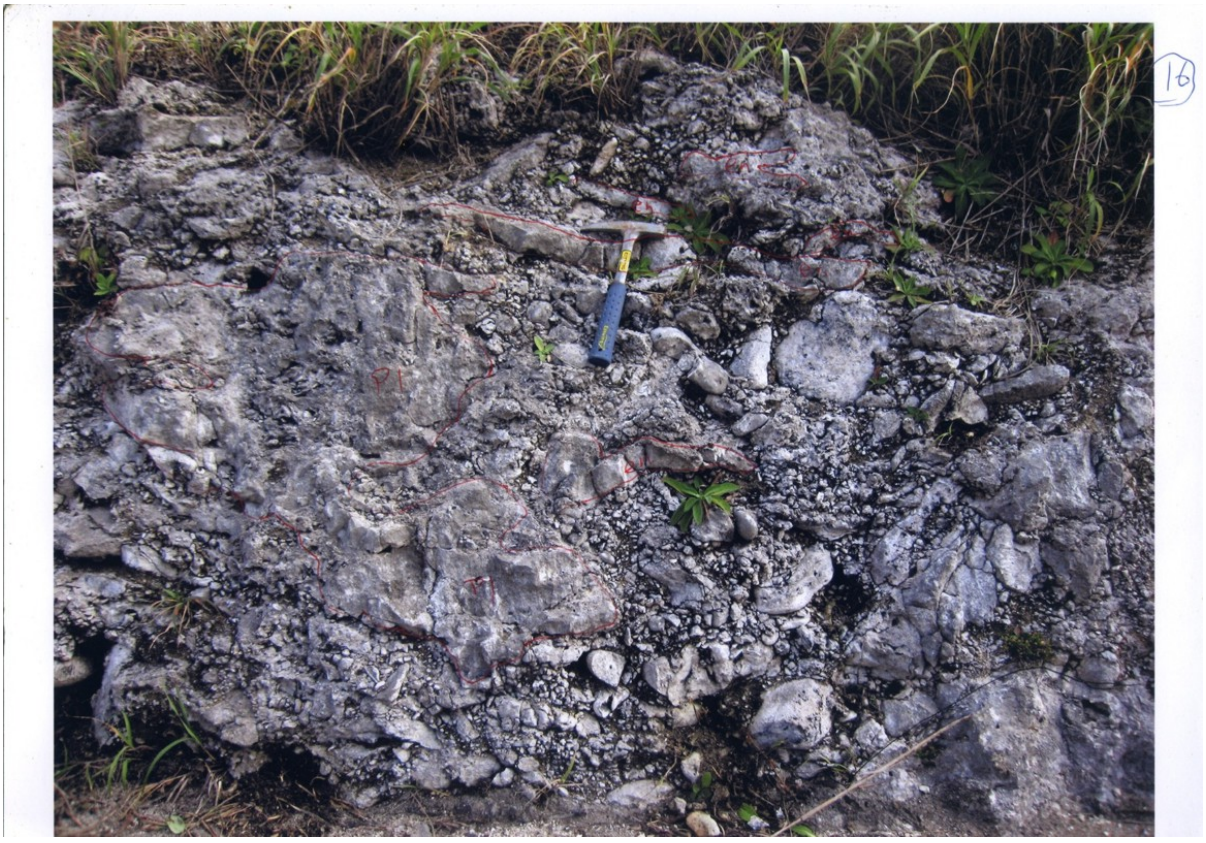
16
P1

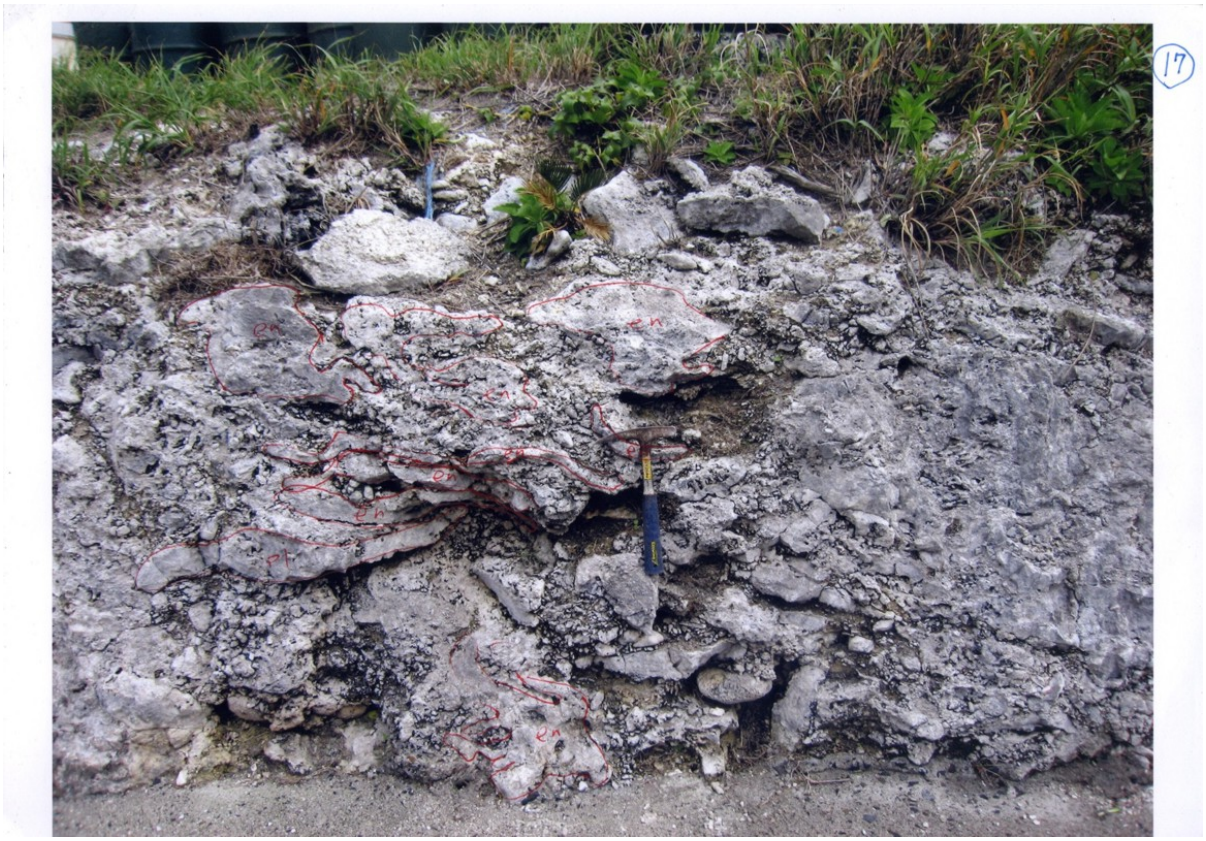
17


18


19


20


21

## A.2 E-2 site


1


2


3


4


5


6


9


10


11


12


13


14


15


16


17


18


19


20


21


22


23


24


25


26


27


28


29


30


31
P1


32
P1
PB


33
P1
PB


34
P1
P1
PB
PB

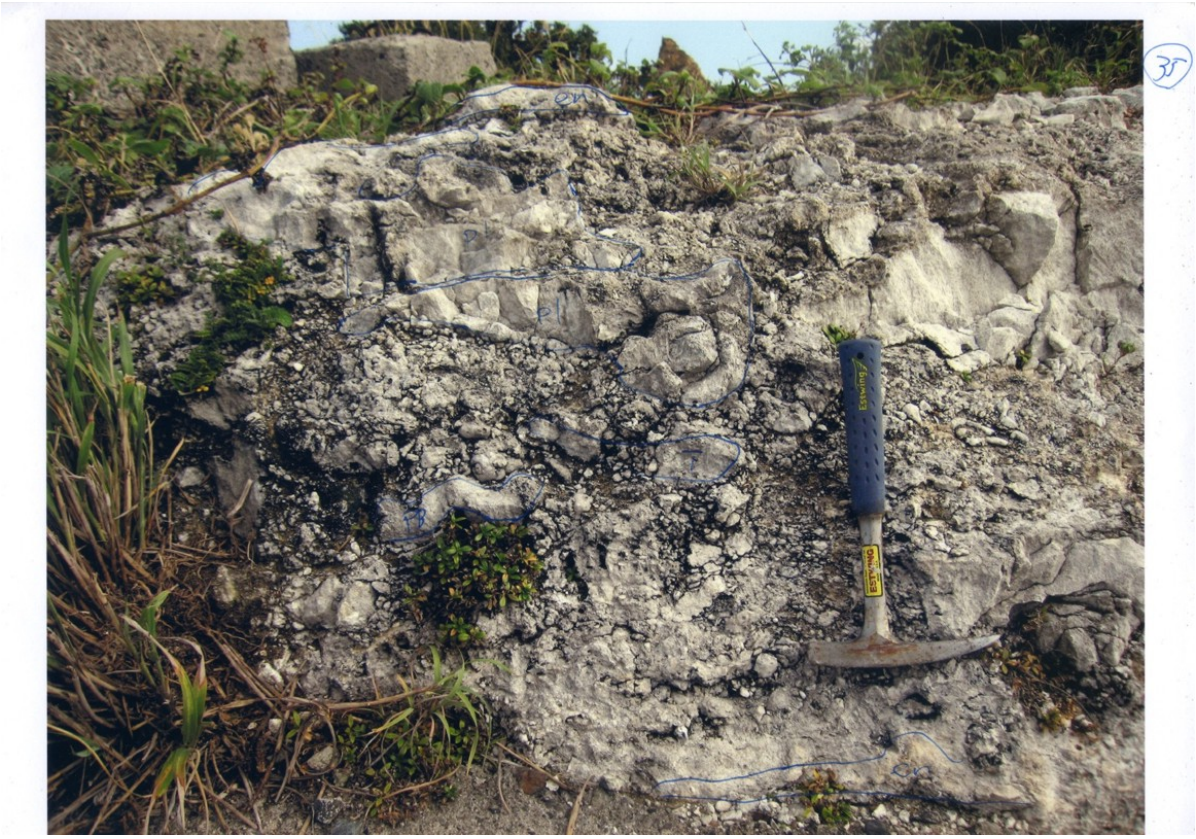

## A.3 E-3 site


1

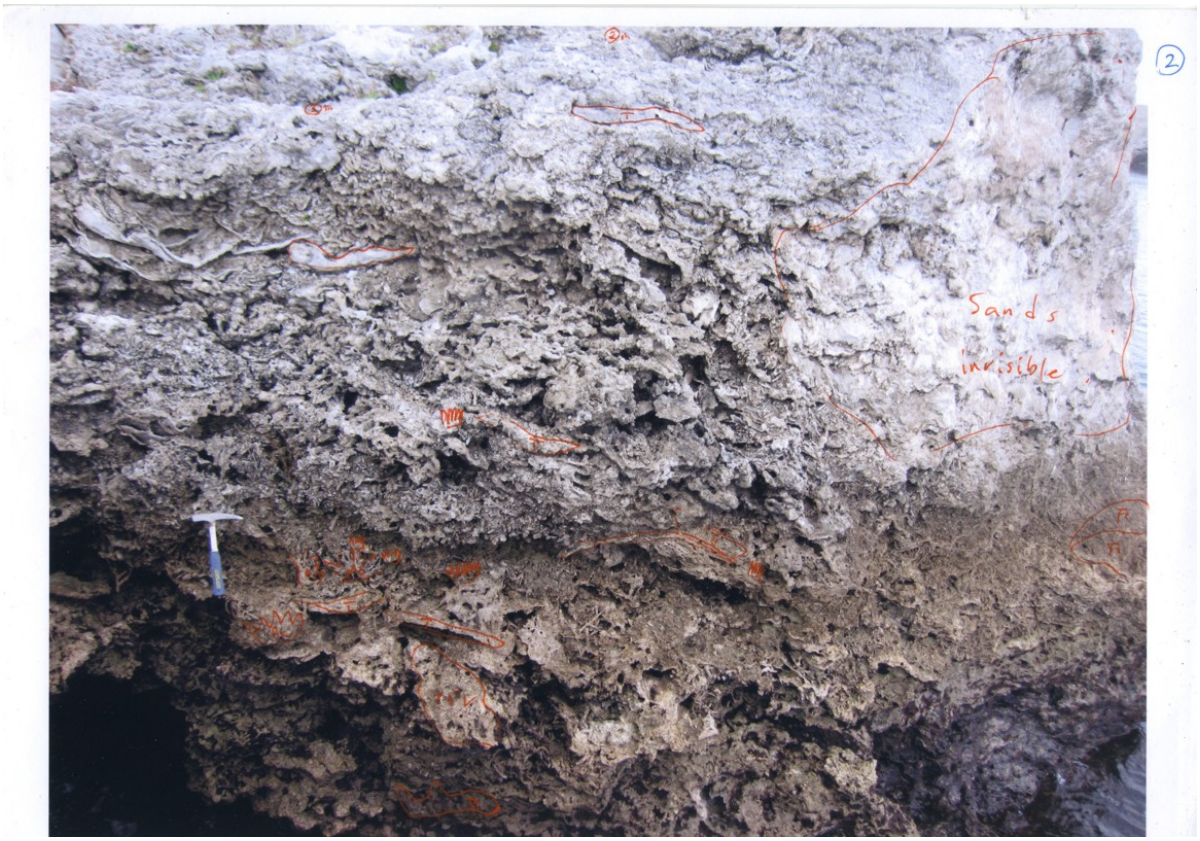
2
Sands
invisible


3
Sands
Sands
Sands
Ech
F


4
PB
PI
Unit 3
Unit 2


5


6


7


8

# Appendix B

## Results of calibration-calibration curves

### B.1 Radiocarbon age vs. calibrated age from cores

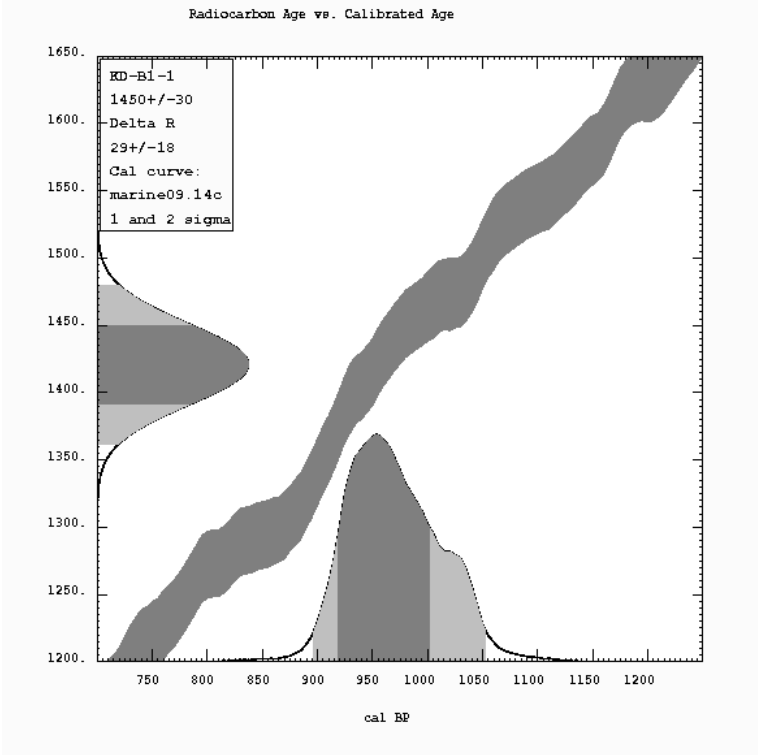
Radiocarbon Age vs. Calibrated Age
KD-B1-1
1450+/-30
Delta R
29+/-18
Cal curve:
marine09.14c
1 and 2 sigma
1650.
1600.
1550.
1500.
1450.
1400.
1350.
1300.
1250.
1200.
750
800
850
900
950
1000
1050
1100
1150
1200
cal BP

KD-B1-1

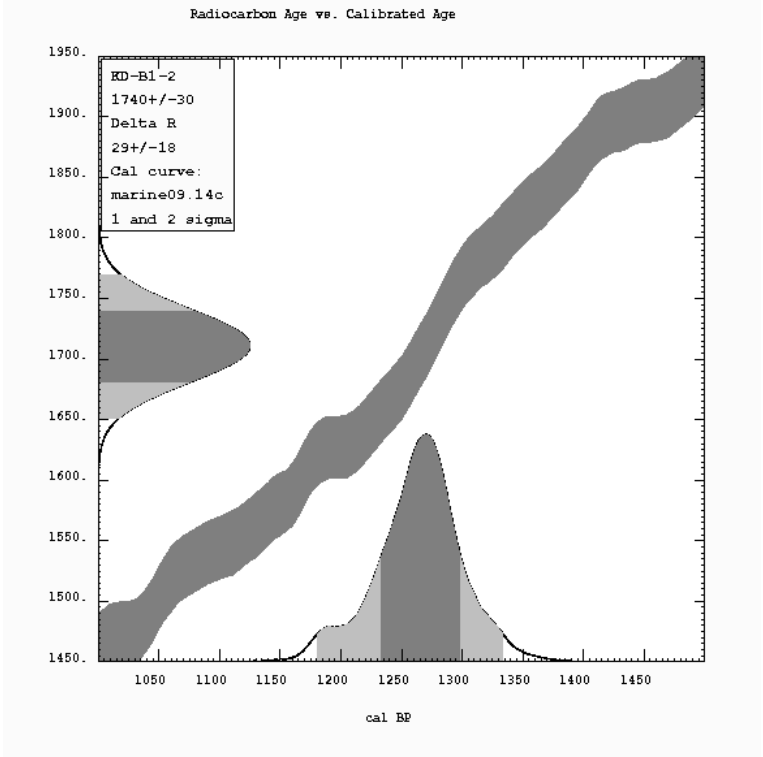
Radiocarbon Age vs. Calibrated Age
KD-B1-2
1740+/-30
Delta R
29+/-18
Cal curve:
marine09.14c
1 and 2 sigma
1950.
1900.
1850.
1800.
1750.
1700.
1650.
1600.
1550.
1500.
1450.
1050
1100
1150
1200
1250
1300
1350
1400
1450
cal BP

KD-B1-2

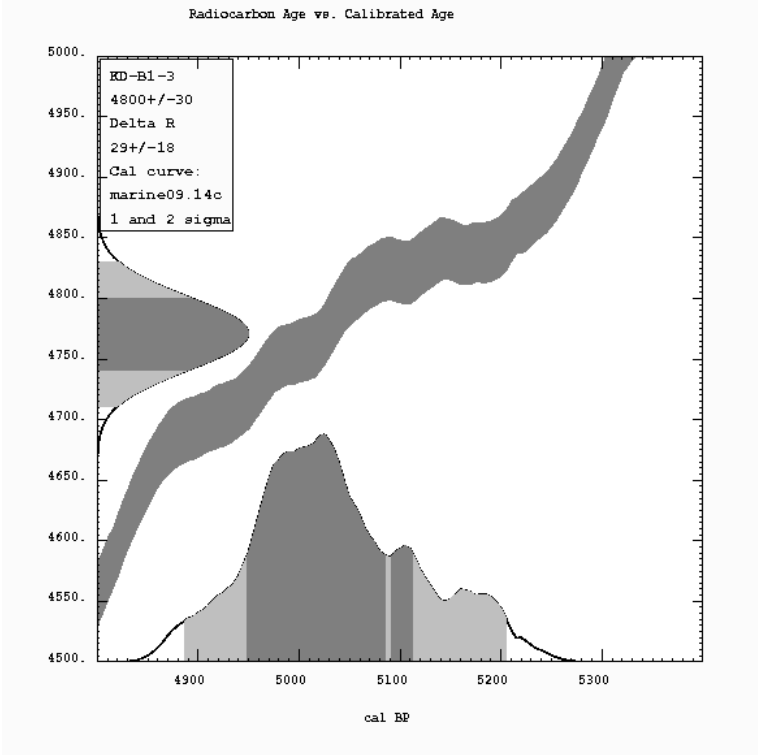
Radiocarbon Age vs. Calibrated Age
KD-B1-3
4800+/-30
Delta R
29+/-18
Cal curve:
marine09.14c
1 and 2 sigma
5000.
4950.
4900.
4850.
4800.
4750.
4700.
4650.
4600.
4550.
4500.
4900
5000
5100
5200
5300
cal BP

KD-B1-3

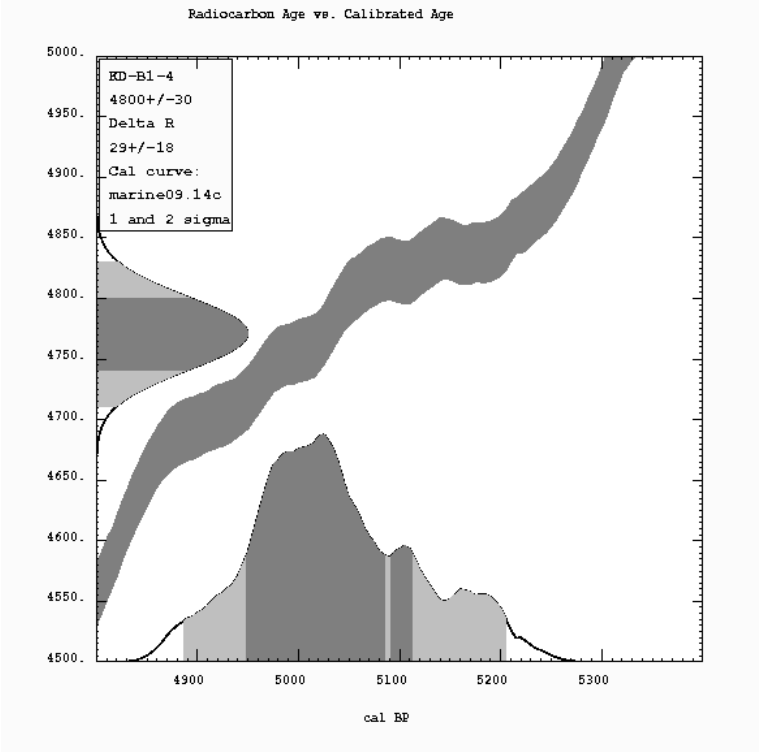
Radiocarbon Age vs. Calibrated Age
KD-B1-4
4800+/-30
Delta R
29+/-18
Cal curve:
marine09.14c
1 and 2 sigma
5000.
4950.
4900.
4850.
4800.
4750.
4700.
4650.
4600.
4550.
4500.
4900
5000
5100
5200
5300
cal BP

KD-B1-4

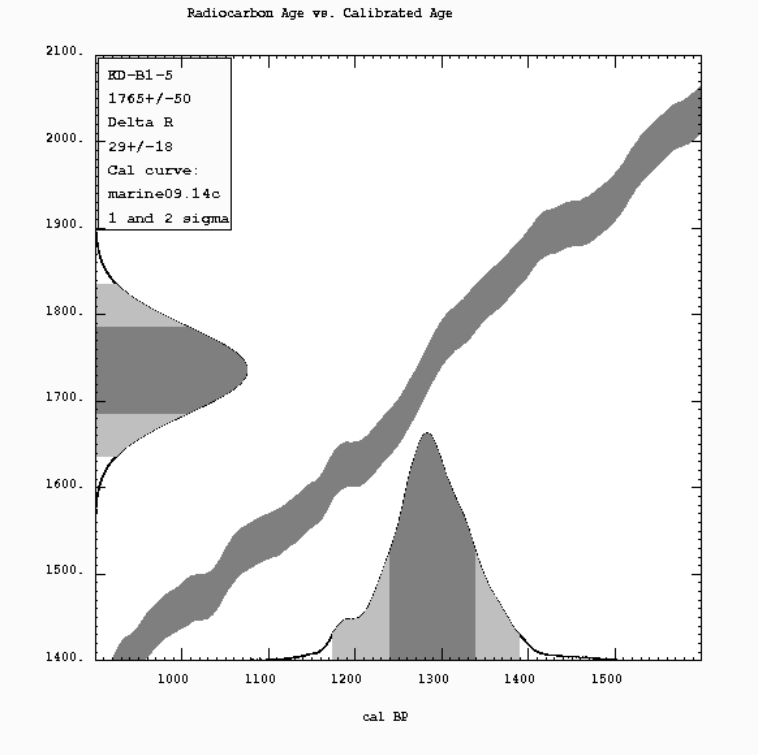
Radiocarbon Age vs. Calibrated Age
KD-B1-5
1765+/-50
Delta R
29+/-18
Cal curve:
marine09.14c
1 and 2 sigma
2100.
2000.
1900.
1800.
1700.
1600.
1500.
1400.
1000
1100
1200
1300
1400
1500
cal BP

KD-B1-5

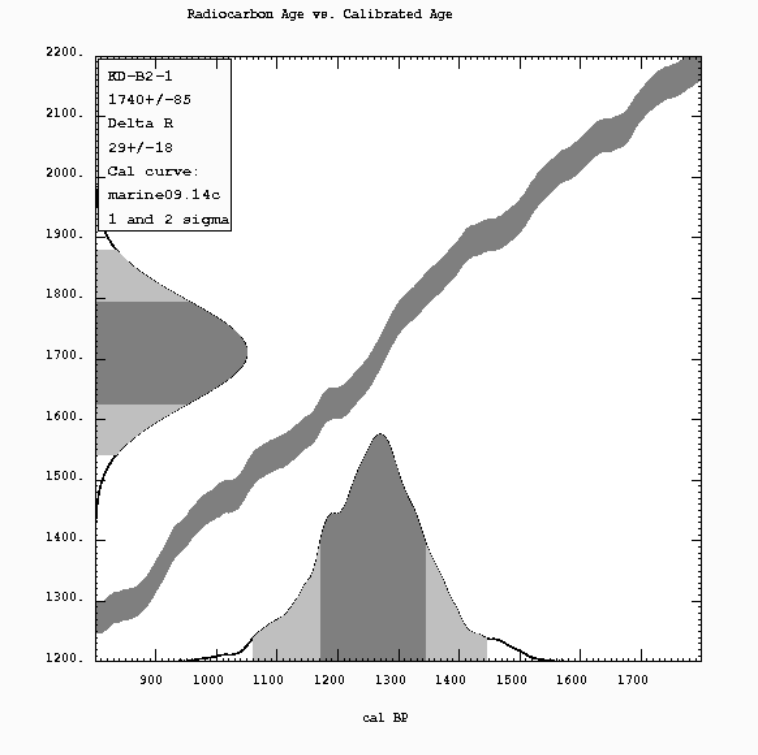
Radiocarbon Age vs. Calibrated Age
KD-B2-1
1740+/-85
Delta R
29+/-18
Cal curve:
marine09.14c
1 and 2 sigma
2200.
2100.
2000.
1900.
1800.
1700.
1600.
1500.
1400.
1300.
1200.
900
1000
1100
1200
1300
1400
1500
1600
1700
cal BP

KD-B2-1

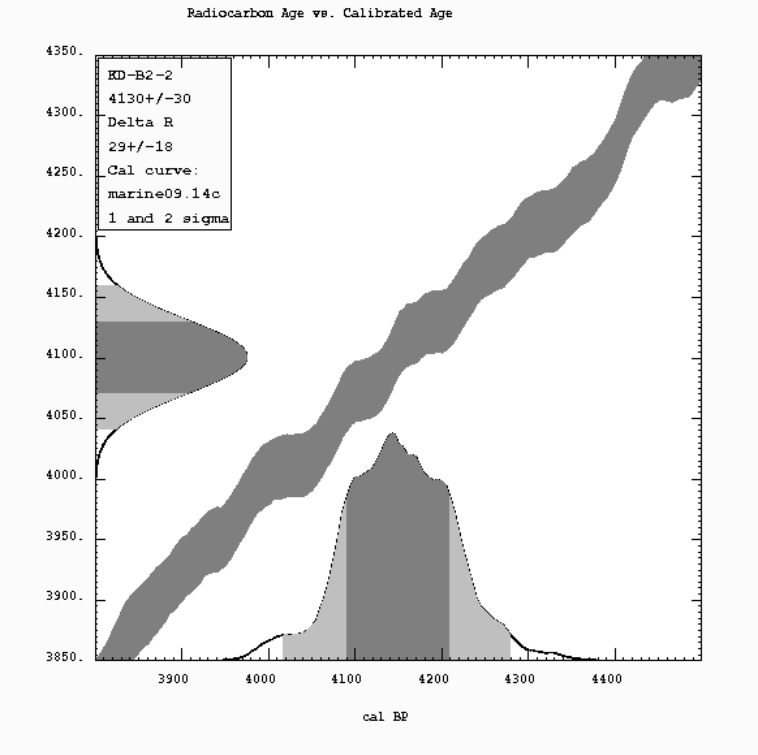
Radiocarbon Age vs. Calibrated Age
KD-B2-2
4130+/-30
Delta R
29+/-18
Cal curve:
marine09.14c
1 and 2 sigma
4350.
4300.
4250.
4200.
4150.
4100.
4050.
4000.
3950.
3900.
3850.
3900
4000
4100
4200
4300
4400
cal BP

KD-B2-2

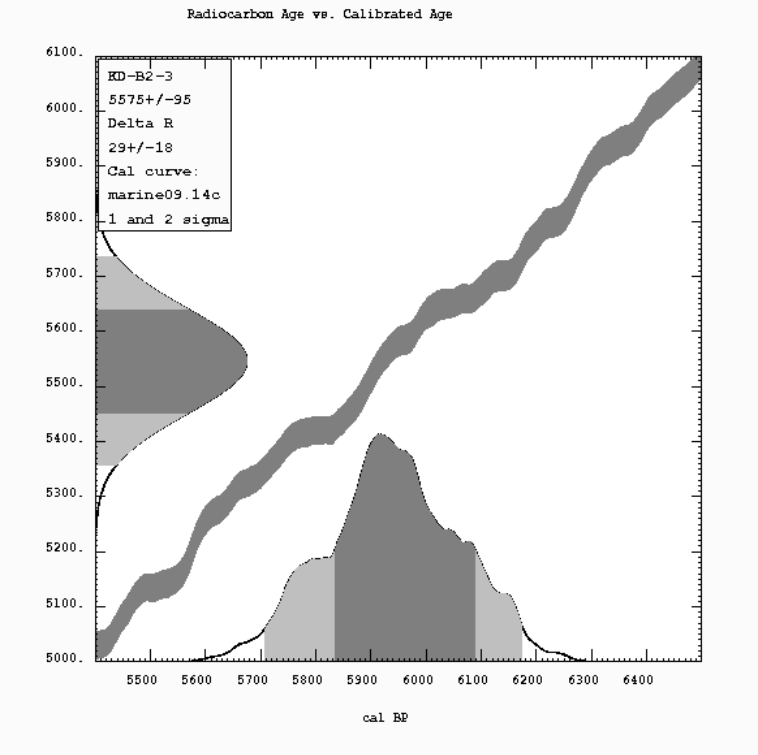
Radiocarbon Age vs. Calibrated Age
KD-B2-3
5575+/-95
Delta R
29+/-18
Cal curve:
marine09.14c
1 and 2 sigma
6100.
6000.
5900.
5800.
5700.
5600.
5500.
5400.
5300.
5200.
5100.
5000.
5500
5600
5700
5800
5900
6000
6100
6200
6300
6400
cal BP

KD-B2-3

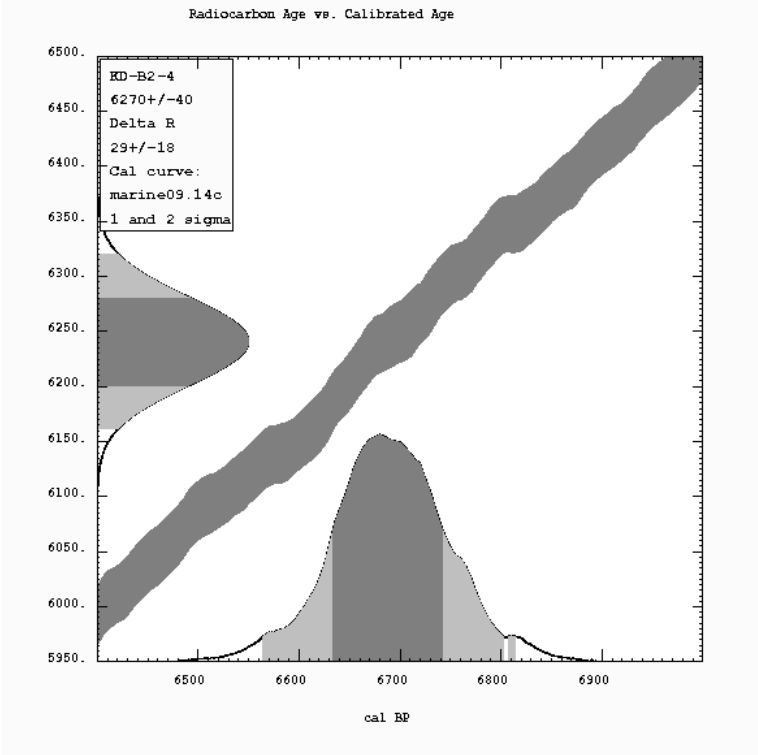
Radiocarbon Age vs. Calibrated Age
KD-B2-4
6270+/-40
Delta R
29+/-18
Cal curve:
marine09.14c
1 and 2 sigma
6500.
6450.
6400.
6350.
6300.
6250.
6200.
6150.
6100.
6050.
6000.
5950.
6500
6600
6700
6800
6900
cal BP

KD-B2-4

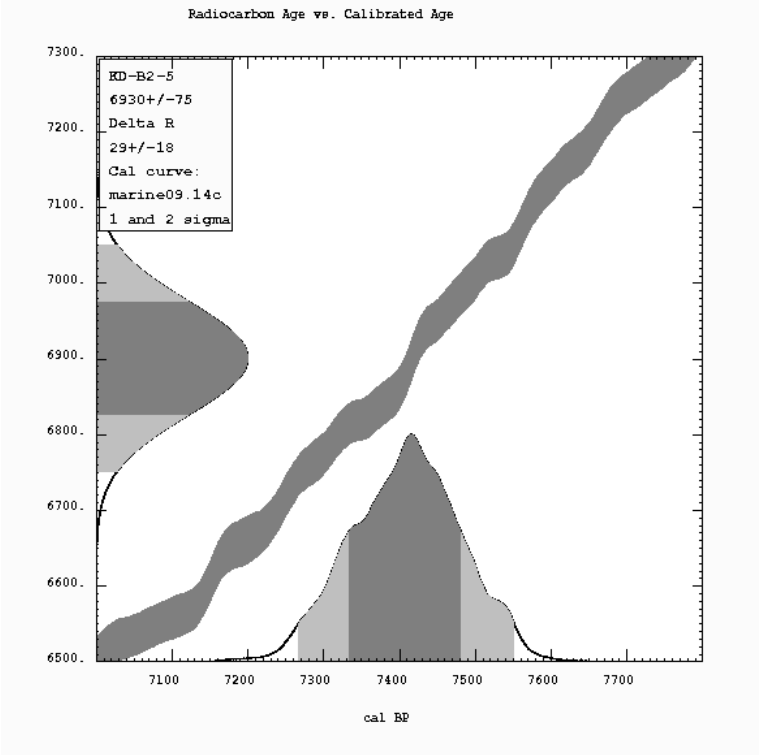
Radiocarbon Age vs. Calibrated Age
KD-B2-5
6930+/-75
Delta R
29+/-18
Cal curve:
marine09.14c
1 and 2 sigma
7300.
7200.
7100.
7000.
6900.
6800.
6700.
6600.
6500.
7100
7200
7300
7400
7500
7600
7700
cal BP

KD-B2-5

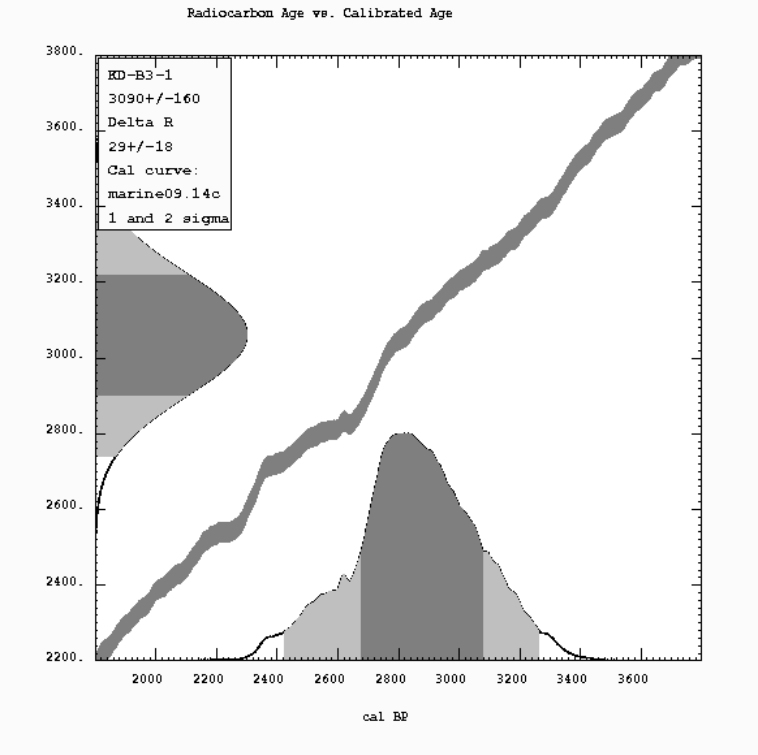
Radiocarbon Age vs. Calibrated Age
KD-B3-1
3090+/-160
Delta R
29+/-18
Cal curve:
marine09.14c
1 and 2 sigma
3800.
3600.
3400.
3200.
3000.
2800.
2600.
2400.
2200.
2000
2200
2400
2600
2800
3000
3200
3400
3600
cal BP

KD-B3-1

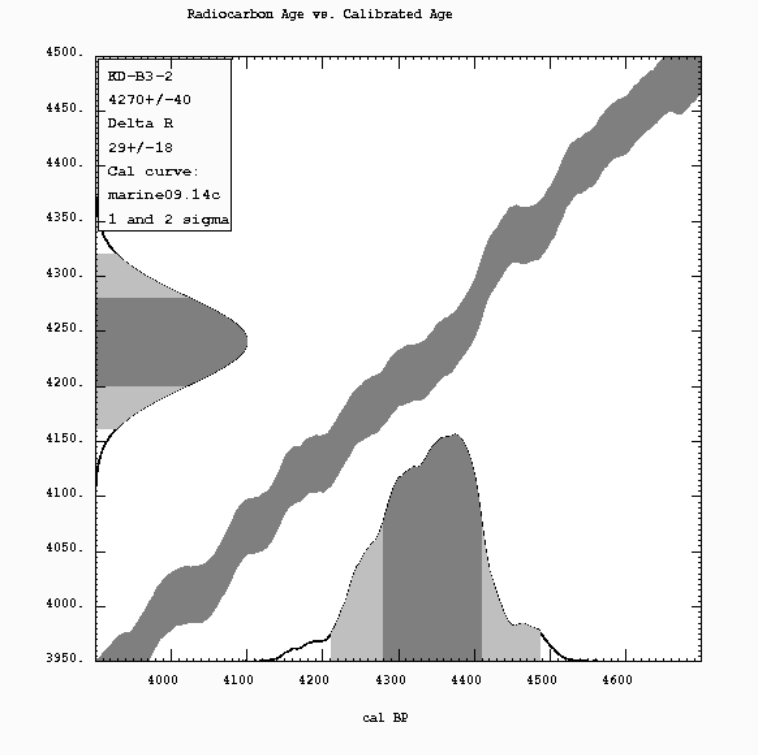
Radiocarbon Age vs. Calibrated Age
KD-B3-2
4270+/-40
Delta R
29+/-18
Cal curve:
marine09.14c
1 and 2 sigma
4500.
4450.
4400.
4350.
4300.
4250.
4200.
4150.
4100.
4050.
4000.
3950.
4000
4100
4200
4300
4400
4500
4600
cal BP

KD-B3-2

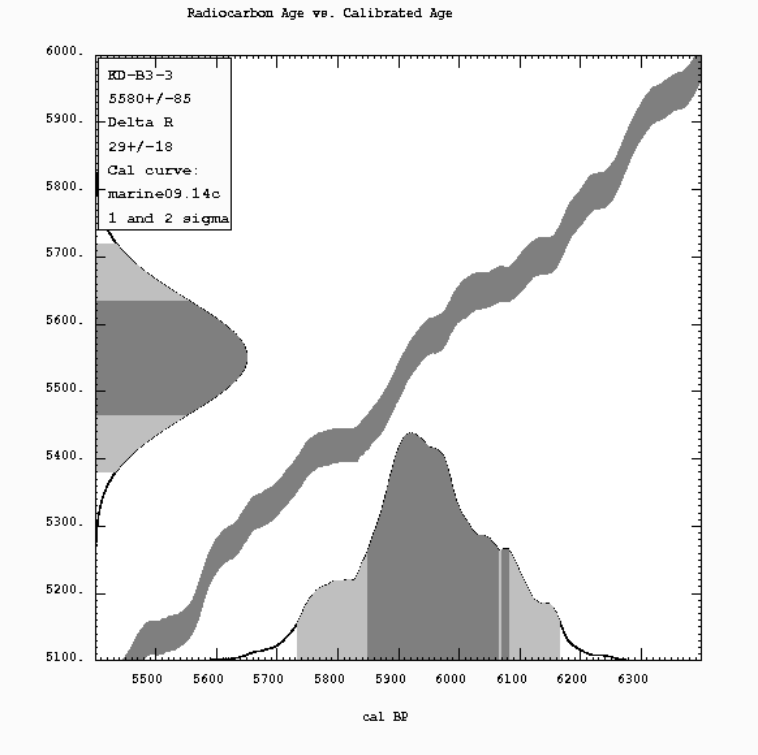
Radiocarbon Age vs. Calibrated Age
KD-B3-3
5580+/-85
Delta R
29+/-18
Cal curve:
marine09.14c
1 and 2 sigma
6000.
5900.
5800.
5700.
5600.
5500.
5400.
5300.
5200.
5100.
5500
5600
5700
5800
5900
6000
6100
6200
6300
cal BP

KD-B3-3

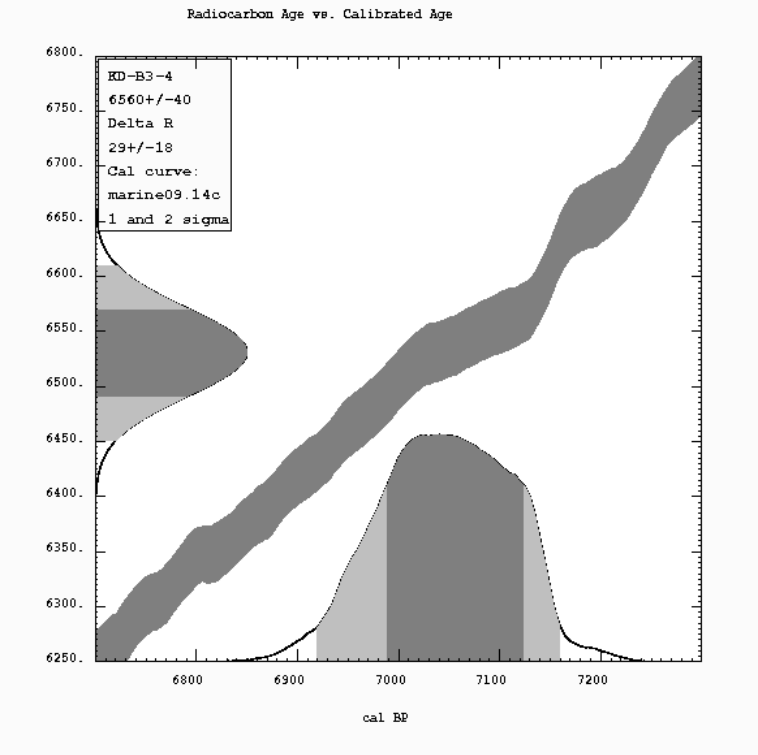
Radiocarbon Age vs. Calibrated Age
KD-B3-4
6560+/-40
Delta R
29+/-18
Cal curve:
marine09.14c
1 and 2 sigma
6800.
6750.
6700.
6650.
6600.
6550.
6500.
6450.
6400.
6350.
6300.
6250.
6800
6900
7000
7100
7200
cal BP

KD-B3-4

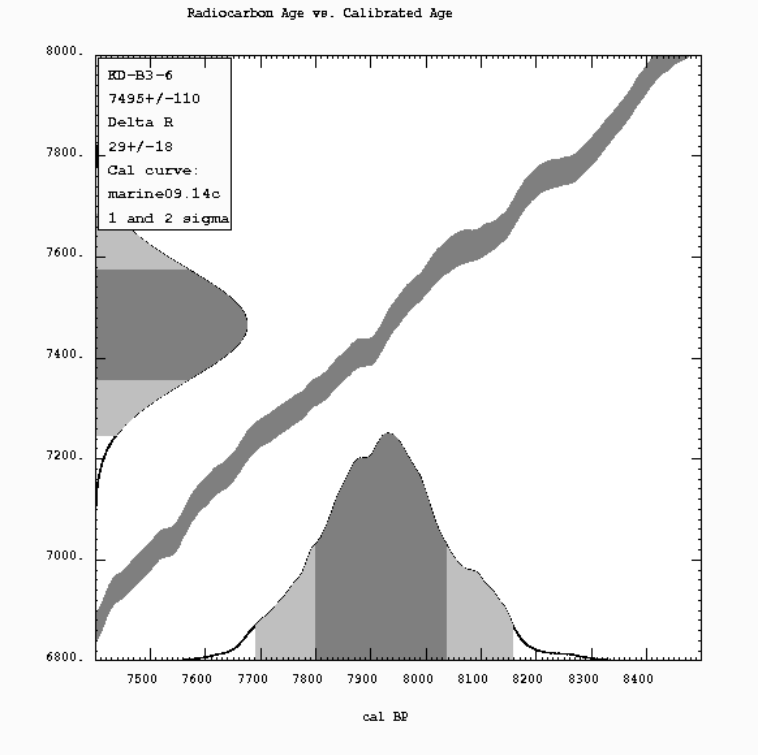
Radiocarbon Age vs. Calibrated Age
KD-B3-6
7495+/-110
Delta R
29+/-18
Cal curve:
marine09.14c
1 and 2 sigma
8000.
7800.
7600.
7400.
7200.
7000.
6800.
7500
7600
7700
7800
7900
8000
8100
8200
8300
8400
cal BP

KD-B3-6

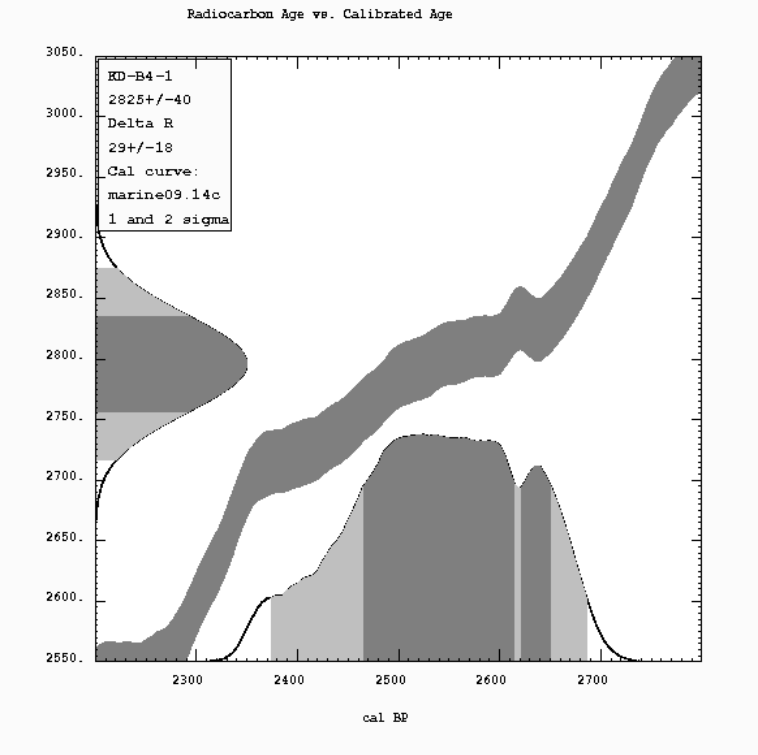
Radiocarbon Age vs. Calibrated Age
KD-B4-1
2825+/-40
Delta R
29+/-18
Cal curve:
marine09.14c
1 and 2 sigma
3050.
3000.
2950.
2900.
2850.
2800.
2750.
2700.
2650.
2600.
2550.
2300
2400
2500
2600
2700
cal BP

KD-B4-1

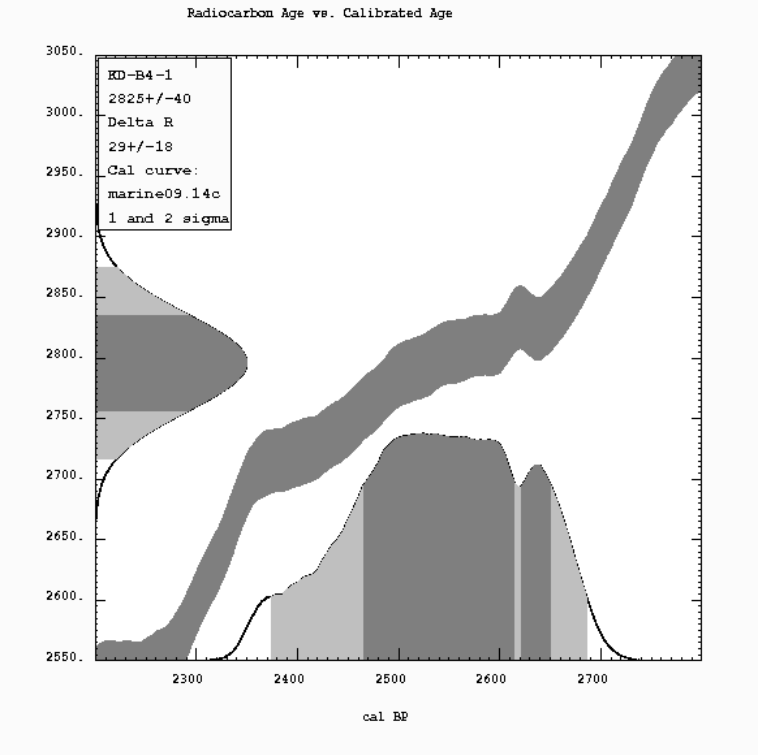
Radiocarbon Age vs. Calibrated Age
KD-B4-1
2825+/-40
Delta R
29+/-18
Cal curve:
marine09.14c
1 and 2 sigma
3050.
3000.
2950.
2900.
2850.
2800.
2750.
2700.
2650.
2600.
2550.
2300
2400
2500
2600
2700
cal BP

KD-B4-2

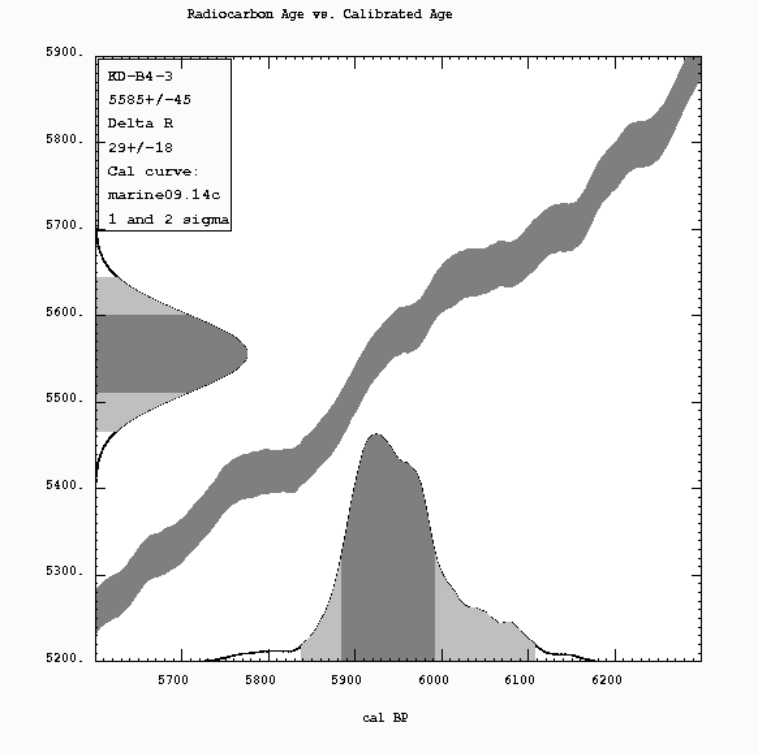
Radiocarbon Age vs. Calibrated Age
KD-B4-3
5585+/-45
Delta R
29+/-18
Cal curve:
marine09.14c
1 and 2 sigma
5900.
5800.
5700.
5600.
5500.
5400.
5300.
5200.
5700
5800
5900
6000
6100
6200
cal BP

KD-B4-3

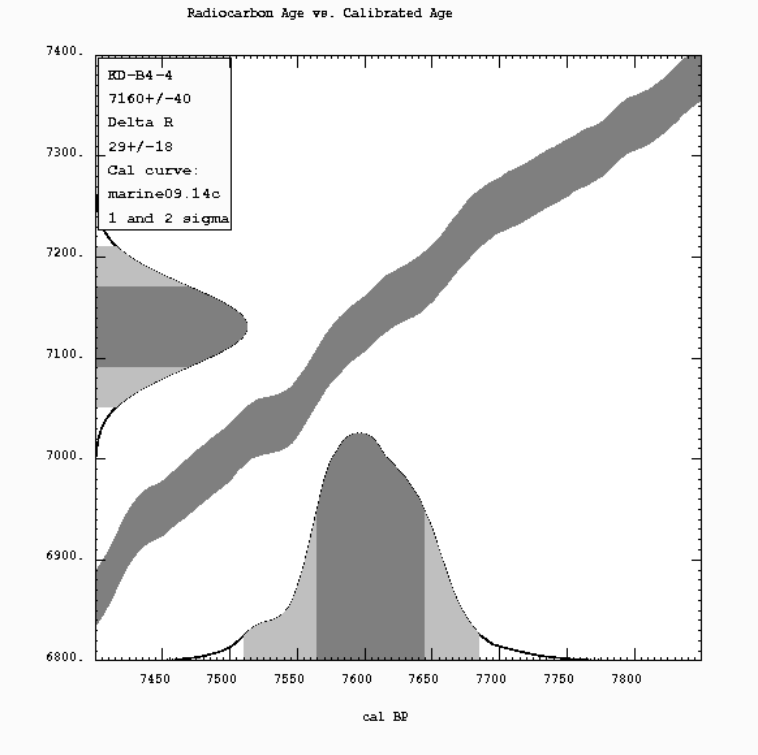
Radiocarbon Age vs. Calibrated Age
KD-B4-4
7160+/-40
Delta R
29+/-18
Cal curve:
marine09.14c
1 and 2 sigma
7400.
7300.
7200.
7100.
7000.
6900.
6800.
7450
7500
7550
7600
7650
7700
7750
7800
cal BP

KD-B4-4

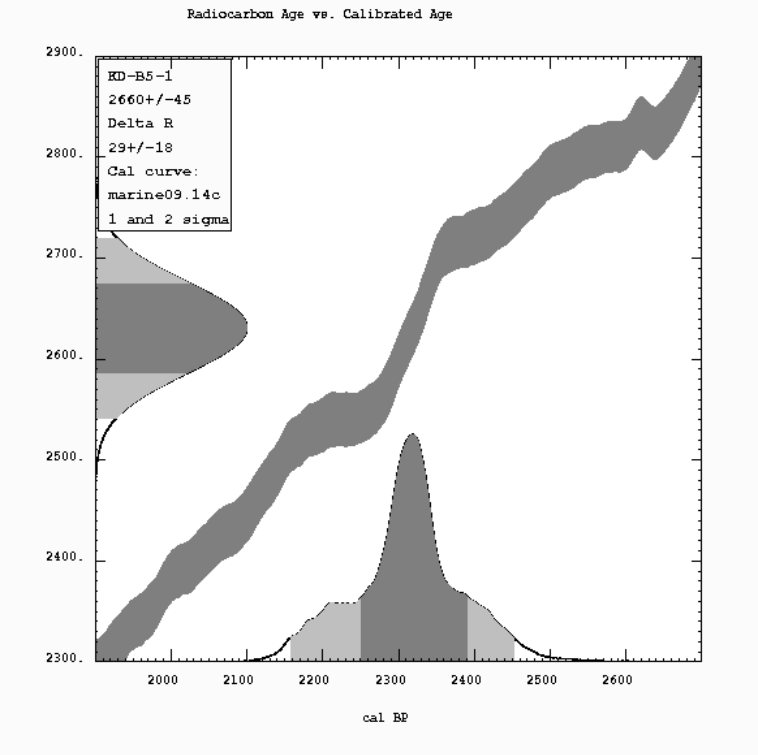
Radiocarbon Age vs. Calibrated Age
KD-B5-1
2660+/-45
Delta R
29+/-18
Cal curve:
marine09.14c
1 and 2 sigma
2900.
2800.
2700.
2600.
2500.
2400.
2300.
2000
2100
2200
2300
2400
2500
2600
cal BP

KD-B5-1

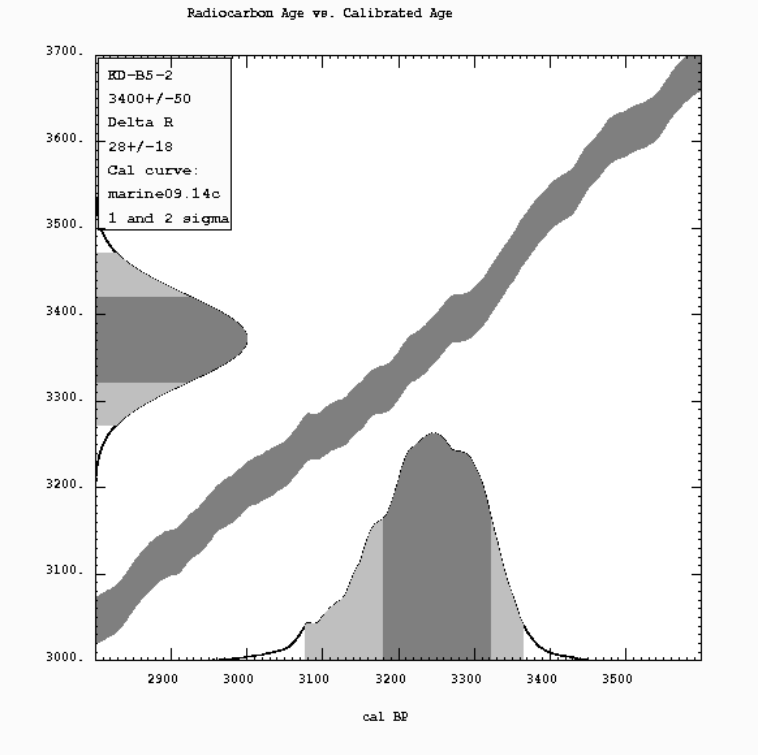
Radiocarbon Age vs. Calibrated Age
KD-B5-2
3400+/-50
Delta R
28+/-18
Cal curve:
marine09.14c
1 and 2 sigma
3700.
3600.
3500.
3400.
3300.
3200.
3100.
3000.
2900
3000
3100
3200
3300
3400
3500
cal BP

KD-B5-2

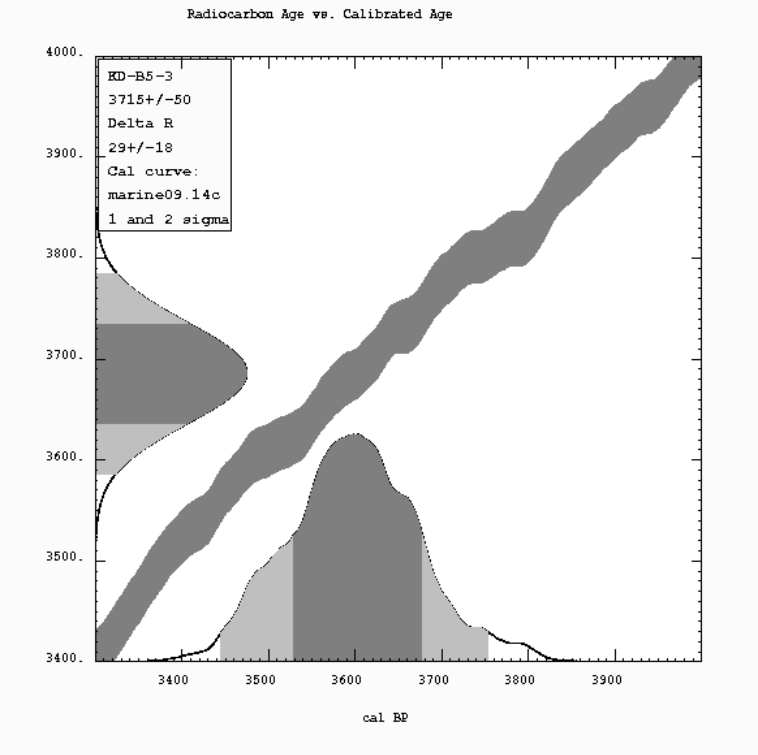
Radiocarbon Age vs. Calibrated Age
KD-B5-3
3715+/-50
Delta R
29+/-18
Cal curve:
marine09.14c
1 and 2 sigma
4000.
3900.
3800.
3700.
3600.
3500.
3400.
3400
3500
3600
3700
3800
3900
cal BP

KD-B5-3

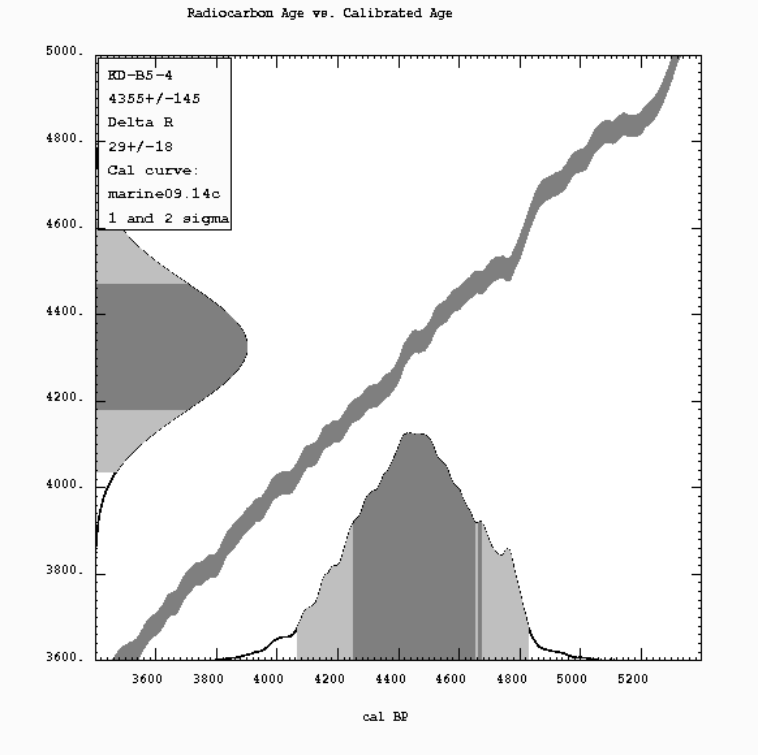
Radiocarbon Age vs. Calibrated Age
KD-B5-4
4355+/-145
Delta R
29+/-18
Cal curve:
marine09.14c
1 and 2 sigma
5000.
4800.
4600.
4400.
4200.
4000.
3800.
3600.
3600
3800
4000
4200
4400
4600
4800
5000
5200
cal BP

KD-B5-4

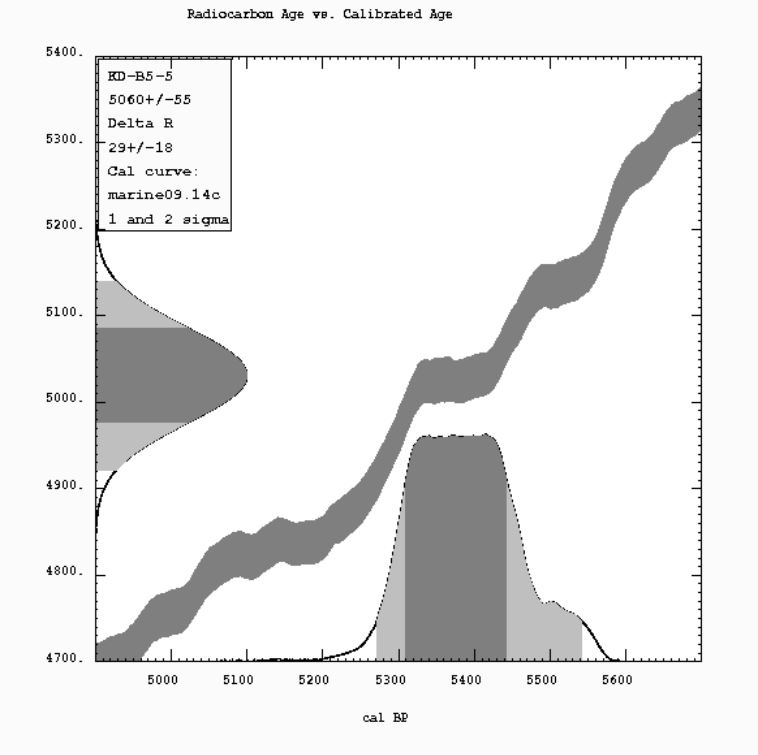
Radiocarbon Age vs. Calibrated Age
KD-B5-5
5060+/-55
Delta R
29+/-18
Cal curve:
marine09.14c
1 and 2 sigma
5400.
5300.
5200.
5100.
5000.
4900.
4800.
4700.
5000
5100
5200
5300
5400
5500
5600
cal BP

KD-B5-5

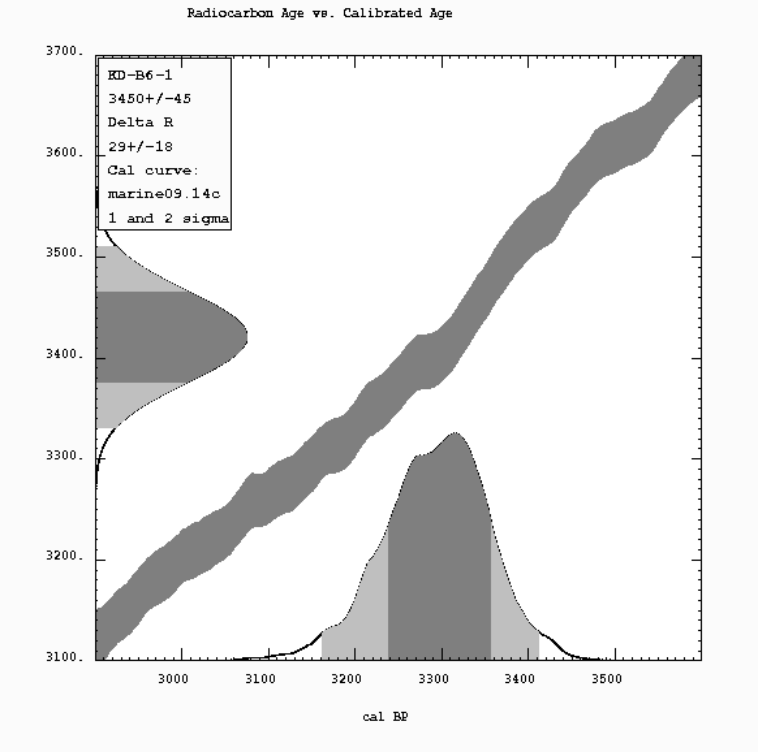
Radiocarbon Age vs. Calibrated Age
KD-B6-1
3450+/-45
Delta R
29+/-18
Cal curve:
marine09.14c
1 and 2 sigma
3700.
3600.
3500.
3400.
3300.
3200.
3100.
3000
3100
3200
3300
3400
3500
cal BP

KD-B6-1

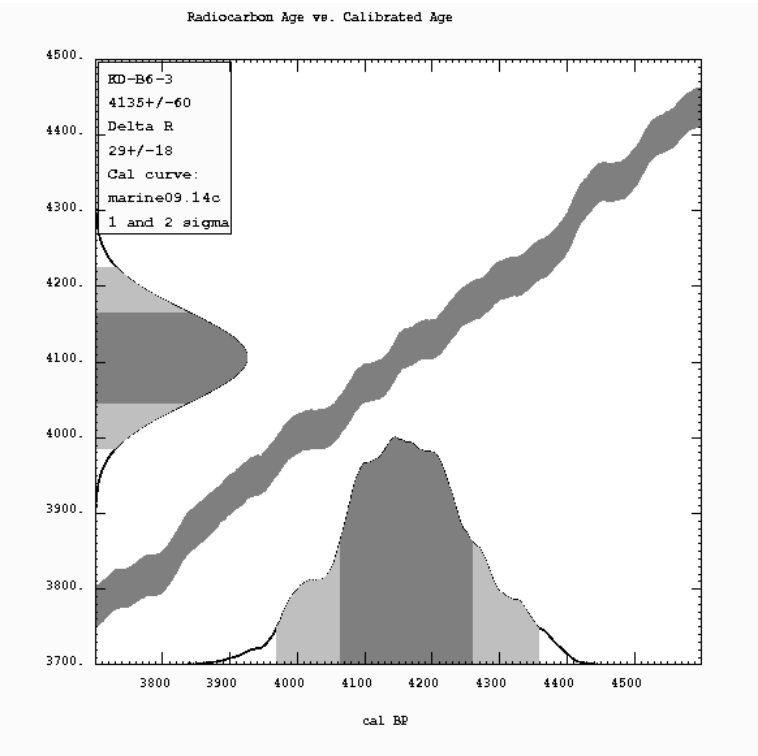
Radiocarbon Age vs. Calibrated Age
KD-B6-3
4135+/-60
Delta R
29+/-18
Cal curve:
marine09.14c
1 and 2 sigma
4500.
4400.
4300.
4200.
4100.
4000.
3900.
3800.
3700.
3800
3900
4000
4100
4200
4300
4400
4500
cal BP

KD-B6-3

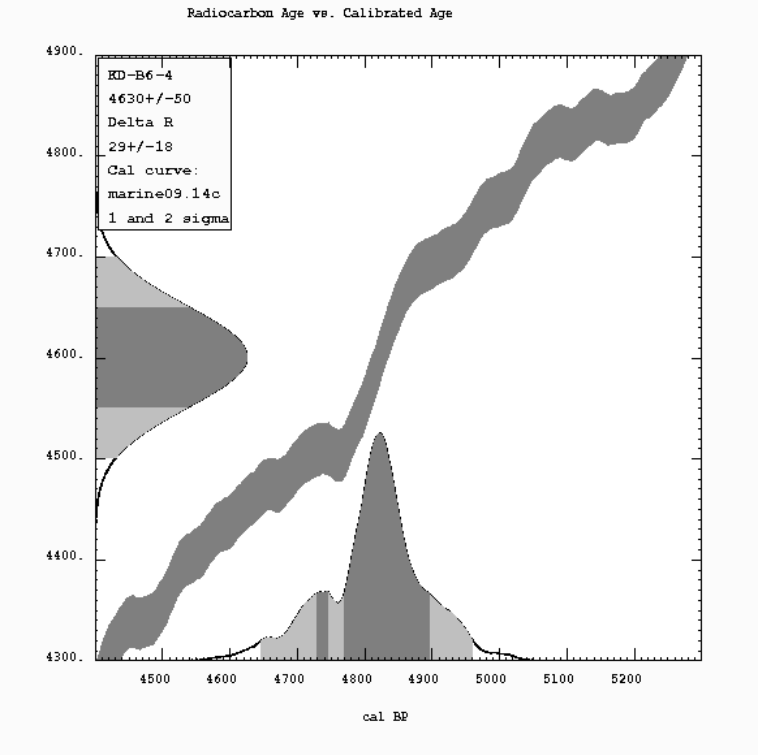
Radiocarbon Age vs. Calibrated Age
KD-B6-4
4630+/-50
Delta R
29+/-18
Cal curve:
marine09.14c
1 and 2 sigma
4900.
4800.
4700.
4600.
4500.
4400.
4300.
4500
4600
4700
4800
4900
5000
5100
5200
cal BP

KD-B6-4

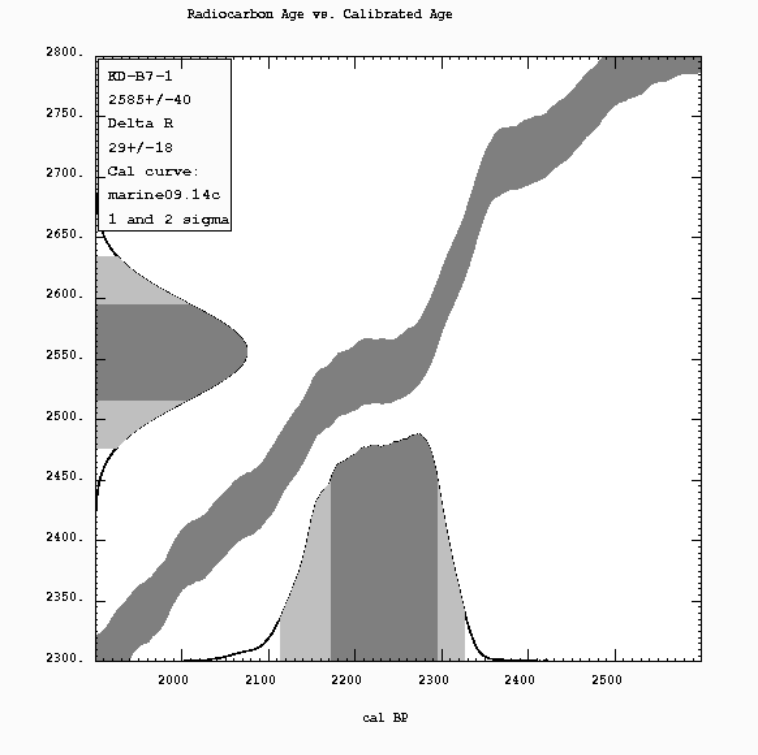
Radiocarbon Age vs. Calibrated Age
KD-B7-1
2585+/-40
Delta R
29+/-18
Cal curve:
marine09.14c
1 and 2 sigma
2800.
2750.
2700.
2650.
2600.
2550.
2500.
2450.
2400.
2350.
2300.
2000
2100
2200
2300
2400
2500
cal BP

KD-B7-1

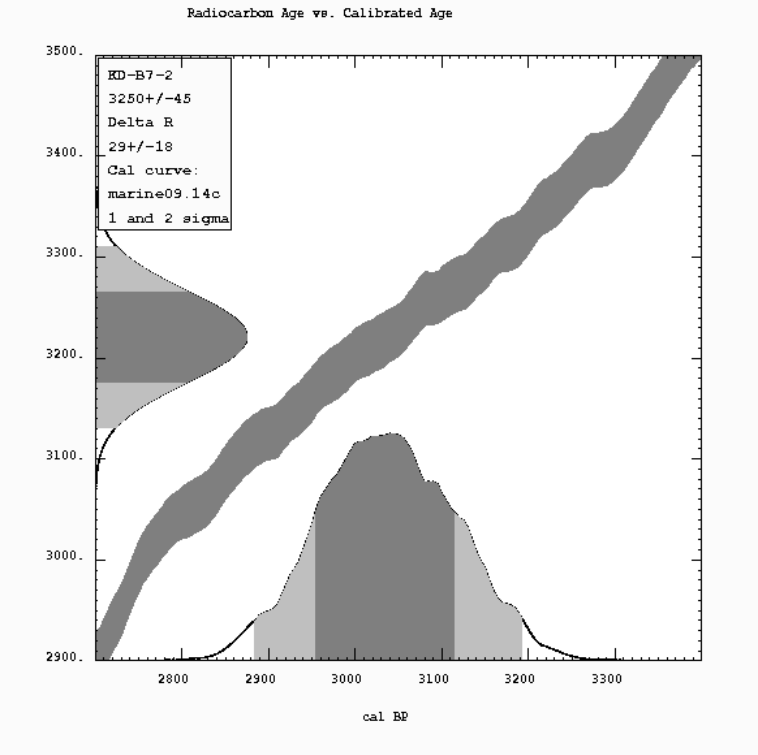
Radiocarbon Age vs. Calibrated Age
KD-B7-2
3250+/-45
Delta R
29+/-18
Cal curve:
marine09.14c
1 and 2 sigma
3500.
3400.
3300.
3200.
3100.
3000.
2900.
2800
2900
3000
3100
3200
3300
cal BP

KD-B7-2

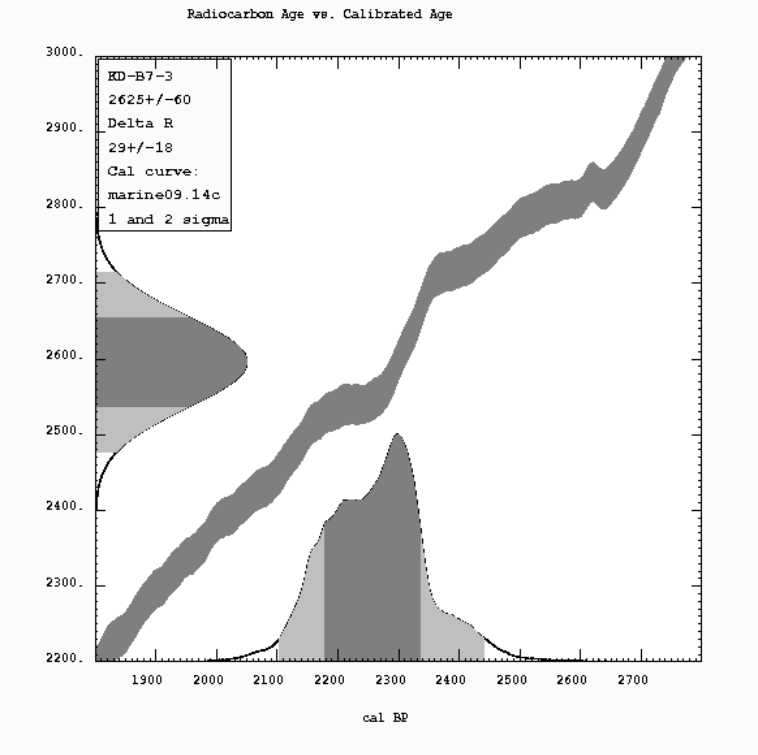
Radiocarbon Age vs. Calibrated Age
KD-B7-3
2625+/-60
Delta R
29+/-18
Cal curve:
marine09.14c
1 and 2 sigma
3000.
2900.
2800.
2700.
2600.
2500.
2400.
2300.
2200.
1900
2000
2100
2200
2300
2400
2500
2600
2700
cal BP

KD-B7-3

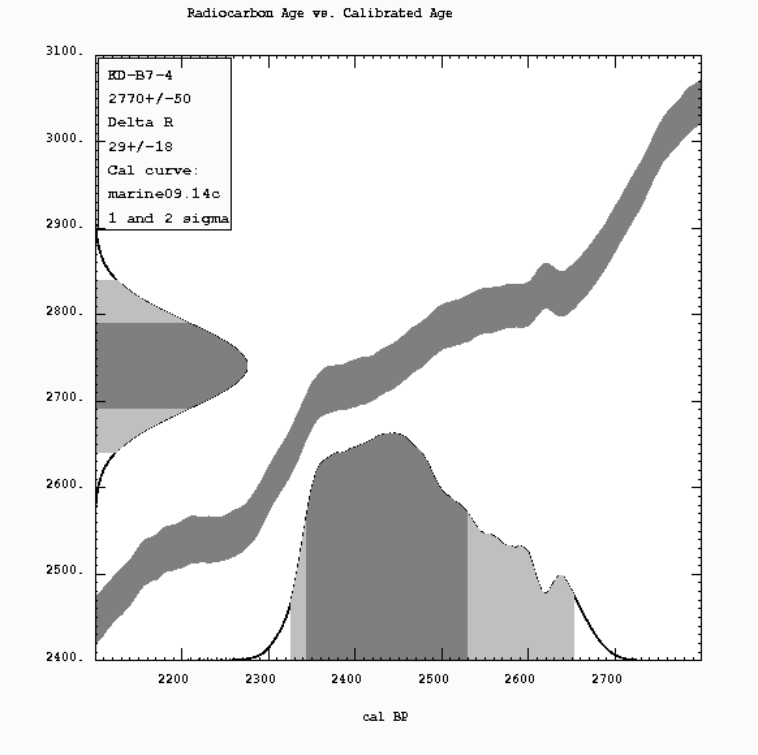
Radiocarbon Age vs. Calibrated Age
KD-B7-4
2770+/-50
Delta R
29+/-18
Cal curve:
marine09.14c
1 and 2 sigma
3100.
3000.
2900.
2800.
2700.
2600.
2500.
2400.
2200
2300
2400
2500
2600
2700
cal BP

KD-B7-4

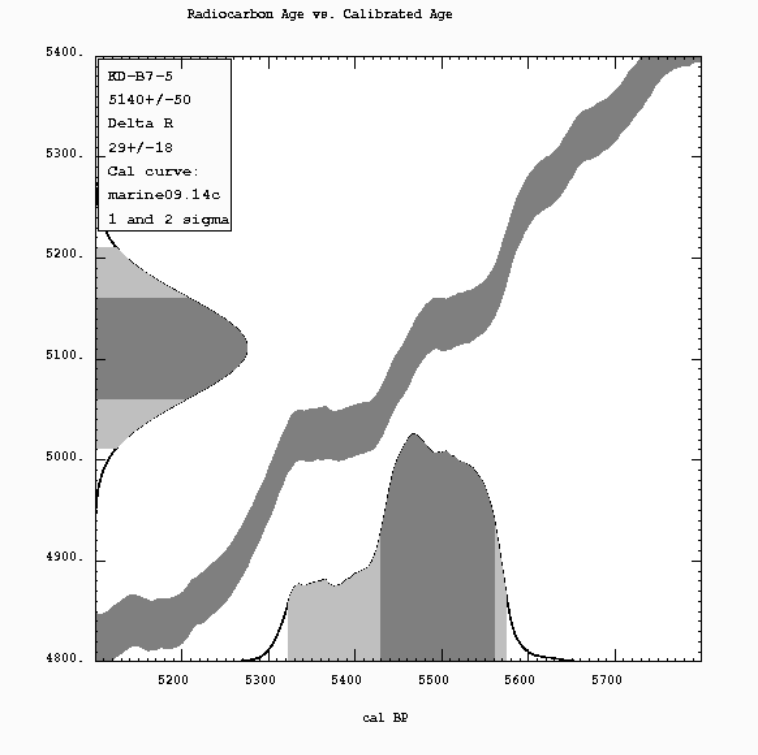
Radiocarbon Age vs. Calibrated Age
KD-B7-5
5140+/-50
Delta R
29+/-18
Cal curve:
marine09.14c
1 and 2 sigma
5400.
5300.
5200.
5100.
5000.
4900.
4800.
5200
5300
5400
5500
5600
5700
cal BP

KD-B7-5

## B.2 Radiocarbon age vs. calibrated age from terraces

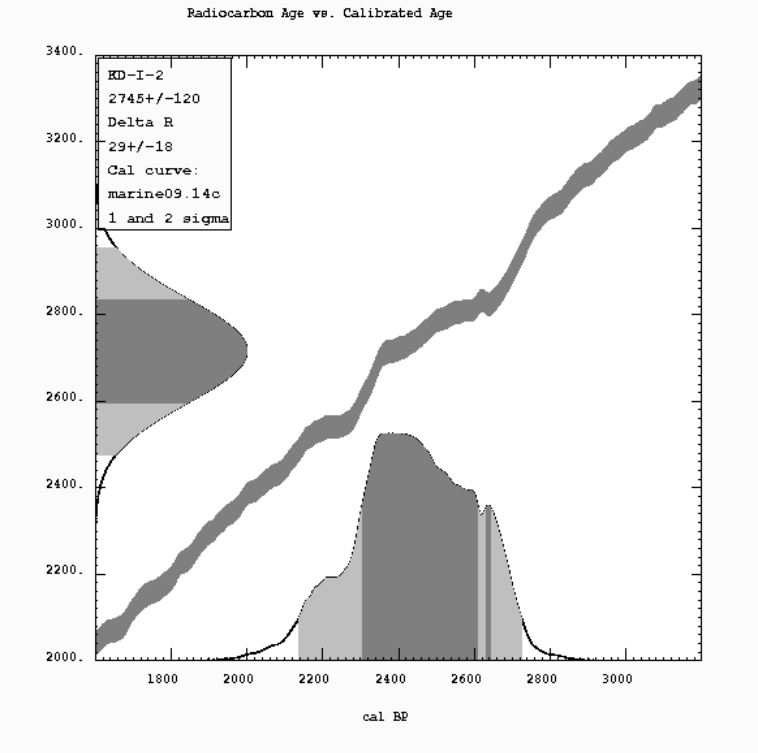
Radiocarbon Age vs. Calibrated Age
KD-I-2
2745+/-120
Delta R
29+/-18
Cal curve:
marine09.14c
1 and 2 sigma
3400.
3200.
3000.
2800.
2600.
2400.
2200.
2000.
1800
2000
2200
2400
2600
2800
3000
cal BP

KD-I-2

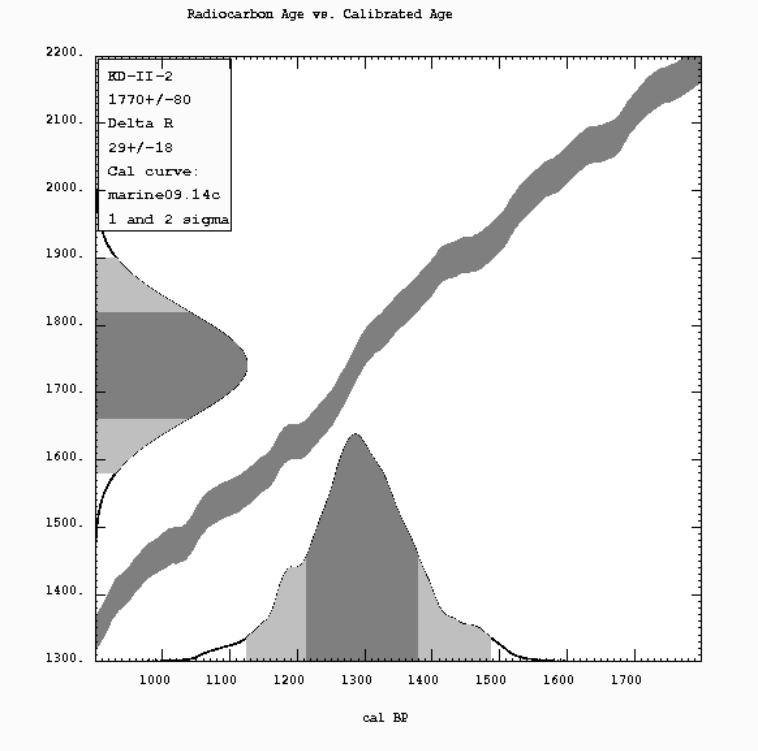
Radiocarbon Age vs. Calibrated Age
KD-II-2
1770+/-80
Delta R
29+/-18
Cal curve:
marine09.14c
1 and 2 sigma
2200.
2100.
2000.
1900.
1800.
1700.
1600.
1500.
1400.
1300.
1000
1100
1200
1300
1400
1500
1600
1700
cal BP

KD-II-2

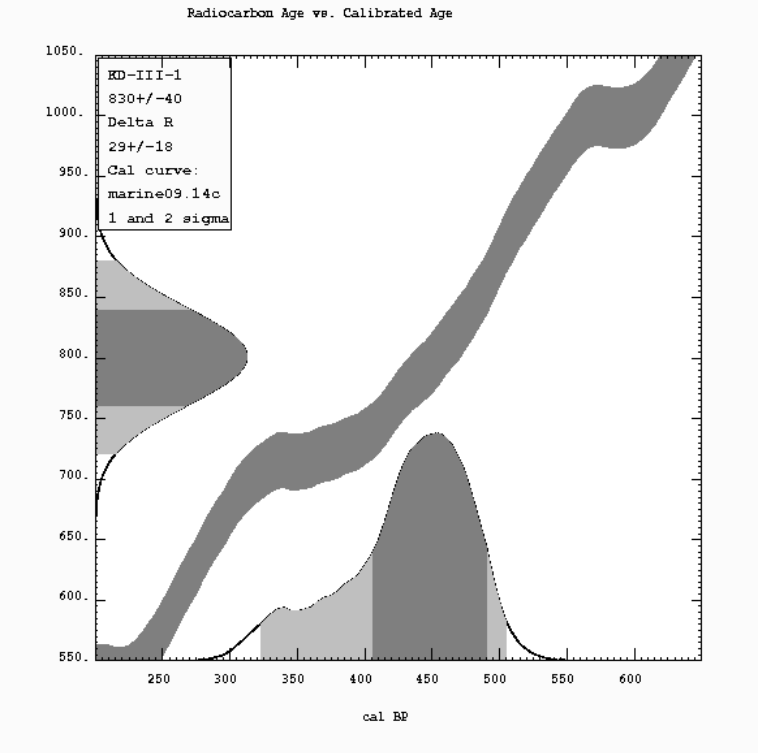


KD-III-1

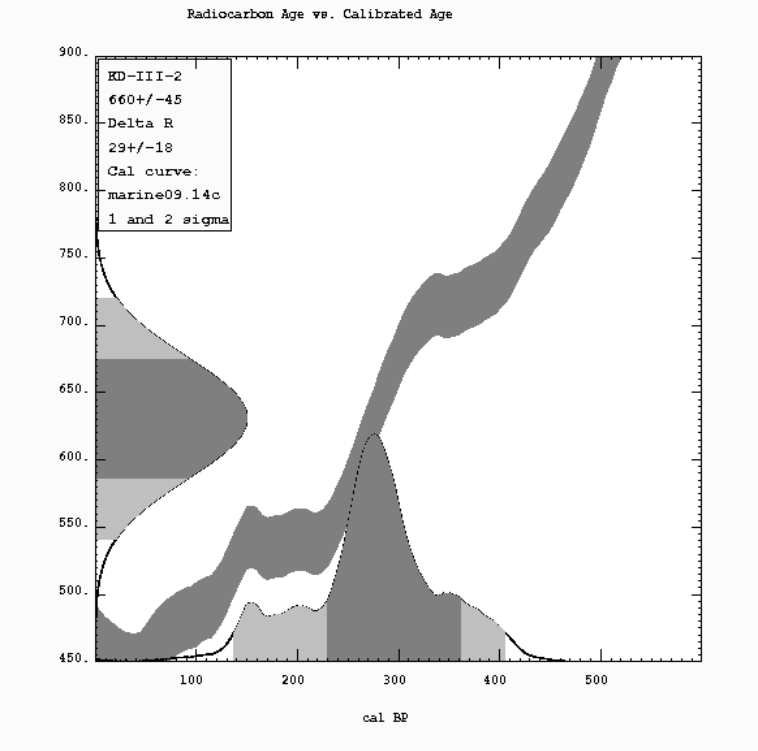


KD-III-2

## B.3 Radiocarbon age vs. calibrated age from trenches

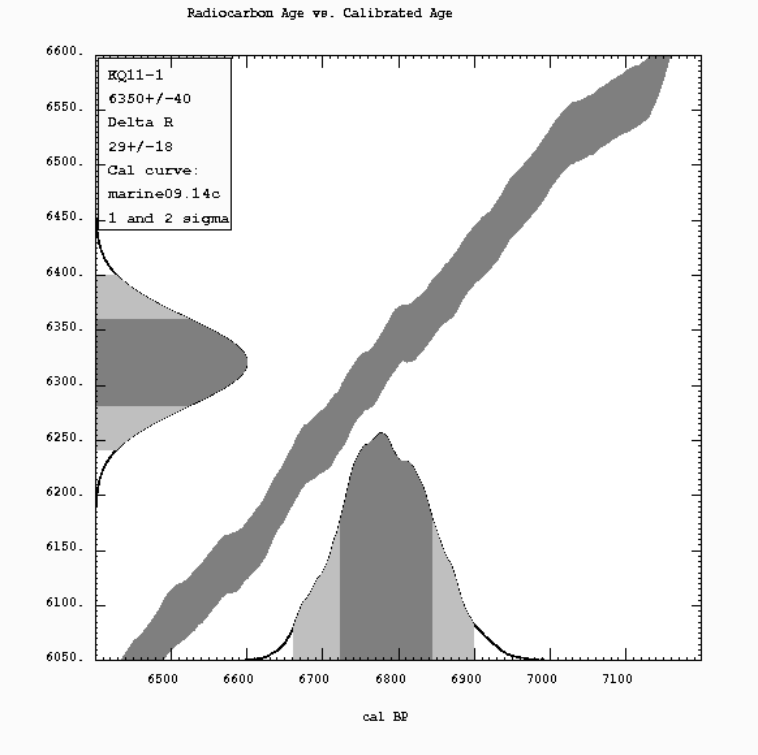


KQ11-1

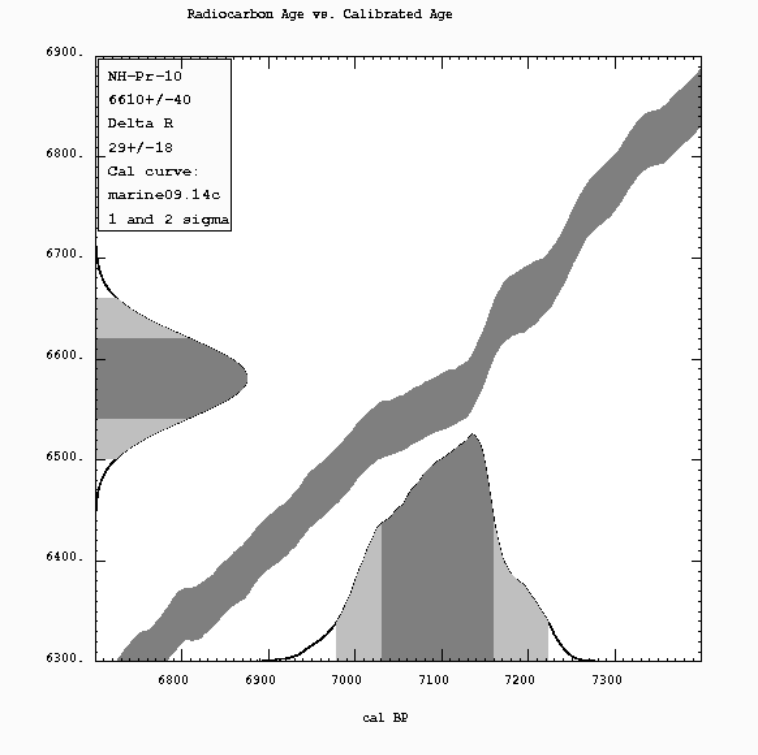


NH-Pr-10

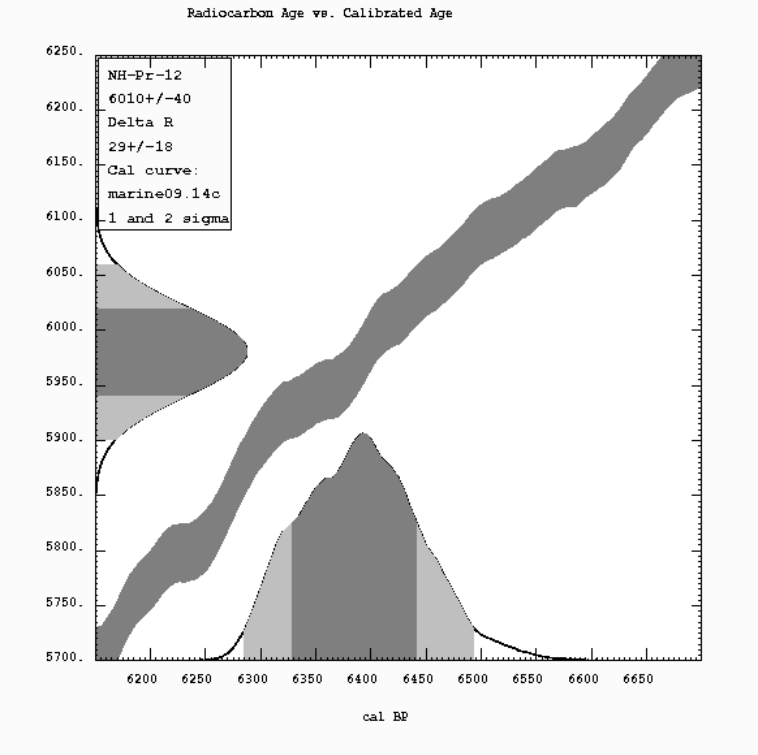


NH-Pr-12

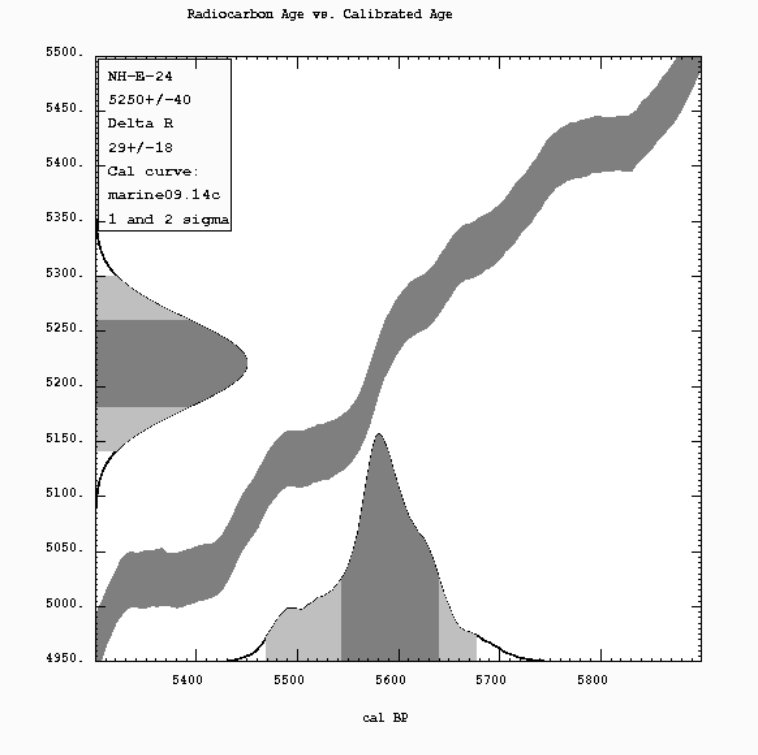


NH-E-24

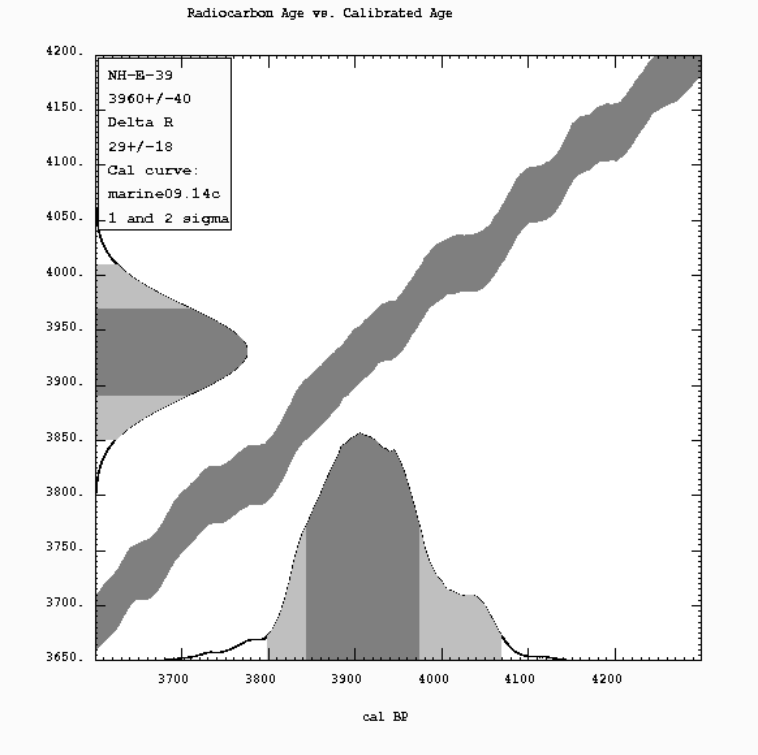
Radiocarbon Age vs. Calibrated Age
NH-E-39
3960+/-40
Delta R
29+/-18
Cal curve:
marine09.14c
1 and 2 sigma
4200.
4150.
4100.
4050.
4000.
3950.
3900.
3850.
3800.
3750.
3700.
3650.
3700
3800
3900
4000
4100
4200
cal BP

NH-E-39

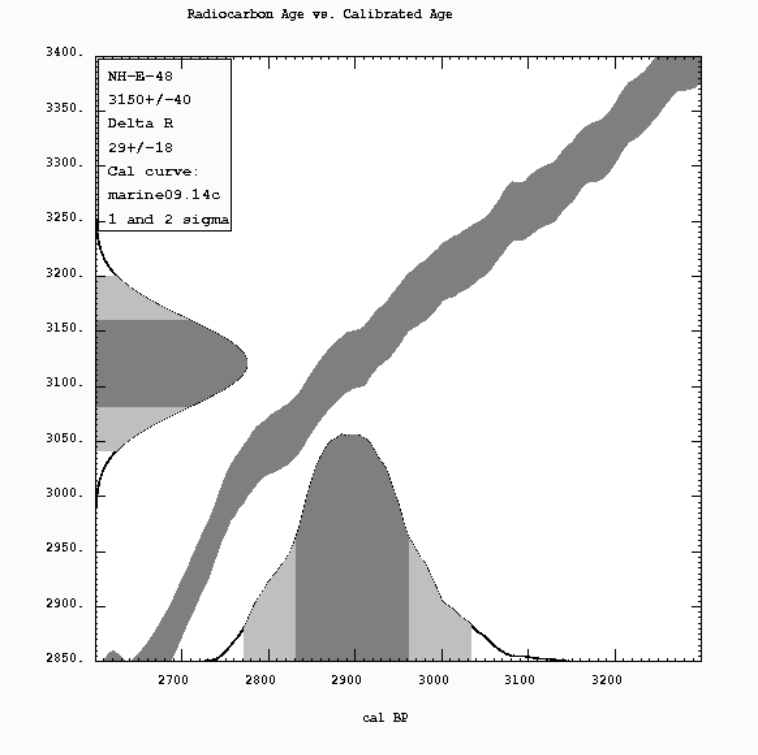
Radiocarbon Age vs. Calibrated Age
NH-E-48
3150+/-40
Delta R
29+/-18
Cal curve:
marine09.14c
1 and 2 sigma
3400.
3350.
3300.
3250.
3200.
3150.
3100.
3050.
3000.
2950.
2900.
2850.
2700
2800
2900
3000
3100
3200
cal BP

NH-E-48

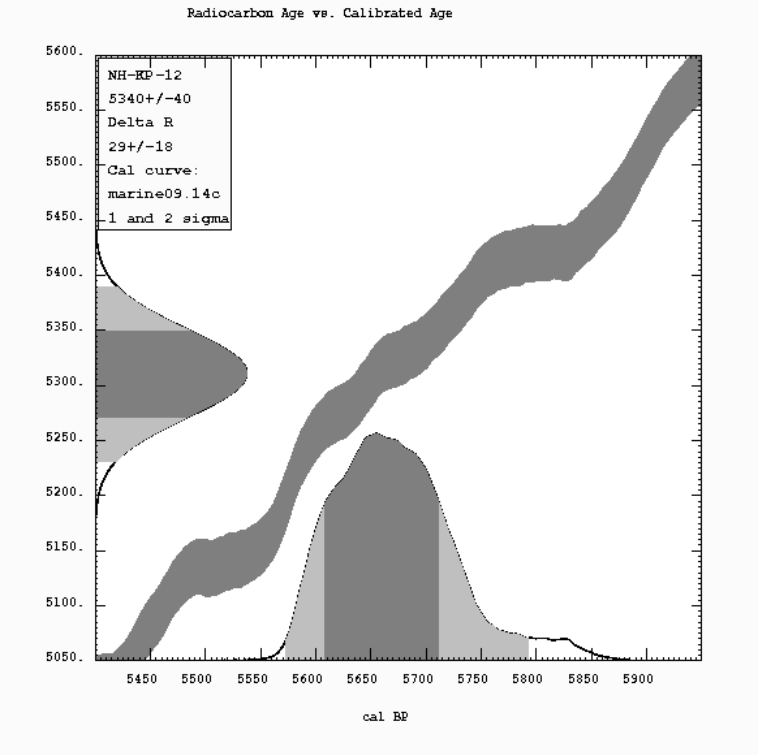


NH-KP-12

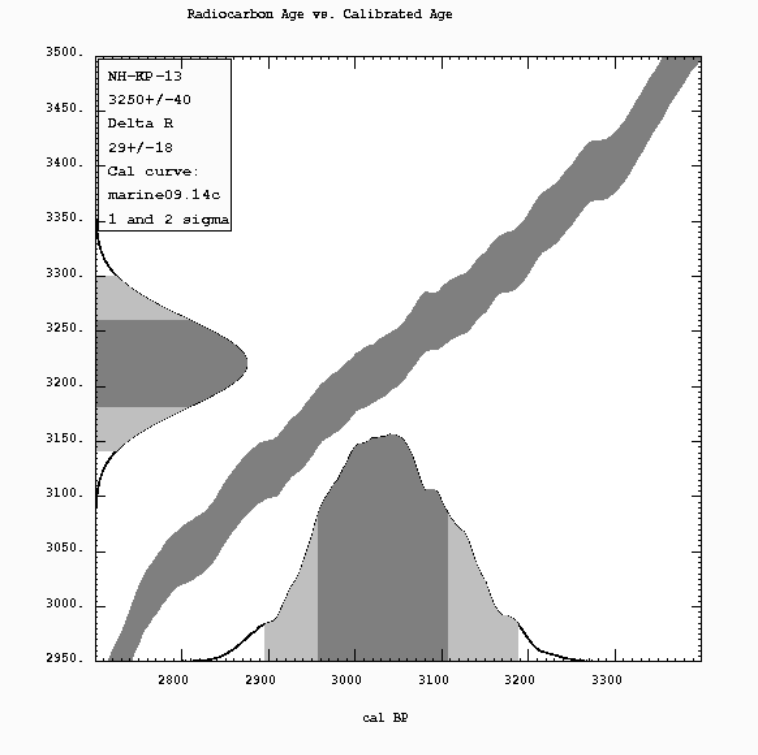


NH-KP-13

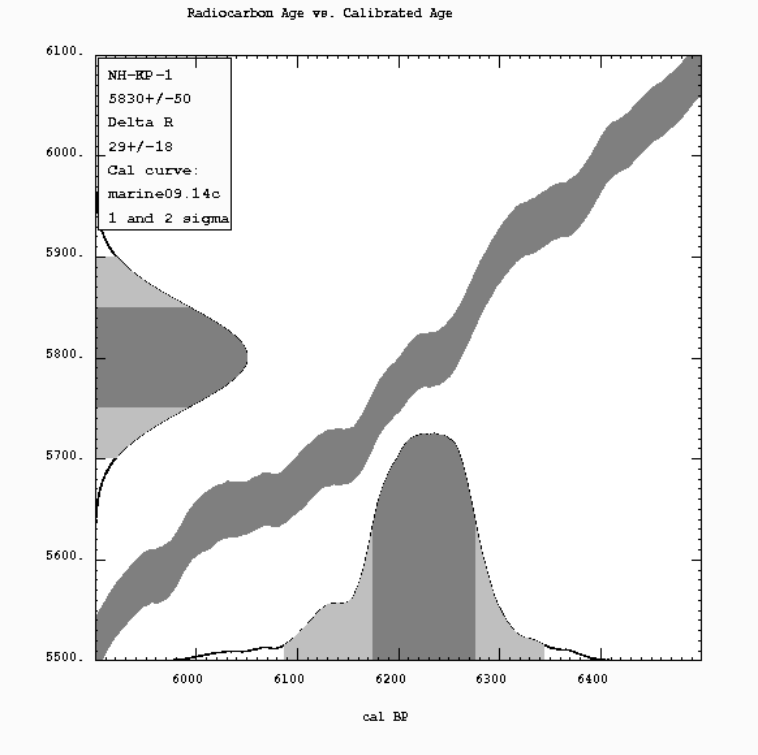
Radiocarbon Age vs. Calibrated Age
NH-KP-1
5830+/-50
Delta R
29+/-18
Cal curve:
marine09.14c
1 and 2 sigma
6100.
6000.
5900.
5800.
5700.
5600.
5500.
6000
6100
6200
6300
6400
cal BP

NH-KP-1

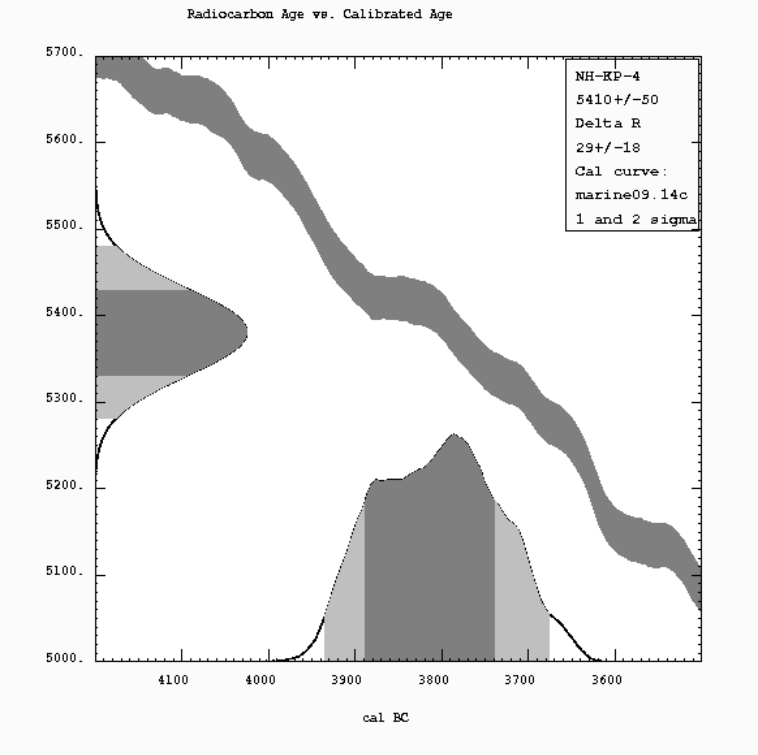
Radiocarbon Age vs. Calibrated Age
NH-KP-4
5410+/-50
Delta R
29+/-18
Cal curve:
marine09.14c
1 and 2 sigma
5700.
5600.
5500.
5400.
5300.
5200.
5100.
5000.
4100
4000
3900
3800
3700
3600
cal BC

NH-KP-4

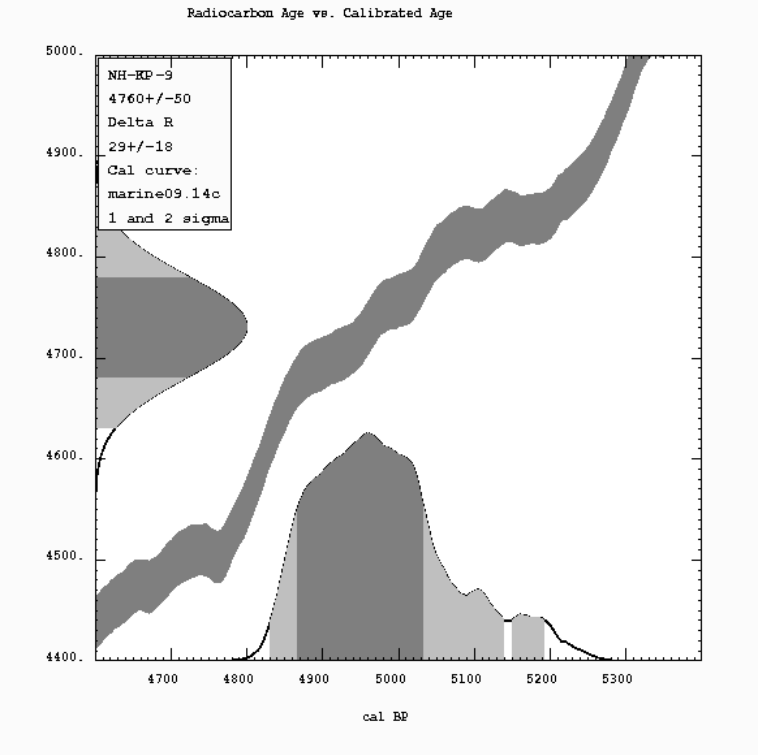


NH-KP-9

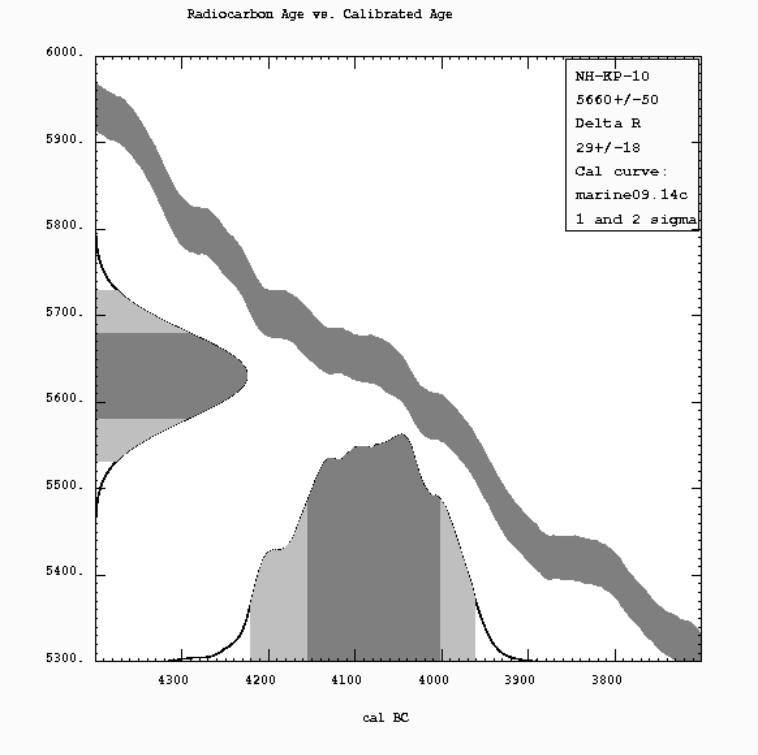


NH-KP-10

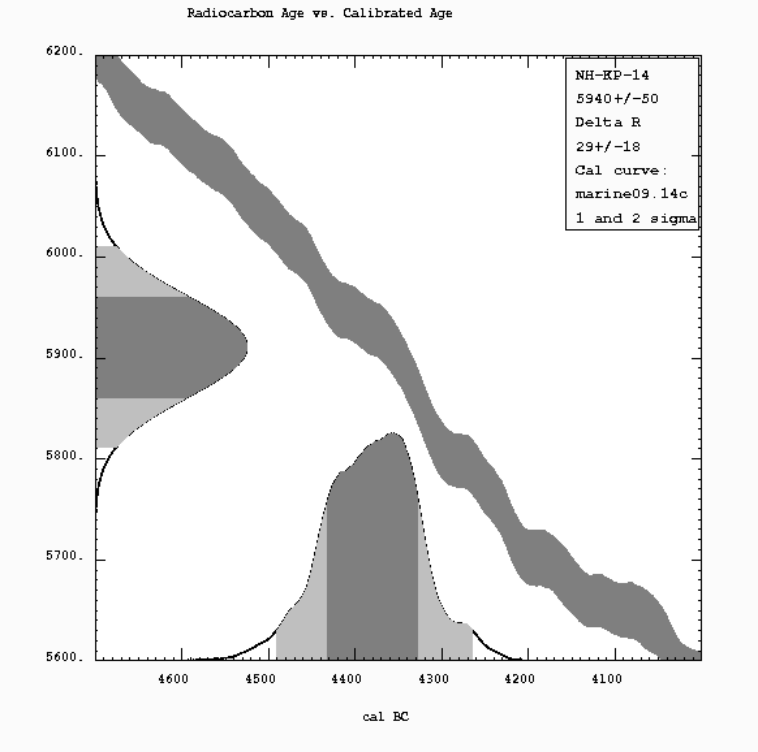


NH-KP-14

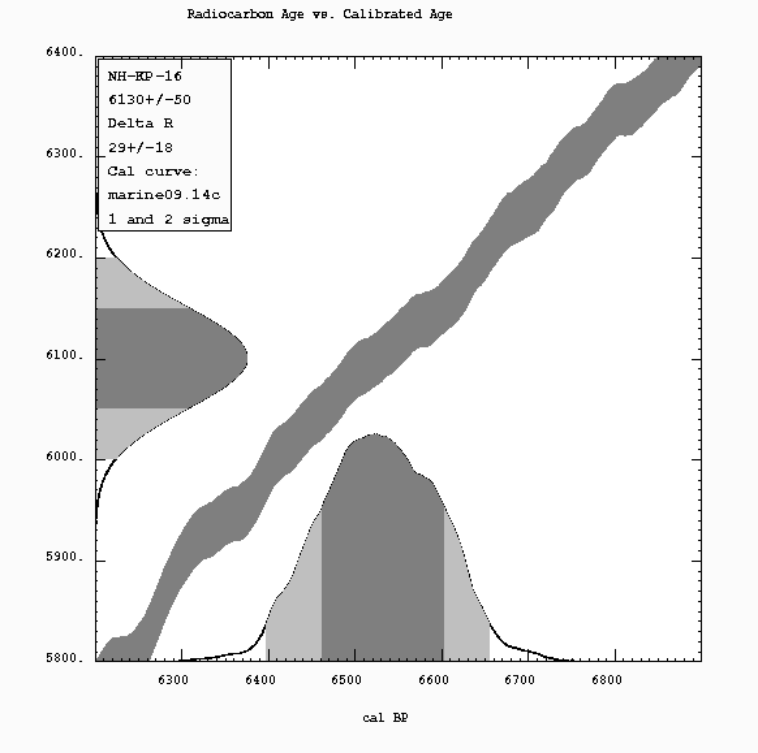


NH-KP-16

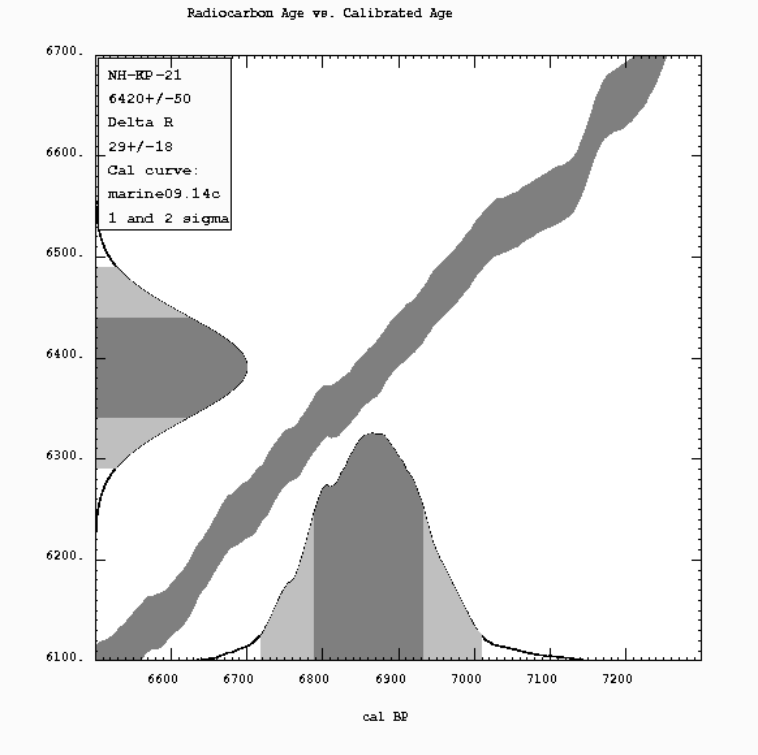


NH-KP-21

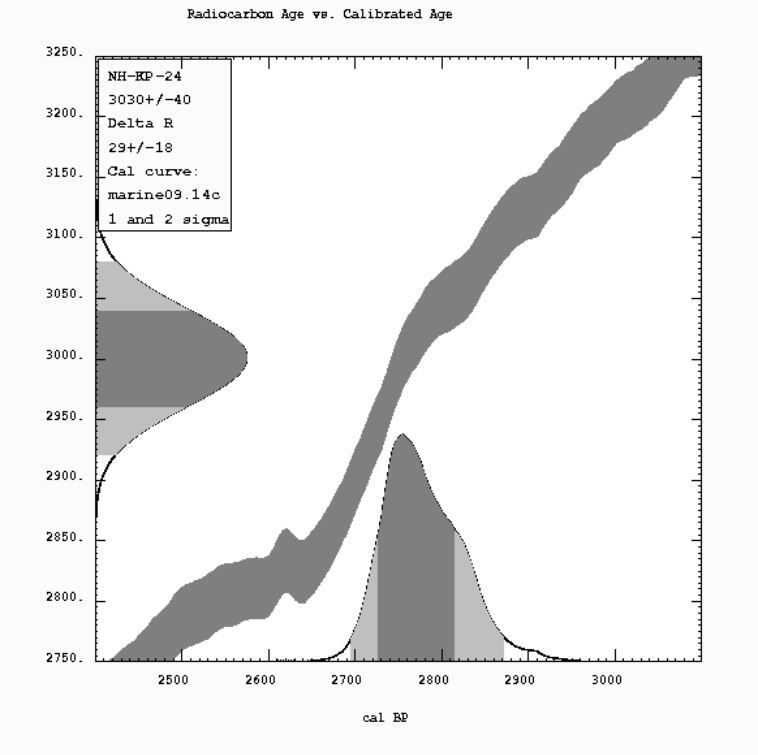


NH-KP-24

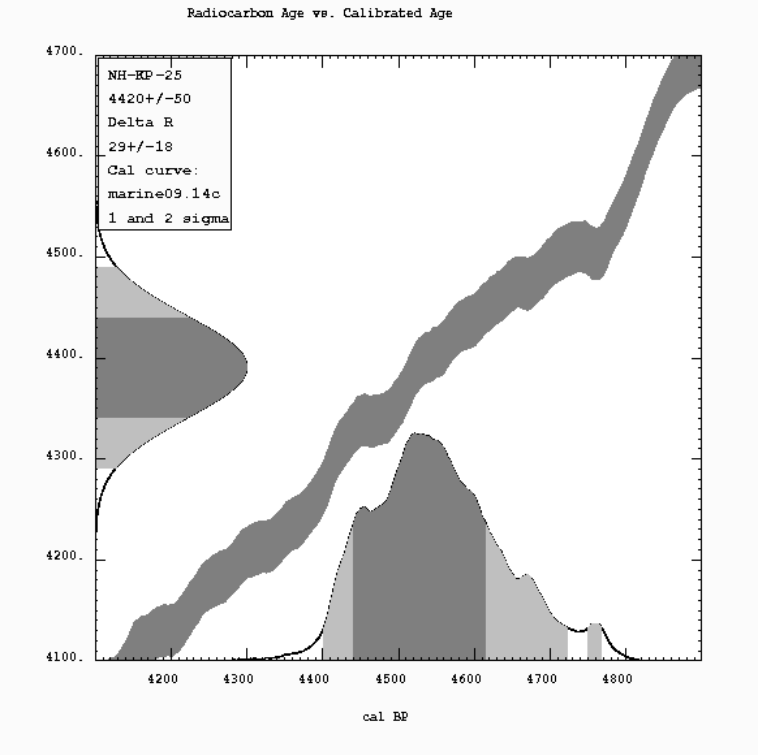


NH-KP-25

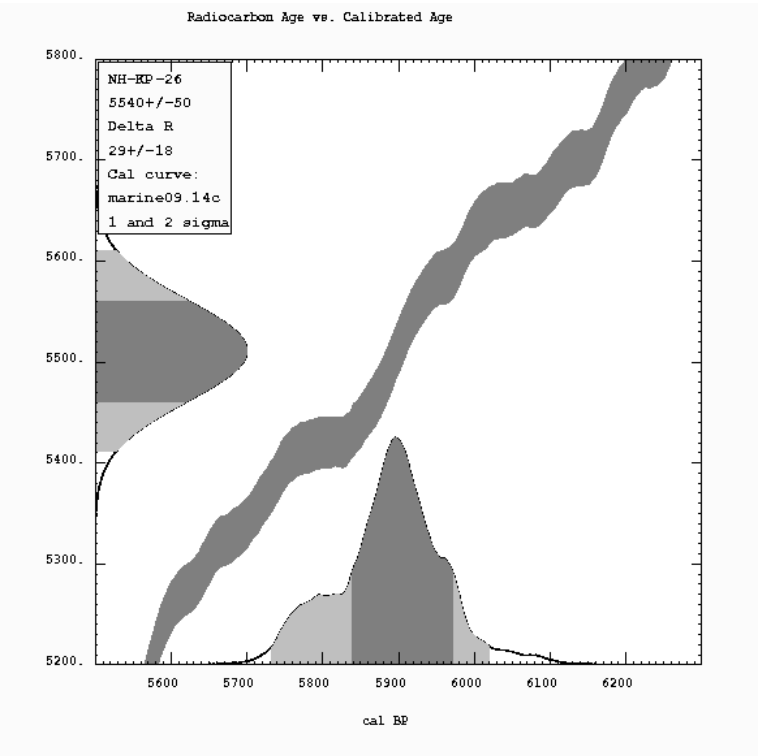


NH-KP-26

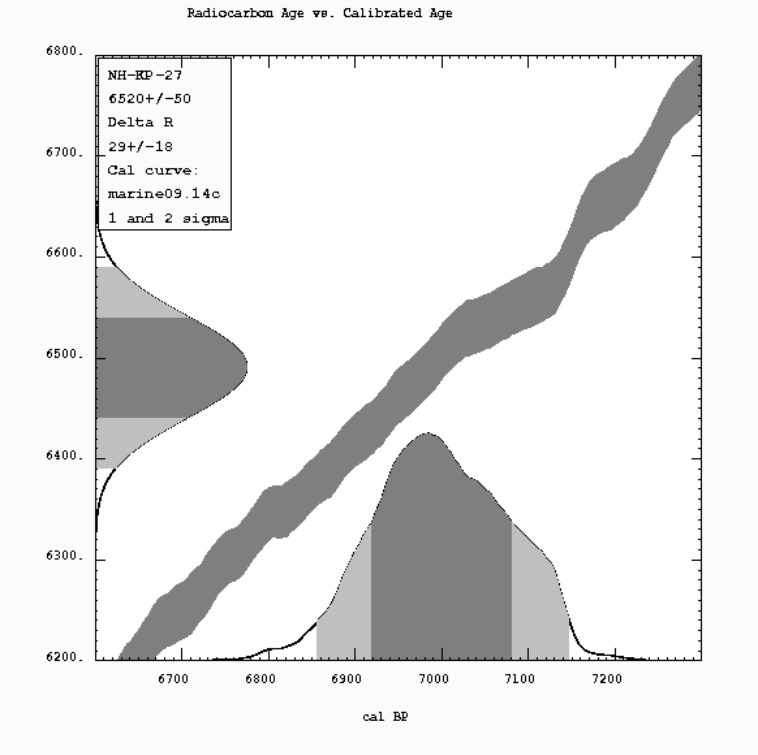


NH-KP-27

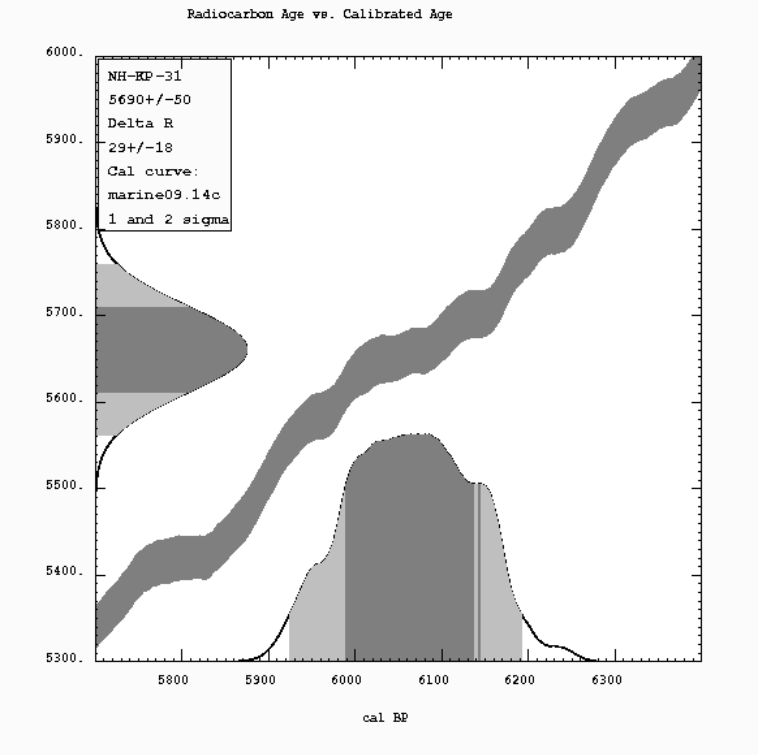


NH-KP-31

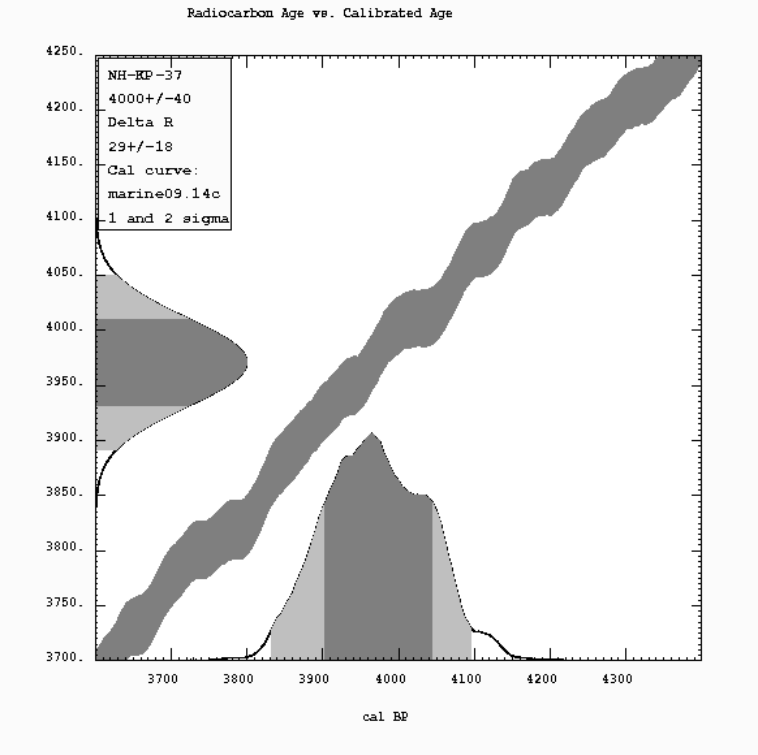


NH-KP-37

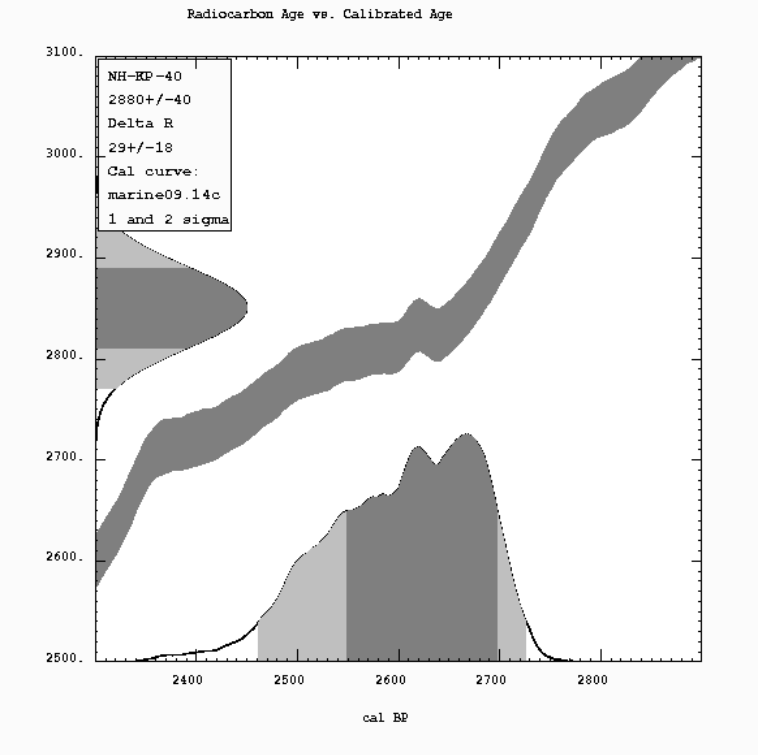


NH-KP-40

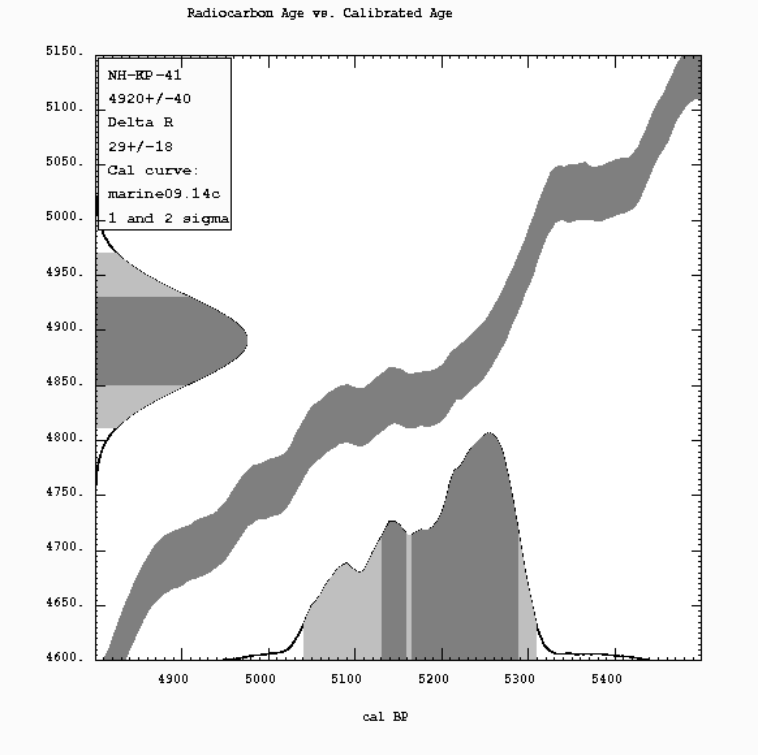


NH-KP-41

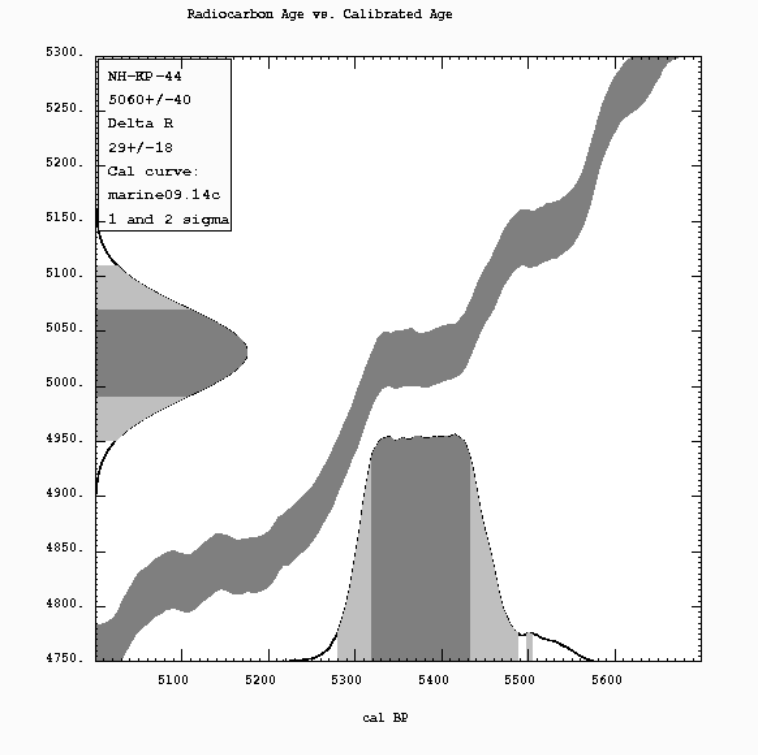


NH-KP-44

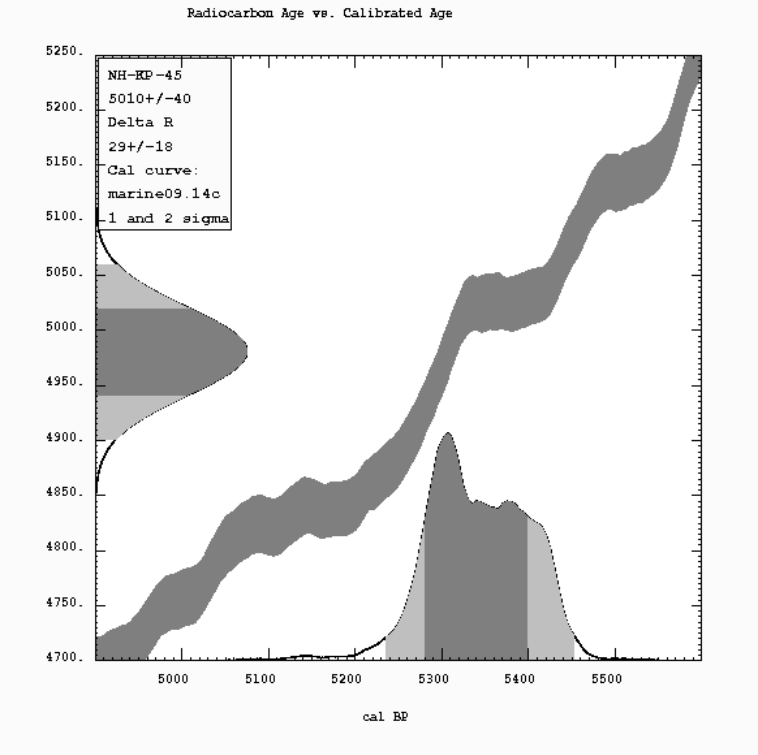


NH-KP-45

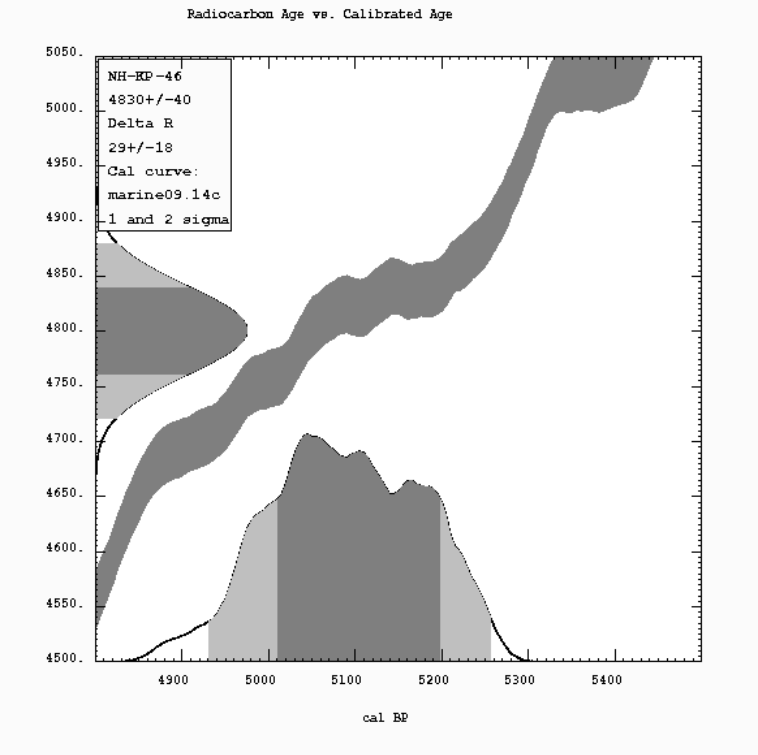


NH-KP-46

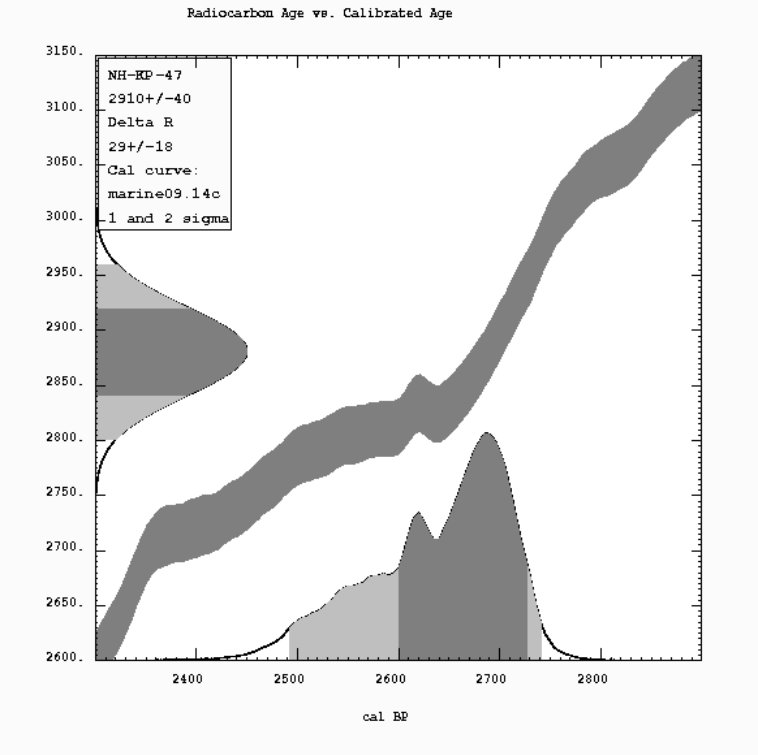


NH-KP-47

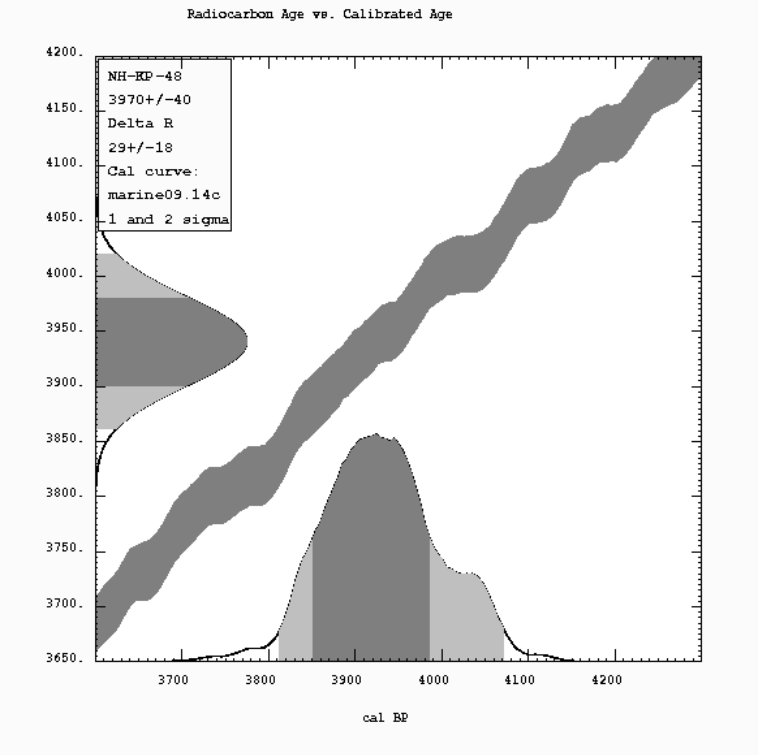


NH-KP-48

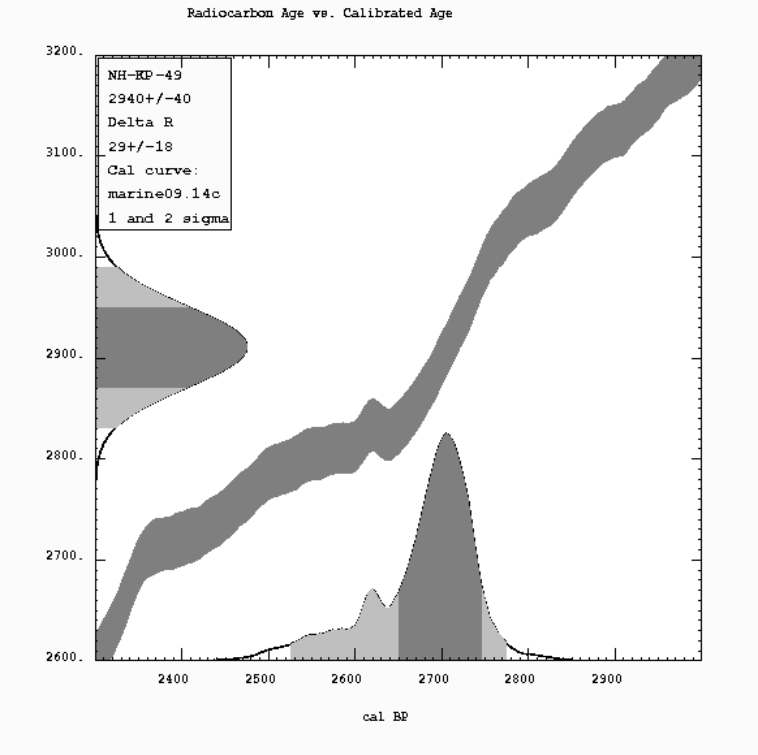


NH-KP-49

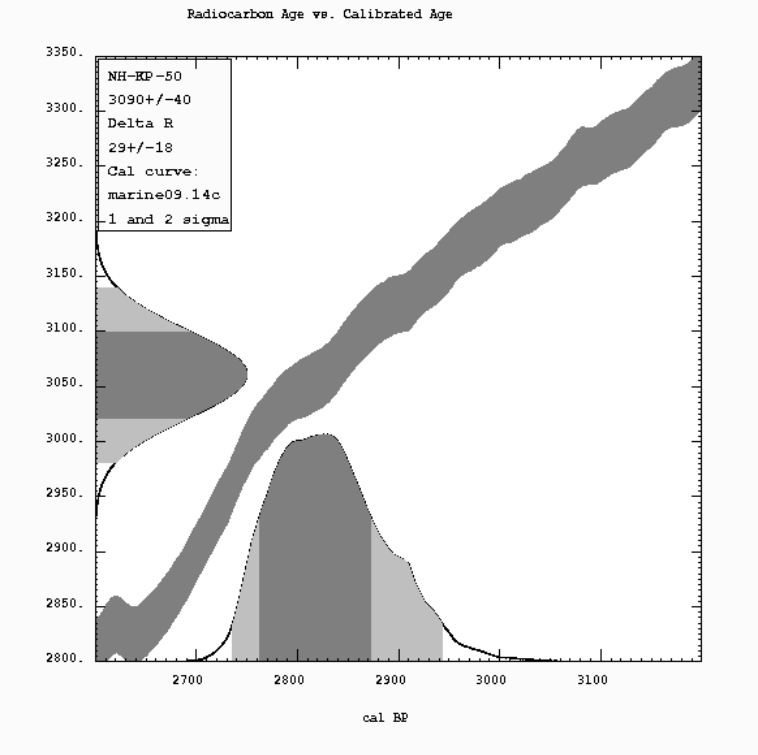


NH-KP-50

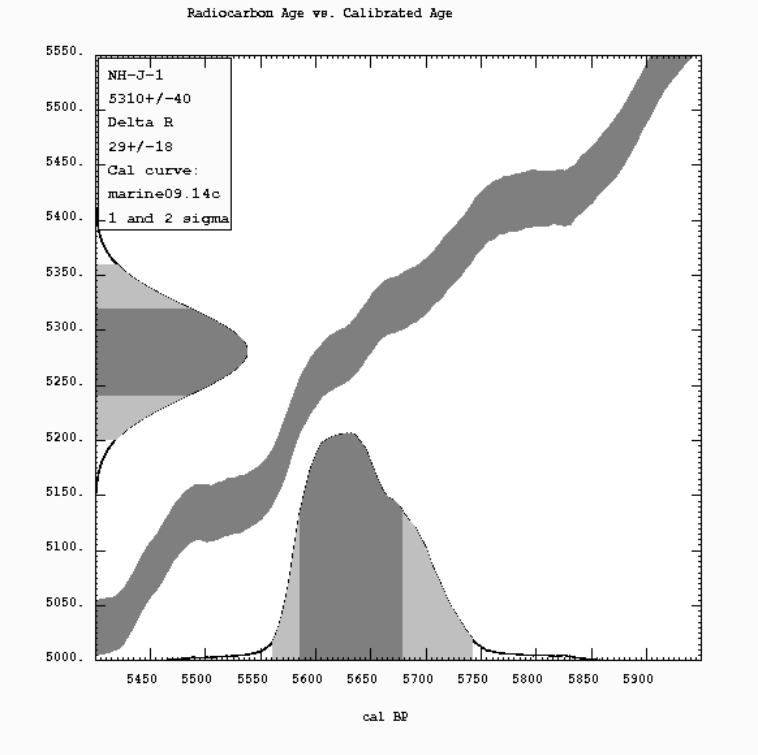
Radiocarbon Age vs. Calibrated Age
NH-J-1
5310+/-40
Delta R
29+/-18
Cal curve:
marine09.14c
1 and 2 sigma
5550.
5500.
5450.
5400.
5350.
5300.
5250.
5200.
5150.
5100.
5050.
5000.
5450
5500
5550
5600
5650
5700
5750
5800
5850
5900
cal BP

NH-J-1

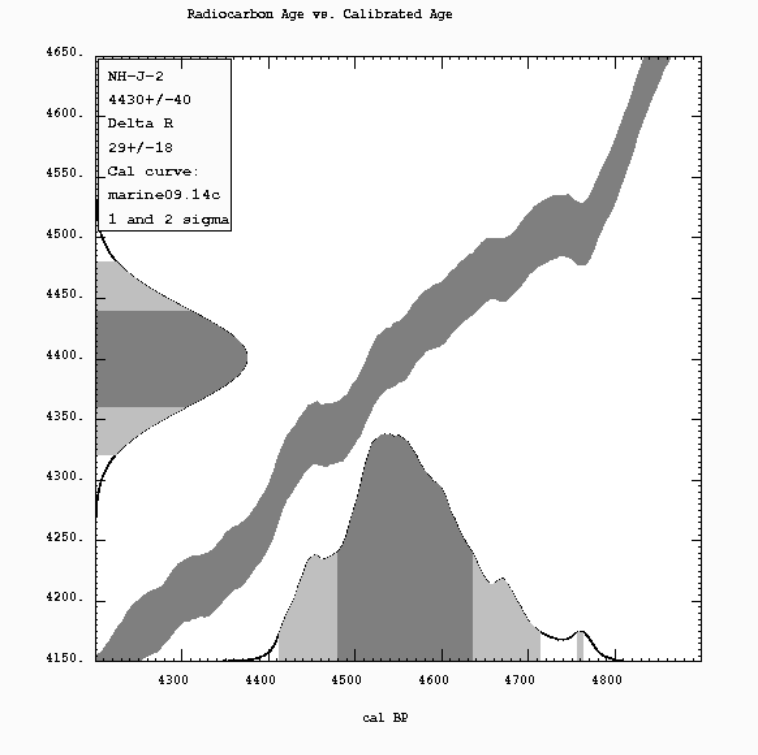
Radiocarbon Age vs. Calibrated Age
NH-J-2
4430+/-40
Delta R
29+/-18
Cal curve:
marine09.14c
1 and 2 sigma
4650.
4600.
4550.
4500.
4450.
4400.
4350.
4300.
4250.
4200.
4150.
4300
4400
4500
4600
4700
4800
cal BP

NH-J-2

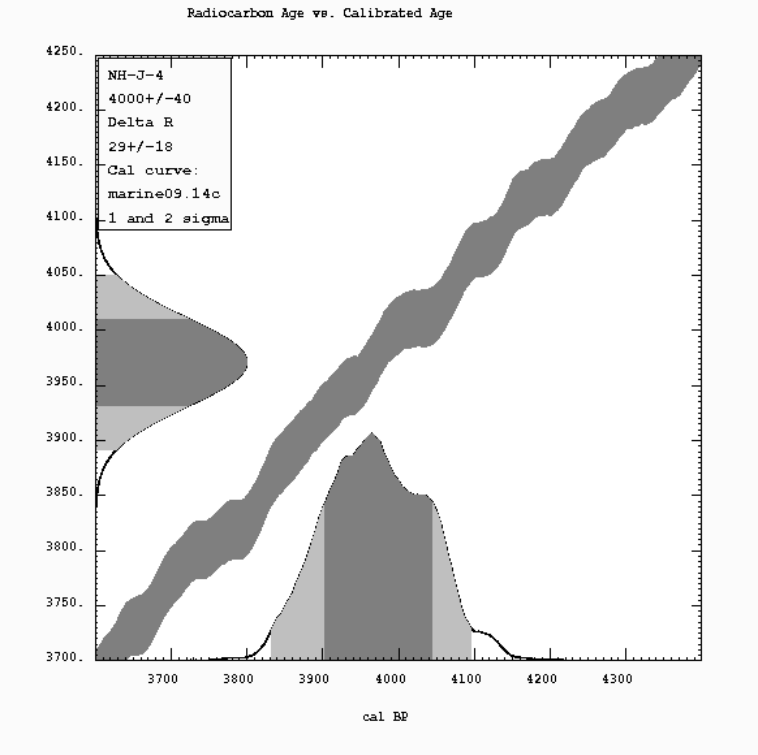
Radiocarbon Age vs. Calibrated Age
NH-J-4
4000+/-40
Delta R
29+/-18
Cal curve:
marine09.14c
1 and 2 sigma
4250.
4200.
4150.
4100.
4050.
4000.
3950.
3900.
3850.
3800.
3750.
3700.
3700
3800
3900
4000
4100
4200
4300
cal BP

NH-J-4

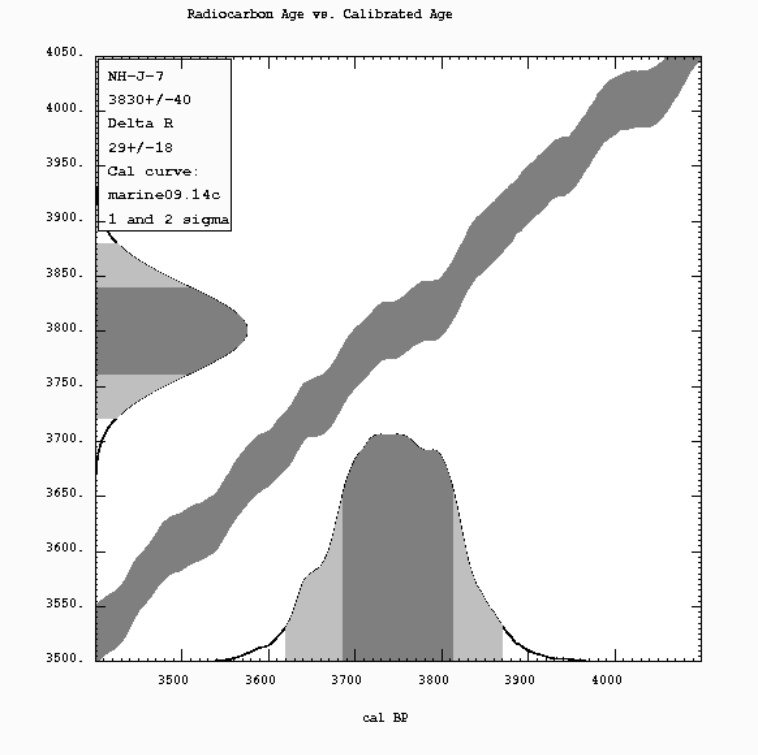
Radiocarbon Age vs. Calibrated Age
NH-J-7
3830+/-40
Delta R
29+/-18
Cal curve:
marine09.14c
1 and 2 sigma
4050.
4000.
3950.
3900.
3850.
3800.
3750.
3700.
3650.
3600.
3550.
3500.
3500
3600
3700
3800
3900
4000
cal BP

NH-J-7

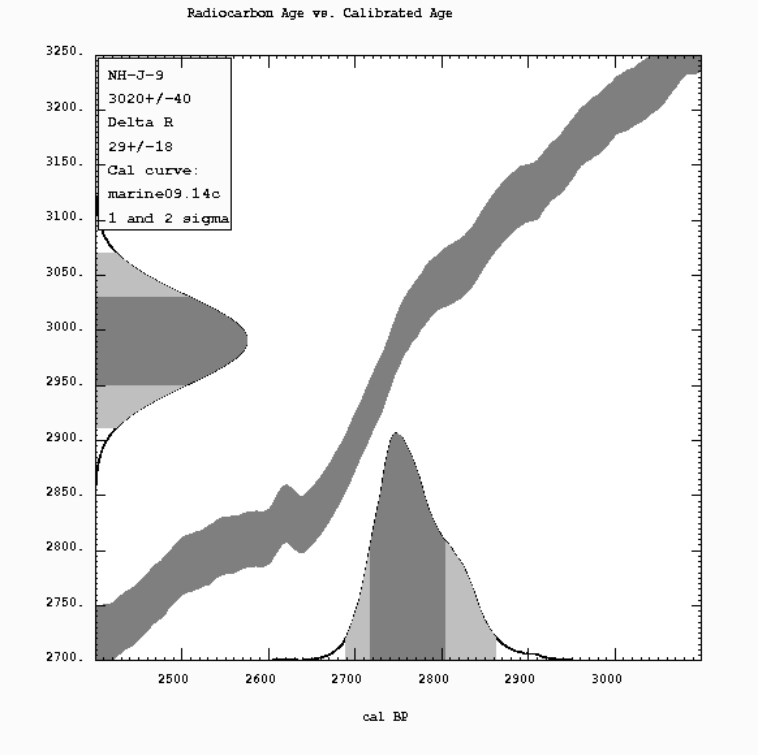
Radiocarbon Age vs. Calibrated Age
NH-J-9
3020+/-40
Delta R
29+/-18
Cal curve:
marine09.14c
1 and 2 sigma
3250.
3200.
3150.
3100.
3050.
3000.
2950.
2900.
2850.
2800.
2750.
2700.
2500
2600
2700
2800
2900
3000
cal BP

NH-J-9

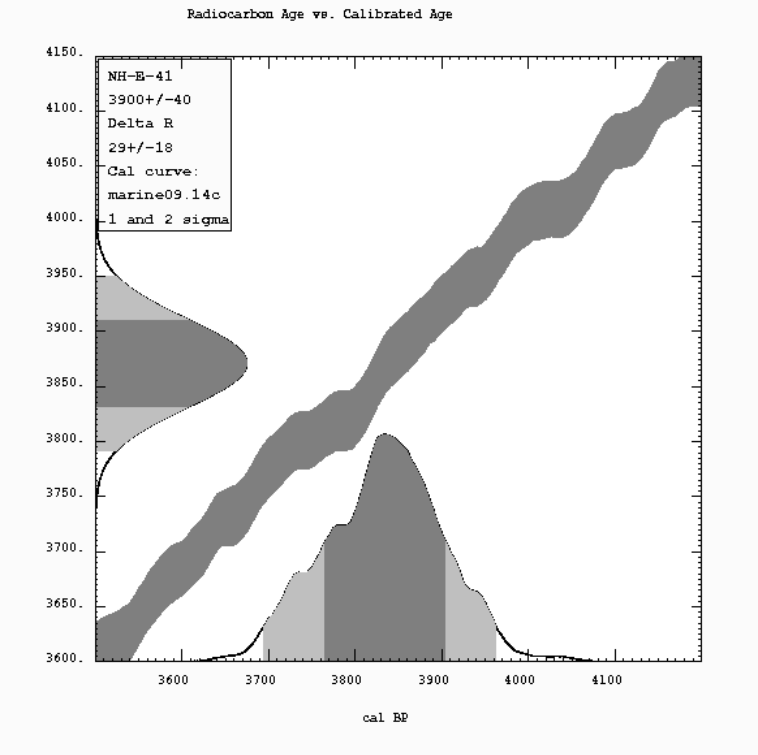
Radiocarbon Age vs. Calibrated Age
NH-E-41
3900+/-40
Delta R
29+/-18
Cal curve:
marine09.14c
1 and 2 sigma
4150.
4100.
4050.
4000.
3950.
3900.
3850.
3800.
3750.
3700.
3650.
3600.
3600
3700
3800
3900
4000
4100
cal BP

NH-E-41

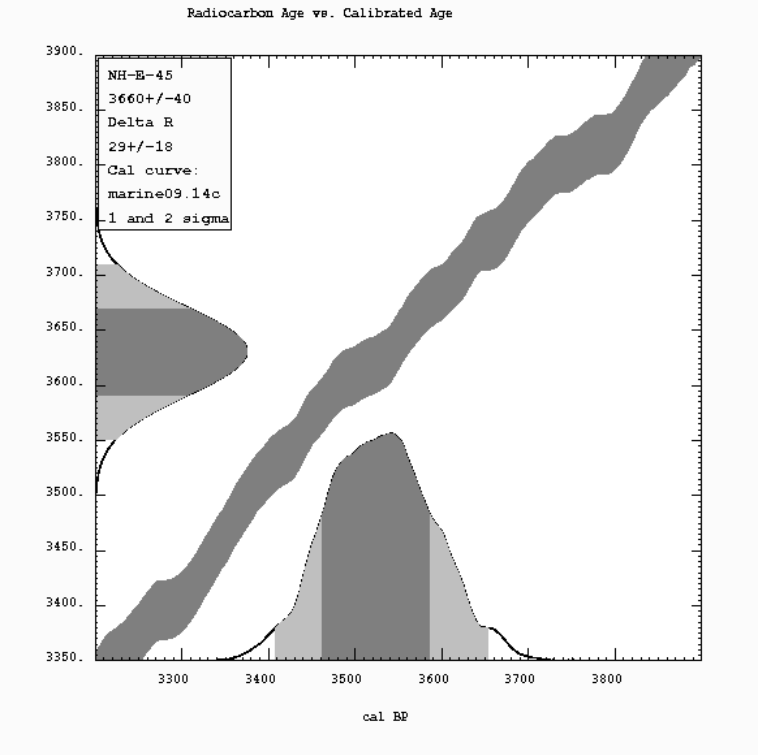
Radiocarbon Age vs. Calibrated Age
NH-E-45
3660+/-40
Delta R
29+/-18
Cal curve:
marine09.14c
1 and 2 sigma
3900.
3850.
3800.
3750.
3700.
3650.
3600.
3550.
3500.
3450.
3400.
3350.
3300
3400
3500
3600
3700
3800
cal BP

NH-E-45

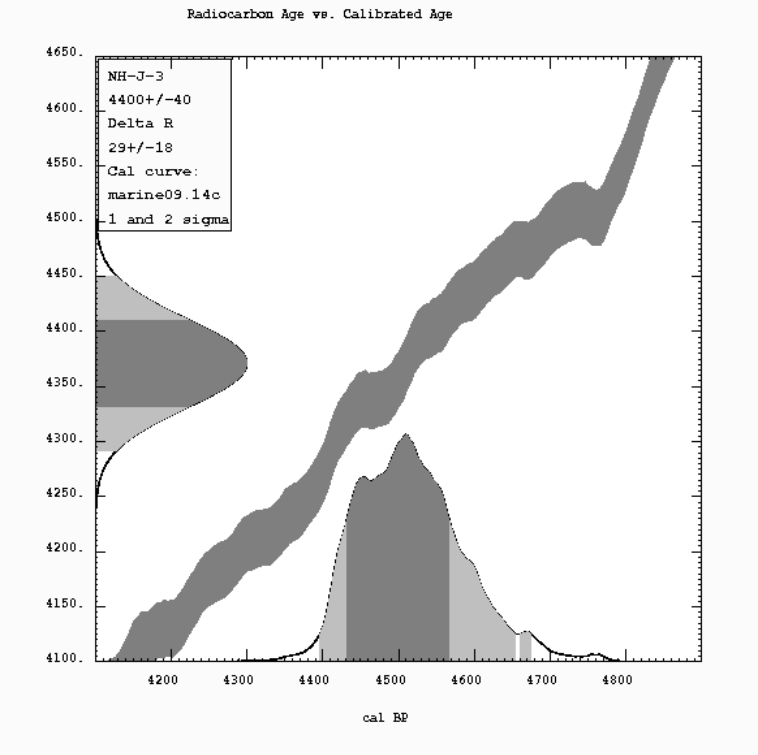
Radiocarbon Age vs. Calibrated Age
NH-J-3
4400+/-40
Delta R
29+/-18
Cal curve:
marine09.14c
1 and 2 sigma
4650.
4600.
4550.
4500.
4450.
4400.
4350.
4300.
4250.
4200.
4150.
4100.
4200
4300
4400
4500
4600
4700
4800
cal BP

NH-J-3

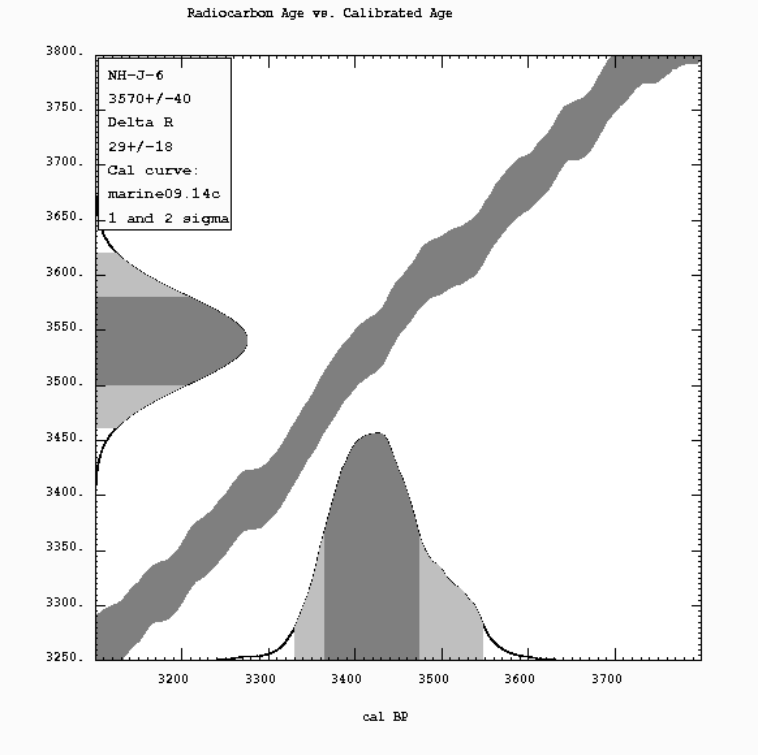
Radiocarbon Age vs. Calibrated Age
NH-J-6
3570+/-40
Delta R
29+/-18
Cal curve:
marine09.14c
1 and 2 sigma
3800.
3750.
3700.
3650.
3600.
3550.
3500.
3450.
3400.
3350.
3300.
3250.
3200
3300
3400
3500
3600
3700
cal BP

NH-J-6

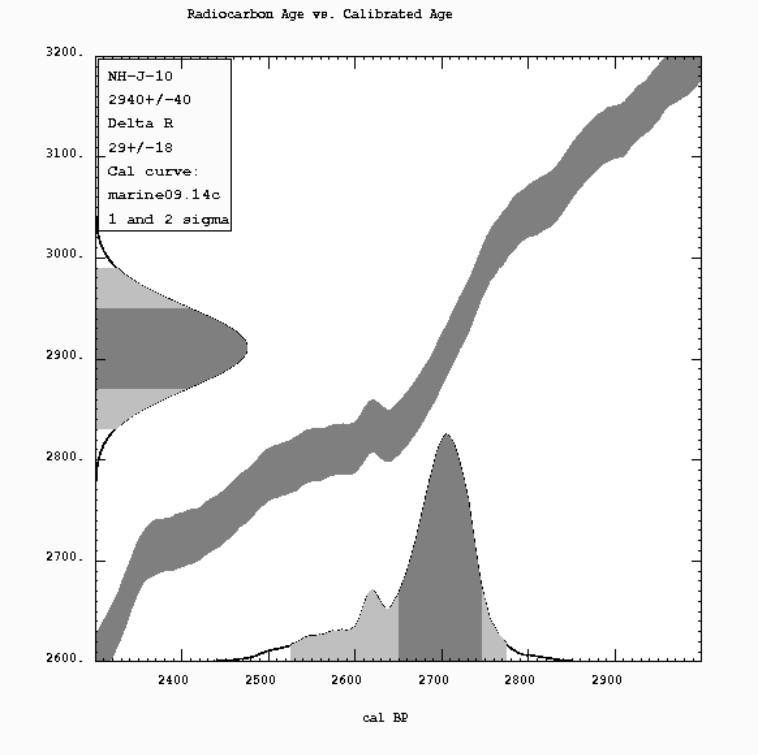
Radiocarbon Age vs. Calibrated Age
NH-J-10
2940+/-40
Delta R
29+/-18
Cal curve:
marine09.14c
1 and 2 sigma
3200.
3100.
3000.
2900.
2800.
2700.
2600.
2400
2500
2600
2700
2800
2900
cal BP

NH-J-10

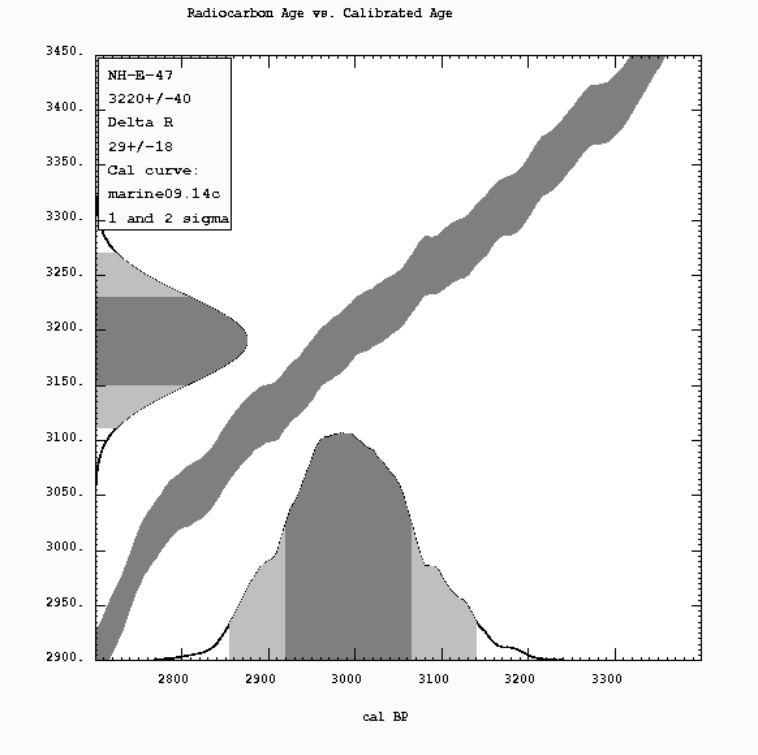


NH-E-47

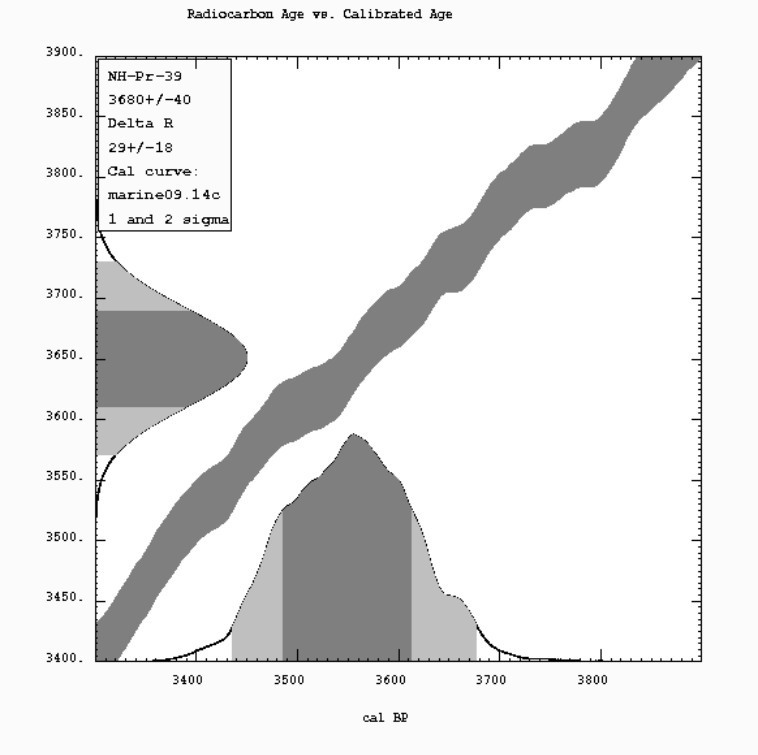


NH-Pr-39

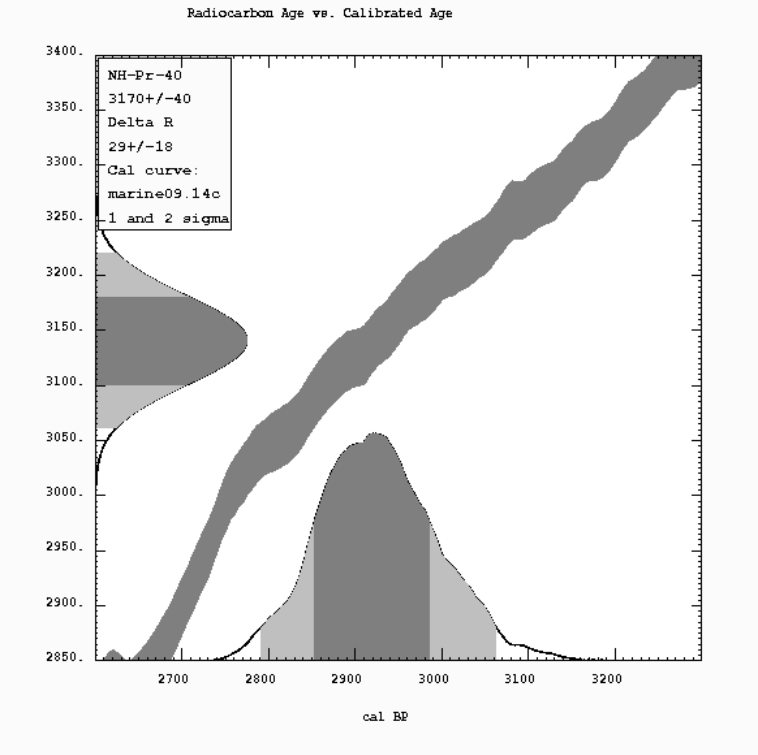


NH-Pr-40

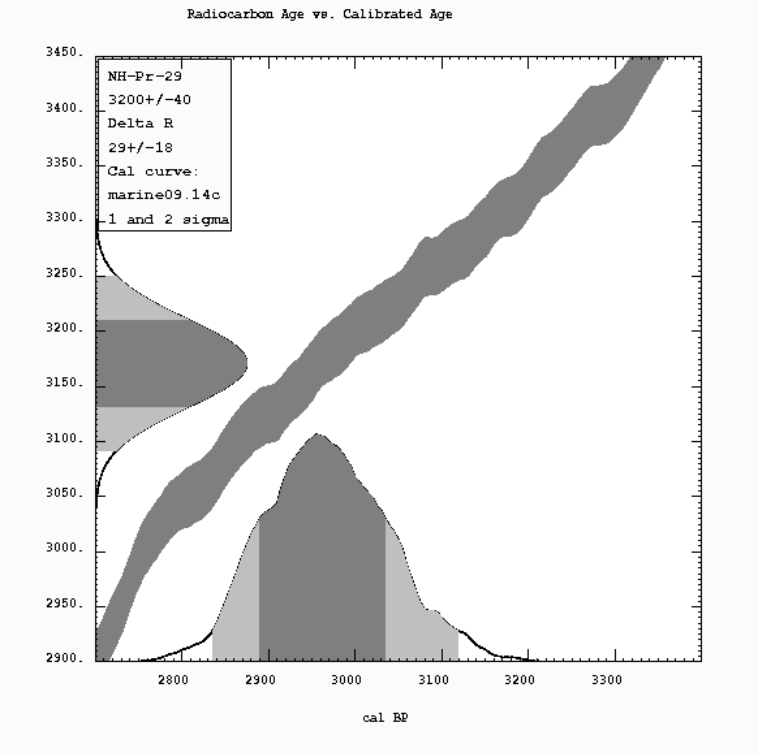


NH-Pr-29

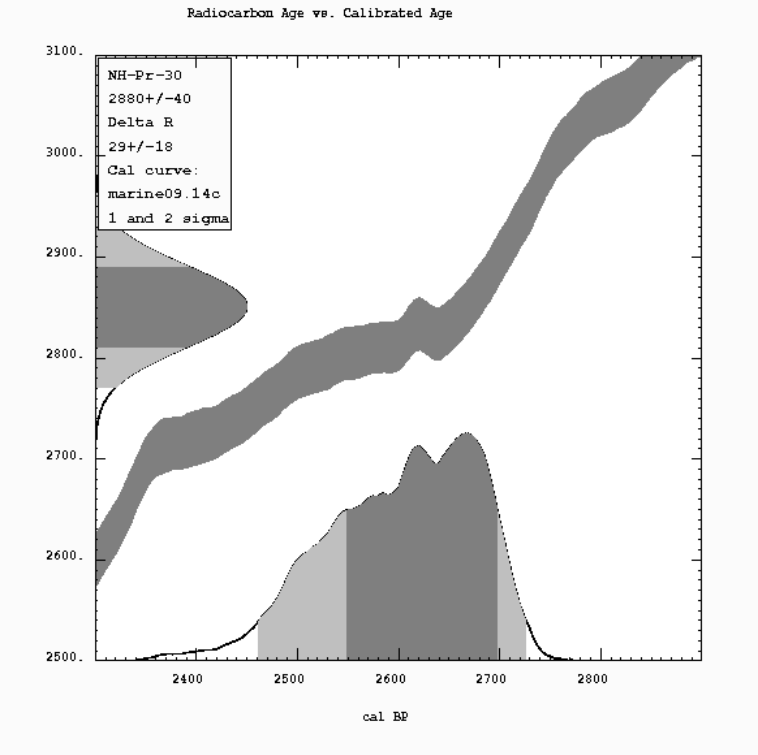


NH-Pr-30

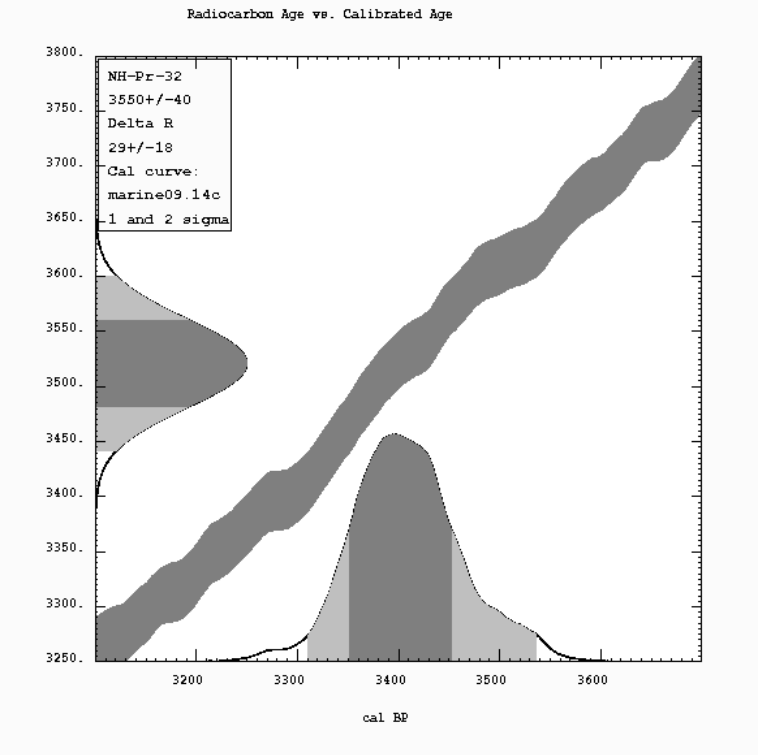


NH-Pr-32

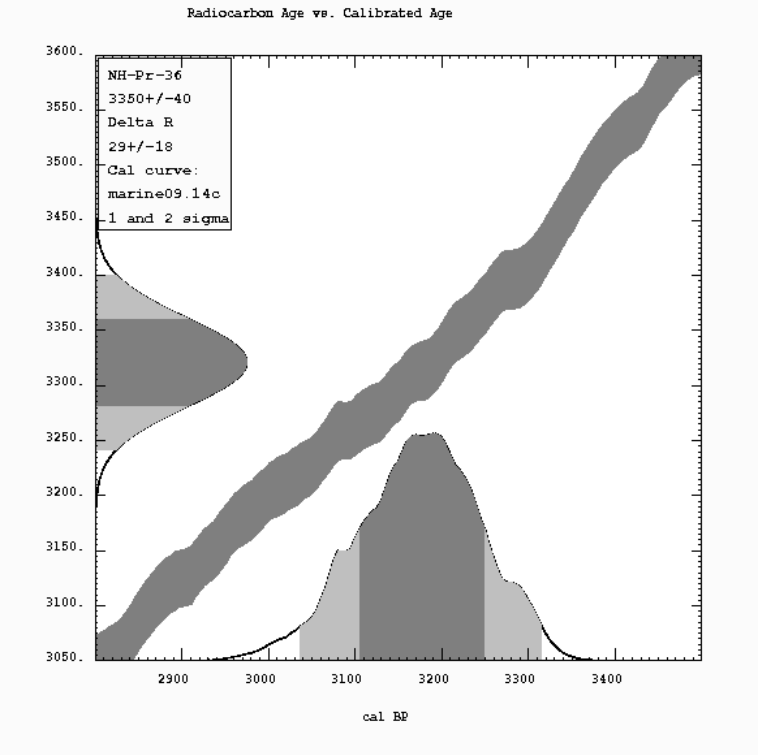


NH-Pr-36

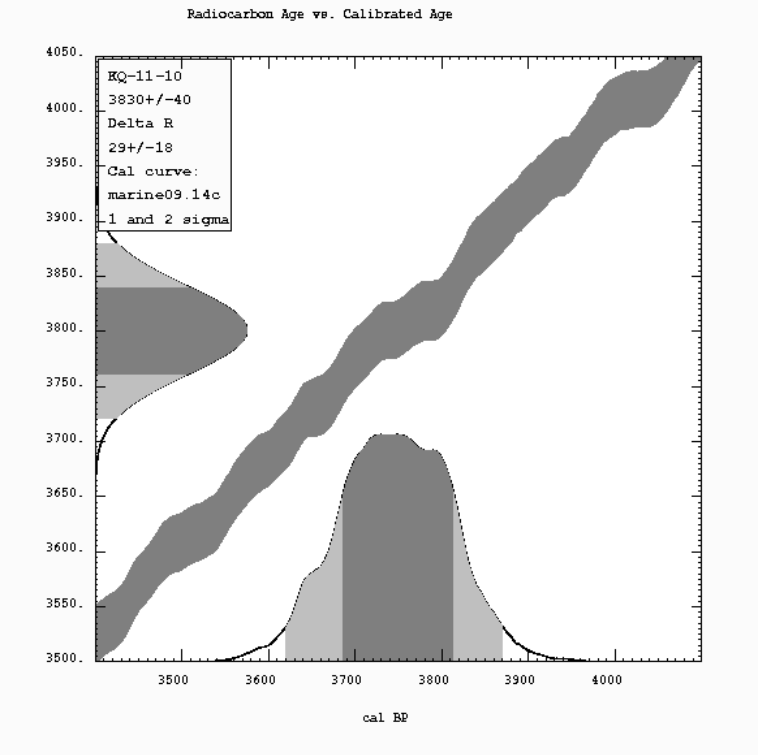


KQ-11-10

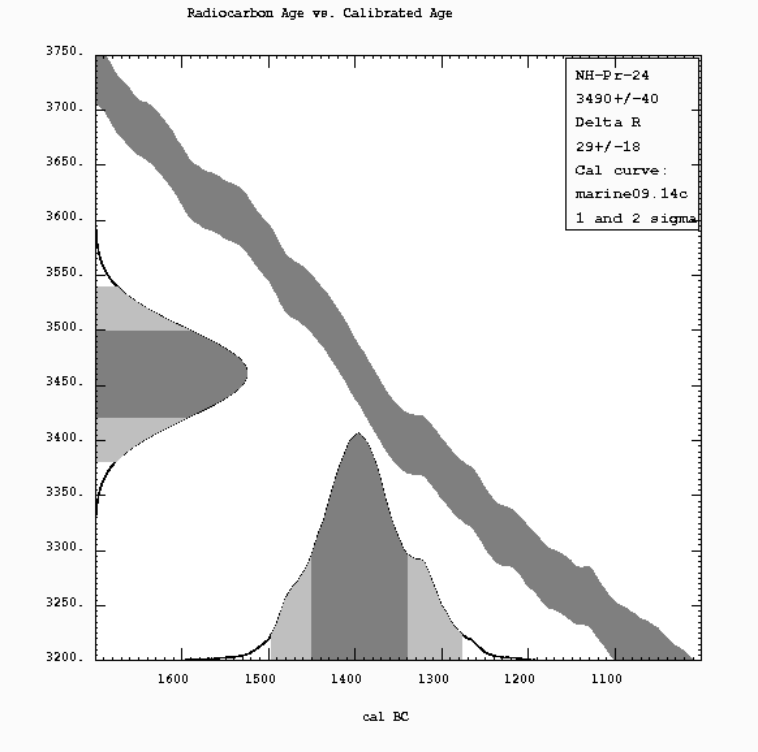


NH-Pr-24

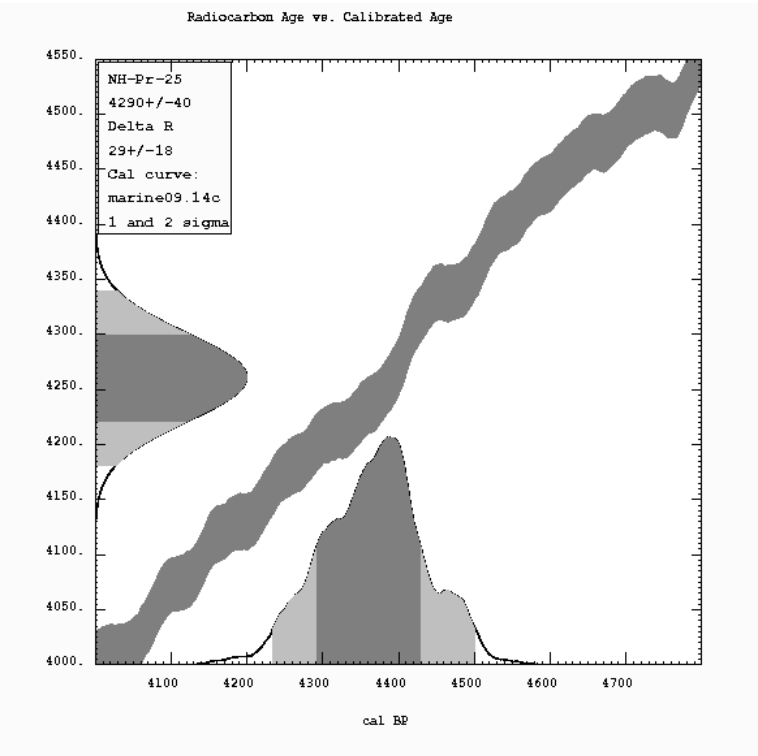


NH-Pr-25